Centre for Molecular Oncology and Imaging

Barts Cancer Institute

Queen Mary's University of London

Development of Virus-infected Cancer Cell Vaccine

Chadwan Al Yaghchi

Supervisors

Professor Yaohe Wang

Professor Nicholas Lemoine

Mr Ghassan Alusi

Submitted in partial fulfilment of the requirements of the Degree of Doctor of Philosophy

Statement of originality

I, Chadwan Al Yaghchi, confirm that the research included within this thesis is my own work or that where it has been carried out in collaboration with, or supported by others, that this is duly acknowledged below and my contribution indicated. Previously published material is also acknowledged below.

I attest that I have exercised reasonable care to ensure that the work is original, and does not to the best of my knowledge break any UK law, infringe any third party's copyright or other Intellectual Property Right, or contain any confidential material.

I accept that the College has the right to use plagiarism detection software to check the electronic version of the thesis.

I confirm that this thesis has not been previously submitted for the award of a degree by this or any other university.

The copyright of this thesis rests with the author and no quotation from it or information derived from it may be published without the prior written consent of the author.

Signature: 

Date: 21/02/2016

Some efficacy experiments were performed in collaboration with the Sino-British Research Centre for Molecular Oncology, Zhengzhou University, Zhengzhou, China. Experimental design, protocols, data analysis and interpretation were performed by me while the experiments were performed by research technicians at the centre. These experiments will be clearly acknowledged in the text.

Certain parts of the introduction relating to vaccinia virus have been adapted from a review article I have written for the Journal of Immunotherapy[1]. The full article is included as appendix IV of this thesis.

To Nada

Acknowledgments

First and foremost I would like to extend my deepest gratitude to my supervisor, Professor Yaohe Wang, for his continuous advice, support, availability, encouragement and trust. Thank you for your infectious enthusiasm and love of science. I would also like to thank Professor Nicholas Lemoine for his constant support, invaluable insight and brilliant ideas. In addition, I would like to thank Mr Ghassan Alusi who has been a constant source of support and mentorship from the first day I walked into the ENT Department as a senior house officer until this day.

I am indebted to every member of the Wang lab. Special thanks goes to Rathi Gangeswaran for teaching me various lab techniques, Ming Yuan and Jay Ahmed for their help and advice on virus cloning and Louisa Chard for her critical eye and brilliant trouble shooting. A heartfelt massive thank you to my lab partner Margot. Her high spirit and infectious enthusiasm made the Molecular Oncology lab a much brighter place. Thanks to Mark, Mo, Anwen, David and Zarah for being such brilliant colleagues.

Finally, sincere gratitude goes to Prof Federica Marelli-Berg, Dr Hongmei Fu, Dr Gunnel Hallden and Dr Jeff Davis for their invaluable help and advice, Vips and Pam for the seamless running of the Molecular Oncology Department, George Elea from histopathology, Dr Becki Pike from the Flowcytometry lab, Arif and James from the BSU and Julia and Tracy from the ATS service.

This project was financially supported by the research fund of the ENT Department at Barts Health NHS Trust and a Project Development Award by Barts Cancer Institute.

Abstract

Oncolytic viruses can be genetically modified to limit their replication in normal cells rendering them a cancer specific treatment. In addition, they can induce a “danger signal” in the form of pathogen- and damage-associated molecular patterns leading to anti-tumour immunity. Furthermore, they can be armed with various immunomodulatory molecules to further enhance anti-tumour immunity. In this project I aim to exploit these qualities to develop a translatable cancer vaccine. Virus-infected cancer cells were injected subcutaneously in a prime/boost regimen. Dying cancer cells will release the required danger signal leading to dendritic cell activation and cross-presentation of tumour associated antigens to T cells to elicit an anti-tumour immune response.

Our results in the murine pancreatic cancer model showed that vaccination with virus-infected DT6606 cells induced tumour specific immunity capable of protecting vaccinated animals against re-challenge with tumour cells. The highest level of interferon gamma production, a surrogate marker of anti-tumour immunity, was achieved when animals were primed with adenovirus-infected cells. There was no significant difference between various boost groups. To enhance the safety of the proposed protocol a secondary treatment was introduced to arrest the proliferation of tumour cells prior to injection. Our results confirmed that secondary treatment with mitomycin does not affect the induction of tumour specific immunity and it does not affect the release of pathogen-associated molecular patterns in the form of viral proteins and DNA.

To test our vaccination regimen in head and neck squamous cell carcinoma (HNSCC) we develop a clinically relevant mouse model using SCC7, B4B8 and LY2 cells to replicate various clinical scenarios including locally advancing disease and post

excision locoregional recurrence. Vaccinating mice with HNSCC cells pre-infected with our recently developed tumour-targeted triple-deleted adenovirus (AdTD) resulted in a cell-specific antitumour immune response. In addition, it resulted in an increase in effector memory T-cells of both CD4+ and CD8+ phenotypes. Efficacy studies showed our vaccination can significantly slow down the growth rate of tumours in locally advancing disease. This led to increase survival of the vaccinated mice although it did not reach statistical significance.

To further enhance the efficacy of our vaccination regimen, we aimed to increase T cell trafficking to the tumour site. CCL25 is a gut homing chemokine. Priming T cells in the presence of CCL25 will lead to upregulation of the surface expression of α4β7 integrin. The latter is a ligand of MAdCAM-1, a cell adhesion molecule highly expressed in the gut and pancreatic tumours. The α4β7/MAdCAM-1 interaction results in preferential homing of activated T cells to these organs. We hypothesised that vaccinating mice with pancreatic tumour cells pre-infected with a CCL25-armed adenovirus will lead to increased T cell trafficking to pancreatic tumours leading to enhanced efficacy. Although we achieved encouraging results in our pilot experiment, we did not detect any significant increase in α4β7 expression once we added a secondary treatment to the vaccination protocol. Similarly, efficacy experiments in the pancreatic cancer transgenic KPC mice did not show any difference in survival between AdTD-CCL25 and the control virus although both groups showed a trend towards increased survival compared to naïve mice.

In conclusion, Virus-infected cancer cell vaccine is a potentially promising immunotherapeutic strategy that can be combined with traditional cancer therapies to increase survival of HNSCC and pancreatic cancer patients.

Table of contents

Table of figures

Table of tables

Abbreviations

Ad5	Human Adenovirus sero-type 5
ADCC	Antibody-dependant cell-mediated cytotoxicity
ADP	Adenovirus Death Protein
AdTD	Triple-deleted adenovirus
AdV	Adenovirus
APC	Antigen Presenting Cells
ATP	Adenosine Triphosphate
BCG	Bacillus Calmette-Guerin
bp	Base pair
BSA	Bovine Serum Albumin
CAR	Coxsackievirus and adenovirus receptor
CAR	Chimeric-antigen receptor
CMV	Cytomegalovirus
CPE	Cytopathic Effect
CsCl	Caesium Chloride
CT	Cycle Threshold (qPCR)
CTA	Cancer testis antigen
CTL	Cytotoxic T Cells
CTLA-4	Cytotoxic T Lymphocyte associated protein 4
DAMPs	Damage Associated Molecular Patterns
DC	Dendritic Cells
DMEM	Dulbecco's Modified Eagle's Medium
DNA	Deoxyribonucleic Acid
dNTP	Deoxynucleotide
DTH	Delayed Type Hypersensitivity
DTT	Dithiothreitol
E1A	Adenovirus early region 1A gene
EC50	Half maximal effective concentration
EDTA	Ethylenediaminetetraacetic acid
EGFR	Epidermal Growth Factor Receptor
ELISA	Enzyme-linked Immunosorbent Assay
ER	Endoplasmic reticulum
FCS	Foetal Calf Serum

FMO	Florescence minus one
GFP	Green Florescent Protein
GM-CSF	Granulocyte-Macrophage Colony-stimulating Factor
GMP	Good Manufacturing Practices
Gy	Gray (Irradiation dose)
HGF	Hepatocyte growth factor
HMGB1	High-mobility group box 1
HNSCC	Head and Neck Squamous Cell Carcinoma
HPV	Human Papilloma Virus
HSV	Herpes Simplex Virus
ICD	Immunogenic Cell Death
IFN	Interferon
IM	Intramuscular
IT	Intratumoural
kbp	kilo base pair
LB	Lysogeny Broth
mAb	Monoclonal antibody
MAdCAM-1	Mucosal addressin cell-adhesion molecule-1
MDSC	Myeloid Derived Suppressor Cells
MHC	Major Histocompatibility Complex
MMC	Mitomycin C
MOA	Modes of Action
MOI	Multiplicity of Infection
MTS	3-(4,5-dimethylthiazol-2-yl)-5-(3-carboxymethoxyphenyl)-2-(4-sulfophenyl)-2H-tetrazolium
MTX	Mitoxantrone
NDV	Newcastle Disease Virus
NK	Natural Killer Cells
OV	Oncolytic Virus
PCR	Polymerase Chain Reaction
PD-1	Programmed Cell Death Protein 1
PDAC	Pancreatic Ductal adenocarcinoma
PAMPs	Pathogen Associated Molecular Patterns
PBS	Phosphate Buffered Saline
PD-L1	Programmed Cell Death Ligand 1
pfu	Plaque forming unit

PRR	Pattern Recognition Receptors
qPCR	Quantitative Polymerase Chain Reaction
RFP	Red Fluorescent Protein
RGD	Arginylglycylaspartic acid
rSAP	Recombinant Shrimp Alkaline Phosphatase
RT	Room temperature
Rx	Irradiation
SC	Subcutaneous
SCC	Squamous Cell Carcinoma
TAA	Tumour associated antigen
TCM	T-cell media
T_{CM}	Central memory T cell
T_{EFF}	Effector T cell
T_{EM}	Effector memory T cell
TGF-β	Transforming Growth Factor Beta
TSA	Tumour specific antigen
Th	T Helper cell
TK	Thymidine kinase
Tregs	Regulatory T cells
VICCV	Virus Infected Cancer Cell Vaccine
VLTF-1	Vaccinia late transcription factor 1
vp	Virus particle
VV	Vaccinia Virus
VVL15	Lister strain vaccinia virus with thymidine kinase gene-deletion
WR	Western Reserve strain vaccinia virus
WRDD	Western Reserve vaccinia virus with double gene deletion (TK and VGF)

Chapter one: Introduction

Despite advances in cancer treatment over the last few decades, cancer remains a major cause of morbidity and mortality in the UK and worldwide. More than 331,000 people a year are diagnosed with cancer in the UK with an estimated 14.1 million new cases a year worldwide. Mortality figures are 162,000 and 8.2 million a year in the UK and worldwide, respectively [2]. Despite significant progress in traditional cancer treatments of surgery, chemotherapy and radiotherapy, survival of patients, with pancreas, lung and head and neck cancers has not improved over the last few decades. In addition, these treatments are often associated with severe morbidity due to poor tumour selectivity. The search for the "Holy Grail" treatment that can target and kill cancer cells sparing normal tissues remains as relevant today as it has always been.

1.1 Oncolytic virotherapy

1.1.1 Oncolytic viruses

An oncolytic virus (OV) is a virus capable of killing cancer cells, which can be utilised as a cancer therapy. The first such use dates back to the late 19th century concurrently with the discovery of viruses. Scientists noticed a temporary regression of malignant disease in cancer patients during viral infections [3, 4]. These were often temporary regressions in leukaemia and lymphoma patients. Nevertheless, this observation led to early attempts to treat cancer with viruses with minimal clinical success. The second wave of virotherapy came in the 1960s with the advancement of tissue culture techniques and the improved understanding of virus biology. The persistent limited clinical success of that era led to the abandonment of virotherapy in the next decade. Only in the early nineties did virotherapy re-emerge with the advancement of

recombinant DNA technology allowing scientists to genetically modify viruses to improve efficacy and selectivity [5].

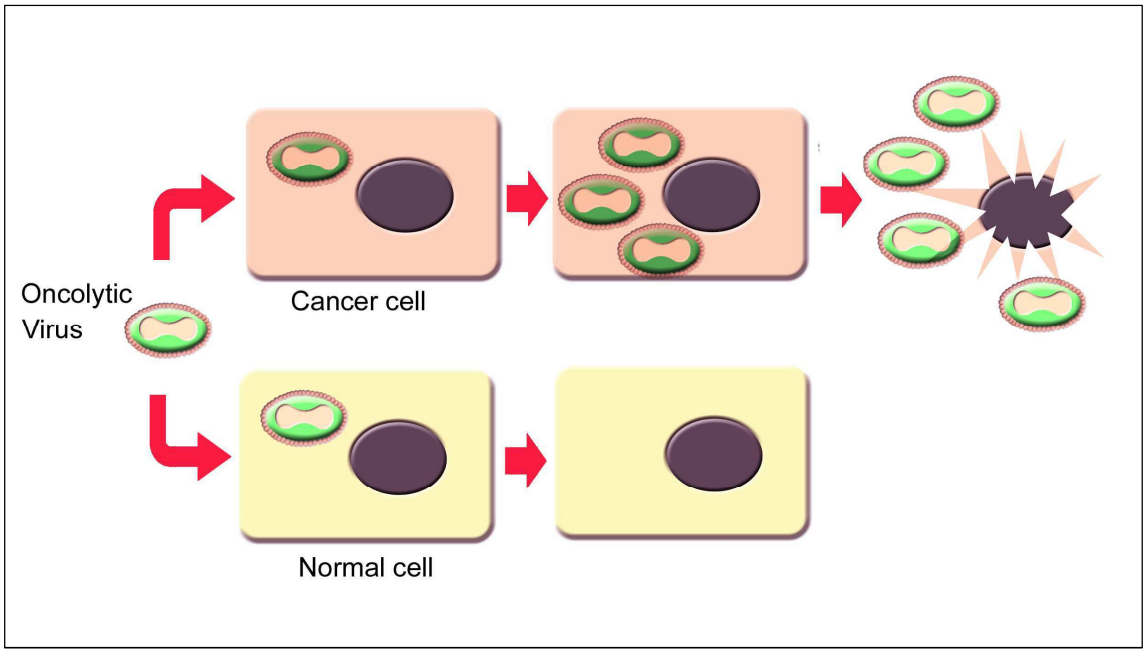

Fig 1.1 Tumour selectivity of oncolytic viruses.
Tumour-targeted oncolytic viruses can exploit defective cellular pathways in cancer cells (top). OVs can infect and replicate in cancer cells leading to cell lysis and release of viral particles. These in turn infect neighboring tumour cells and so forth. In normal cells (bottom) cellular defense mechanisms prevents viral replications

Oncolytic virotherapy is based on the ability of OVs to specifically target and replicate in tumour cells (Fig. 1.1). To facilitate such a process, the injected virus needs to reach tumour cells, infect them and start the lytic process. It needs to replicate within these cells producing more viral particles leading to tumour cell lysis, which releases viable virions capable of infecting neighbouring tumour cells. This process would continue until all tumour cells are lysed sparing normal cells. In reality this process would be short lived as the immune system will clear the virus limiting its clinical benefit. In fact, clinical trials have not shown that direct tumour lysis to be an important antitumour mechanism [3]. However the ability of the virus to alter the immune composition of the, ordinarily, immune-suppressive tumour microenvironment led to a new line of thinking

of the role of OVs (Fig. 1.2). Current evidence suggests that anti-tumour immunity, where the virus is acting as an oncotropic immunomodulator, is the key determinant of a successful oncolytic virotherapy [6-9]. This will form the basis of this study and will be discussed in detail later. In addition, OVs can target multiple cellular pathways [10-12] minimising the risk of tumour resistance and induce different modes of cell death [13-16]. Furthermore, OVs can function in synergy with conventional cancer treatments of chemoradiotherapy [17-20]. Finally, OVs as a treatment platform are amenable to adjustment and development following our ever-increasing understanding of cancer cells, the virus and host immune responses to both tumour and virus.

Tumour selectivity is the main feature of OVs. It is related to the ability of OVs to exploit the altered cellular pathways and deregulated metabolic activity to their advantage [6]. In fact, many of the hallmarks of cancer [21] make tumour cells susceptible to viral replication including immune escape, sustained cell proliferation and resistance to cell death [22]. OVs fall broadly into two categories: viruses that have natural preferential replication in tumour cells such as Newcastle disease virus, myxoma virus and reovirus; and viruses that are genetically engineered to be tumour selective such as vaccinia virus, measles virus and adenovirus [23, 24].

OVs can additionally be utilised as a vector system to deliver genetic material to cancer cells or the tumour microenvironment. They can be armed to express a variety of immunomodulatory proteins such as granulocyte-macrophage colony-stimulating factor (GM-CSF) [25, 26], interleukin-12 [27] and interleukin-10 [28]. These expressed cytokines can change the immune profile of the tumour microenvironment and enhance the anti-tumour response.

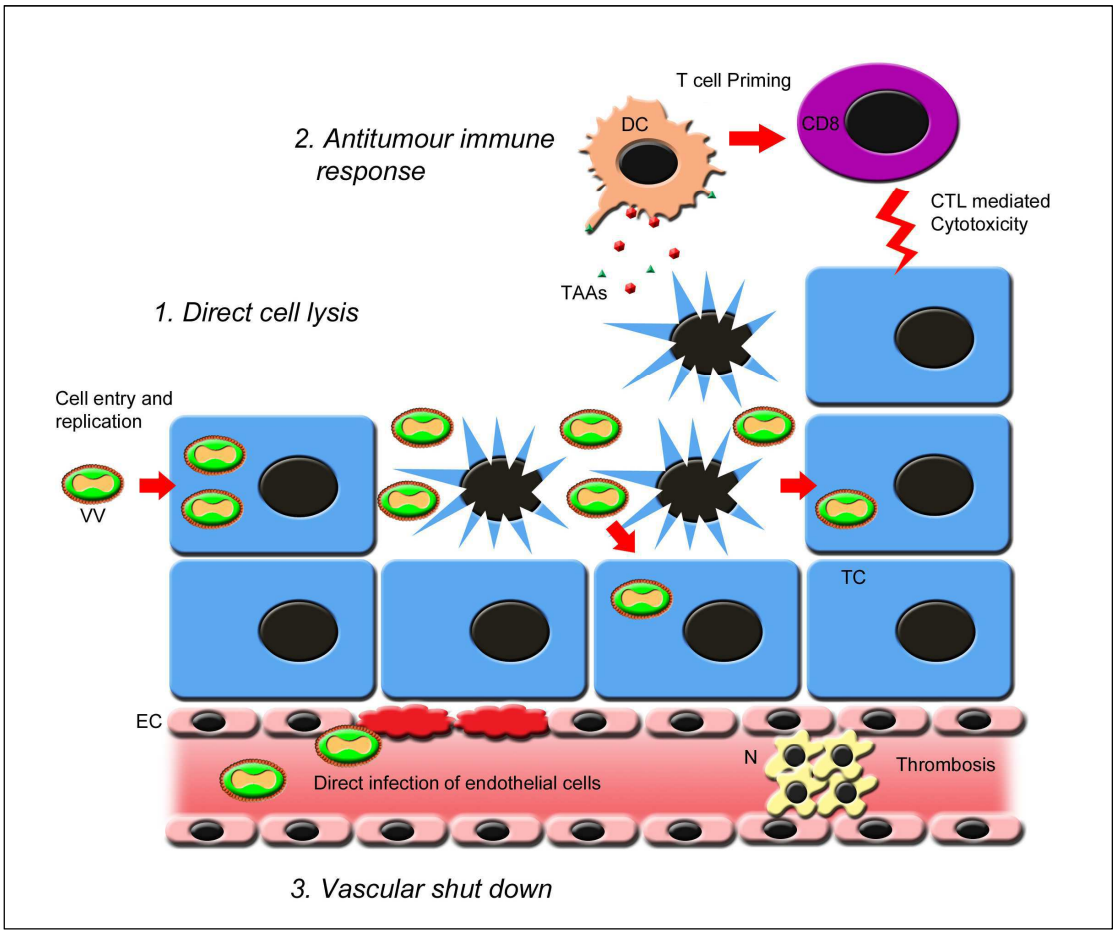

Fig 1.2 Multiple modes of action (MOA) of tumour-targeted oncolytic viruses.
OVs can kill cancer cells via a variety of mechanisms. First, they directly infect, replicate and lyse tumour cells sparing normal cells. Released virions can infect neighbouring tumour cells and so forth. Second, OVs can induce immunogenic cell death associated with the release of PAMPs and DAMPs. In addition viral infection results in the release of cytokine and chemokines deviating the immune response towards a cytotoxic profile. Dendritic cells can pick TAAs released from lysed tumour cells and prime CD8+ T cells to induce a tumour-specific immune response. Third, OV infection can result in vascular shutdown caused by direct viral infection of endothelial cells and thrombosis caused by cytokine-mediated neutrophil accumulation. Key: (TC) tumour cells, (DC) dendritic cells, (N) neutrophils, (CD8) Cytotoxic T cells, (EC) endothelial cells, (TAAs) tumour associated antigens and (VV) vaccinia virus.

1.1.2 Vaccinia virus

Vaccinia virus (VV) has played a prominent role in one of the greatest achievements in medical history: the eradication of smallpox. Since then, VV has been developed as a vector for vaccines against infectious diseases such HIV, influenza, malaria and tuberculosis, as well as in immunotherapies [29] and oncolytic therapies for cancer [30, 31].

1.1.3.1 Positive features of Vaccinia virus as an oncolytic virotherapy agent

Vaccinia virus is a member of the poxvirus family. It is a double stranded DNA virus approximately 192kbp in size, carrying approximately 200 genes [32] with the free ends connected via a hairpin loop [33]. It can stably accommodate up to 25kbp of cloned exogenous DNA [34]. Structurally it consists of a core region composed of viral DNA and various viral enzymes including RNA polymerase and polyA polymerase encased in a lipoprotein core membrane. The outer layer of the virus consists of double lipid membrane envelope [35, 36]. VV has two major forms of infectious virions; the intra cellular mature virions (IMV), as described above, which is released upon cell lysis and the extra cellular enveloped virion (EEV) released from the cells via cell membrane fusion. The latter has an additional lipid bilayer membrane wrapped around the IMV particle.

Vaccinia virus has many inherent characteristics that make it an ideal choice for oncolytic virotherapy. Unlike other OVs, VV does not have a specific surface receptor for cell entry allowing it to infect a wide range of cells unhindered by the lack of expression of that specific receptor. It depends on a number of membrane fusion pathways for cell entry which are not fully characterised [37, 38].

VV has a short life cycle of eight hours that take place in its entirety in the cytoplasm eliminating the risk of genome integration. Following viral core entry into the cell, packaged viral proteins are released into the cytoplasm. Within 20 minutes this core produces a set of early mRNAs encoding the required proteins for the cytoplasmic DNA replication [39]. This usually starts two hours after infection, at which time the host cell nucleic acid synthesis shuts down as all cellular resources are directed towards viral replication, and takes place in structures called viral factories or virosomes. DNA replication initiate the transcription of late genes encoding for the late proteins that are necessary for viral assembly and viral enzymes which are packaged within the viral particle cores [40-42]. VV independence from host mechanisms for mRNA transcription makes it less susceptible to biological changes of the host cell. Cell lyses takes place between 12-48 hours releasing packaged viral particles.

The existence of various antigenically-distinct forms of the mature virus allows it to evade host immune system. EEV form of the virus is encapsulated in a host-derived envelope, with incorporated viral proteins, that contains several host complement control proteins [43-45]. In addition, VV infected cells secretes Vaccinia compliment control protein (VCP) which binds an inactivate C4b and C3B inhibiting the classic and alternative complement activation pathways [46-48]. VV therefore can be disseminated relatively unharmed in the blood stream to reach distant tumours allowing systemic delivery of the virus [49], which is more suitable for the treatment of the advanced cancers. Recent clinical trial evidence has demonstrated the feasibility of intravenous injection for VV oncolytic therapy [50].

Hypoxia is a feature of many cancers that contributes to treatment resistance. In contrast to adenovirus [51], our group has found that hypoxic conditions did not affect replication, viral proteins production, cytotoxicity and transgene expression of the Lister

strain of vaccinia virus [52]. To the contrary, recent evidence from our group and others suggests that hypoxic condition can actually enhance the oncolytic effect of VV due the enhanced internalization of the virus. This is due to the hypoxic induction of vascular endothelial growth factor A (VEGF-A) expression [53]. In addition, VEGF signaling sensitises endothelial cells to vaccinia virus infection facilitating viral spread to tumour cells following IV viral delivery [54].

Finally, VV has a good safety track record following its use as a vaccine for over a century. Minor and less severe side effects include fever, rash and inadvertent inoculation. Moderate to severe side effects include eczema vaccinatum, generalized vaccinia, progressive vaccinia, and postvaccinial encephalitis [55]. Sides effects are rare with an incident of less than 1:10,000 and severe side effects in particular are extremely rare [56]. Genetically modified recombinant VV could be potentially safer due to their tumour selectivity. Recent clinical trial of JX-594 virus in hepatocellular carcinoma showed the treatment to be well tolerated with mainly flu-like symptoms in all patients and a single severe side effect [31].

1.1.3.2 Cancer selectivity and modes of action of vaccinia virus

Vaccinia virus has a natural tropism to cancer cells [57, 58]. The virus can utilise activated molecular pathways in tumour cells to aid its replication [59-61]. In fact, many of the hallmarks of cancer [21] make tumour cells susceptible to viral replication including immune escape, sustained cell proliferation and resisting cell death. In the case of vaccinia virus, the epidermal growth factor receptor (EGFR) family [62], potentially plays an important role in tumour selectivity. The viral smallpox growth factor (SPGF), an EGF-like growth factor carried by vaccinia virus, can activate host cellular pathways leading to increased viral replication [63]. In addition, Ras-GTP-activating protein S3H domain-binding protein (G3BP), over-expressed in most human

cancers [64], plays a role in VV replication by complementing the activity of the viral intermediate transcription factor-2 (VITF-2) [65].

Various techniques can be utilised to enhance tumour selectivity of VV. The virus depends for its replication in normal cells on a set of genes that prepare the cell resources for viral replication and block apoptotic pathways. Deleting these genes will limit the virus ability to replicate in normal cells. However, these pathways are often disrupted in cancer cells allowing the virus to replicate despite the defective genes. One such example is the disruption of the vaccinia thymidine kinase gene affecting the virus ability to synthesise deoxyribonucleotides [66, 67]. Normal cells have a much smaller reserve of deoxyribonucleotides, compared to tumour cells, limiting the ability of VV to replicate. Another example is the deletion of the B18R gene encoding the secreted IFN-binding protein that blocks IFN-α signaling [68]. In normal cells this gene deletion attenuates viral replication due to IFN antiviral effect while cancer cells remain permissive to VV replication as IFN signaling is often disrupted [69, 70]. In addition, altering the expression of crucial vaccinia viral gene by microRNA (miRNA) also enables tumour-specific viral replication, which is a potentially novel and versatile platform for engineering vaccinia viruses for cancer virotherapy [71].

Vaccinia virus kills cancer cells via a combination of necrosis and immunogenic apoptosis resulting in the release of damage associated molecular patterns (DAMPs) [72-75] and pathogen associated molecular patterns (PAMPs) [76-78] as well as the release of viral antigens into the tumour. This process leads to a strong inflammatory response that can overcome the immune suppression within the tumour microenvironment. In addition, tumour cell lysis releases tumour-associated antigens (TAAs) into this inflammatory environment. Dendritic cells can in turn pick up these exposed TAAs and cross-prime CD8+ T cells resulting in a potent anti-tumour adaptive

immune response. It has been demonstrated that an oncolytic VV (JX549) could induce tumour-specific immunity in human cancer patients [79] and pre-clinical study [80]. Therefore, oncolytic virotherapy with VV may be considered as a method of vaccination in situ, enabling the adaptive immune response to clear residual disease and provide long-term surveillance against relapse.

Finally, VV can utilise vascular shut down to kill non-infected tumour cells [25, 49, 81]. This is believed to be caused by accumulation of neutrophils in blood vessels, mediated by cytokines and chemokines, leading to intravascular thrombosis [81]. In addition, VV can infect and destroy tumour-associated endothelial cells further contributing to vascular collapse [69].

1.1.3.3. Strain selection and gene deletions

Selecting the "right" strain of VV could be of significant importance to the safety and efficacy of the oncolytic viral treatment. The non-vaccine strain Western Reserve (WR) VV is widely used in experimental preclinical trials. JX-963, a GM-CSF armed mutant of WR VV with deletion of both the Thymidine Kinase and the Viral Growth Factor gene (vvDD-GM-CSF), has been reported as the most potent tumour-targeted oncolytic VV [60]. Other strains, such as the European vaccine Lister strain, are largely untested. Our group recently evaluated the anti-tumour potency and bio-distribution of different vaccinia virus strains using *in vitro* and *in vivo* models of cancer including pancreatic, head and neck and colorectal cancer models. The Lister strain virus with a Thymidine Kinase gene deletion (VVL15) demonstrated superior anti-tumour potency and cancer-selective replication *in vitro* and *in vivo*, compared to WRDD, especially in human cancer cell lines and immune-competent hosts [82]. Further investigation of functional mechanisms revealed that Lister VVΔTK presented favorable viral bio-distribution within the tumours, with lower levels of pro-inflammatory cytokines compared to

WRDD, suggesting that Lister strain may induce a diminished host inflammatory response [82]. This comprehensive study indicates that the Lister strain vaccinia virus with TK deletion, used in my work, is a particularly promising vaccinia virus strain for the development of the next generation of tumour-targeted oncolytic therapeutics.

1.1.3 Adenovirus

Adenovirus (AdV) is the most commonly used viral vector for cancer gene therapy. It is a member of the Adenoviridae family. The name is derived from its initial isolation from adenoid tissue in 1953 [83]. They have broad range of vertebrate hosts. There are 59 serotypes of human adenovirus divided into seven subgroups, A to G according to their clinical manifestations [84, 85]. Ad5, the adenovirus used in this study, belongs to group C.

1.1.2.1 Positive features of adenovirus as an oncolytic virotherapy agent

Adenovirus is a non-enveloped, icosahedral-shaped, double stranded DNA virus. The icosahedral capsid has 20 faces composed of hexon proteins and 12 vertices of penton proteins. A fibre protein ending with a globular knob domain extends outward from each of the penton bases. The latter is responsible for attachment to the host cell receptors [86, 87].

Adenovirus has many favourable characteristics making it an attractive oncolytic virus. The genomic structure of adenovirus is well characterised and their modes of replication, infection and pathogenesis is known. Its linear DNA core is approximately 35-40kbp in size encoding for approximately 35 proteins. These genes are expressed in two phases; early which occurs in the first few hours after infection prior to DNA replication, and late which occurs afterwards. The early genes are regulatory genes that allow the virus to divert host cell resources and initiate viral DNA replication. They

are arranged into five transcription units; E1A, E1B, E2A, E3A and E4A. Late genes encode for viral structural proteins are arranged into; L1, L2, L3, L4, L5 and ADP [88, 89]. The latter is a gene encoding for Adenovirus Death Protein which mediates cell lysis to release assembled viral particles [90].

Adenoviruses are non-integrating DNA viruses with extensively studied life cycle. AdV attaches to the host cells through binding of the knob domain of the fibre protein to the cell receptor. The most studied adenovirus receptor is the coxsackievirus and adenovirus receptor (CAR) [91], however there are a number of other receptors including CD46 [92], heparan sulfate glycosaminoglycans [93], CD80 and CD86 [94] to name a few. This is followed by attachment between an exposed arginylglycylaspartic acid (RGD) motifs on the penton base to cell surface integrin molecule. Integrins known to facilitate adenovirus attachment and entry include $\alpha_v\beta_1$ [95], $\alpha_v\beta_3$ and $\alpha_v\beta_5$ [96]. This attachment induces cellular signals, including activation of PI3 kinase, which leads to actin cytoskeleton rearrangement and initiation of viral internalistion [97]. The virus then enters the cell in a clathrin-coated pit that forms into an endosome. Acidification leads to partial disassembly of the capsid and virion escapes into the cytoplasm [98]. The capsid is then transported to the nucleus where its DNA is injected via the nucleic membrane pores where early gene transcription starts utilising cellular enzymes. Early mRNA is then transported to the cytoplasm for translation. DNA replication starts after the late phase. In addition viral structural proteins are produced at high levels during the late phase and translocated to the nucleus to be assembled into viral particles.

Adenoviruses can be safely used as vaccine vector and oncolytic virotherapy agents with limited morbidity. In fact millions of US army personnel have received live AdV vaccination of serotypes 4 and 7 with excellent safety track record [99]. They only

cause mild self-limiting diseases in human mainly in the form of respiratory tract infection. They can however lead to severe infections, or even mortality, in immunodeficient patients [100]. Further genetic modifications *(section 1.1.2.2)* can enhance AdV safety. In fact, such modified AdVs (serotype 5) have been used in various clinical trials with excellent safety track record [101, 102].

Finally, AdV is amenable to genetic modifications, deletion and transgene cloning. They can be produced to Good Manufacturing Practice (GMP) with high-level titration and purity.

1.1.2.2 Cancer selectivity and gene deletions of adenovirus

Earliest anticancer clinical trials in the fifties used non-attenuated wild type adenovirus to treat a variety of cancers. Various AdV serotypes delivered systematically or intratumourally resulted in initial tumour necrosis but failed to achieve significant sustained therapeutic results [103-105], however they demonstrated the safety of AdV-based therapies and highlighted the need for better tumour-targeted viruses.

Wild-type AdV has wide tropism and can infect proliferating and non-proliferating cells. This wide tropism could be a useful tool for gene therapy applications in somatic diseases and cancer; however it can lead to toxicity when administered in high doses [106, 107]. Replication-deficient AdV vectors were developed in the early nineties to overcome this potential off-target effect. This can be achieved by deleting the E1A or E2A gene, both essential genes for viral replication, and replacing them with a promoter from a different organism, such as the cytomegalovirus (CMV) promoter, to drive the expression of the therapeutic gene. Advexin and Gendicine are first generation replication-defective adenovirus vectors with double gene deletions of E1A and E3B. Both viruses have been armed with p53 gene driven by CMV promoter and

Rouse Sarcoma Virus promoter respectively [108, 109]. The rationale is that expression of the p53 gene in tumour cells will lead to cell cycle arrest. These two viruses have been used extensively in clinical trials over the years with excellent safety but modest clinical outcome when used as monotherapeutic agents [109-112]. Numerous other replication-defective AdV with various therapeutic genes have entered clinical trials [113]. These replication defective vectors can be made tumour selective by using tissue specific promotor to drive transgene expression selectively in tumour cells [114, 115].

The focus of scientific research then moved to tumour-targeted replication-competent AdV. The shift was encouraged by safety of replication-defective AdV in clinical trials and better understanding of the genomic structure and life cycle of adenovirus and its relation to the host cell cycles. Various approaches could be adopted to achieve tumour selectivity. Using a tumour or tissue-specific promoters, such as PSA promoter [116], allows AdV to selectively replicate and lyse tumour cells expressing that specific gene.

However the most common strategy, as with vaccinia virus, is viral gene deletions. *dl1520* (also known as Onyx-015) is an E1B55K and E3B gene-deleted AdV designed to selectively replicate and lyse cancer cells carrying the mutant p53 gene but causes limited damage to normal tissue [117-119]. p53 is a pro-apoptotic protein that is activated by viral infection leading to further activation of apoptotic genes leading to cell apoptosis. E1B55k protein is a p53 inhibitor allowing wild-type adenovirus to continue replication in normal cells and avoid apoptosis. Deleting this protein will render the adenovirus to be replication-dependent on the presence of a mutant p53 gene as is the case in many cancer cells [120]. However, later studies showed that *dl1520* is also cytopathic in p53-intact tumour cells [121]. It is now believed that *dl1520* tumour

selectivity is mainly due to late viral gene mRNA export [122, 123]. *dl1520* has been used in many clinical trials for various types of cancer with limited clinical success but excellent safety record [102, 124-132]. Such limited efficacy was reported to be due to attenuated replication and reduced viral progeny production limiting its anti-tumoural effect. The E1B55K gene was found to be essential to viral life cycle through its interaction with E4orf1 protein [133]. In addition, deletion of gene products encoded by the E3B region could further weaken its oncolytic effect due to increased macrophage infiltration and higher TNF and IFN-γ secretion leading to rapid viral clearance [134]. Our group has found recently that E3B can supress transcription factor STAT1 in monocytes leading to inhibition of chemokine expression [135]. *dl1520*, and other E3B-delted viruses, lack this inhibitory function leading to high chemokine expression and macrophage infiltration. Despite its shortcoming, H101 (an adenovirus similar to *dl1520*) remains the only licensed oncolytic virus for treatment of Head and Neck cancers in China [136].

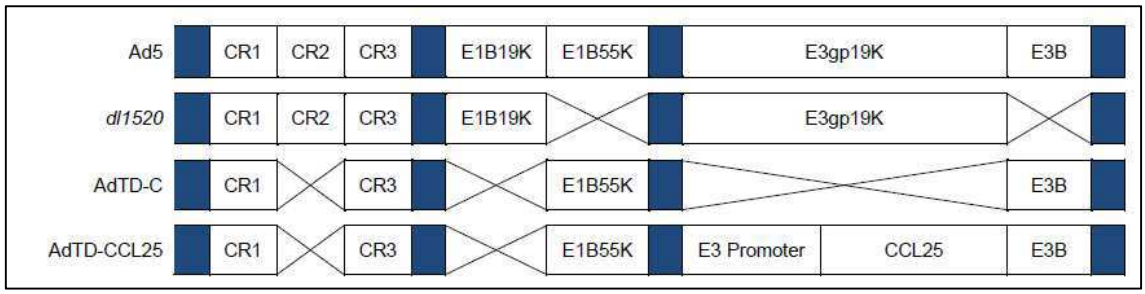

Fig 1.3 A schematic diagram of viruses used in this study in comparison with wild-type adenovirus (Ad5).
dl1520 virus contains a deletion in the E1b55K and E3B regions. Our triple deleted virus (Ad-TD-C) contains three deletions in the E1A conserved region 2, E1B19K and E3gp19K. CCL25 gene was inserted in the latter region to create the Ad-TD-CCL25 virus.

In order to improve on the limited clinical success of *dl1520* and to create a potent yet safe oncolytic virus, our group and others have targeted other AdV genes for deletions (Fig 1.3). E1A conserved region 2 (E1ACR2) viral protein binds to retinoblastoma

protein (pRB) releasing the E2F transcription factor to drive the cell cycle from G1 to S phase. Deleting this region will reduce viral replication in normal quiescent cells while maintaining its ability to replicate in cancer cells with altered cell cycle control. One such virus, *dl922-947*, was shown to be more potent when compared to *dl1520* [137].

E1B19K viral protein inhibits both extrinsic and intrinsic apoptosis induction pathways. It acts as a homologue for Bcl2 capable of binding to Bax and Bak preventing the downstream process of apoptosis, allowing the cell to survive while viral replication takes place [138]. In addition, E1B19K can inhibit Fas-mediated extrinsic apoptosis pathway by inhibiting FADD oligomerisation [139]. Deleting this gene will therefore reduce the ability of AdV to survive and replicate in normal cells. On the other hand these pathways are often inhibited in cancer cells which allows the virus to replicate [140]. In addition, deleting this antiapoptotic gene will sensitise tumour cells to DNA-damaging cytotoxic drugs [141].

E3gp19K is an endoplasmic reticulum (ER) membrane glycoprotein. It can bind to major histocompatibility complex (MHC) class I and inhibits its transport to cell surface allowing the virus to evade cytotoxic T cells (CTL) recognition [142]. In addition, it can inhibit recognition by natural killer (NK) by intracellular sequestration of NK ligands MICA and MICB [143]. Deleting the E3gp19K gene can enhance CTL recognition and killing of infected tumour cells enhancing the antitumour efficacy of the virus [134]. In addition cloning transgenes at this site, as the case with the adenovirus mutant cloned for this study, allows high level expression under the control of the endogenous E3 promoter [144].

In this study, we will use our latest generation of adenovirus with triple deletions of E1A conserved region 2, E1B19K and E3gp19K genes (AdTD), the resultant virus is

replication-competent selectively in cancer cells. It promotes apoptosis of tumour cells and sensitise them to chemotherapy cytotoxic drugs and it recruits the immune system to aid tumour clearance.

1.2. Cancer immunity

1.2.1 Cancer immune escape

The process of “immunoediting”, as described by Dunn and colleagues suggests a dual capacity of the immune system to both promote and suppress tumour growth [145]. At early stages of tumour development the immune system can eliminate the most immunogenic tumour cells. The process reaches equilibrium where tumour cells with less immunogenic phenotypes can continue to divide until it reaches a stage where it can escape immune surveillance and develop into overt cancer [146].

Various mechanisms contribute to tumour immune escape. Tumour cells can down regulate expression of tumour antigen via down regulation of MHC I [147-149], or down regulate the transporter for antigen presentation proteins (TAP) [150] reducing expression of tumour associated antigen on the cell surface, which in turn reduce the ability of CTLs to recognise tumour cells. In addition, tumour cells often lack co-stimulatory molecules leading to anergy of T cells [151].

Regulatory T cells (Tregs), and tumour-derived Tregs in particular, play major role in immune suppression [152, 153]. These cells are recruited into the tumour microenvironment via tumour-mediated chemokine production [154, 155]. In addition, transforming growth factor beta (TGF-β) can aid the conversion of T helper cells to Tregs in situ [156]. Myeloid derived suppressor cells (MSDCs) can suppress CTL mediated antitumour immune response and play a role in tumour initiation, angiogenesis and metastasis [157, 158]. Furthermore, immature dendritic cells (DCs)

present in the tumour microenvironment can contribute to CTL suppression. Gangliosides expressed on some tumour cells can alter the phenotype of DCs to express lower levels of CD80, CD86 and CD40 [159].

Cancer cells and other non-cancerous cells in the tumour microenvironment can produce a variety of immuno-suppressive cytokines. TGF-β is believed to play a major role in this process [160-162]. In addition TGF-β combined with IL-10 expression can shift T helper cell profile from Th1 to Th2 leading to reduced CTL activation [162]. Various mediators such as vascular endothelial growth factor (VEGF), IL-10, TGF-β can inhibit differentiation of progenitors to DCs and prevent the maturation of DCs resulting in immune tolerance as antigens are presented to T cells without the appropriate co-stimulatory factors [163, 164].

Immune checkpoints have emerged in recent years as an essential mechanism to regulate the function of the immune system and maintain self-tolerance. Cytotoxic T lymphocyte-associated antigen 4 (CTLA-4) was the first immune check point to be discovered. In normal tissue CTLA-4 is progressively expressed on the surface of CTLs following their TCR binding to its cognate antigen. CTLA-4 counteracts the activity of T cell co-stimulatory receptor CD28 by competitively binding to its ligands CD80 and CD86 (also known as B7.1 and B7.2 respectively) [165, 166]. In normal tissue CTLA-4 down-modulates immune response to chronic antigen stimulation preventing autoimmunity, while in cancer it promotes tolerance and immune escape [167, 168]. Programmed cell death protein 1 (PD1) is expressed on the surface of T cells. Its main function is to limit the activity of T cells in peripheral tissues during inflammatory response [169-171]. Tumour cells can express immune inhibitory molecules such as programmed cell death ligand 1 (PD-L1) which can negatively

regulate T cell responses [172, 173]. This expression can be upregulated as a response to an antitumour immune response [174].

Finally, tumour cells have been shown to induce apoptosis in T cells leading to peripheral immune tolerance [175, 176].

1.2.2 The "Danger" model in immunity

The original "Self *vs*. Non-Self" model of immunity was first suggested by Burnet [177]. It proposes that the immune system distinguishes between tolerated self and attacked non-self. This theory was further reinforced with the work of Medawar *et al* on clonal selection [178, 179]. Despite changes to this model over the years and the addition of the helper cell [180] and the second costimulatory signal generated by antigen-presenting cells [181] the model still failed to explain a number of immunological phenomena mainly the failure of antigen-presenting cells (APC) to present self-antigen despite being non-antigen-specific cells. To address this point an "Infectious non-self" model was proposed [182] where APCs have the capacity to distinguish and be activated by non-self evolutionary-conserved pathogen associated molecular patterns (PAMPs) via their pattern recognition receptors (PRR). However, this model fell short when it came to anti-tumour immunity, graft rejection and non-cytopathic viral infections.

Matzinger proposed the "danger" model of immunity where the main function of the immune system is to recognise and protect against danger [183]. This model suggests that APCs not only recognise PAMPs but also can recognise, and be activated as a result, of stimulation from damaged distressed cells. This damage could be the result of infection, trauma, oncogenic transformation, toxins and so on. These distressed cells would release or express what was collectively termed damage associated molecular

patterns (DAMPs). These were later discovered to include, among others, lipoproteins, uric acid, serum amyloid A protein, lipopolysaccharides, tumour necrosis factor-4, adenosine triphosphate (ATP) and so forth [184].

1.2.3 Oncolytic viruses and anti-tumour immunity

Oncolytic viruses have a number of advantages as cancer immunotherapy agents. They kill cancer cells through a variety of immunogenic and non-immunogenic mechanisms including apoptosis, necrosis, autophagy and pyroptosis [185, 186]. The most dominant form of cell death varies depending on the individual OV. This oncolytic process provides the necessary "danger signal" to dendritic cells to initiate a potent anti-tumour immune response. These signals include DAMP from dying tumour and stroma cells and PAMP from the OV itself [182, 183, 187]. In turn, activated DCs can take up released tumour associated antigens (TAA) and induce an adaptive immune response that can target the tumour [22].

Table 1.1 List of PAMPS and DAMPS associated with Adenovirus and Vaccina Virus

	PAMPs	**DAMPs**
Adenovirus	Adenovirus DNA [188-190]	ATP [16] Ectopic Calreticulin [16] HGMB1 [16] Uric Acid [191]
Vaccinia Virus	Unknown ligand of TLR2 [76-78] Viral RNA [192]	ATP [74] HGMB1 [72, 73, 75]

Immunogenic cell death (ICD) is a type of cell death, induced by certain chemotherapeutic agents, characterised by the expression of calreticulin on the

surface of dying tumour cells with the active release of DAMPs such as ATP and high-mobility group box 1 (HMGB1) [193, 194]. However, other types of cell death such as necrosis, pyroptosis and autophagy share many of the immunogenic features of ICD including the release of DAMPs and pro-inflammatory cytokines from dying cells [8, 195, 196]. OVs including AdV [16, 197], herpes simplex virus (HSV) [198], measles [15] and pox viruses [74] can kill tumour cells via a variety of mechanisms leading to the induction of ICD features resulting in a potent anti-tumour immunity.

Autophagy is another important mechanism of OV-induced anti-tumour immunity. It mediates the sequestration, degradation and recycling of cellular components and intra-cellular pathogens. It plays an important role in the activation of both innate and adaptive immunity [199, 200]. OV such as AdV [201, 202], HSV [203], and Newcastle Disease virus (NDV) [204] can induce autophagy in tumour cells. Autophagy has been shown to stimulate antigen processing and cross-presentation by DC cells to naïve T cells [205, 206] resulting in the cross-priming of TAAs and viral antigen to generate tumour and virus specific CD8+ T cells [207-209].

1.3 Cancer vaccination

1.3.1 The concept of therapeutic cancer vaccination

Prophylactic vaccination in the field of infectious disease has been one of modern medicine biggest success stories resulting in the eradication of smallpox and the near-eradication of polio. It was a major contributor to the increase in life expectancy over the last two centuries [210]. This success has extended to cancers of an infectious pathogen origin. Vaccines against human papilloma virus [211, 212] and hepatitis B virus [213, 214], the leading causes of cervical cancer and hepatocellular carcinoma respectively, are now in routine medical practice.

Following in the footsteps of such a success, a huge effort and interest in the medical and scientific community has been directed towards developing a therapeutic cancer vaccine. The prospect of harnessing the power of the immune system to fight cancer is a highly attractive approach. It aims to generate an anti-tumour immune response that can be effective, safe and long-lasting. Such a treatment can clear any residual disease or microscopic metastasis that remains after conventional treatments. It can even provide an immune memory that can protect against tumour recurrence or a second primary.

An effective cancer vaccine can, in theory, be achieved if it can combine the “right” antigen, the “right” adjuvant and the “right” immune response [215].

Tumour antigens that can be recognised by the immune system were first discovered in human melanoma [216-218]. Normal proteins are ignored by the immune system due to self-tolerance. Tumour protein that can be recognised by the immune system can be generally categorised into three categories: cancer testis antigens (CTAs), tumour specific antigens (TSAs) and tumour associated antigens (TTA). CTAs are proteins that are expressed in testis and foetal ovaries but can also be expressed by tumour cells such as oncofoetal proteins [219-221]. TSAs are antigens not normally encoded in the normal host genome. They represent proteins of oncogenic viruses or arise from somatic mutations form of normal proteins (neoantigens) [222-224]. TTAs are normal proteins that are expressed in tumours in a quantitatively (abnormally high expression levels) or qualitatively (post-transcriptional modifications) different form [225-227].

However, tumour antigens by their very nature are weakly immunogenic. In addition, they represent a small minority of the total molecules released from the dying vaccine

cells, while the vast majority are non-immunogenic normal cellular components further dampening the immune response [228]. To overcome these factors, and other immune escape mechanisms discussed above, the immune system requires an adjuvant molecule that can activate APCs leading to T cell-mediated immune response as discussed previously.

1.3.2 Cancer vaccine approaches

Various different approaches to cancer vaccination have been trialled in the last few decades. These include peptides, naked DNA, *ex vivo* antigen presenting cells, viral vectors and whole cell vaccines.

TAA peptide epitopes that contain the specific major histocompatibility complex (MHC)-restricted amino acid sequence can be used as a cancer vaccine. Following injection they can be picked up by host APCs and cross-presented to T cells for the generation of an immune response. This process will often require an immune adjuvant molecule that can be injected simultaneously to stimulate APCs [229, 230]. This approach has a number of advantages that include safety, ease of production and the ability to generate high levels of T cell response [231, 232]. However they have a number of limitations including high level degradation *in-vivo*, low immunogenicity due to poor MHC affinity and the restriction of a certain peptide to a specific HLA type limiting its applicability across patients [230].

Naked DNA vaccines are used to deliver a gene encoding the specific peptide of the relevant TAA in an expression vector. This can be injected directly subcutaneously (SC) or intra-muscularly (IM) where it can transfect host cells and express the protein of interest, which in turn can be picked by APC and presented to T cells. Naked DNA vaccines have a number of advantages including low cost, ease of production, safety

and the possibility to co-express immunostimulatory molecules [233]. While naked DNA vaccines have shown a great potential to generate immune responses against exogenous pathogen-derived antigens [234, 235], while they have low immunogenicity when expressing self-antigens due to central and peripheral immune tolerance limiting their clinical applications [236].

Dendritic cell vaccines exploit the ability of these cells to capture released TAAs and present them to T cells. *Ex vivo* DCs generated from haematopoietic progenitor cells can be loaded with TAA peptides or whole proteins then re-injected in the patient to generate an antigen specific immune response [237, 238]. Other approaches have been utilised to generate antigen-specific DCs include transfection with tumour DNA, transduction with viral vectors containing the gene of interest, pulsing DC with dying tumour cells or cell lysate and fusing DCs with tumour cells [215, 239]. These are not without their challenges. It requires the selection of the correct DC population capable of activating the right subset of T cells. In addition DC cells need to undergo a maturation process to enhance their T cell-activation properties [215]. Although DC vaccination has been shown to induce an antigen-specific response [240, 241] it has yet to be translated into a successful vaccine in day to day medical practice [239].

Whole cancer cell vaccine has an advantage over antigen-specific vaccines in that it can target multiple or even undefined antigens simultaneously. This approach allows the immune system to select the most immunogenic antigen to target. However when whole cells are used as vaccine they release, in addition to tumour-specific cell-surface protein, a proportionately vast amount of intra cellular proteins and non-specific molecules [242] potentially dampening the immune response [228]. To overcome weak immunogenicity, tumour cells can be gene-modified to express an immunostimulatory

molecules such as GM-CSF [243] or a combination of cytokine and co-stimulatory molecule such as B7.1 (CD80) [244, 245].

Another approach (adopted in this study) to enhance the immunogenicity of a whole cell vaccine is the addition of a pathogen or a pathogen-derived product to act as an immune adjuvant and provide the necessary “danger signal” to stimulate APCs. This will be discussed in more detail in the following section.

1.3.3 Pathogen-based cancer vaccines, what has been achieved to date?

The idea of using pathogens to treat cancer goes back to the late 1800s when William Coley injected a mixture of various dead bacteria into his patients’ tumours leading to tumour regression [246, 247].

The tuberculosis vaccine, Bacillus Calmette-Guerin (BCG), was the first successful pathogen-based immunotherapeutic agent to enter routine clinical practice. Early clinical trials in the 1970s using irradiated non-modified allogeneic melanoma cells mixed with BCG showed some encouraging results [248, 249]. However, two phase III trials using the same strategy showed no significant benefit to patients and was subsequently discontinued. Other phase III trials targeting renal cell carcinoma and colorectal cancer showed promising results [250-252]. However, a subsequent large multi-centre trial targeting colorectal cancer failed to show significant difference between the treatment groups [253]. The inconsistent results, according to the author, of this trial could be related to the variability of the quality of vaccine produced locally at various trial centres and the failure to develop delayed type hypersensitivity (DHT) to tumour cells. Encouragingly, survival analysis showed a correlation between survival and DHT reactivity.

The discovery of hypomethylated CpG sequence from bacterial DNA as the immunogenic component of BCG [254, 255] led to its use in clinical trials. PF-3512676 (CpG 7909, a Toll-like receptor 9 agonist) has been used as an adjuvant to autologous cell vaccine in renal cell carcinoma in combination with IFN-α and GM-CSF and led to a reported 20% clinical response. In keeping with BCG trials, clinical response correlated to DHT reactivity [256].

Melacine is another whole cell vaccine that entered clinical trials and was subsequently licensed for clinical use in some countries. The vaccine is a lysate of two melanoma cell lines given with DETOX adjuvant (altered mycobacterium cell wall skeleton and monophosphorilyl lipid A). An early phase II trial confirmed the safety of the vaccine and showed a 10% response rate. However, phase III trial comparing Melacine to chemotherapy showed no significant difference between the two groups however quality of life was strongly in favour of Melacine [257, 258].

Newcastle disease virus is an enveloped avian RNA paramyxovirus. It has been used as an immune adjuvant, where tumour cells are pre-infected with the virus then irradiated before injection subcutaneously as a vaccine. Animal trials showed 50% protection from metastasis in a lymphoma model [259]. This vaccine model was used in phase I and II clinical trials in breast, colorectal, renal cell carcinoma leading to an increased survival rate between 24 – 36% [260]. A small phase II/III trial on melanoma showed no statistical difference in survival [261]. A phase III trial in patients with colorectal cancer showed no overall survival improvement however subgroup analysis showed an improved disease free survival and metastasis free survival in patients with colon cancer but not rectal disease [262]. A much larger clinical trial involving 592 colorectal cancer patients showed an average survival of 5.13 years in the vaccination plus surgery group compared to 4.46 in the surgery alone group ($p<0.01$) [263].

1.4 Immunotherapy in head and neck cancers

1.4.1 Introduction to head and neck cancer

Head and neck squamous cell carcinoma (HNSCC) is an aggressive cancer with severe impact on the quality of life of patients and significant morbidity and mortality rates. It is the sixth most common form of cancer affecting more than 50,000 in the United States and half a million people worldwide [264, 265]. HNSCC is a set of malignancies arising from the epithelium of the upper aerodigestive tract including oropharynx, nasopharynx, oral cavity, nasal cavity, sinuses and larynx. In the United Kingdom oral cavity tumours affects 6,800 people every year with a 2,100 deaths in 2012. Incidence levels and mortality rates have increased by approximately 33% and 10% respectively in the last decade [266]. While laryngeal SCC affected 2,360 people with 78 deaths in 2012 [267]. Male-to-female ratio of HNSCC incidence could be as high as 2:1, however this ratio is declining due to increased incidence in women due to higher use of tobacco [267, 268].

HNSCC incidence and mortality are higher in disadvantaged population groups [269]. Tobacco and alcohol use remains the main risk factor for the development of these cancers, however oncogenic viruses could play a major role in tumour development such as Epstien-Bar virus in nasopharyngeal carcinoma and human papilloma virus in oral or oropharyngeal cancers. In fact, developed countries have seen an epidemic of oropharyngeal cancers due to HPV infection possibly contracted during sexual activity [265].

Surgery, radiation and chemotherapy remain the mainstay treatments for HNSCC. However, changes to their delivery timing and combinational approach have led to improved clinical outcome especially in advanced disease. In such cases all three

modalities should be used with chemotherapy delivered as a combination chemoradiotherapy. The latter has been shown to be more beneficial compared to radiation alone. Induction chemotherapy could shrink primary tumour prior to surgical excision. It has been shown to increase local control and reduce metastasis with an overall survival increase of about 5% [270, 271]. Radiotherapy treatment has witnessed similar advancement with the introduction of hyper-fractionated radiotherapy, accelerated radiotherapy and intensity modified radiotherapy [270].

Despite the advances in traditional treatments, research in new treatment modalities is required to improve the lives of our patients. Survival rates of HNSCC patients has not improved over the last few decades [272]. In addition these treatments continue to have high morbidity rate and significant impact on quality of life. Surgery is often invasive with high complication rate. Major head and neck surgery is associated with temporary or permanent loss of voice, taste and swallowing functions. In addition, it has a significant aesthetic, social and psychological impact on patients [273]. Similarly chemoradiotherapy has a high morbidity and complications rates and significant impact on quality of life [274, 275]. Furthermore, although the advances in traditional treatments has improved the rate of locoregional control it has made little impact on metastatic disease [276].

1.4.2 HNSCC and the immune system

HNSCC is an immunosuppressive disease. These tumours can induce deficiency in quantity [277] and quality of T cells [278, 279] and anergy in NK cells [280, 281]. They express a tumour-permissive cytokine profile leading to a proinflammatory immune response and increased angiogenesis [282-285]. In addition, these tumours often show defective antigen processing and presentation further contributing to their immune escape [286, 287]. On the contrary, developing an effective host immune response

correlates with a better outcome in HNSCC. Immunosuppressed patients have a higher risk developing HNSCC with worse clinical outcome [288, 289]. Higher levels of tumour-infiltrating lymphocytes (TIL) seem to be associated with better outcome in HPV positive oropharyngeal cancer patients [290, 291]. In oral squamous cell carcinoma the density of CD8+ TILs correlates with tumour size, clinical stage and metastasis [292]. Higher levels of CD8+ T cells and CD20+ B cells in metastatic lymph nodes has been reported to correlate with favourable outcome in pharyngeal cancers [293].

As previously discussed, immune check points plays a major role of tumour development and evasion of the immune system. PD-L1/PD-1 interaction in particular seems to play an important role in HNSCC. PD-L1 is expressed in 66% of these tumours [294]. Premalignant lesion in the head and neck are reported to express high levels of PD-L1 [295, 296] which could be a target area for immunotherapy. The role of PD-L1 is most studied in HPV associated oropharyngeal carcinoma where the increased expression of PD-L1 due to chronic viral infection can contribute to T cell dysfunction [297]. Similarly, Tobacco and alcohol related HNSCC shows increased expression of PD-L1 [298]. And although PD-L1 expression doesn't correlate with overall survival [292, 299] it appears to correlate with distant metastasis [299].

The success of immunotherapy in any cancer depends of the expression of tumour associated antigen that are either uniquely expressed by tumour cells or expressed in increased levels compared to normal cells and the ability of the immune system to detect these antigens. HNSCC can express a variety of TAAs with clinical importance such as MUC-1, RAGE and CAGE tumour antigens and the cancer-testis antigen (NY-ESO-1) [300, 301]. Patients with advanced disease can express higher serum levels of MUC-1 and anti MUC-1 antibodies [302]. Antibodies to p53 have also been reported to

be expressed in higher levels in HNSCC undergoing surgical treatment which correlated with the presence of distal metastasis [303]. In addition to humoral immunity, CD4+ and CD8+ T cells isolated from HNSCC patients can be activated with synthetic MUC-1 protein fragments [304].

1.4.3 Current Immunotherapy approaches to HNSCC

Immunotherapy in HNSCC has been an area of great interest in the last decade. While prophylactic vaccines targeting EBV or HPV viruses carry a great potential they are beyond the scope of this study. Therapeutic immunotherapy approaches in HNSCC aim to stimulate a generalised immune response, target cell surface receptors using monoclonal antibodies (mAb), reverse HNSCC-induced immunosuppression, or generate an antitumour immune response via vaccination.

Cytokines can be powerful stimulators of the immune system. Earlier studies of peri-tumour and peri-lymphatic administration IL-2 in HNSCC can lead to increased levels of NK cells and TILs [305, 306] with evidence of improved survival in certain patient groups [307]. A phase III clinical trial (NCT00002702) aiming to study the effect of IL-2 when administered in conjunction with surgery and radiotherapy is currently in progress. IRX-2 is a biological product that contains cell-derived multiple cytokines including IL-1, IL-2, IL-6, IL-8, TNF-α, IFN-γ and GM-CSF [308]. A phase II trial (NCT00210470) showed promising results including increased lymphocytes infiltration and minimal toxicity. Two year survival and disease free survival were increased compared to matched control group [309, 310]. A phase III trial is currently being planned according to the manufacturing company website.

EGFR is expressed by 90% of HNSCC and is associated with radioresistance, locoregional recurrence and inferior survival rates [311, 312]. It is involved in most

aspects of HNSCC tumourigenesis. Cetuximab is a chimeric mAb which targets the extra cellular domain of EGFR. It was the first FDA approved molecularly targeted agent for the management of HNSCC. Cetuximab main action mechanism is interference with the binding of natural ligands such as EGF, disrupting its signalling pathway [313]. In addition, cetuximab can activate the antibody-binding receptor FcγR IIIa on NK cells leading to antibody-dependant cellular cytotoxicity (ADCC). These activated NK cells can secrete higher levels of IFN-γ leading to maturation of dendritic cells. This NK-DC cross-priming increases the antigen presenting capacity of DC cells leading to the induction of TAA-specific antitumour immunity [314]. When combined with radiotherapy or platinum-based chemotherapy it can increase overall survival in advanced HNSCC patients [315, 316]. Another approach to target EGFR using chimeric antigen receptor (CAR) T cell transfer is currently undergoing phase I clinical trial (NCT01818323) [317].

HNSCC induces a tumour-permissive cytokines profile including VEGF and hepatocyte growth factor (HGF) [282, 283, 318]. These cytokines can be targeted by monoclonal antibodies to neutralise their function. Bevacizumab is an anti-VEGF mAb. It is currently being tested in combination with chemotherapy in a phase III trial (NCT0058870) despite modest success in a phase II trial when combined with cetuximab [319]. Ficlatuzumab is a mAb that binds and neutralises HGF. It is currently undergoing phase I trials in combination with cetuximab or chemoradiotherapy (NCT02277197 and NCT02277184 respectively).

Another approach to reverse the immune suppression induced by HNSCC is to target the immune check points. Both CTLA-4 and PD-1 are highly expressed in tumour infiltrating lymphocytes in HNSCC [320, 321]. Ipilimumab, an anti-CTLA-4 mAb, is currently being tested in a phase I trials in combination with cetuximab and

radiotherapy in HNSCC (NCT01860430). Similarly, anti-PD-1 mAb, nivolumab, is currently undergoing a phase III trial in recurrent HNSCC (NCT02105636).

HNSCC express a variety of TAAs making these tumours suitable for therapeutic vaccine approaches. Melanoma antigen E (MAGE)-A3 is a cancer testis antigen originally found in melanomas but later identified in HNSCC [322, 323]. A recent phase I trial targeting MAGE-A3 and HPV-16 using a Trojan peptide vaccination technique, where the peptide contain a “penetrin” sequence that allows the entire peptide to translocate through the cell membrane and penetrate directly into the endoplasmic reticulum where they can form peptide-HLA complexes [324], was found to be safe and well tolerated. It generated an immune response to HLA-II peptides but not HLA-I. There was no demonstrable clinical benefit and one patient suffered severe neurological events post vaccination [325]. Vaccination with lethally irradiated semi-allogeneic human fibroblasts (MRC-5) transfected with tumour DNA is currently in phase I trial (NCT02211027). Another cellular vaccine in phase I trial is AlloVax$^{(TM)}$, a personalized anti-cancer vaccine combining Chaperone Rich Cell Lysate as a source of tumour antigen prepared from patient's tumour and AlloStim$^{(TM)}$ activated CD4+ cells [326] as an adjuvant (NCT01998542).

Although not currently in clinical trials, but relevant to our treatment model, is the vaccination with HNSCC autologous tumour cells pre-infected with Newcastle disease virus to act as vaccination adjuvant. In a phase II trial, 20 patients with HNSCC of various anatomical locations were recruited. They all received surgical treatment +/- radiotherapy to be followed after three months with vaccination. Autologous tumour cells were isolated, expanded, infected with NDV then irradiated before being injected subcutaneously. The treatment was well tolerated with only flu-like symptoms, fatigue and induration at injection site recorded. Of the advanced disease patients (stage III

and IV, n=18) 11 survived over 5 years (61%) [327], remarkably higher than the 38% 5-year survival reported at that time [328]. Despite the study shortcomings of small patient cohort and poorly reported functional immunological response data, the overall survival rate is impressive and further validates our own approach of virus-infected cancer cell vaccine.

1.5 T cell homing role in pancreatic adenocarcinoma therapeutic vaccines

The success of any vaccination protocol relies on the ability of memory T cells to localise to peripheral tissue were they are required. This is achieved by expression of homing receptors on these lymphocytes during activation. Vaccination efficacy can be improved by inducing a specific homing receptors pattern relevant to the targeted organ on the resultant memory cells. In human pancreatic adenocarcinoma prognosis correlates with the level of tumour infiltrating CD8+ cells [329]. However, evidence from human disease and animal models show that the desmoplastic stroma of this disease forms a barrier to immune cell infiltration, especially CD8+ [330, 331]. We hypothesised that a vaccination strategy that can induce a pancreas-specific homing capacity in CD8+ cells can overcome this barrier and improve the prognosis of these patients.

1.5.1 Introduction to pancreatic cancer

Pancreatic cancer remains one of the most difficult cancers to diagnose and treat. It is the fifth most common cause of cancer death in the UK with one and five-years survival of 20.8% and 3.3% respectively. These figures have hardly improved since the early 1970s [332]. Complete surgical resection remains the only curative treatment. Unfortunately less than 20% of pancreatic tumours are amenable to surgical excision at the time of diagnosis. However, even with complete surgical resection prognoses remains poor with five years survival around 20% [333, 334]. Gemcitabine is the main chemotherapeutic agent approved for advanced pancreatic cancer. Despite being

shown to improve life expectancy compared to 5-flurouracil, effect remains modest with median survival around 6 months [335]. Combining gemcitabin therapy with erlotinib led to minimal increase in life expectancy from 5.9 to 6.2 months [336].

Immunotherapy is a promising new avenue in the management of pancreatic cancer. Early clinical trials of peptide-based [337, 338] and dendritic cells vaccines [339, 340] have demonstrated the ability of these treatments to induce an antitumour immune response and a promising clinical potential. However the most successful vaccine to enter clinical trials is a whole cell vaccine, similar to our approach. G-Vax is a GM-CSF expressing allogeneic whole cell vaccine that was shown to induce an antitumour immune response involving CD4+ and CD8+ cells [341]. Importantly, patient vaccinated with G-Vax developed mesothelin-specific IFN-γ-producing $CD8^+$ T cells, which provided evidence of *in vivo* cross-priming by antigen-presenting cells of this tumour-associated antigen [342]. This led to the introduction of CRS-207, a live-attenuated *Listeria monocytogenes*-expressing mesothelin to the vaccination regimen. A recent phase III clinical trial using G-Vax prime and CRS-207 boost resulted in an increase of overall survival compared to G-Vax alone [343].

Other vaccination approaches utilising the immunogenic abilities of oncolytic viruses, and vaccinia virus in particular has been reviewed by the author recently [1] (*appendix IV*).

1.5.2 T-cells homing

Leukocytes adhesion to the vascular endothelium and the subsequent migration into adjacent tissue is an integral part of the immune system function. It allows lymphocytes, and other white blood cells, to reach the site of the body where their services are required. This is a multistep process involving; *tethering and rolling* where

lymphocytes are loosely attached to an adhesion molecule on the surface of endothelial cells, *activation* by exposure of the lymphocyte G-protein-coupled receptor to a chemoattractant chemokine and *arrest* where lymphocytes are firmly attached via their activated integrin to the endothelial cells. Transmigration follows were lymphocytes cross the endothelium into surrounding tissue via the junctions between endothelial cells [344, 345]. Each of these steps is mediated by specific interaction between adhesion molecules and surface receptors. In order to extravasate a lymphocyte needs to engage all these receptors in a sequential manner. The various different combination of these receptors and ligands give each tissue type a specific molecular “post code” that allows specific T cells to target a specific area [345].

Chemokines play an essential role in all steps of the adhesion and migration process. They increase the affinity of integrin for their adhesion molecule ligands, provide the necessary signal at the activation stage via interaction with their cognate receptor, and provide the chemotactic gradient to direct lymphocytes migration into the relevant tissue compartment following extravasation [346]. More than 50 chemokines and 20 receptors have been identified. Chemokines are divided into four groups depending on the arrangement of the first two cytosine residue; CC, CX, C and CX3C. They are further divided into inflammatory and homeostatic based on their function [346, 347]. Chemokine receptors are composed of seven transmembrane domain coupled with G-protein that are expressed on the surface of lymphocytes. Each receptor can interact with several chemokines and *vice versa* [348].

Naïve T cells circulate between blood and lymph nodes (and other secondary lymphoid organs) constantly. This migration to lymph nodes depends on the expression of L-Selectin (CD62L) and the chemokine receptor CCR7 on lymphocytes and interaction with their prospective ligands peripheral lymph node addressin (PNad), and

chemokines CCL19 and CCL21 [349]. In the guts, migration to Payer's patch requires the engagement of α4β7 integrin in addition to L-Seletin [350]. This interaction takes place in post-capillary high endothelial venules where shear forces of the blood flow are reduced and accumulation of lymphocytes doesn't interfere with gas and fluid exchange [351].

Upon activation of T cells in the lymph nodes by dendritic cells, they proliferate and became either effector or memory cells and they leave the lymphoid compartment. Some activated T cells maintain expression of CD62L and CCR7 and can migrate to lymph nodes. These cells are referred to as central memory T cells (T_{CM}), while effector T cells (T_{EFF}) and effector memory T cells (T_{EM}) lose their expression and the ability to migrate to lymph nodes but they migrate peripheral and non-lymphoid tissue [352, 353]. However, the difference between these subsets can be subtle. T_{CM} can be as efficient as T_{EM} in providing effector function when faced with antigen challenge [354]. In addition, T_{EM} can convert back to T_{CM} and localise to lymphoid tissue [355].

1.5.3 Gut and non-lymphod T cell homing

T_{EFF} and T_{EM} cells show migratory selectivity to various organs, including the gut, based on expression of various selectin ligands and chemokines receptors as discussed earlier. Gut-tropic T cells express high levels of α4β7 integrin and the chemokine receptor CCR9 [356-358]. These cells migrate preferentially to the small intestine lamina propria venules where mucosal addressin cell adhesion molecule 1 (MAdCAM-1), α4β7 ligand, and CCL25, the main ligand of CCR9, are highly expressed [359, 360].

The site of antigen entry into the body influences the traffic qualities of T_{EFF}. Pathogen entering through the skin primes lymphocytes with skin homing receptors [361]. Similarly, oral vaccination induces higher level of α4β7 compared to intramuscular or

subcutaneous vaccination allowing the primed T cells to home to the guts [362]. In addition, the homing potential of lymphocytes depends on the lymphoid microenvironment where these cells are primed. T cells primed in mesenteric lymph nodes express higher levels of α4β7 and CCR9 compared to those primed in skin draining lymph nodes [363, 364].

Dendritic cells play an essential role in inducing a tissue-specific homing potential into T cells. Intestinal DCs from Peyer's patch and mesenteric lymph nodes induces gut homing capacity while those derived from peripheral lymph nodes induces a skin homing pattern [365-367]. The capacity of DCs to induce tissue specific homing capacity in T cells is believed to depend on the ability of the DCs to produce active metabolites from tissue-derived factors such as retinoic acid by gut-derived DCs [368] and vitamin D3 by skin DCs [369].

MAdCAM-1/α4β7 and CCR9/CCL25 mediated T cell homing plays a role in the pathogenesis of various diseases outside the guts. In normal circumstances MAdCAM-1 expression is confined to the blood vessels of the small intestines [370]. MAdCAM-1 is not detected in normal liver while it can be expressed in chronic inflammatory liver disease [371] and liver cirrhosis [372]. Similarly, the mucosal immune composition in Barrett's oesophagus including high level expression of MAdCAM-1 resembles that of the small intestine suggesting that the disease process is caused by intestinal homing signals rather than to an active local inflammatory response [373].

In the pancreas, MAdCAM-1 is highly expressed in normal and diabetic neonate mice and plays a critical role in the pathogenesis of type 1 diabetes [374]. This expression is down regulated in normal adult mice [374] but remains high in diabetic animals

although restricted to inflamed islets [375]. In human pancreatic cancer, tumour-derived endothelial cells express higher levels of addressins including MAdCAM-1 compared to those derived from normal tissue, allowing selective transmigration of Treg cells from peripheral blood to tumour tissue [376].

1.5.4 Induction of homing capacity via vaccination

The induction of T cells with specific homing capacity requires tissue-derived DCs as discussed above. This can be achieved by enteral vaccination to generate gut-homing phenotype [362] or via intranasal route to target the head and neck region [377]. However this approach has some practical disadvantages in a clinical setting. This will be especially relevant to our vaccination approach that depends on delivering viable tumour cells infected with an oncolytic virus, neither of which is resistant to gastric enzymes.

One approach to overcome that would be to recreate the tissue-specific microenvironment in the lymph nodes via the delivery of tissue specific chemokines. Unpublished work of our collaborator showed that priming of T cells in the presence of CCL25 *in vivo* and *in vitro* would induce higher expression of α4β7 integrin on CD4+ and CD8+ cells, in consequence a gut homing phonotype [F Marelli-Berg, unpublished data]. We speculated that a similar approach can be utilised to generate an anti-tumour immune response with a pancreas-targeting phenotype.

1.6 Hypothesis, aims and objectives

1.6.1 Hypothesis

Based on the work of our group and others demonstrating the induction of antitumour immunity following infection of tumour cells with oncolytic viruses, we hypothesised that prime/boost vaccination with virus-infected tumour cells would induce a therapeutic T cell-mediated antitumour immune response. In addition, arming these oncolytic viruses with CCL25 chemokine would generate tumour-targeting T cells with higher expression of α4β7 integrin preferentially homing to the MAdCAM-1-rich pancreatic tumour.

1.6.2 Major aim:

- To develop a virus-infected cancer cell vaccine (VICCV) that can be translated into the clinic (Fig 1.4).

1.6.3 Objectives

- To optimise the viral dose and the best prime/boost combination to induce a tumour specific immunity.
- To optimise the safety of the vaccination regimen with a secondary treatment of irradiation or cytotoxic drugs to arrest cell proliferation.
- To evaluate the effect of the secondary treatment on viral life cycle and anti-tumour immunity.
- To investigate the immunological functions involved in VICCV.
- To test the efficacy of the vaccination regimen in therapeutic and prophylactic Head and Neck and pancreatic tumour models.
- To generate a T cell immune response with pancreatic-homing phenotype to enhance the therapeutic efficacy of the VICCV in pancreatic cancers.

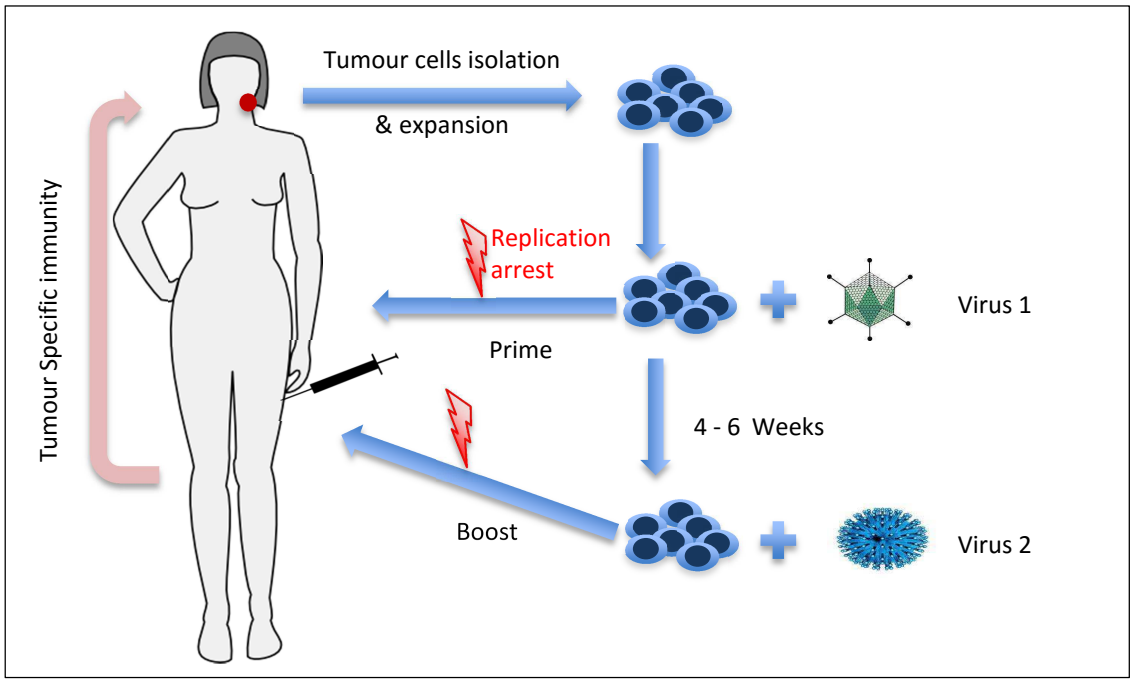

Fig 1.4 A schematic diagram of the virus-infected cancer cell vaccine (VICCV). Tumour cells collected during tumour excision are isolated and expanded, infected with an oncolytic virus, replication-arrested and injected subcutaneously. The same is repeated after 4 – 6 weeks using virus 2. The resultant tumour specific immunity could in theory clear any minimal residual disease or micro metastasis and prevents tumour recurrence.

Chapter two: Materials and Methods

2.1 Cell lines

Murine pancreatic ductal adenocarcinoma (PDAC) cell lines DT6606 and TB11381 cells were kindly provided by Professor David Tuveson (Cold Spring Harbour Laboratory & John Hopkins University, NY, USA). They were obtained from pancreatic tumours of the transgenic mouse strains KC (K-ras$^{LSL.G12D/+}$; PdxCre) and KPC (K-ras$^{LSL.G12D/+}$; p53$^{R172H/+}$; PdxCre) [378, 379] respectively. 32Dp210 is a leukaemia cell line derived from C3H/HeN mice [380]. It was kindly provided by Professor Farzin Farzaneh (Kings College London, London, UK). Lewis Lung cancer (LLC), CT26, CMT93, 4T1, SUIT2 and Mia PaCa cell lines were all obtained from the Cancer Research UK cell bank. SCC7 is a head and neck derived squamous carcinoma, from C3H/HeN mice and was kindly provided by Dr Osam Mazda, (Department of Microbiology, Kyoto Prefectural University of Medicine, Japan). B4B8 is murine SCC cells derived from oral keratinocytes treated with chemical carcinogene 4NQO [381]. LY-2 cell line was isolated from lymph node metastasis after inoculation with PAM212 squamous cell carcinoma cells [382, 383]. They were kindly provided by Dr Carter Van Waes (National Institute of Health, Bethesda, MD, USA). Pkpa130200 is a pancreatic cancer cell line isolated from tumours developed in progenies of KPC mice crossed with Atg7$^{fl/fl}$ [384]. They were kindly provided by Professor Kevin Ryan (Beatson Institute, Glasgow, UK). CV1, HEK-293 and JH293 cell lines were all obtained from ATCC (VA, USA) and were used for virus production and titration. All other cell lines were obtained from Cancer Research UK cell bank. All cell lines are listed in Table 2.1.

All cell lines, except 32Dp210, were grown in Dulbecco's Modified Eagle's Medium (DMEM) high glucose (Sigma-Aldrich, MO, USA) supplemented with 5-10% foetal calf serum (Gibco®, Life Technologies, CA, USA) and 1% penicillin-streptomycin (Sigma-

Aldrich, MO, USA) at 37℃ in a humidified atmosphere containing 5%CO2. 32Dp210 cells were grown in RPMI-1640 (Sigma-Aldrich, MO, USA) supplemented with 10% FCS and 1% penicillin-streptomycin.

Table 2.1 List of all cell lines used in this study

Cell line	Organism	Strain	Disease
DT6606	Mouse	KC	Pancreatic Ductal Adenocarcinoma
TB11381	Mouse	KPC	Pancreatic Ductal Adenocarcinoma
Pkpa130200	Mouse	KPC $Atg7^{fl/fl}$	Pancreatic Ductal Adenocarcinoma
LLC	Mouse	C57BL/6	Lewis Lung Carcinoma
32Dp210	Mouse	C3H/HeN	Leukaemia
SCC7	Mouse	C3H/HeN	Head and Neck SCC
B4B8	Mouse	BALB/c	Head and Neck SCC
LY-2	Mouse	BALB/c	Head and Neck SCC
CT26	Mouse	BALB/c	Colon Carcinoma
CMT93	Mouse	C57BL/Icrf	Colorectal Carcinoma
4T1	Mouse	BALB/c	Breast Adenocarcinoma
JC	Mouse	BALB/c	Breast Adenocarcinoma
SUIT2	Human	-	Pancreatic Carcinoma
Mia PaCa	Human	-	Pancreatic Carcinoma
CV1	Green Monkey	-	Normal Kidney Fibroblasts
HEK293	Human embryonic	-	Epithelial kidney transfected with E1A
JH293	Human embryonic	-	Slow growing subclone of HEK293

2.2 Generation of Renilla Luciferase stable cell lines

2.2.1 Puromycin killing curve

Cells were plated in 6-wells plates at $1x10^5$ cell/well, one plate per cell line, and incubated at 37℃ in a humidified atmosphere containing 5% CO_2 overnight. Puromycin serial dilutions were made in DMEM medium supplemented with 5% FCS as described *(section2.1)* starting with 10µg/ml then 5, 2, 1, 0.5 and negative control of medium only. Puromycin dilutions were added to each well and incubate for 7 days. Cell death was monitored and 2µg/ml dilution was chosen as it resulted in 100% cell killing.

2.2.2 Lentivirus transduction

B4B8, LY-2 and SCC7 cells were plated at $2x10^4$ cells/well in two wells of a 24-wells plate and incubate at 37℃ in a humidified atmosphe re containing 5% CO_2 overnight. On day two, medium was replaced with fresh medium containing hexadimetherine bromide (Sigma-Aldrich, MO, USA) to a final concentration of 4 µg/ml. RediFect Green Renilla-Puromycin Lentivirus vector (#CLS960004, PerkinElmer, MA, USA) was added directly to the cells at MOI=15 units/cell and incubated for 24 hours. One well was left un-infected as negative control for puromycin selection. On day three, virus-containing medium was replaced with fresh pre-warmed medium. Day four, medium was replaced with fresh medium with puromycin at the required concentration (2µg/ml) Renilla Luciferase positive cells were selected in puromycin for 5-7 days. Luciferase expression was confirmed using Renilla luciferase expression assay from Promega (#E2810, Madison, WI, USA) following kit instructions. Stable cells were expanded and frozen 10% DMEM medium supplemented with 10% DMSO.

2.3 Animals

5-7 weeks old male C57BL/6, 5-7 weeks old female C3H/HeN and 5-7 weeks old female BALB/c mice were purchased from Charles River Laboratories (UK) and housed at the BSU, Charterhouse Square.

KPC (K-$ras^{LSL.G12D/+}$; $p53^{R172H/+}$; PdxCre) mice were bread and genotyped in-house by the author by cross-breading KP (K-$ras^{LSL.G12D/+}$; $p53^{R172H/+}$) mice with PDX-Cre mice [379]. Parental mice were kindly provided by Professor David Tuveson (Cold Spring Harbour Laboratory & John Hopkins University, NY, USA).

All animals were housed and all experiments were conducted in accordance with Home Office regulations [385].

2.4 Radiation and chemotherapeutic agents

Cells were irradiated using a RS2000 Biological Irradiator (Rad Source Technology Inc., GA, USA) with a total dose of 30Gy, unless otherwise indicated.

Chemotherapeutic agents used in this study were mitomycin C (Roche Applied Science) used at 50 µg/ml and mitoxantrone (Onkotrene, Baxter, Norfolk, UK) used at 2µM/ml.

2.5 Viruses

2.5.1 Vaccinia virus

VVL15 (VVΔTK) is a thymidine kinase-deleted Lister strain vaccinia virus with E. coli LacZ and firefly luciferase reporter genes inserted in its locus [386]. VVL15-RFP was constructed by Dr L Chard from our group and is equivalent to VVL15 but contains an RFP transgene replacing LacZ.

All Vaccinia viruses used in this study were mass produced by Miss M El-Khouri or Dr L Chard. The virus was grown in 40 T175 flasks of CV-1 cells and purified by ultra-centrifuge sucrose gradient banding. All viruses were re-titrated by the author *(section 2.8)* prior to use.

2.5.2 Adenovirus

Ad5 is a wild type class C Human adenovirus serotype 5. *dl1520* has an 827 base deletion in the region encoding the E1B 55-kDA protein. Ad5-GFP-PL11 is a wild type Ad5 with the GFP gene inserted in the E4 untranslated region [387]. It was kindly provided by Dr G Hallden (Queen Mary University of London, London, UK).

All adenoviruses used in this study were mass produced by the author with the exception of *dl1520* which came from our lab stock. HEK-293 cells were expanded and plated in a Cell Factory-10 system (equivalent to 36 T175 flasks) (Thermo Fisher Scientific, MA, USA) and infected with viral primary expansion. Cells were harvested two days later and spun down before three cycles of freeze/thaw to release viral particles. Adenovirus was purified by sequential ultra-centrifuge CsCl banding. Purified virus was aliquoted and stored at -80℃.

2.6 Plasmids and AdTD-CCL25 virus construction

AdTD plasmid was constructed by Dr Pengju Wang of Sino-British Research Centre for Molecular Oncology, Zhengzhou University of China. This vector contains the full genome of Ad5 with triple gene deletions; *E1ACR2*, *E1B19K* and *E3gp19K.* The latter was replaced with chloramphenicol resistance gene flanked by two SwaI restriction enzyme sites. In addition, the *AdTD* vector contains a kanamycin resistance gene located outside the Ad5 genome, flanked by two PacI restriction enzyme sites.

AdTD vector was digested with SwaI (New England Biolabs, Ipswich, MA, USA) at 25° for four hours. Blunt digested ends were then dephosphorylated using Shrimp Alkaline Phosphatase (New England Biolabs, Ipswich, MA, USA) at 37° for 60 minutes. Enzymes were deactivated at 65° for 20 minutes. DNA was purified using Phenol:Chloroform:Isoamyl Alcohol 25:24:1 (Sigma-Aldrich, MO, USA) followed by DNA precipitation using sodium acetate and ethanol 96-99% at -80° overnight. DNA suspension was centrifuged at 13,000 rpm for five minutes. DNA pellet was washed with Ethanol 70% and centrifuged again and left to air-dry. DNA was eluted in distilled water and concentration measured using NanoDrop 1000 Spectrophotometer (Thermo Fisher Scientific, MA, USA).

PCMV6-Entry-mCCL25-MycDDK plasmid was purchased from Origene (#PS100001, Rockville, MD, USA). It contains a full murine CCL25 cDNA with MycDDK expression tag at the C-terminal. Plasmid was digested using EcoRI (New England Biolabs, Ipswich, MA, USA) at 37° for two hours followed by blunting of the DNA free ends using Quick Blunting™ Kit (New England Biolabs, Ipswich, MA, USA) supplemented with Deoxynucleotide (dNTP) (New England Biolabs, Ipswich, MA, USA) and dithiothreitol (DTT) (Sigma-Aldrich, MO, USA). A second digestion with SmaI (New England Biolabs, Ipswich, MA, USA) at 25° for four hours followed. DNA bands were separated via electrophoresis in 1% UltraPure™ Low Melting Point Agarose gel (Invitrogen, Thermo Fisher Scientific, MA, USA). CCL25 band was cut from the gel and DNA was extracted using illustra GFX PCR DNA and Gel Band Purification Kit (GE Healthcare Life Sciences, Buckinghamshire, England) following the manufacturer instruction.

T4 DNA ligase (New England Biolabs, Ipswich, MA, USA) was used to ligate mCCL25 fragment into AdTD vector. Insert and vector were mixed with enzyme and buffer at a free-ends ratio of 20:1 insert to vector. Reaction tube was incubated at 16° overnight. Vector-only ligation reaction was used as a control for dephosphorylation efficacy. Both ligation products were transformed into One Shot® TOP10 Electrocomp™ competent E.coli using electroporation. Transformed E.Coli were plated and grown over night on kanamycin agar dishes at 37°. Ten colonies were picked from AdTD-CCL25 plate and each was grown in kanamycin liquid lysogeny broth (LB) for 15 hours with shaking at 37°. The following day DNA was extracted using QIAprep Spin Miniprep kit (Qiagen, Venlo, Netherland) following manufacturer instruction. Insertion and direction were confirmed by Polymerase Chain Reaction (PCR) *(Section 2.7).*

Positive clone DNA was digested using PacI digestion enzyme (New England Biolabs, Ipswich, MA, USA) to linearise the plasmid and remove the kanamycin resistance gene. DNA was purified as described above. In addition, AdTD backbone plasmid was digested with PacI to create AdTD-C control virus.

HEK293 cells were plated in 6-wells plate at $1x10^5$ cells/well and incubated overnight at 37° and 5% CO_2. The following day, linearised AdTD and AdTD-CCL25 plasmids were transformed into the cells using Effectene Transfection Reagent (Qiagen, Venlo, Netherland) following the manufacturer instructions (Fig 2.1). Plates were incubated for 7 days and observed for cytopathic effect (CPE). Once most cells showed signs of infection, supernatant was collected for confirmation of CCL25 expression. Cells and remaining culture media were harvested by scrapping the wells and underwent three cycles of freeze/thaw to release viral particles. 100 µl of the virus suspension was used to infect a T25 flask of HEK293 cells which in turn used to infect a T175 flask to make the viral primary expansion. DNA was extracted from the remaining viral suspension using Blood DNA extraction kit (Qiagen, Venlo, Netherland) and used for construct validation by PCR.

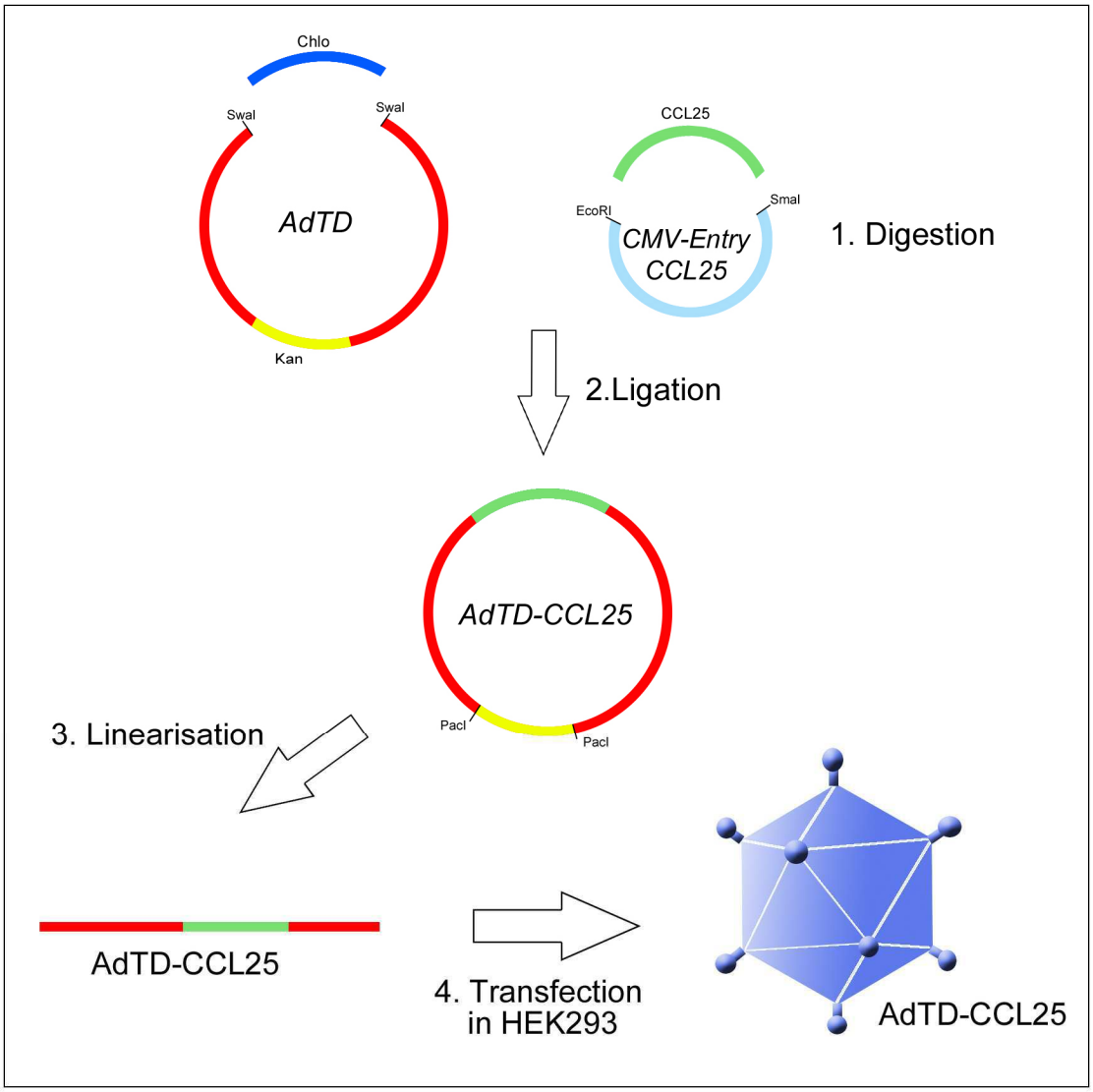

Fig 2.1 Schematic diagram of AdTD-CCL25 construction.

AdTD plasmid and *PCMV6-Entry-mCCL25-MycDDK* were digested with SwaI and EcoRI+SmaI respectively. Isolated DNA fragments were then ligated and transformed into competent E.Coli. The correct clone was then linearised using PacI before transfection into HEK293 cells to be packaged into AdTD-CCL25 virus. Key: Kanamycin resistance gene (Kan), Chloramphenicol resistance gene (Chlo)

2.7 PCR validation of adenovirus constructs

AdTD-CCL25 plasmid constructs were validated for transgene insertion and direction by PCR. E3gp19K external primers were used to screen colonies for successful ligation. The expected size of the amplified segment using these primers is 733 bp in an *AdTD-CCL25* plasmid compared to 1019 bp in the *AdTD* vector. CCL25 gene

insertion was further validated using CCL25 internal primers. Direction of the insert was confirmed using an E3gp19K forward primer and CCL25 reverse primer. Successful amplification of DNA using these primers indicates the insert is in the right direction (*section 6.1*).

Standard Ad5 primer sets [388] (Table 2.2) were used to validate the triple gene deletions of both AdTD-C and AdTD-CCL25 viruses prior to viral mass production (*Section 6.1*).

All PCR reactions contained 1-2 µl DNA (approximately 100ng), 0.5 µl forward primer, 0.5 µl reverse primer, 10 µl distilled water and 12.5 µl ReddyMix PCR Master Mix (Thermo Fisher Scientific, MA, USA). PCR reactions were run for 25-30 cycles each consisting of 94℃ for 30 seconds, 62℃ for 30 seco nds and 72℃ for one minute. Cycles were proceeded by a single incubation at 95°C for one minute and followed by a single incubation step at 72℃ for seven minutes, to be followed by a hold step at 4℃.

Table 2.2 List of all PCR primers used for this study

Primer	Primer	Sequence
Ad5 set 1	Forward	CCCGGTGAGATTCCTCAAGAGGCCAC
	Reverse	CCGGACCCAAGGCTCTCTGCTCTCCGGCTGCTCGGGC
Ad5 set 2	Forward	GTAATGTTGGCGGTGCAGGAAGGGATTG
	Reverse	GGGTCCCCCGTATTCCTCCGGTGATAATGAC
Ad5 set 3	Forward	GTGTTCGCTTTGCTATATGAGGACCTGTGGC
	Reverse	CCTCGATACATTCCACAGCCTGGCGACGCCCACC
Ad5 set 4	Forward	CCTGTGATTGCGTGTGTGG
	Reverse	GACAACAGTAGCAGGCGATTC
Ad5 set 5	Forward	GCATCTGTGGAGAGCGGTTGTGAGACAC
	Reverse	GCGCCAAGCAGATCAAGCTCATTAGCGC
Ad5 set 6	Forward	GCTTAATGACCAGACACCGTCCTGAGTG
	Reverse	GCACCAAGTGATCGGGCCTCAGCTCC
Ad5 set 7	Forward	CACCCTCACGCTCATCTGCAGCCTCATCACTGTGG
	Reverse	CTTCAGACGGTCTTGCGCGCTTCATCTGC
Ad5 set 8	Forward	CGCTGGGGTCGCCACCCAAGATGATTAGG
	Reverse	GAGTAGGGTACAGACCAAAGCGAGCACTG
E3gp19k ext	Forward	CTCTGCCTAAGGCTCGCCG
	Reverse	GCAAGCAGCGAGTAAAGCAGTT
CCL25 int	Forward	TCGCCATGAAACTGTGGCTT
	Reverse	GCGTACGCGTATTGTTGGTC

2.8 Virus titration

Purified virus titre was determined using the 50% tissue culture infective dose (TCID50) method. 8,000 cells/well of CV1 or JH293 cells, for vaccinia virus and adenovirus respectively, were plated in 96-well plates in 200µl DMEM supplemented with 5% FCS as described *(section2.1)* and incubated at 37℃ in a humidified atmosphere containing 5% CO_2 overnight. The purified virus was diluted $1{:}10^5$ in DMEM 5%CSF. 20µl of the diluted virus were used to infect each well of the top row of the plate. Serial 1:10 dilutions were made to the next six rows. The last row was left uninfected as a negative control. Plates were incubated as above and the number of infected wells was counted on day 7 days for vaccinia virus and day 10 for adenovirus. The titre (pfu/ml) was calculated using the Reed Muench method [386, 389].

Table 2.3 List of all viruses used for this study.

Virus	Batch No.	Titre (pfu/ml)
VVL15	010612	$6.34X10^{10}$
VVL15	010814	$8.14X10^{9}$
VVL15-RFP	060509	$2.1X10^{9}$
Ad5	221013	$1x10^{9}$
Ad5	141113	$1.95x10^{10}$
dl1520	111105	$7.13x10^{9}$
Ad5-GFP-PL11	010313	$2.47x10^{9}$
AdTD-C	290514	$1x10^{10}$
AdTD-CCL25	020714	$2.59x10^{9}$

2.9 Picogreen assay

Adenovirus particle count was determined using a Quant-iT™PicoGreen®dsDNA Assay Kit (Invitrogen, Eugene, OR, USA). Stock virus was diluted 1:2 in TE (Tris-ethylenediaminetetraacetic acid (EDTA)) and inactivated at 56℃ for 15 minutes. The viruses were then diluted 1:6 and 1:10, and incubated at room temperature for 10 minutes to allow equal distribution. Lambda DNA was diluted in TE to a concentration of 1 µg/ml. This was serially diluted to generate a standard curve 0-750 ng/ml. The viral dilutions and DNA standard samples were further diluted 1:20 and added in triplicate to a photosensitive 96-well plate (100 µl/well). 1x picogreen reagent was added to each well (100 µl/well) and the plate was left to incubate for two minutes at room temperature. The plate was read at 485 nm/535 nm on a Dynex Opsys MR 96 Well Microplate Reader and the samples were quantified from the standard curve. The virus particle (vp)/ml concentration was then determined using costumised GraphPad Prism 5.0 and Excel spreadsheet.

2.10 Virus replication assay

Cells were plated at $2x10^5$ cell/well in a total of 2ml MDEM 5%FCS in a 6-wells plate to a total of 51 plates per cell line and incubated overnight. The next day cell count per well was obtained by averaging the cell count of three of the wells. The remaining 48 wells were infected with 1pfu/cell for VVL15 and 50pfu/cell for Ad5. Cells were incubated for two or four hours for VVL15 and Ad5 respectively.

Cells were then treated with irradiation (Rx), mitomycin C (MMC), mitoxantrone (MTX) or left untreated as negative control. After two hours of treatment, medium was aspirated and the cells were washed with phosphate buffered saline (PBS) twice. Following this 2ml of fresh medium was added to each well and incubated at 37℃.

Twenty-four hours later cells of each well were scraped and transferred with medium to a cryotube and placed into -80℃ freezer. The proce dure was repeated at 48, 72 and 96 hours. The cells were then lysed by two rapid freeze/thaw cycles to release viral particles.

TCID50 assay with top dilution of 1:1,000 was used to determine virus titre for each sample, as described above *(section 2.8)*.

2.11 Cell viability assay, MTS

2.11.1 Dose-response cell kill assay

Cells were plated at 1,000 cell/well in 96-wells plate in 90µl DMEM 5%FCS. 6 hours later, triplicate plates were infected per tested virus. The first column was infected at 100pfu/cell for vaccinia virus and $1x10^4$pfu/cell for adenovirus diluted in 10µl DMEM 5%FCS. Virus was serially diluted at 1:10 a further 8 times through the other columns.

Uninfected cells acted as the negative control and media only wells as the positive control. Plates were incubated at 37℃. Six days after infection 20µl of MTS reagent (Cell titer 96AQueous MTS Reagent, Promega, Madison, WI, USA) supplemented with 5 % PMS (Sigma-Aldrich, MO, USA) was added to each well and plates were incubated at 37℃ for 2 hours. Optical density was measured at 490 nm using a 96-well plate reader. Dose response curve and EC50 values were calculated using customised Excel spreadsheet and Graphpad Prism 5.0 software.

2.11.2 Time course cell kill assay

Cells were plated in triplicate at $2x10^4$ cell/well in 96-wells plate in 200µl DMEM 5%FCS. Six hours later cell were infected with AdTD or AdTD-CCL25 virus at an MOI=10 pfu/cell. One plate was used per time point. Triplicate wells of un-infected cells and media only were used as negative and positive controls respectively. Plates were incubated at 37℃. 24 hours later MTS reagent was added and cell kill percentage was calculated as above. The same procedure was repeated at 48, 72 and 96 hours.

2.12 Cell proliferation assay

This assay was used to determine irradiation, MMC or MTX dose and incubation period required to arrest the proliferation of tested cells over a period of 96 hours.

Cells were plated at $2x10^5$ cell/well in a total of 2ml MDEM 5%FCS in a 6-wells plate and incubated overnight. The next day cell count per well was obtained by averaging the cell count of three of the wells. Triplicate wells were then treated with either MMC and incubated for 2 hours, or MTX and incubated for 2, 4 or 24 hours. Additionally triplicate wells were irradiated at increasing irradiation dose from 15 to 120 Gy. 24 hours later triplicate wells were trypsinised for each treatment group and live cell count was determined using the Trypan blue exclusion test [390].

2.13 Virus infectivity assay using fluorescence

32Dp210 cells were plated at $2x10^5$ cell/well in a total of 2ml RPMI 10%FCS in 6-well plates and incubated overnight. The next day cell count per well was obtained by averaging the cell count of three of the wells. Cells were infected at MOI=10 or 20 pfu/cell for VVL15-RFP, and 50 or 100 pf/cell for Ad5-GFP-PL11. After 24 hours incubation at 37℃, florescent cells percentage (as a marker of infected cells) was measured using BD LSRFortessa™ cell analyzer (BD Biosciences, CA, USA).

2.14 Western blot

$2x10^5$ cells in 6-well plates were lysed for 5 min on ice with 100 µl of lysis buffer containing 50 mM Tris pH7.4, 150 mM NaCl, 10 mM CaCl2, 1% NP40 and 1 protease inhibitor tablet for each 50 ml of buffer (Roche Applied Science, Mannheim, Germany). Protein concentration in samples was determined by using a Bradford assay (BioRad, CA, USA) and measuring optical density at 595nm using a 96-well plate reader. Proteins were resuspended in 5 µl of Laemmli sample buffer 5X (50 mM Tris, 4% SDS, 10% glycerol, 5% Mercaptoethanol, 0.01 % Bromophenol Blue) and distilled water to give a final concentration of 30µg in 25µl. Samples were heated to 95℃ for 5 min. Samples were separated according to molecular weight on 10% SDS-polyacrylamide gels and transferred onto a polyvinylidene difluoride membrane (GE Healthcare, Little Chalfont, Buckinghamshire, UK) using a wet transfer system. Membranes were blocked in 0.1% Tween 20 in PBS supplemented with 5% fat-free powdered milk for 40 minutes. They were then incubated with primary antibodies overnight at 4℃ specific to the following proteins: E1A (MS-587-P1, NeoMarkers, CA, USA), Hexon (LF-PA0099, Seoul, Korea), vaccine virus proteins (9503-2057, Biogenesis Ltd, Poole, UK). Alpha tubulin was used as a loading control (ab52866, Abcam, Cambridge, UK). Antibodies

were diluted 1:1,000 – 1:2,000 in 0.1% Tween 20 in PBS supplemented with 5% bovine serum albumin (BSA).

Membranes were then transferred to the appropriate horseradish peroxidase-labelled secondary antibodies (Santa-Cruz Technology, Santa Cruz, CA, USA). Secondary antibodies were then detected using ECL Western Blotting Detection System (GE Healthcare, Little Chalfont, Buckinghamshire, UK).

2.15 Quantitative PCR

DT6606 cells were plated, infected and secondary treatment with Rx, MMC or MTX was performed as with the viral replication experiment *(Section 2.10)*. 24 hours later, cells were scrapped, transferred to 15mls conical tubes and spun down at 1500rpm for 5 minutes. Supernatant was discarded. Viral DNA was extracted from cell pellets using the Blood DNA extraction kit (Qiagen, Venlo, Netherland). DNA samples were diluted in Nuclease-free water to 20ng/µl (100ng/reaction). Quantitative PCR (qPCR) was performed using SYBR® Green PCR Master Mix (Applied BioSystems, Thermo Fisher Scientific, MA, USA). Primers sets used for this assay are shown in table 2.4. Data were interpreted as either viral copy numbers using a standard curve of serially diluted viral DNA.

Table 2.4 List of primers used for qPCR

Gene	Primer	Sequence
Ad5 E1A	Forward	TGCCAAACCTTGTACCGGA
	Reverse	CGTCGTCACTGGGTGGAAA
Ad5 Penton	Forward	GATCGGAAAACCTCTCGAGAAA
	Reverse	CGTAGGAGGGAGGAGGACCTT
VVL15 VLTF-1	Forward	AACCATAGAAGCCAACGAATCC
	Reverse	TGAGACATACAAGGGTGGTGAAGT
18s	Forward	ATCCCTGAAAAGTTCCAGCA
	Reverse	CCCTCTTGGTGAGGTCAATG

2.16 CCL25 ELISA

Supernatant samples harvested from viral construction, virus replication assay and cell killing assay were diluted 1:5 in 1x Reagent Diluent Concentrate (R&D Systems, Minneapolis, MN, USA). CCL25 levels were measured using Mouse CCL25/TECK DuoSet ELISA (R&D Systems, Minneapolis, MN, USA) following the manufacturer instructions. Data was analysed using GraphPad Prism 5.0.

2.17 CCR9 expression

Cells were trypsinised and washed twice with FACS buffer (PBS + 1% BSA). A triplicate of $1x10^6$ cells of each cell line were spun down and resuspended in Anti-mouse CCR9 APC (eBioscience, San Diego, CA, USA) diluted 1:100 in FACS buffer and incubated on ice away from light for 45 minutes. Stained cells were washed twice in FACS buffer. Unstained samples of each cell line were used as negative control. Data was acquired on BD LSRFortessa (BD Biosciences, San Jose, CA, USA).

2.17 Cancer vaccination (Prime/Boost)

Cells were grown in T-175 flasks to a 70% confluence. The next day cell count per flask was obtained by averaging the cell count of two flasks. The flasks were infected with MOI= 1pfu/cell for VVL15 and 50pfu/cell for Ad5 (or as otherwise indicated in the individual experiment). Cells were incubated for two or four hours for VVL15 and Ad5 respectively.

Cells were then treated with irradiation (Rx), mitomycin C (MMC), mitoxantrone (MTX) or left untreated as control. After two hours of treatment, medium was aspirated and the cells were washed with phosphate buffered saline (PBS) twice. Other control groups are: PBS, cell lysate obtained by three freeze/thaw cycles, Rx-treated cells,

MMC-treated cells or MTX-treated cells. The cells were diluted to $2x10^7$ cell/ml in PBS ($2x10^6$ cells per 100µl vaccination dose). The treated cells were then injected into the right flank of mice.

The same procedure was repeated after two to four weeks (boost).

2.18 IFN-γ Assay

This assay is based on the release of IFN-γ when CD8 cells are activated by their cognate epitope-MHC complex. The level of released IFN-γ correlates to the level of tumour/antigen specific immunity.

Two weeks after vaccination *(section 2.17)*, mice were euthanised via cervical dislocation and spleens were harvested under sterile conditions. A single-cell suspension of splenocytes was obtained by gentle mashing of the spleens using the flat end of a 2ml syringe plunger in a 70µm nylon cell strainer over a 50ml conical tube. Cells were flushed using T-cell media (TCM) (RPMI-1640 supplemented with 10% FCS, 1% Penicillin-Streptomycin, 1% essential amino acids and 1% sodium pyruvate) all from Sigma-Aldrich (MO-USA). Red blood cells were then lysed using red blood cell lysis buffer (Sigma-Aldrich, MO, USA). Splenocytes were then washed with PBS, spun down at 1,200rpm for 5 minutes then re-suspended at $5x10^6$ cells/ml.

Target cells and control cells (DT6606 and LLC respectively, or 32DP210 and SCC7) were trypsinised and treated with MMC for two hours at 37℃. They were then washed with PBS, spun down at 1,200rpm for 5 minutes and re-suspended in TCM at $5x10^5$ cells/ml.

In a round-bottomed 96-well plate, 100µl of the splenocytes re-suspension were co-cultured in duplicate wells with 100µl of target cell solution giving an effector to target ratio of 10:1 ($5x10^5$ splenocytes and $5x10^4$ target cells). Control wells contained splenocytes only in 200µl TCM. Plates were incubated for 72 hours at 37℃.

Plates were spun down at 1,200rpm for 5 minutes and supernatant collected from each well. IFN-γ levels were measured using Murine IFN-γ ELISA kit (Biolegend, San Diego, CA, USA) following the manufacturer's instructions.

2.19 Immune cells phenotyping using flowcytometry

Single cell suspension from spleen or inguinal lymph nodes was obtained as described above from vaccinated mice and washed twice in FACS buffer (PBS + 1% BSA). A master mix for each phenotyping group was prepared in advance (Table 2.6).

$1x10^6$ cells of each organ were spun down and resuspended in the relevant master mix and incubated on ice away from light for 45 minutes. All antibodies were purchased from eBioscience (San Diego, CA, USA) and diluted 1:100 in FACS buffer. Stained cells were washed twice in FACS buffer and fixed in 2% formaldehyde diluted in FACS buffer. The latter was washed and cells were resuspended in FACS buffer and kept at 4℃ away from light over night when necessary. In a ddition, a representative sample of each organ was left unstained or stained in single colours and FMO (florescence minus one). These were used to set up voltages and gates. Data was acquired on BD LSRFortessa (BD Biosciences, San Jose, CA, USA).

Table 2.5 Labelled antibodies used for flowcytometry

Marker	Fluorochrome	Laser and filter	eBioscience ref	FMO
Adaptive immunity				
CD3	PE	Yellow-Green 582/15	12-0031-83	
CD4	PE Cy7	Yellow-Green 780/60	25-0041-82	
CD8	FITC	Blue 530/30	11-0081-85	
CD44	eFluor 450	Violet 450/50	48-0441-82	Yes
CD62L	PerCP5.5	Blue 695/40	45-0621-82	Yes
CXCR3	APC	Red 670/14	17-1831-82	Yes
Dendritic cells activation				
CD11c	PerCP5.5	Blue 695/40	45-0114-80	Yes
CD86	PE	Yellow-Green 582/15	12-0862-81	Yes
CD80	eFluor 450	Violet 450/50	48-0801-82	Yes
MHCII	APC	Red 670/14	17-5321-81	Yes
T cell homing				
CD3	PerCP5.5	Blue 695/40	35-0031-82	
CD4	PE Cy7	Yellow-Green 780/60	25-0041-82	
CD8	FITC	Blue 530/30	11-0081-85	
α4β7	PE	Yellow-Green 582/15	12-5887-82	Yes
CCR9	APC	Red 670/40	17-1991-82	Yes

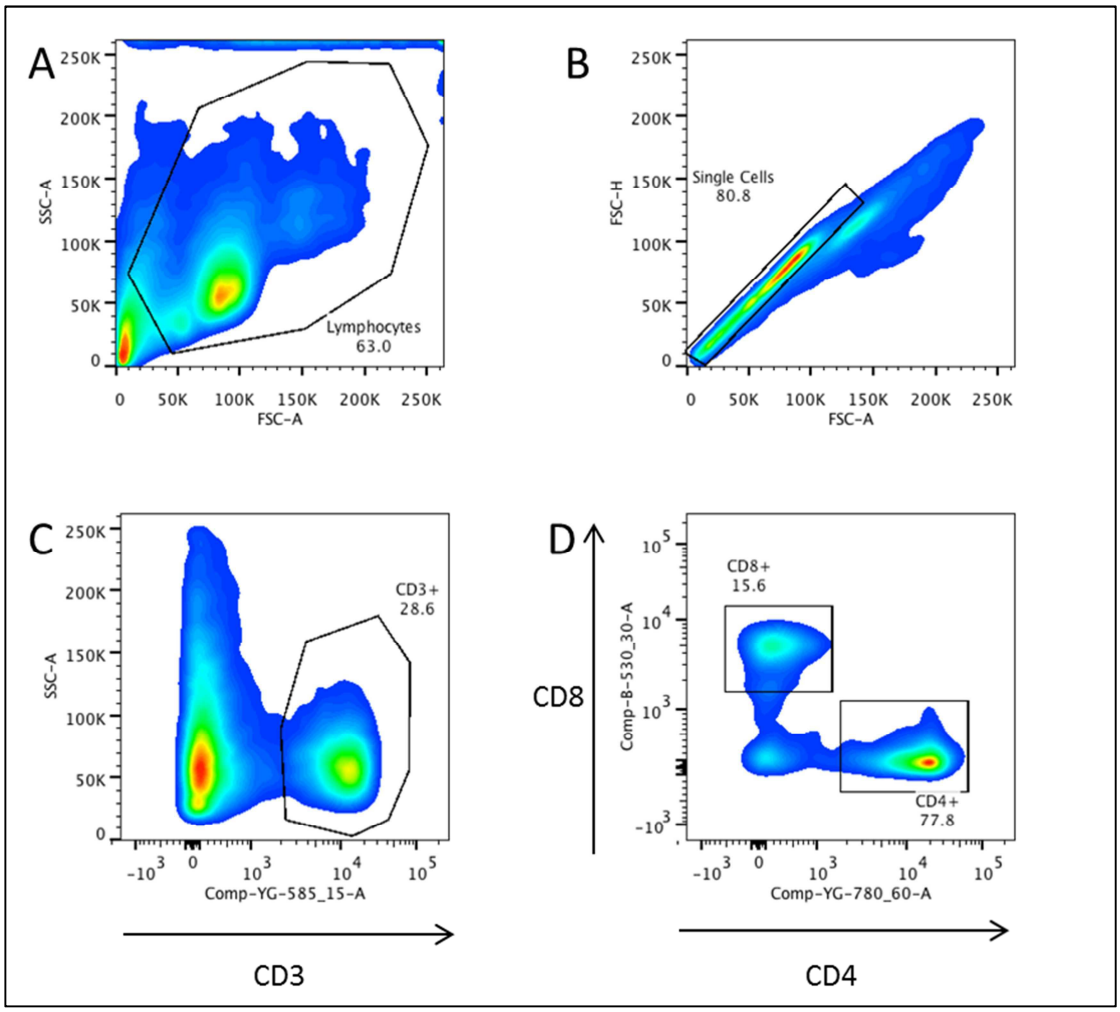

Fig 2.2 Selecting for CD3+, CD4+ and CD8+ T cells.

Flow cytometry was used to isolate T cells subtypes. The plots depict a representative sample of the gating strategy to isolate different T cell populations within the splenocytes obtained from a vaccinated mouse. A, B) Using FCS-A, SSC-A and FSC-H profiles, gates were drawn to exclude cell debris and cell duplets. C) CD3+ cells were selected within the single cell population. D) CD3+CD4+ and CD3+CD8+ T cells were selected using the relevant lasers and filters.

Intact cells were sorted using forward scatter area (FSC-A) and side scatter area (SSC-A) profiles. Single cells were then selected using FSC-A and forward scatter height (FSC-H) profiles. A minimum of 20,000 events were recorded for each sample within the single cell gate. A detailed gating plan is explained in figures 2.2, 2.3, 2.4 and 2.5. Data was analysed using FlowJo V10 software (Tree Star Inc., San Carlos, CA, USA).

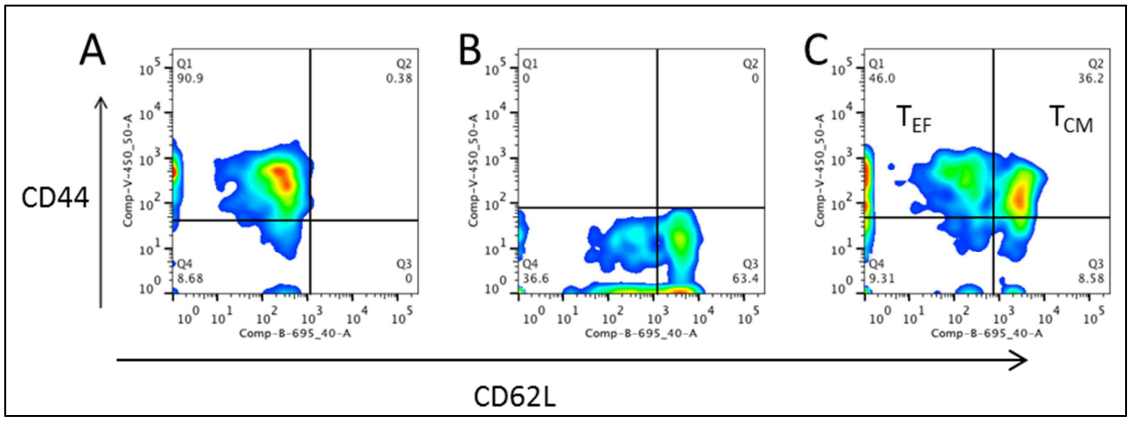

Fig 2.3 Selecting effector memory and central memory T cell populations.
Cells were stained using Anti-mouse CD44 and CD62L conjugated antibodies. The plots depict a representative sample of CD3+ CD4+ (as shown in Fig 2.2) splenocytes obtained from a vaccinated mouse. Cells were sorted using the blue 695/40 and violet 450/50 lasers. A) Using CD62L FMO sample, gate was set to separate CD62L+ and CD62L- cells. B) Similarly, CD44+ and CD44- cells were identified. C) A representative fully stained sample showing effector and central memory cells population.

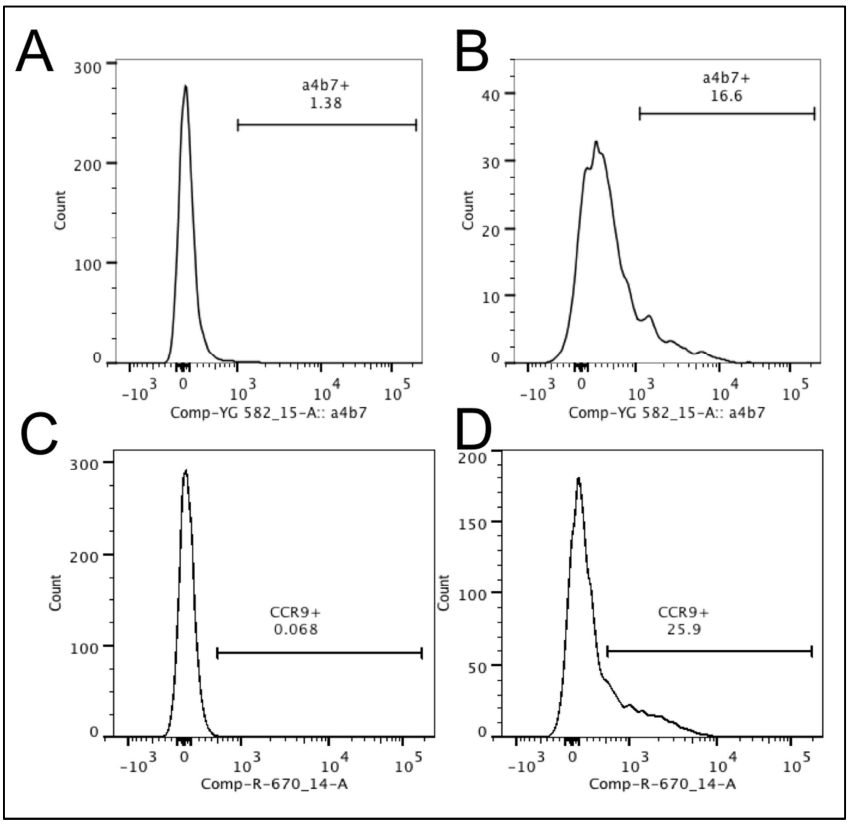

Fig 2.4 Selecting α4β7+ and CCR9+ T cells.

Cells were stained with anti-mouse α4β7 integrin PE and anti-mouse CCR9+ APC. A and C) histograms show FMO samples histograms that were used to set the gating. B and D) histograms shows representative sample of CD4+ cells (as isolated in Fig 2.2). The number depicts the percentage of positive cells out of the total population.

2.20 Head and Neck tumours animal model

SSC7, SSC-RLuc, B4B8, B4B8-RLuc, LY2 or Ly2-RLuc were trypsinised, washed with PBS and re-suspended to a concentration of $1x10^7$-$5x10^7$ cell/ml in PBS. Mice were then injected with 100µl of the cell suspension either intra-orally in the right cheek or subcutaneously in the right lower flank giving a total of $1x10^6$ to $5x10^6$ cells /mouse depending on the cell line and individual experiment. Tumour growth, weight and clinical signs of lymph node metastasis were monitored twice a week. Mice were sacrificed according to Home Office guidelines if showing signs of tumour ulceration, bleeding, dyspnoea, distress or severe cachexia, if tumour size reached 1.44 cm^2 or if

they lost 20% of total body weight. Tumours, lungs and draining lymph nodes were harvested and sent for histopathology analysis.

2.20.1 Subcutaneous surgical excision model

Tumour cells were injected as above. Tumours were carefully excised under continuous inhalation anaesthesia using isoflurane via nose cone once they reached 200 mm^3 in size or earlier if they started to ulcerate. A cuff of healthy skin and/or underlying muscle was excised as necessary to allow complete tumour clearance. Wounds were closed with interrupted sutures using 4.0 Vicryl Rapide™ (Polyglactin 910, Ethicon, Edinburgh, UK) and Vetbond™ Tissue Adhesive (3M, St Paul, MN, USA). Buprenorphine ('Vetergesic', Alstoe Veterinary, York, UK), diluted 1:10 in Normal Saline (0.9% NaCl), was injected subcutaneously at an approximate dose of 0.1 mg/kg to provide post-operative analgesia. Tumour recurrence, weight and clinical signs of lymph node metastasis were monitored twice a week. Mice were sacrificed and organs harvested as above.

2.20.2 Orthotopic surgical excision model

$2x10^6$ LY2 cells were injected orthotopically as above. Tumours were excised five days after injection via external skin incision under injection anaesthesia using ketamine (Narketane-10, 100 mg/ml, VÉTOQUINOL (UK) Ltd, Great Slade, UK) and xylazine (Rompun, 20 mg/ml, Bayer, Kiel, Germany) at an approximate dose of 100/10 mg/kg via intraperitoneal injection. Wound closure, post-operative care and monitoring were conducted as above.

2.21 Efficacy studies

Mice were vaccinated as described previously (section 2.17).

Two weeks after vaccination mice were injected subcutaneously in the left flank with $5x10^6$ viable DT6606 cells (unless otherwise specified) suspended in 100µl sterile PBS. Tumour growth and weight were monitored twice a week. Mice were sacrificed according to Home Office guidelines if showing signs of tumour ulceration, bleeding, dyspnoea, distress or severe cachexia, if tumour size reached 1.44 cm^2 or if they lost 20% of total body weight.

3.22 Statistical analysis

Statistical analysis was performed using Graphpad Prism 5 software. Specific statistical tests will be stated for each experiment in the results section.

Chapter three: Proof of concept

3.1 Induction of tumour-specific immunity using virus-infected cancer cells

3.1.1 Optimising the VICCV viral dose

MTS assay was used to determine the required viral dose to kill 50 percent of DT6606 and TB11381 murine pancreatic cancer cells. EC50 values were 12.8 pfu/cell and 0.35 pfu/cell in DT6606 for Ad5 and VVL15 respectively and 23.1 pfu/cell and 0.05 pfu/cell for TB11381 (Fig. 3.1). To “guarantee” all tumour cells are killed by the virus and to prevent tumour developing in the vaccination site, an MOI=50 pfu/cell and 1 pfu/cell for Ad5 and VVL15 were selected.

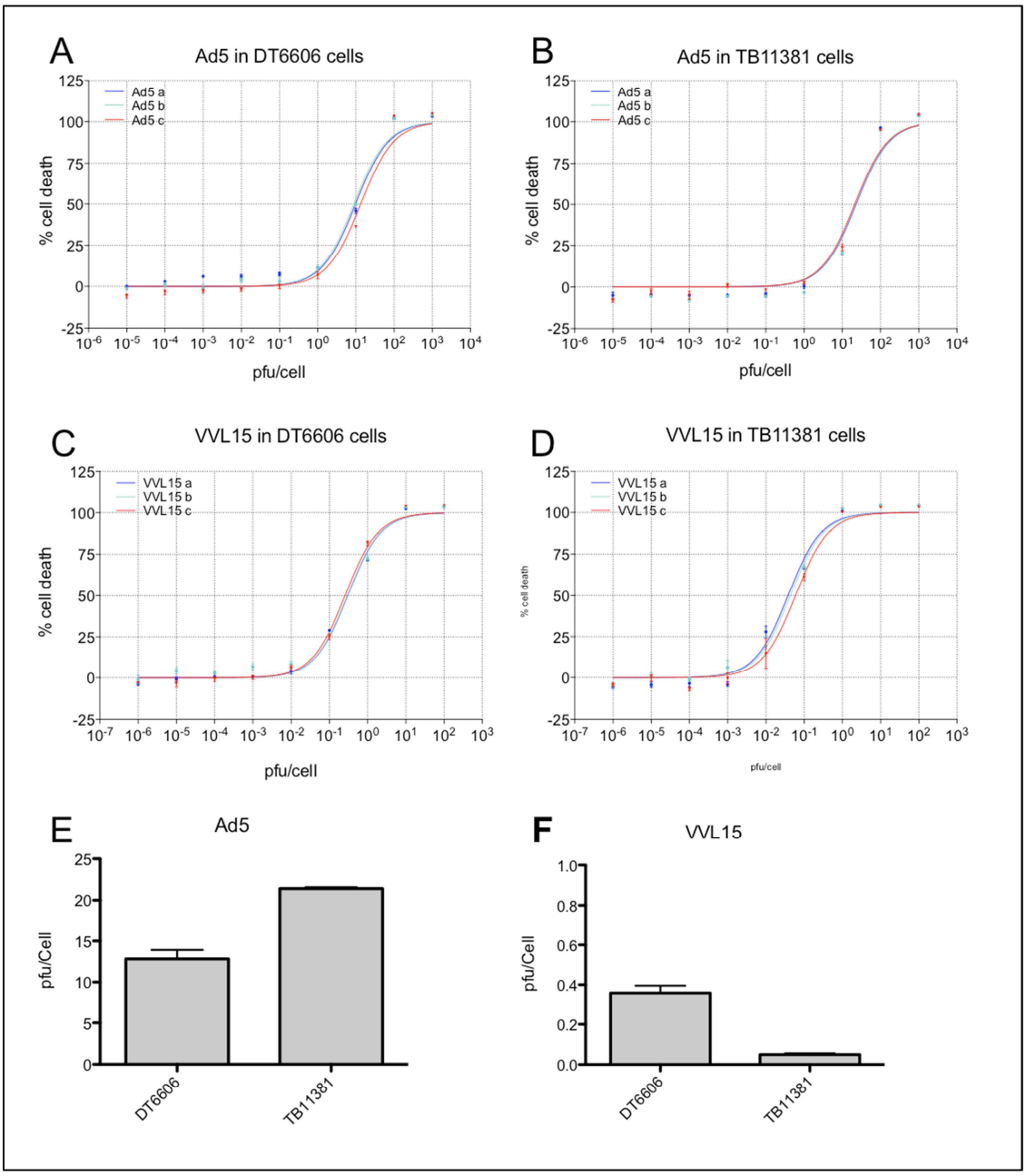

Fig 3.1 Cytotoxicity of oncolytic viruses Ad5 and VVL15 in murine pancreatic cell lines.

DT6606 and TB11381 cells were infected with 1:10 serial dilutions of Ad5 (top dilution MOI=1x10^4 pfu/cell) or VVL15 (Top dilution MOI=100 pfu/cell). Figures represent dose-response curve for A) Ad5 in DT6606. B) VVL15 in DT6606. C) Ad5 in TB11381. D) VVL15 in TB11381. E-F) EC50 values of both cell lines.

3.1.2 Induction of tumour specific immunity in a murine pancreatic cancer model

An IFN-γ assay was performed to test the ability of the VICCV regimen to induce tumour-specific immune response in this murine pancreatic cancer model. This assay is based on the release of IFN-γ when CD8 cells are activated by their cognate epitope-MHC complex. The level of released IFN-γ correlates to the level of antigen specific tumour immunity.

Four groups of mice (n=3) were vaccinated with $2x10^6$ DT6606 cells infected with various prime/boost viral combinations. Additionally, three control groups were vaccinated with PBS, cell lysate obtained by three freeze/thaw cycles or MMC-treated cells. When harvested, splenocytes were co-cultured with DT6606 cells, and the highest level of secreted IFN-γ, indicating the strongest anti-tumour response, was in the Ad/Ad group. This was significantly higher than all other treatment groups except Ad/VV (Fig. 3.2 A). This anti-tumour response appears to be tumour specific as the level of IFN-γ were significantly higher in the Ad/Ad group ($p=0.0481$, Paired *t*-test) and the Ad/VV group ($p=0.032$, Paired *t*-test) compared to the levels secreted from splenocytes co-cultured with LLC control cells (Fig 3.2 B).

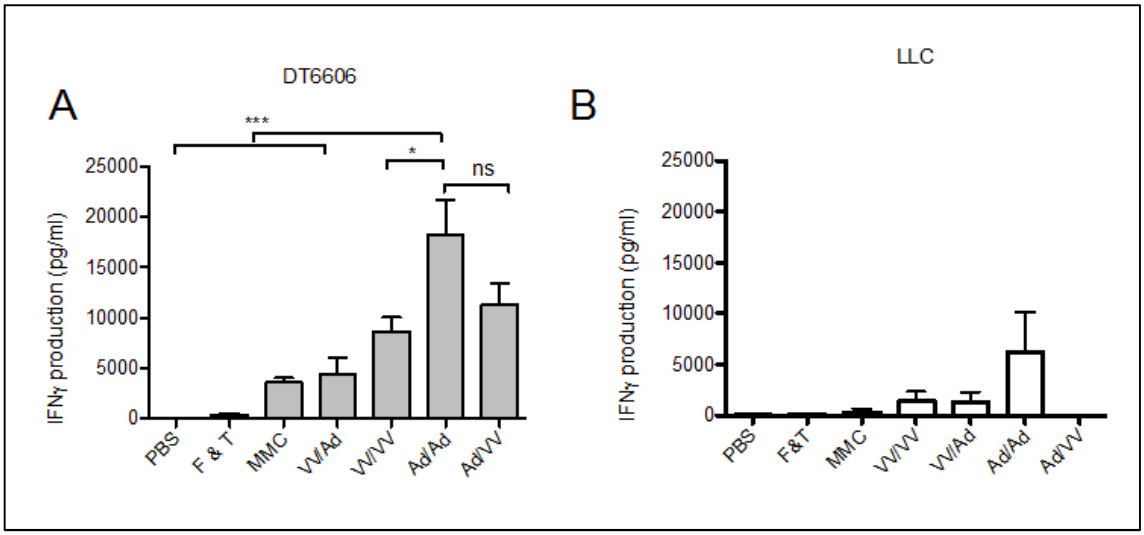

Fig 3.2 Ad/Ad and Ad/VV prime/boost VICCV combination induce the higest level of antitumour immunity.

Seven groups of C57BL/6 mice (n=3) were vaccinated with PBS, DT6606 cell lysate or DT6606 tumour cells pre-treated with MMC, Ad5 or VVL15. Mice were boosted four weeks later. Spleens were harvested and processed two weeks after boost. Isolated splenocytes were incubated for 72 hours with proliferation arrested A) DT6606 cells or B) control LLC cells. IFNγ production, as an indicator of CD8 activation, in the supernatant was measured by ELISA**.** IFNγ levels were normalized by subtracting background release from non-stimulated splenocytes. One-way ANOVA with Tukey post-hoc test was used to compare groups. Columns represent the means ± SEM; asterisks denote the significance levels as comparing: ns non-significant; * $p \leq 0.05$; ** $p \leq 0.01$; *** $p \leq 0.001$.

3.2 Enhancing the safety of the vaccination regimen using secondary treatment

The virus-infected cancer cells, as described above, are viable at the time of injection, albeit virus-infected. The success of the VICCV relies on the oncolytic virus, along with host defence mechanisms, to eradicate injected cells. Failure of these mechanisms represents a serious safety issue that would limit the translatability of the VICCV. To reduce such risk we added an extra safety measure by arresting the proliferation of the virus-infected cells using irradiation or chemotherapy agents.

To validate the irradiation dose required to arrest the proliferation of DT6606 cells a cell proliferation assay was performed. The results (Fig. 3.3 A) suggest that 30Gy dose was sufficient to inhibit growth in this cell line.

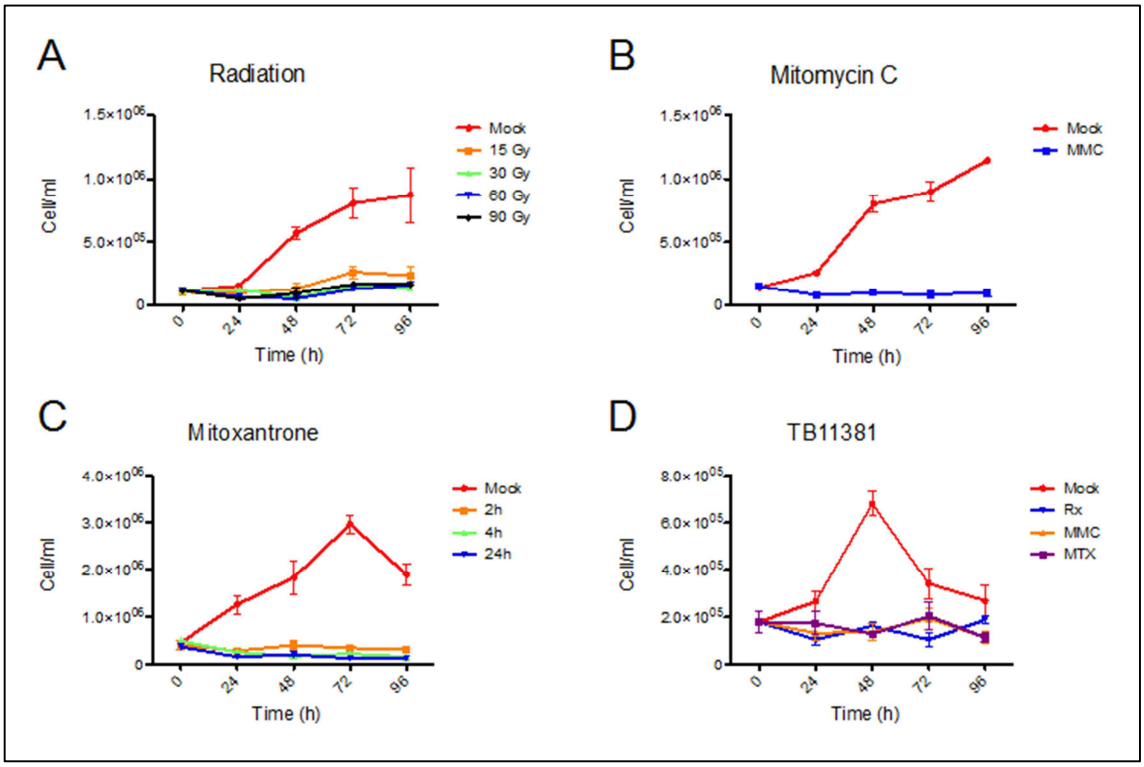

Fig 3.3 Arrest of proliferation of murine pancreatic cancer cells using irradiation or chemotherapeutic agents.

Figures represent DT6606 cell proliferation curve comparing number of viable cell over a 96 hours period after treatment with A) Increasing dose of irradiation from 15Gy to 120 Gy B) 50µg/ml MMC C) 2µM MTX applied for 2, 4 or 24 hours. D) Optimal doses were tested in TB11381 cell lines

MMC dose of 50µg/ml for 2 hours was previously validated by our group members [Ahmed *et al.* unpublished data] to be sufficient to arrest the proliferation of DT6606 cells. The results were further confirmed (Fig 3.3 B).

An MTX dose of 2µM applied for 24 hours was similarly validated by our group [El-Khoury *et al*. unpublished data]. However the incubation period was not compatible with my VICCV regimen as life cycle of vaccinia virus is much shorter (8 hours). This

means that by 24 hours many of the infected cells would have died and virus particles released into the supernatant potentially affecting the efficacy and safety of the VICCV. Shorter exposure periods of 2 and 4 hours were tested (Fig. 3.3 C) and both appear sufficient.

These doses were confirmed in a second murine pancreatic cell line, TB11381 (Fig 3.3 D).

3.3 Induction of tumour specific immunity using virus-infected cancer cells plus secondary treatment

3.3.1 Heterologous vaccination using Ad5 and VVL15 viruses

To test the effect of the secondary treatment on the anti-tumour immunity of the VICCV, three groups of mice (n=3) were vaccinated with DT6606 infected with adenovirus prime and vaccinia virus boost. Two of these groups had a secondary treatment of Rx or MMC (MTX was introduced at a later stage in this study). Control groups of PBS and MMC-proliferation arrested cells were used. The results suggest that the secondary treatment had no effect on the level of the anti-tumour immunity induced by VICCV (Fig 3.4). Tumour specificity was similarly preserved. Comparing IFN-γ released when stimulated with DT6606 vs LLC showed significant difference across all treatment groups (Ad/VV group p=0.0097, Ad/VV+MMC group p=0.0182, Ad/VV group p=0.023, Paired *t*-test).

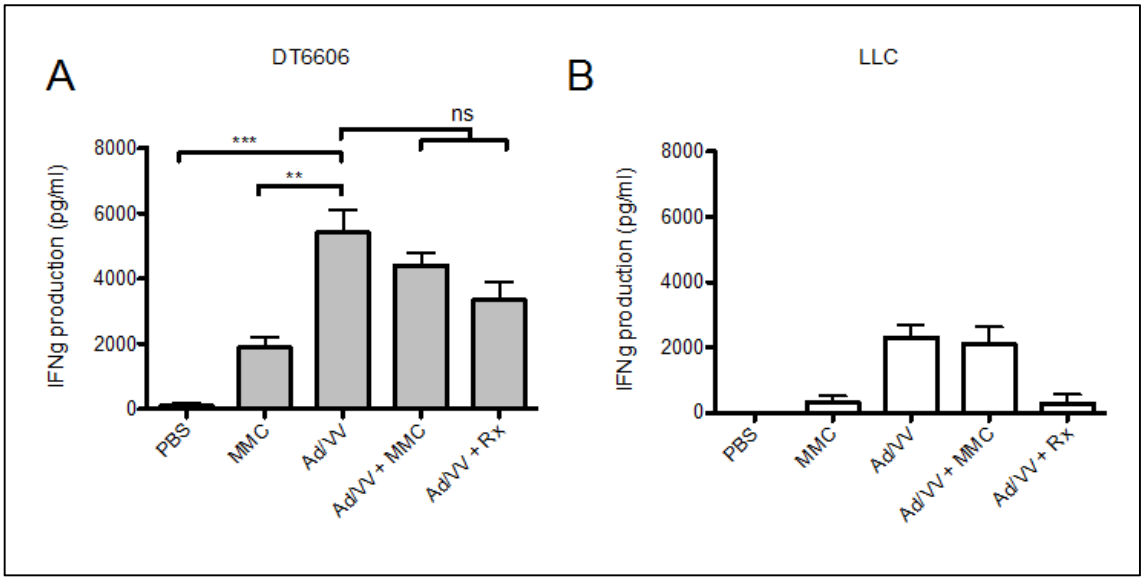

Fig 3.4 Secondary treatment does not affect tumour-specific splenocyte activation post VICCV.

Five groups of C57BL/6 mice (n=3) were vaccinated with PBS, MMC-treated DT6606 cells, Ad5-infected cells or Ad5 plus irradiation or MMC. Mice were similarly boosted four weeks later using VVL15. Spleens were harvested and processed two weeks after boost. Isolated splenocytes were incubated for 72 hours with proliferation arrested A) DT6606 cells or B) control LLC cells. IFNγ production, as an indicator of CD8 activation, in the supernatant was measured by ELISA. IFNγ levels were normalized by subtracting background release from non-stimulated splenocytes. One-way ANOVA with Tukey post-hoc test was used to compare groups. Columns represent the means ± SEM; asterisks denote the significance levels as comparing: ns non-significant; * $p \leq 0.05$; ** $p \leq 0.01$; *** $p \leq 0.001$.

3.3.2 Homologous regimen using *dl1520* virus

The *dl1520* mutant of adenovirus was chosen for this experiment as it is the only oncolytic virus licensed for clinical use (in China, H101 virus, Shanghai Sunway Biotech, China). The established safety record and the commercial availability of GM-standard virus would make a potential clinical trial more feasible.

Additionally we have tested MTX as a secondary treatment group due to the drug's ability to induce immunogenic cell death [391] and enhance the anti-tumour immunity when combined with OVs [392].

In this experiment, four groups of mice (n=3) were treated with homologous prime/boost VICCV using *dl1520* alone or with one of three secondary treatments. In addition, to validate if the observed anti-tumour response was due to the virus infection or the secondary treatment, three control groups were introduced in which the cells were treated with Rx, MMC or MTX but no virus infection. PBS acted as a negative control. These results confirmed the previous finding that secondary treatment does not affect the induction of anti-tumour immunity and the specificity of the VICCV (Fig. 3.5).

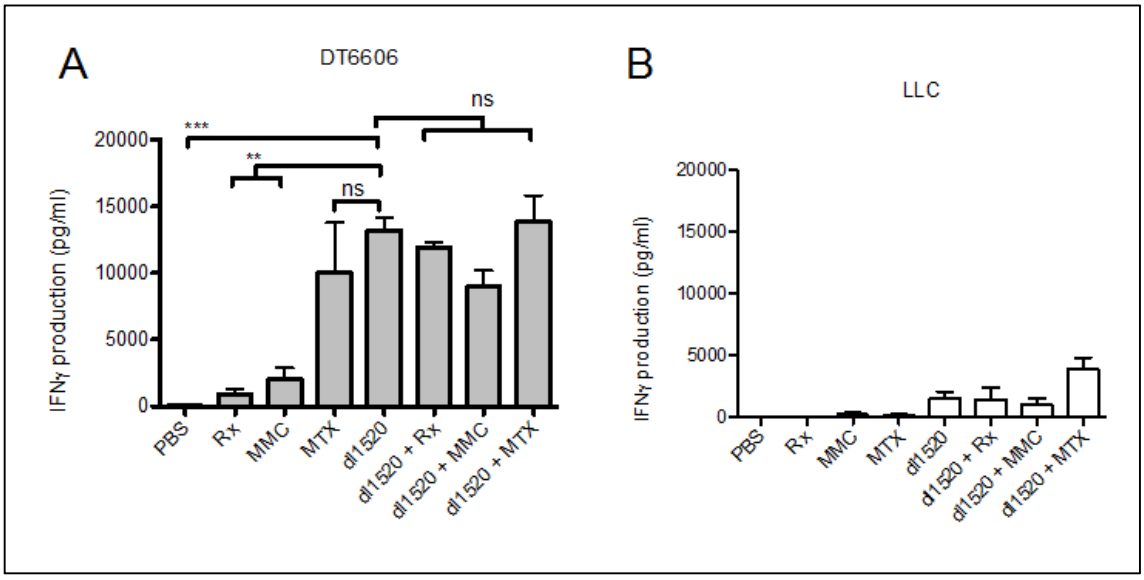

Fig 3.5 Secondary treatment does not affect tumour-specific splenocyte activation post VICCV.

Eight groups of C57BL/6 mice (n=3) were vaccinated with homologous prime/boost regimen using PBS or DT6606 cells treated with MMC, MTX, RX, *dl1520* or *dl1520* plus a secondary treatment. Spleens were harvested and processed two weeks after boost. Isolated splenocytes were incubated for 72 hours with proliferation arrested A) DT6606 cells or B) control LLC cells. IFNγ production, as an indicator of CD8 activation, in the supernatant was measured by ELISA. IFNγ levels were normalized by subtracting background release from non-stimulated splenocytes. One-way ANOVA with Tukey post-hoc test was used to compare groups. Columns represent the means ± SEM; asterisks denote the significance levels as comparing: ns non-significant; * $p \leq 0.05$; ** $p \leq 0.01$; *** $p \leq 0.001$.

Of note, DT6606 treated with MTX only resulted in high level anti-tumour immunity comparable to the virus treated groups. However, this was a single experiment with wide variation between the IFN-γ secreted from splenocytes derived from the three mice in the treatment group (as demonstrated with high error bars in fig 3.5 above). This high level expression was not seen in multiple comparable experiments performed by other team members [El-Khouri *et al*, unpublished data].

3.4 Efficacy of vaccination regimen

3.4.1 Efficacy of various homologous and heterologous VICCV combinations

To validate if the level of IFN-γ release from stimulated CD8 cells *(section 3.1.2)* correlates with clinical efficacy, five groups of mice (n=6 or 7) were vaccinated with either MMC-treated DT6606 cells or various homologous and heterologous Ad5 or VVL15-infected cells with a secondary treatment of MMC. Two weeks after boost mice were re-challenged with $5x10^6$ DT6606 cells via subcutaneous injection in the contra lateral flank. Ad/Ad VICCV group showed significantly longer survival compared to other groups (Fig. 3.6 A). The shorter survival in the Ad/VV group was not related to tumour growth but to the death of four mice around day 35 due to fighting between male mice. In fact the Ad/Ad and Ad/VV groups were identical in terms of protection against tumour re-challenge (Fig. 3.6 B).

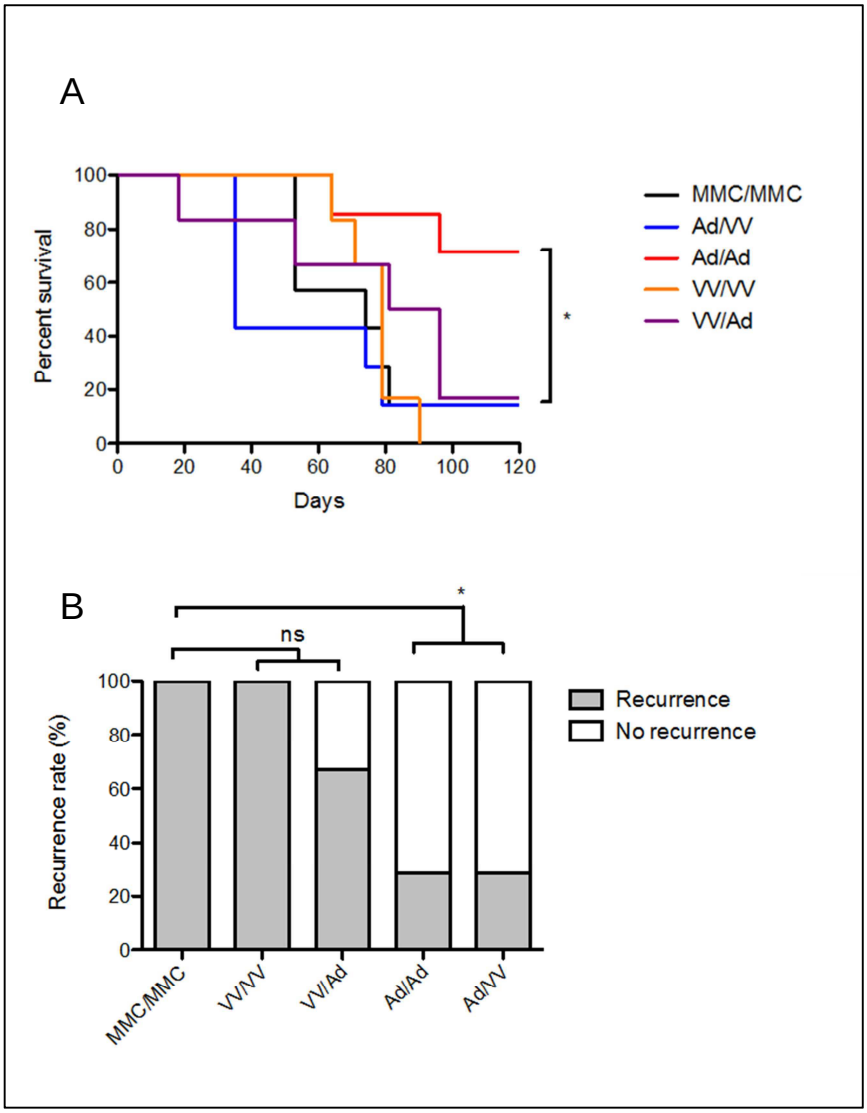

Fig 3.6 Efficacy study of VICCV using various homologous and heterologous virus combinations.

5 groups of mice (n=6 or 7) were vaccinated with $2x10^6$ MMC-treated DT6606 cells or heterologous VICCV regimen using the same number of cells infected with various combinations of AdV or VV plus MMC. Two weeks after boost, mice were re-challenged via subcutaneous injection with $5x10^6$ viable DT6606 cells. A) Ad/Ad vaccination group resulted in significantly longer survival compared to other groups. B) The same data presented as recurrence rate after tumour re-challenge to account for mice dying from non-tumour related injuries. Fisher's Exact test was used to compare various groups to control. p values were corrected to account for multiple group analysis. Asterisks denote the significance levels as comparing: ns non-significant; * $p \leq 0.05$; ** $p \leq 0.01$; *** $p \leq 0.001$.

3.4.2 Escalating tumour re-challenge dose

High tumour burden remains a significant challenge facing any immunotherapy [393]. To test the limit of tumour burden our VICCV regimen can protect against, four groups of mice were vaccinated with DT6606 cells infected with adenovirus prime and vaccinia virus boost plus MMC secondary treatment. One control group vaccinated with MMC-treated cells was also included. Two weeks later mice were challenged with an escalating dose of DT6606 subcutaneously. These results suggest that VICCV can protect against a tumour challenge three times the amount of the vaccination dose (Fig. 3.7).

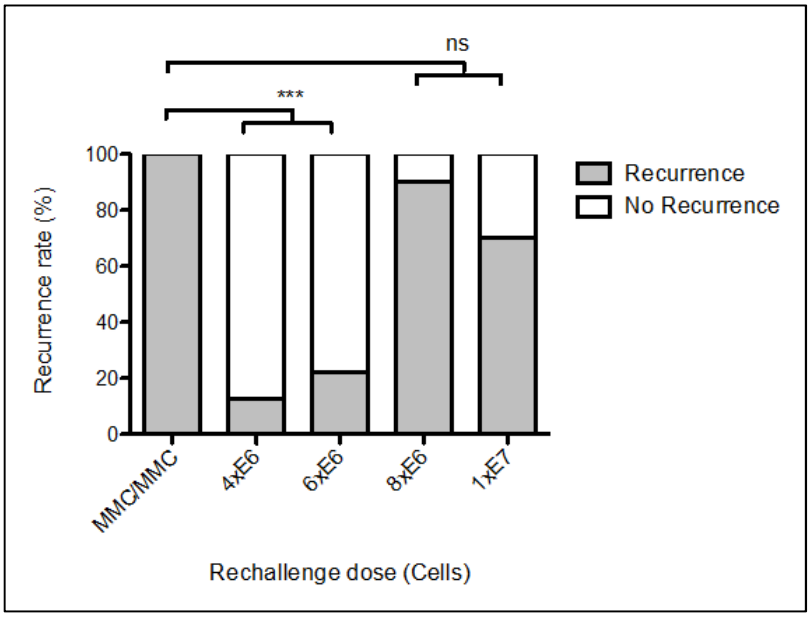

Fig 3.7 Escalating tumour re-challenge dose after VICCV.
5 groups of mice (n=10 to 14) were vaccinated with $2x10^6$ MMC-treated DT6606 cells or heterologous VICCV regimen using the same amount of cells infected with Ad5 plus MMC prime and VVL15 plus MMC boost. Two weeks after boost, mice were re-challenged via subcutaneous injection with increasing dose of viable DT6606 cells. VICCV appears to protect against tumour challenge three times the amount of vaccination dose. Fisher's Exact test was used to compare various groups to control. p values were corrected to account for multiple group analysis. Aasterisks denote the significance levels as comparing: ns non-significant; * $p \leq 0.05$; ** $p \leq 0.01$; *** $p \leq 0.001$.

3.5 32Dp210 murine leukaemia model

Having proved the efficacy of the VICCV in the pancreatic cancer model we wanted to test it in other models. We chose a leukaemia model as it is significantly different from other epithelial cancer models where the challenges are likely to be similar to pancreatic models. In addition, if this regimen proves successful, it will be easier to translate in leukaemia patients due to the ease of which we can harvest autologous cancer cells compared to pancreatic cancer.

3.5.1 MTS and viral infectability

To calculate the required viral dose for a safe VICCV regimen, MTS assay was performed on 32Dp210 cell line for both Ad5 and VVL15 giving EC50 values of 1945 pfu/cell and 36 pfu/cell respectively (Fig 3.8 A). This is almost 500 times higher than that of pancreatic cell lines. Such high viral dose could lead to severe toxic effect on the mice. However, with the induction of secondary treatment, such high viral dose may not be necessary as the secondary treatment will arrest the proliferation of any cells not killed by the virus.

We hypothesised that if a sufficient percentage of vaccine cells are infected there will be enough virus at the vaccination site to provide that “danger signal” required for an effective anti-tumour immunity.

To test the infectibility of the 32Dp210 cells we infected them with AD5-GFP-PL11 and VVL15-RFP. Percentage of infected cells was determined using flow cytometry (Fig 3.8 B-C). Based on these results we decide to use an MOI of 100 pfu/cell for Ad5 and 10 pfu/cell for VVL15.

5.5.2 Secondary treatment

Cell proliferation arrest using secondary treatment was validated (Fig. 3.8 D). These cells were sensitive to treatment with MMC, MTX or radiation at the doses used previously.

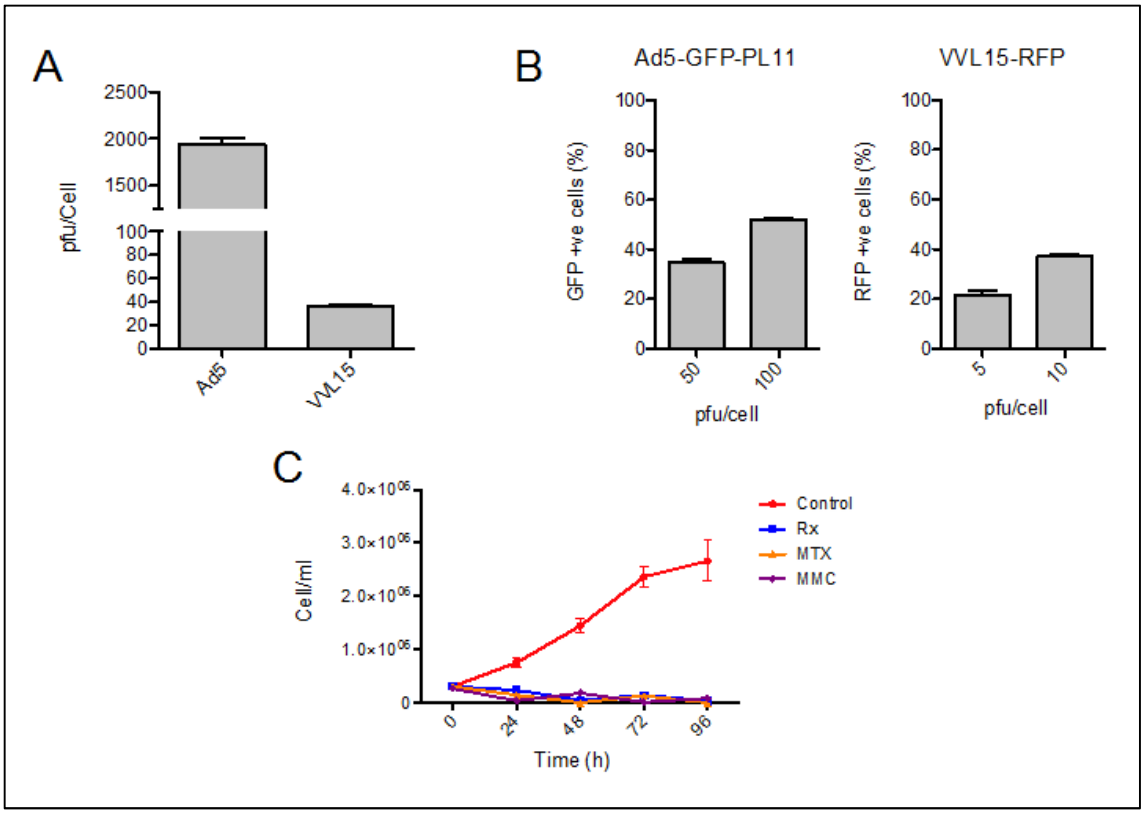

Fig 3.8 Validation of cell kill, infectibility and cell proliferation arrest in 32Dp210 cell line.

A) The graph represents EC50 values of both Ad5 and VVl15 in 32Dp210 cell line obtained from viral dose-response curve using MTS assay. B) Cell infectability represented as a percentage of fluorescent cells out of the total viable cells after infection with Ad5-GFP-PL11 or VVL15-RFP with two different MOIs for each virus. C) Figure compares cell proliferation over a 96 hours period after treatment with Rx, MMC or MTX.

3.5.3 Induction of tumour specific immunity

C3H/HeN mice were vaccinated as described previously with $1x10^6$ 32Dp210 cells infected with various combinations of Ad5 and VVL15 plus MMC secondary treatment.

Unfortunately, our hypothesis was proven incorrect as there was no difference between viral groups and MMC control or between target and control cell line (Fig. 3.9).

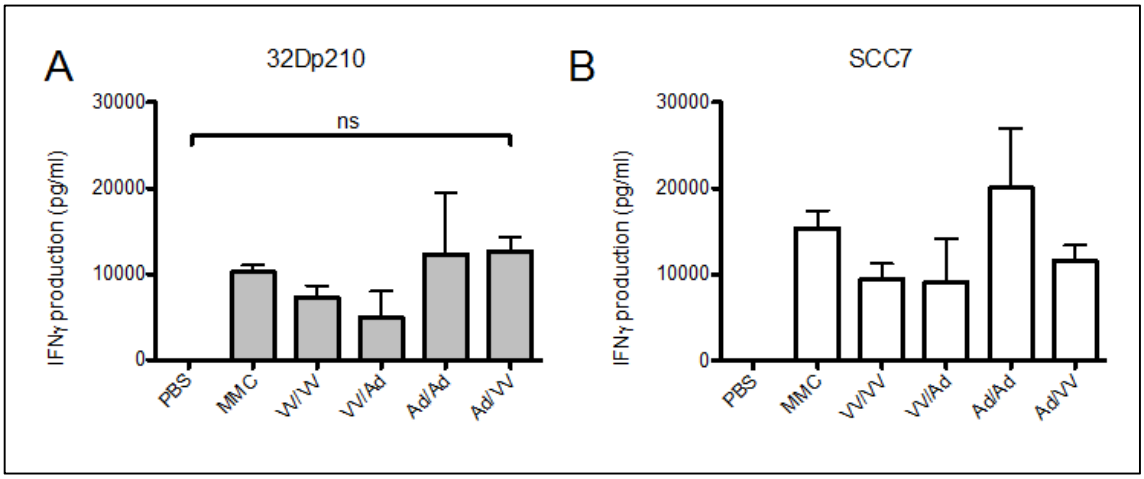

Fig 3.9 VICCV did not induce tumour specific immunity in the 32Dp210 model compared to control.

Seven groups of C3H/HeN mice (n=3) were vaccinated with PBS, 1x 10^6 MMC-treated 32dp210 cells or various homologous and heterologous prime/boost combinations using Ad5 plus MMC and VVL15 plus MMC-treated cells. Spleens were harvested and processed two weeks after boost. Isolated splenocytes were incubated for 72 hours with proliferaion arrested A) 32Dp210 cells or B) control SCC7 cells. IFNγ production, as an indicator of CD8 activation, in the supernatant was measured by ELISA**.** IFNγ levels were normalized by subtracting background release from non-stimulated splenocytes. One-way ANOVA with Tukey post-hoc test was used to compare groups. Columns represent the means ± SEM; asterisks denote the significance levels as comparing: ns non-significant; * $p \leq 0.05$; ** $p \leq 0.01$; *** $p \leq 0.001$.

3.6 Effects of secondary treatment on oncolytic viruses

Various aspects of the virus life cycle have been examined to establish how they are affected by the secondary treatment and to explain how that contributed to the difference in anti-tumour immune response observed between the DT6606 and the 32Dp210 cell lines. All experiments were designed to match the *in vivo* work including viral dose, incubation period and secondary treatment.

3.6.1 Viral replication

The viral replication assay was performed. In the two pancreatic cell lines irradiation led to the reduction of the replication of both viruses while MMC and MTX treatments resulted in a near complete arrest of viral replication. The 32Dp210 cell line did not support adenovirus replication. On the other hand, vaccinia virus did replicate in these cells albeit to a much lower level compared to the other two (Fig 3.10 A-F).

3.6.2 Viral proteins synthesis

Despite the effect of secondary treatment on adenovirus replication, viral protein synthesis does not seem to be affected in both pancreatic cell lines. Similar levels of E1A protein were expressed regardless of the secondary treatment (Fig. 3.11 A and C).

Vaccinia virus showed a similar picture for irradiation. However MMC and MTX treatment resulted in significant reductions in viral protein synthesis (Fig. 3.11 B and D).

In comparison viral protein levels were significantly lower in the 32Dp210 cell lines (Fig. 3.11 E and F)

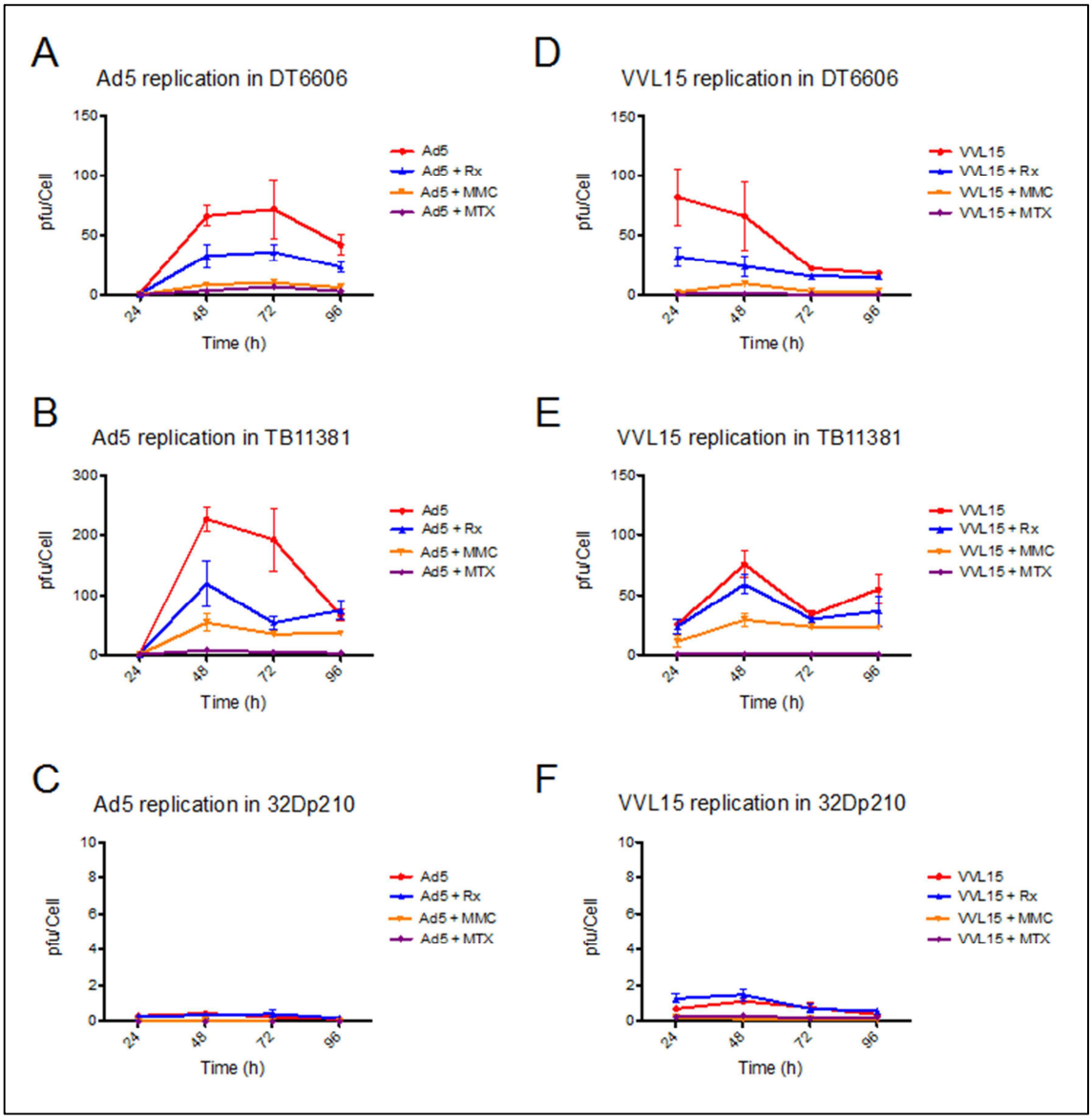

Fig 3.10 The effect of secondary treatments on viral replication in DT6606, TB11381 and 32Dp210 cell lines.

DT6606 and TB11381 cells were infected with Ad5 at MOI=50 pfu/cell or VVL15 at MOI=1 pfu/cell. 32Dp210 cells were infected at MOI 100 and 10 pfu/cell for Ad5 and VVL15 respectively. Cells were then treated with Rx, MMC, MTX or left untreated as control. Cell lysate were then harvested at 24, 48, 72 and 96 hours. Viral titers were determined using TCID50 assay. Each virus/cell line/treatment/time point combination was performed in triplicates. A, C and E) represent Ad5 replication in corresponding cell line. B, D and F) represent vaccinia virus replication.

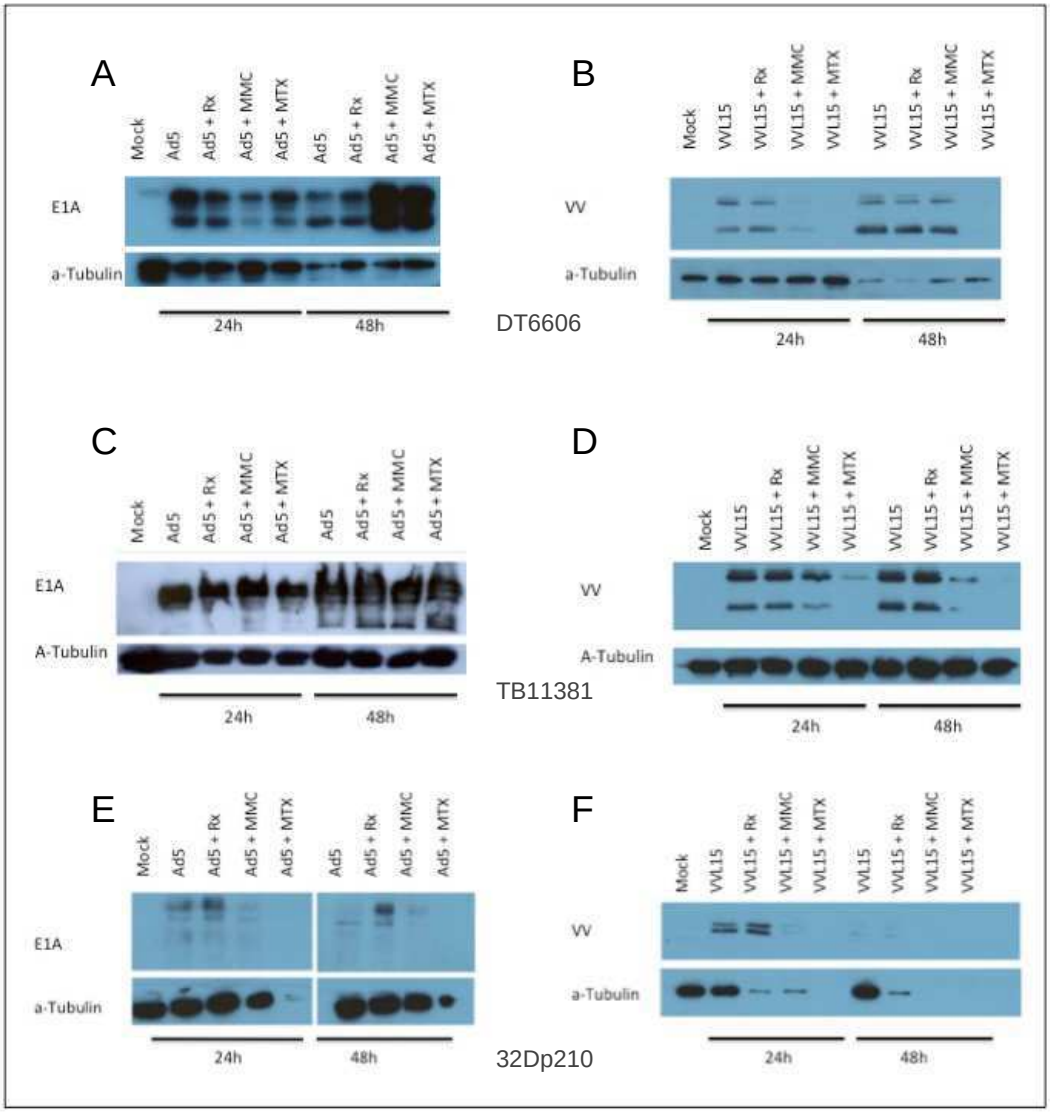

Fig 3.11 The effect of secondary treatments on viral protein expression in DT6606, TB11381 and 32Dp210 cell lines.

DT6606 and TB11381 cells were infected with Ad5 at MOI=50 pfu/cell or VVL15 at MOI=1 pfu/cell. 32Dp210 cells were infected at MOI 100 and 10 pfu/cell for Ad5 and VVL15 respectively. Cells were then treated with Rx, MMC, MTX or left untreated as control. Cell lysate were then harvested at 24 and 48 hours for western blotting using primary antibodies against adenovirus E1A protein and vaccinia virus. α-Tublulin was used as a loading control. A, C and E) represent Ad5 E1A protein expression in corresponding cell line. B, D and F) represent vaccinia virus protein expression.

3.6.3 Viral DNA replication

In the DT6606 cell line viral DNA replication was measured using qPCR. Copy numbers of viral DNA have more or less mirrored the pattern of protein expression (Fig 3.12 A and B).

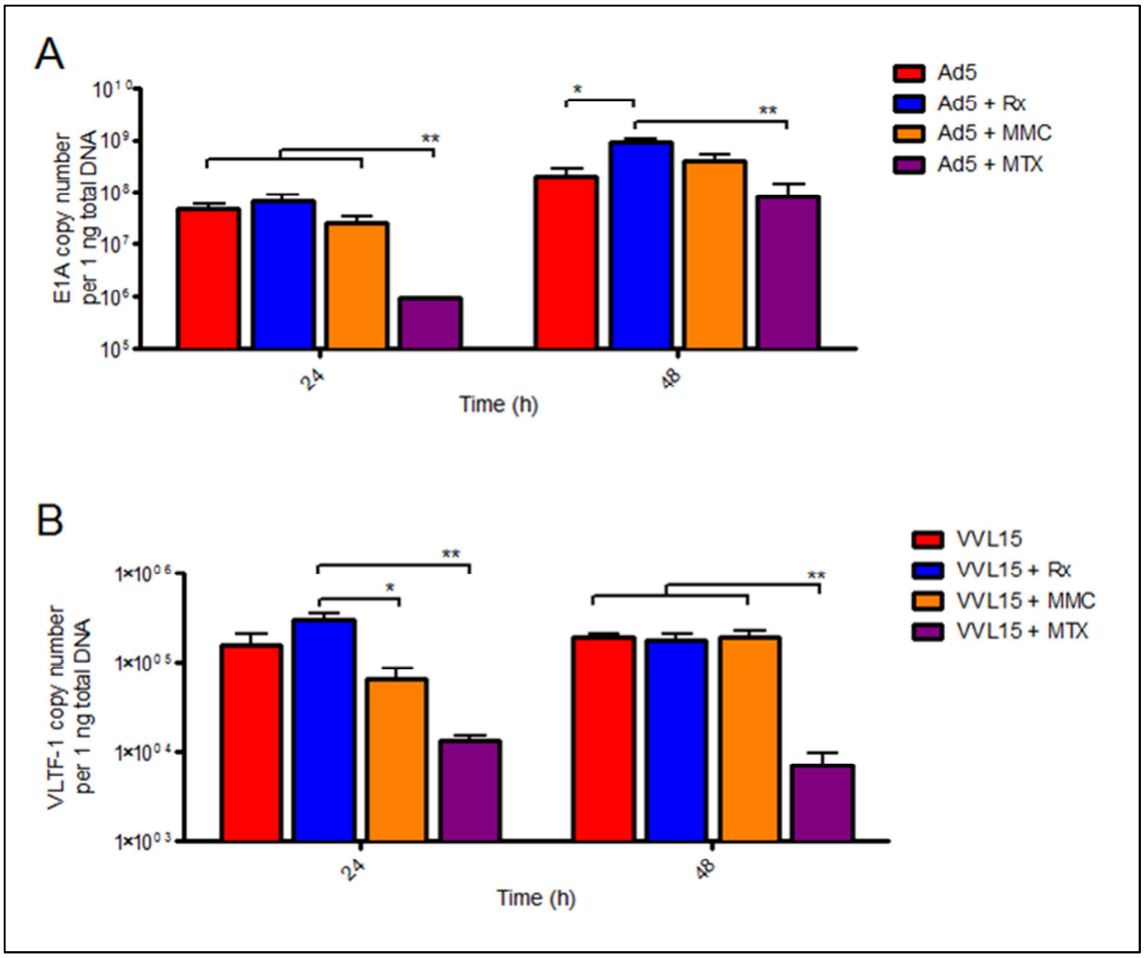

Fig 3.12 The effect of secondary treatments on viral DNA reapplication in DT6606 cell line.

DT6606 cells were infected with Ad5 at MOI=50 pfu/cell or VVL15 at MOI=1 pfu/cell. Cells were then treated with Rx, MMC, MTX or left untreated as control. Cell lysate were then harvested at 24, 48, 72 and 96 hours. DNA was extracted from and qPCR was performed as previously described. Each virus/cell line/treatment/time point combination was performed in triplicates. A) Graph represents adenovirus E1A gene copy numbers as compared to standard curve using purified viral DNA at 24 and 48 hours. B) Vaccinia virus VLTF-1 gene copy numbers calculated similarly. Columns represent the means ± SEM; asterisks denote the significance levels as comparing: ns non-significant; * $p \leq 0.05$; ** $p \leq 0.01$; *** $p \leq 0.001$.

3.7 Chapter three results summery

- Virus infected cancer cell vaccine can induce tumour specific immune response.
- The highest antitumour immune response was elicited in mice primed with cells pre-infected with adenovirus
- There was no difference in immune response when mice were boosted with either adenovirus or vaccinia virus pre-infected cells
- To enhance safety and arrest the proliferation of cancer cells prior to injection, a secondary treatment of radiation , mitomycin or mitoxantrone was added prior to injection
- Secondary treatment did not affect antitumour immunity
- Irradiation resulted in a reduction of both adenovirus and vaccinia virus replication. Mitomycin and mitoxantrone led to complete arrest of viral replication.
- Irradiation and mitomycin had limited effect on viral protein and viral DNA production while mitoxantrone reduced both.
- Moving forward, mitomycin was chosen as a secondary treatment rather than mitoxantrone for the following reasons:
    - There was no difference in immune response, as measured by IFN-γ, between MTX and MMC treatment groups
    - MTX resulted in rapid cell killing. This varied depending on the cell line. MMC was more predictable, allowing better reproducibility of results
    - Cells treated with MMC survived longer *in vitro*. Although, not demonstrated in our experimental work, we anticipate the same to apply

in vivo allowing longer exposure of the infected tumour cells to the immune system

- MTX interfered significantly in viral DNA and protein production especially in vaccinia virus making interpretation of results more difficult
- MTX is known to induce an immunogenic cell death while MMC does not. It will be difficult to distinguish if elicited immune response is due to the viral infection or MTX.

Chapter four: Head and Neck cancer animal model

For the purpose of this study three murine head and neck squamous cell carcinoma cell lines were obtained from our collaborators. These were SCC7, B4B8 and LY2 cells. These cells were injected orthotopically or subcutaneously to establish tumours. The growth of these tumours can be easily monitored. However, lung and lymph node metastasis will require sacrificing a large number of animals to allow histopathological examination of these tissues. Alternatively, imaging techniques can be utilised to monitor metastasis. We decided to use luciferase bioluminescence due to its high sensitivity and fast turnaround time compared to CT or MRI scans.

4.1 Establishment of Renilla luciferase stable head and neck cell lines

B4B8, LY2 and SCC7 cell line were transfected with Renilla-puromycin lentivirus vector and selected in puromycin for 2 weeks. Luciferase expression was confirmed in all cell lines (Fig. 4.1)

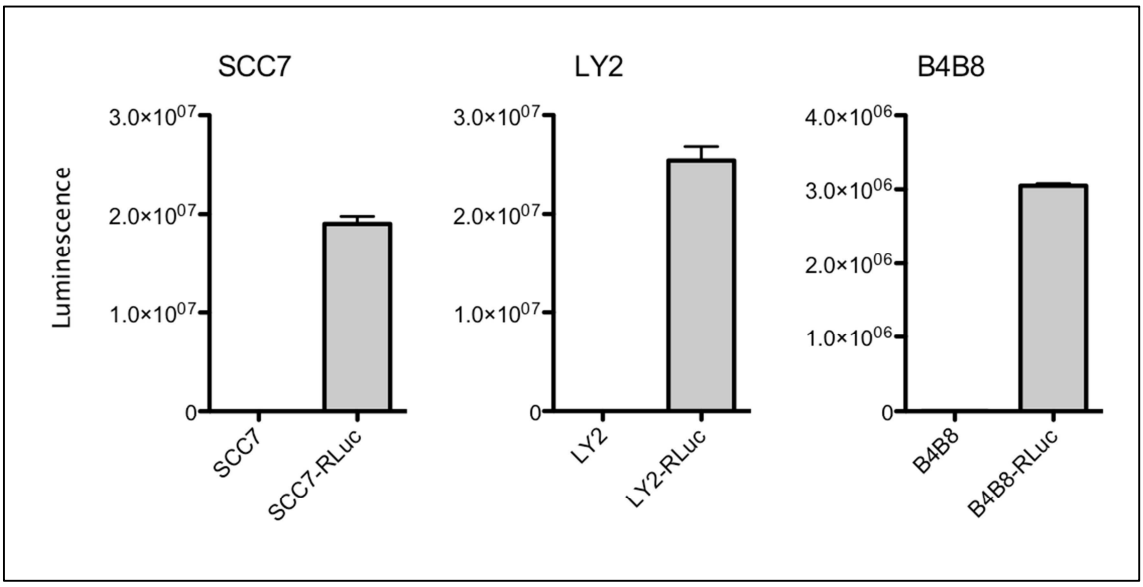

Fig 4.1 Validation of luciferase expression from stable cell lines.
$1x10^5$ SCC7, SCC7-RLuc, LY2, LY2-RLuc, B4B8 and B4B8-RLuc cells were plated in triplicate in a 24-wells plate and incubated overnight before being lysed. Coelenterazine was added to cell lysate and luminescence measured. Bar charts compares luminescence levels between parental and stable cell lines. Columns represent the means ± SEM.

4.2 HNSCC tumour model

4.2.1 Subcutaneous tumour model

To test the ability of Renilla luciferase-expressing cell lines to form tumours and metastasise to local lymph nodes and lungs, $1x10^6$ cells were injected subcutaneously in the right flank of BALB/c mice. Tumour volumes were measured twice a week. Mice were culled according to Home Office guidelines. Tumours, lungs and ipsilateral inguinal lymph nodes were harvested at the point of sacrifice, fixed with 4% formaldehyde and sent to Barts Cancer Institute Pathology lab for histopathological haematoxylin and eosin (H&E) staining. We chose not to use the B4B8-RLuc cells for this model as it is known from literature that these cells do not metastasise [394] limiting its clinical relevance. SCC7-RLuc tumours showed a rapid growth pattern leading to all mice being culled around three weeks after tumour inoculation. However

there was no lung or node metastasis on histological examination (Fig 4.2). LY2-RLuc tumours did not grow and the experiment was terminated after 30 days.

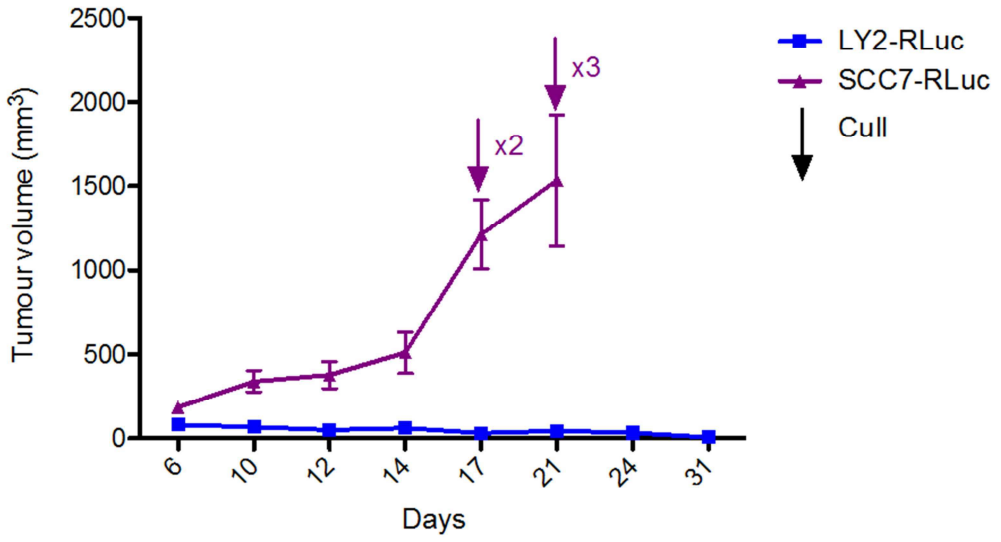

Cell line	Primary tumour	Lung mets	Node mets
SCC7-RLuc	5/5	0/5	0/5
LY2-RLuc	0/5	Experiment terminated	Experiment terminated

Fig 4.2 Growth pattern and metastasis rates in subcutaneous HNSCC murine model. $1x10^6$ SCC7-RLuc and LY2-RLuc cells were injected subcutaneously in the flank of 5 C3H/HeN and BALBC/c female mice respectively. Tumour sizes were measured twice a week. Lungs and lymph nodes were harvested at the point of animal sacrifice, fixed and stained to evaluate metastasis. The graph shows tumour growth curves over time. Points represent the means. Error bars represent SEM. ↓Xn indicates the number of animals culled at that time point. Table shows the number of animals developing primary tumours, lung metastasis and lymph node metastasis.

4.2.2 Orthotopic tumour model

Similarly we tested the ability of the three luciferase tumour cell lines to form tumour and metastasise when implanted orthotopically in the right cheeks via intraoral injection under inhalation anaesthesia. Similar to the subcutaneous model, SCC7-RLuc cells showed a rapid growth pattern leading to the animals being culled at 17 days (Fig 4.3).

Only one animal showed a single lung metastatic tumour nodule (Fig 4.4) but no lymph nodes metastasis was seen.

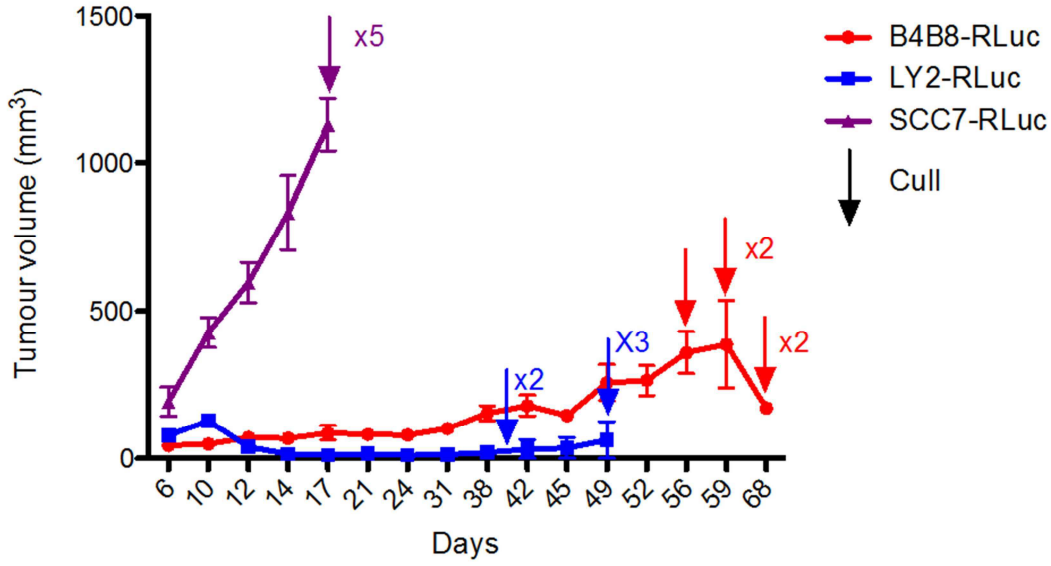

Cell line	Primary tumour	Lung mets	Node mets
SCC7-RLuc	5/5	1/5	0/5
LY2-RLuc	2/5	3/5	4/5

Fig 4.3 Growth pattern and metastasis rates in orthotopic HNSCC murine model.
$1x10^6$ SCC7-RLuc, B4B8-RLuc and LY2-RLuc cells were injected in the cheek of 5 C3H/HeN and BALBC/c female mice respectively. Tumour sizes were measured twice a week. Lungs and lymph nodes were harvested at the point of animal sacrifice, fixed and stained to evaluate metastasis. The graph shows tumour growth curves over time. Points represent the means. Error bars represent SEM. ↓Xn indicates the number of animals culled at that time point. Table shows the number of animals developing primary tumours, lung metastasis and lymph node metastasis.

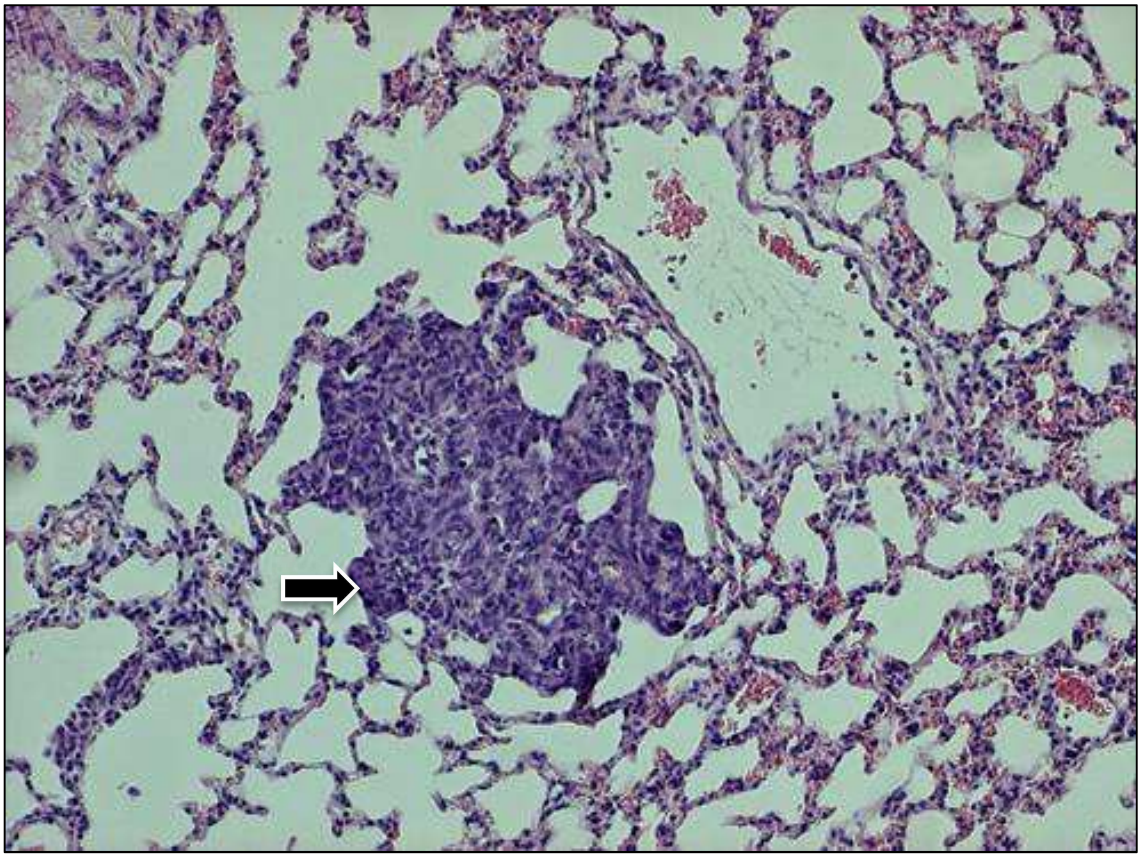

Fig 4.4 Lung metastasis from SCC7-RLuc orthotopic tumour
H&E high power view (x100) showing single metastatic SCC7-RLuc tumour deposit (arrow) within lung tissue.

B4B8-RLuc showed a very slow growth with the animals surviving more than two months (Fig 4.3). Only two of the LY2-RLuc injected animals developed palpable tumours and even these two grow very slowly. However these mice started to lose weight around 30 days following tumour injection and started to develop large cervical lymph nodes (Fig 4.5). Histological examination showed 60% and 80% rate of lung and lymph nodes metastasis respectively (Fig 4.5).

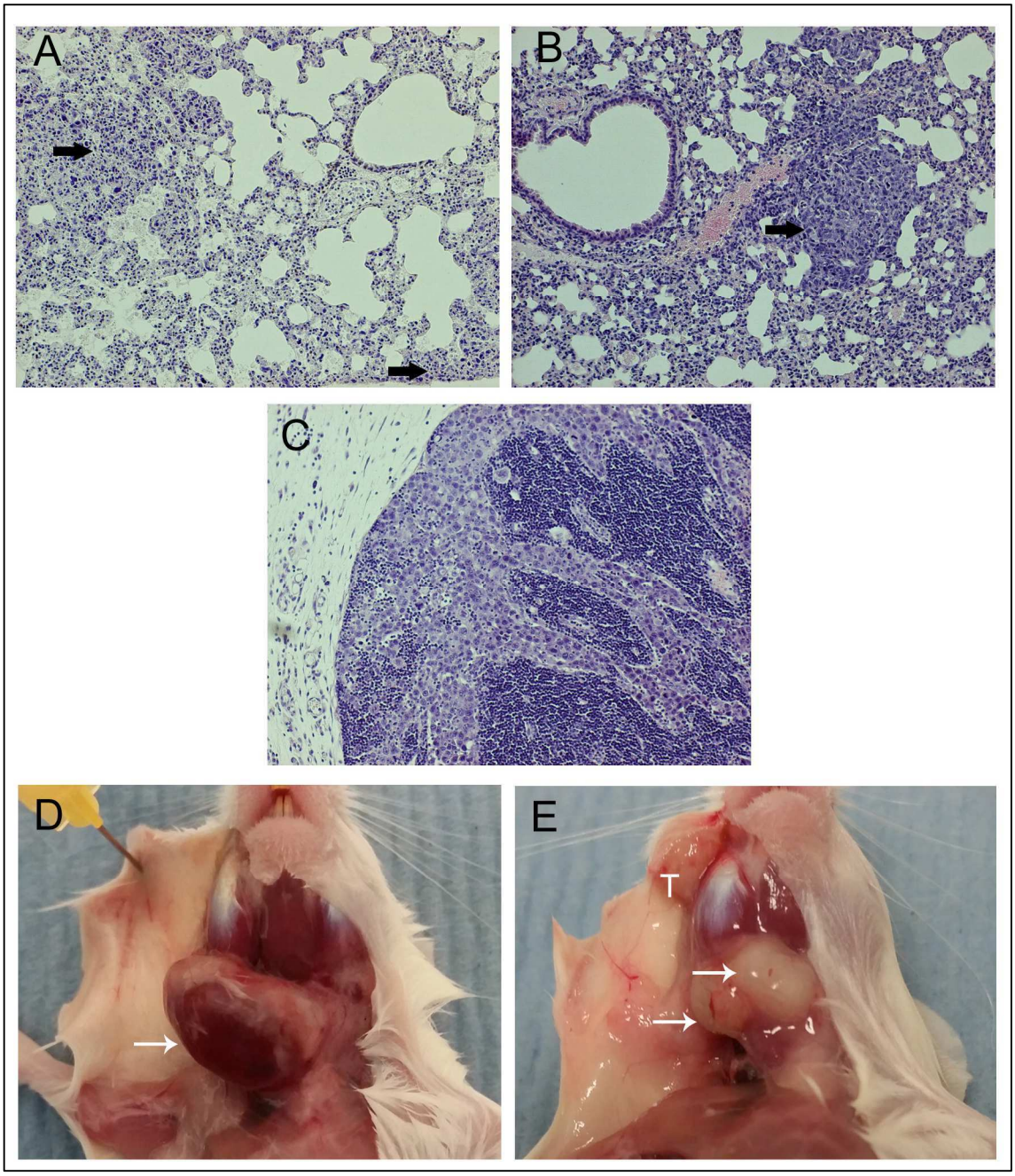

Fig 4.5 Lung and lymph node metastasis in orthotopic LY2-RLuc tumour model.

H&E high power view (x100) showing A) disseminated metastatic LY2-RLuc tumour infiltration (arrows) within the lung tissue. B) metastatic nodule in the lung. C) lymph node metastasis destroying the normal architecture of the node. D and E) post-mortem examination showing primary tumour (T) and metastatic cervical lymph nodes (white arrows).

To validate if the slow growth rate in LY2-RLuc and B4B8-RLuc tumours is related to luciferase transfixion or low number of injected tumour cells, we repeated the experiment using both parental and luciferase-expressing cell lines at a higher dose of $5x10^6$ cells. B4B8 tumours (Fig 4.6) showed an initial rapid growth phase followed by tumour regression. Tumours started to grow gradually after 30 days. On the other hand B4B8-RLuc tumours showed a very slow steady growth rate. Neither cell line showed lung or lymph node metastasis (Fig 4.7).

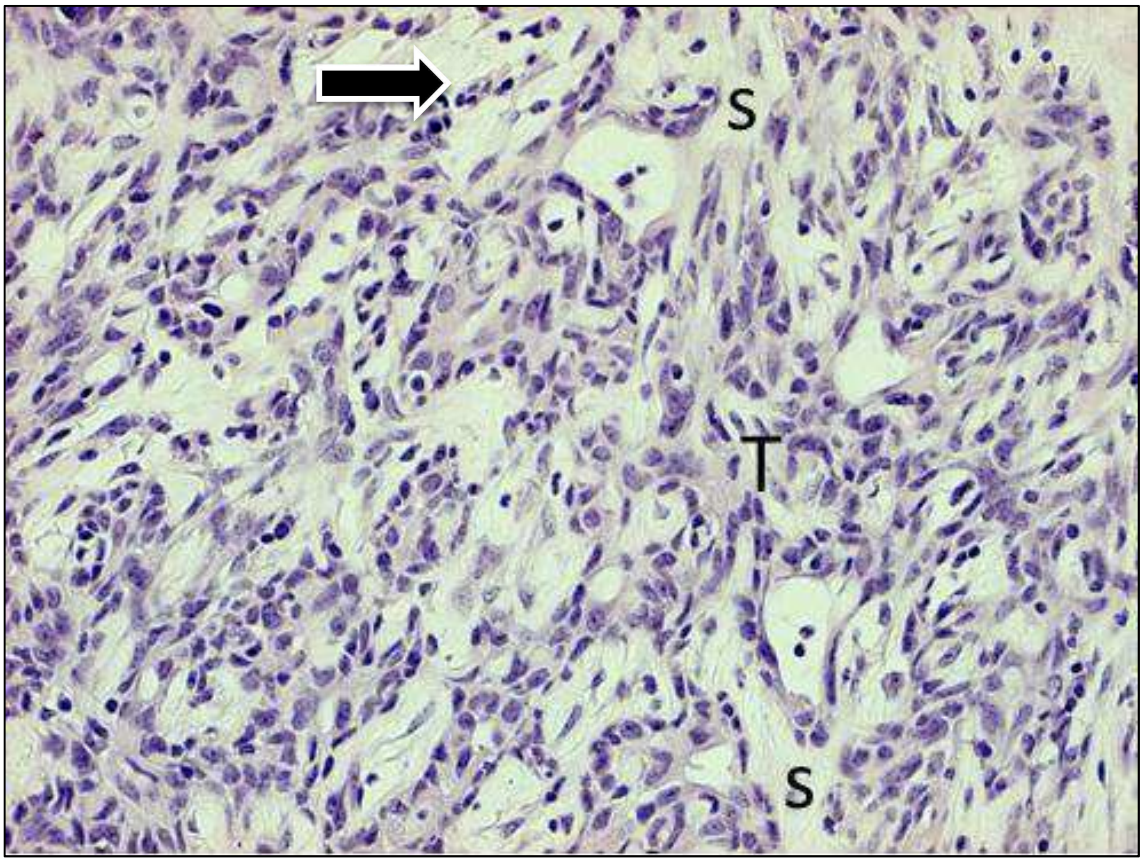

Fig 4.6 Histological features of B4B8 tumours.

H&E high power view (x200) of the orthotopic B4B8 tumours. T) shows tumour cells, s) shows fibrous stroma and arrow) shows infiltrating immune cells.

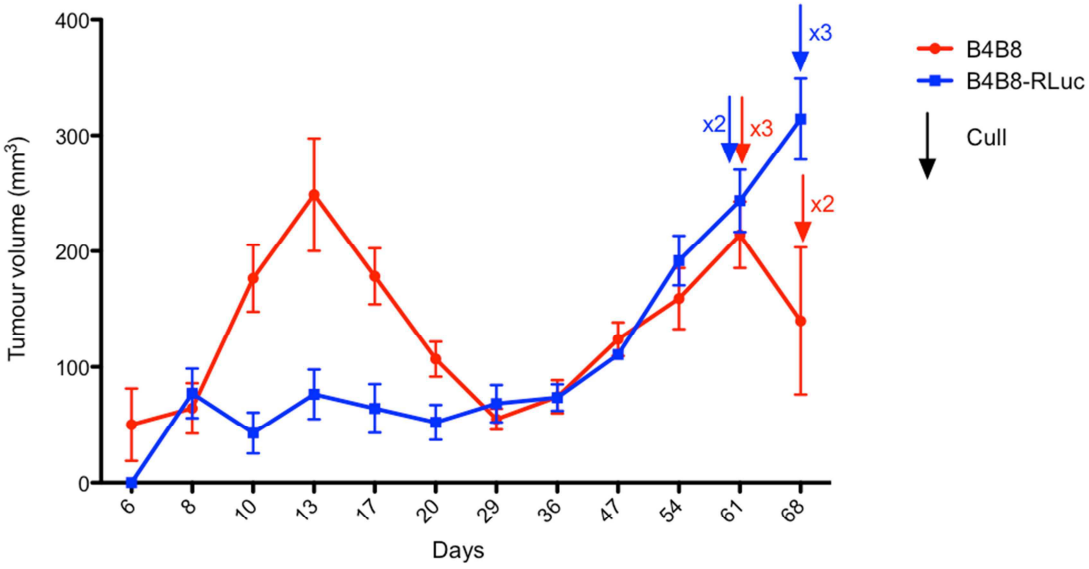

Cell line	Primary tumour	Lung mets	Node mets
B4B8	5/5	0/5	0/5
B4B8-RLuc	5/5	0/5	0/5

Fig 4.7 Growth pattern and metastasis rates in orthotopic B4B8 murine tumour model. $5x10^6$ B4B8 and B4B8-RLuc cells were injected in the cheek of 5 BALBC/c female mice. Tumour sizes were measured twice a week. Lungs and lymph nodes were harvested at the point of animal sacrifice, fixed and stained to evaluate metastasis. The graph shows tumour growth curves over time. Points represent the means. Error bars represent SEM. ↓Xn indicates the number of animals culled at that time point. Table shows the number of animals developing primary tumours, lung metastasis and lymph node metastasis.

LY2 tumours grew rapidly with the animal losing weight rapidly leading to cull at 2 weeks. 4 out of 5 mice developed lymph node metastasis but no lung metastasis. This was likely related to rapid tumour progression and early culls. The luciferase-expressing cells did not grow into overt tumours except in one animal, however all animals had lung and lymph node metastasis (Fig 4.8). We suspect that the absence of primary tumours is likely to be a detection failure as the tumours are likely to be very small and embedded in the masseter muscle. This speculation is supported by our

observation in subcutaneous tumours where all mice developed tumours, albeit small (Fig 4.12).

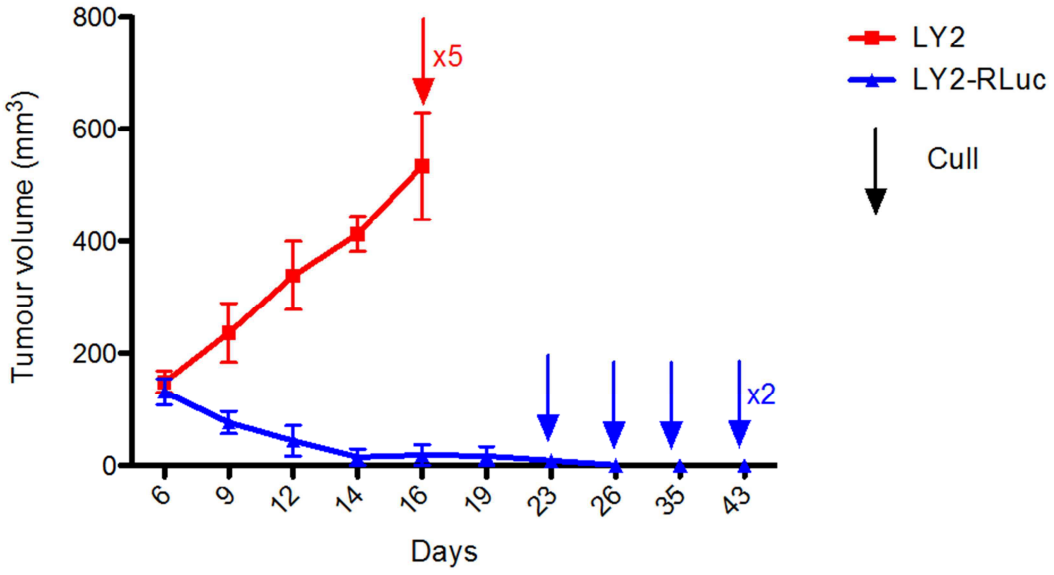

Cell line	Primary tumour	Lung mets	Node mets
LY2	5/5	0/5	4/5
LY2-RLuc	1/5	5/5	5/5

Fig 4.8 Growth pattern and metastasis rates in orthotopic LY2 murine tumour model. $5x10^6$ LY2 and LY2-RLuc cells were injected in the cheek of 5 BALBC/c female mice. Tumour sizes were measured twice a week. Lungs and lymph nodes were harvested at the point of animal sacrifice, fixed and stained to evaluate metastasis. The graph shows tumour growth curves over time. Points represent the means. Error bars represent SEM. ↓Xn indicates the number of animals culled at that time point. Table shows the number of animals developing primary tumours, lung metastasis and lymph node metastasis.

4.3 Surgical excision model

4.3.1 Subcutaneous surgical excision model

Head and neck cancer management often include surgical excision of the tumour followed by chemoradiotherapy. These tumours have a high rate of neck node metastasis [395, 396] and the most mortalities are due to locoregional recurrence [397]. To simulate these clinical characteristics we implanted LY2, LY2-RLuc, SCC7 or SCC7-RLuc tumour cells subcutaneously in the right flank of the animal. Tumour were excised when approaching 1 cm^2 in size (maximum size permitted by Home Office is 1.44 cm^2) or if ulcerating. Animals were monitored for change of weight, local tumour recurrence and lymph node involvement. Animals were culled according to guidelines. Tumours, lungs and lymph nodes were harvested as previously described.

SCC7 and SCC7-RLuc tumours (Fig 4.9) were injected subcutaneously at a dose of $1x10^6$ cells. They grew rapidly and recurred after surgical excision. However the animals remained healthy throughout with no weight loss or cachexia. Animals were culled due tumours reaching the maximal permitted size. None of these animals developed lung or lymph node metastasis (Fig 4.10).

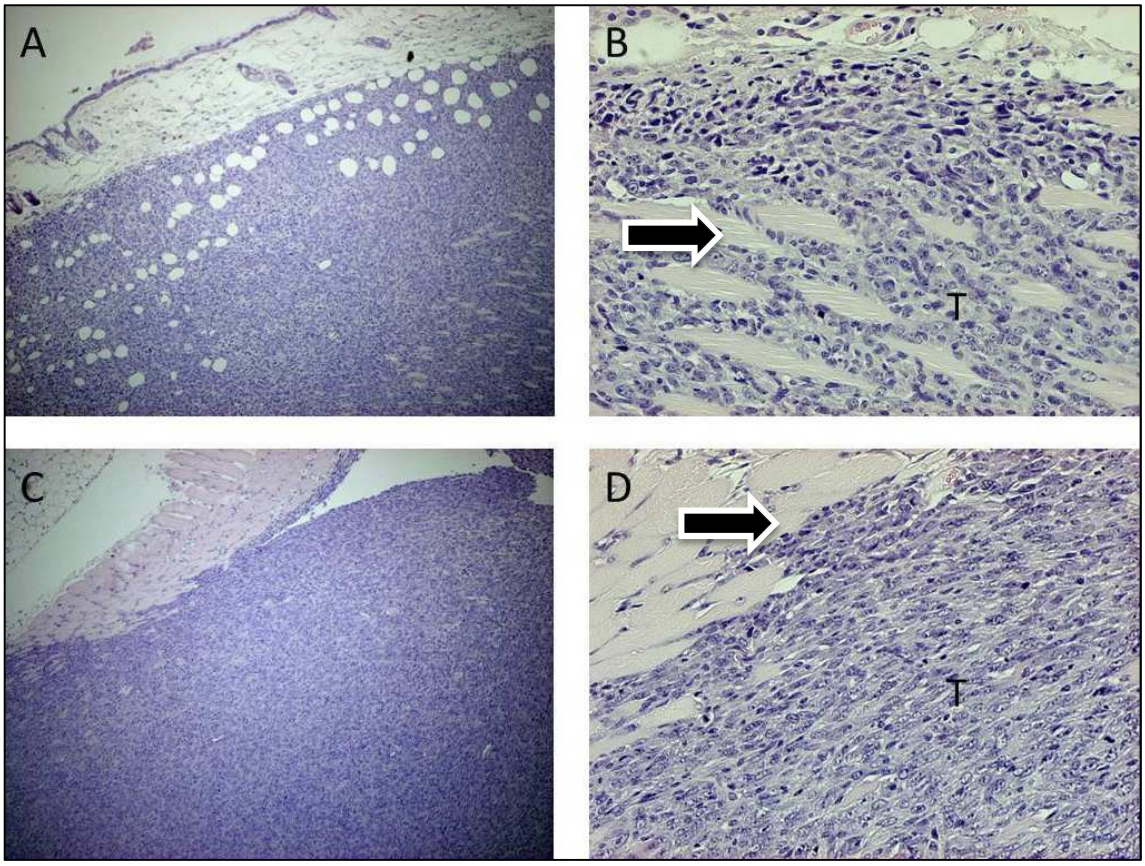

Fig 4.9 Histological features of SCC7 tumours.

A) H&E low power view (x40) of subcutaneous SCC7 tumours. B) high power view (x200) showing tumour cells (T) invading subcutaneous muscles (arrow). C and D) Similar features were seen in SCC7-RLuc tumours.

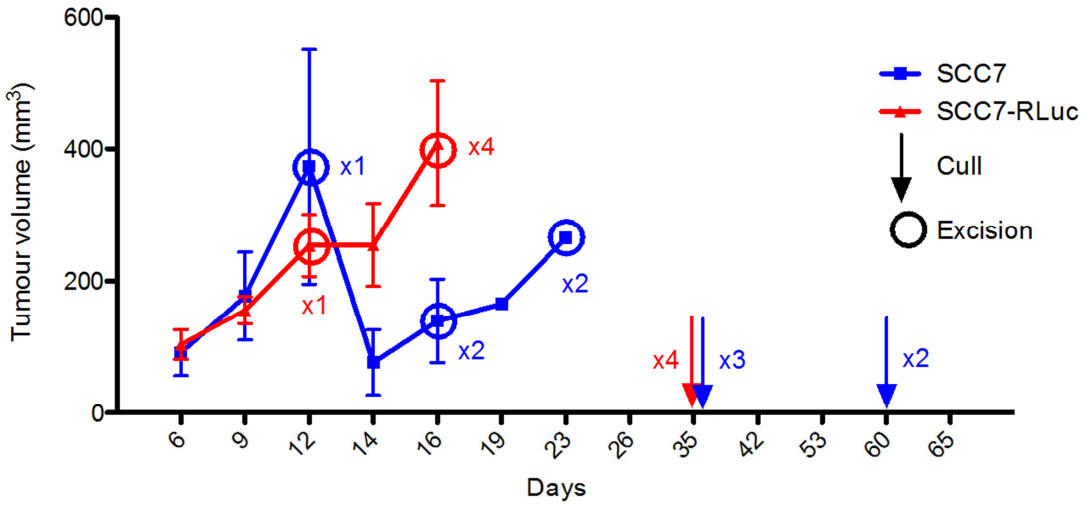

Cell line	Primary tumour	Recurrent tumour	Lung mets	Node mets
SCC7	5/5	4/5	0/5	0/5
SCC7-RLuc	5/5	4/4 (one mouse culled due to wound breakdown)	0/4	0/4

Fig 4.10 Growth pattern, recurrence and metastasis rates in surgical excision HNSCC murine model using SCC7 cells.

$1x10^6$ SCC7 and SCC7-RLuc cells were injected subcutaneously in the right flank of 5 C3H/HeN female mice. Tumour sizes were measured twice a week and excised around 1 cm^2 in size or if ulcerating. Animals were monitored for tumour recurrence and weight loss. Lungs and lymph nodes were harvested at the point of animal sacrifice, fixed and stained to evaluate metastasis. The graph shows tumour growth curves over time. Points represent the means. Error bars represent SEM. Open circles represent time point of tumour excision. Arrows represent time point of animal cull. Xn indicates the number of animal treated or culled at that time point. Table shows the number of animals developing primary and

LY2 tumours (Fig 4.11) showed a slow initial growth pattern followed by a rapid increase in volume. All tumours showed tumour ulceration and invaded underlying muscle. Animals became severely cachexic around 10 days after excision and they all showed lung and node metastasis. The pattern was fairly similar, albeit slower, in the LY2-RLuc tumours (Fig 4.12).

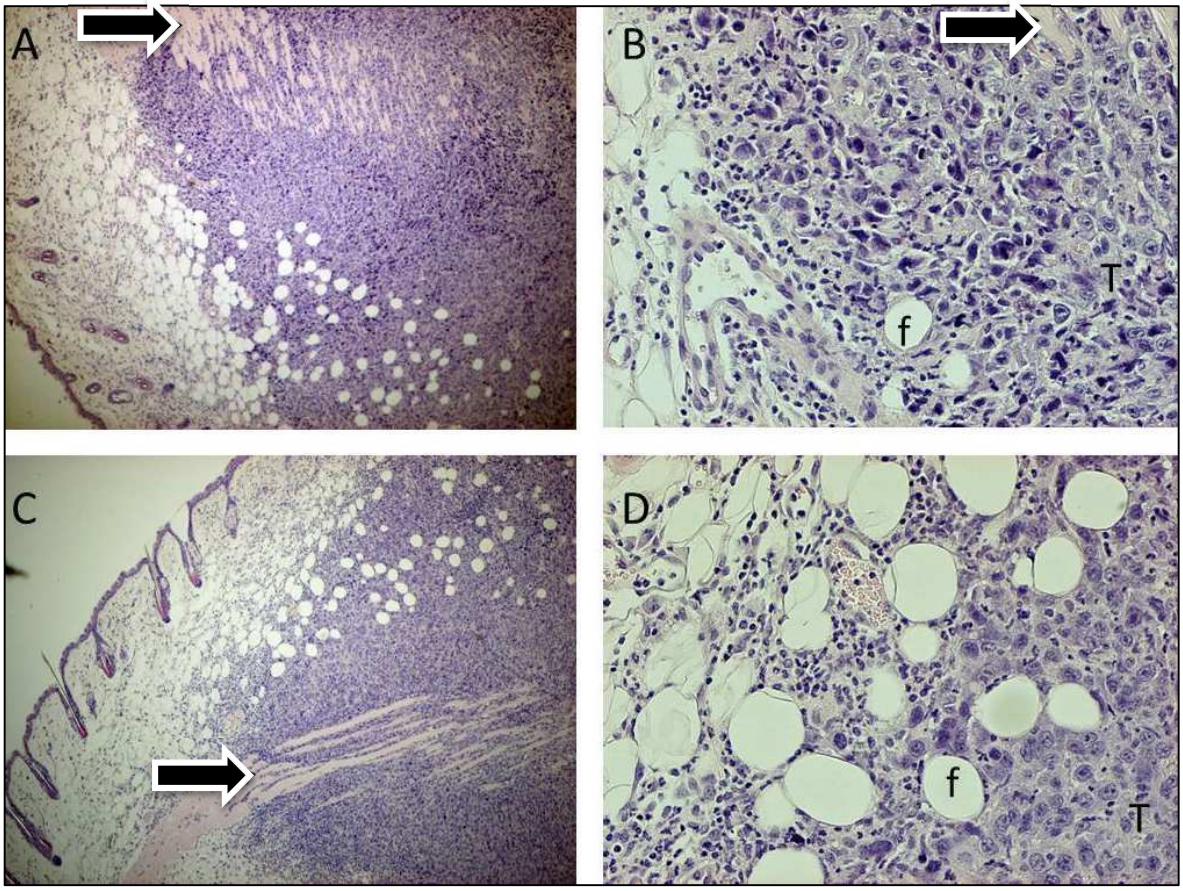

Fig 4.11 Histological features of LY2 tumours.
A) H&E low power view (x40) of subcutaneous LY2 tumours showing less cohesive tumour front and more soft tissue infiltration compared to SCC7 tumours (Fig 4.9). B) high power view (x200) showing tumour cells (T) invading subcutaneous muscles (arrow) and subcutaneous fat tissue (f). C and D) Similar features were seen in LY2-RLuc tumours.

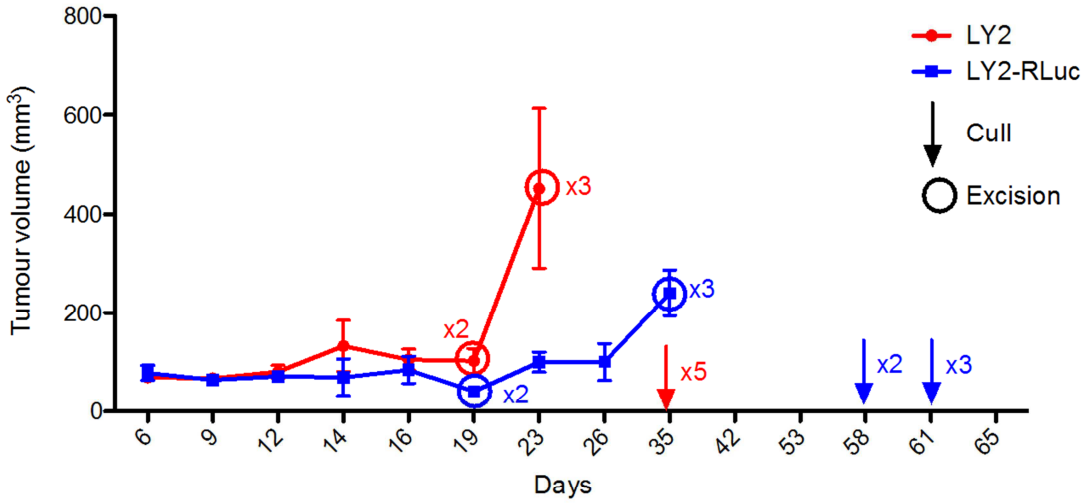

Cell line	Primary tumour	Recurrent tumour	Lung mets	Node mets
LY2	5/5 (Ulceration all tumours)	3/5	5/5	5/5
LY2-RLuc	5/5 (Ulceration all tumours)	1/5	3/5	4/5

Fig 4.12 Growth pattern, recurrence and metastasis rates in surgical excision HNSCC murine model using LY2 cells.

$5x10^6$ LY2 and LY2-RLuc cells were injected subcutaneously in the right flank of 5 BALB/c female mice. Tumour sizes were measured twice a week and excised around 1 cm^2 in size or if ulcerating. Animals were monitored for tumour recurrence and weight loss. Lungs and lymph nodes were harvested at the point of animal sacrifice, fixed and stained to evaluate metastasis. The graph shows tumour growth curves over time. Points represent the means. Error bars represent SEM. Open circles represent time point of tumour excision. Arrows represent time point of animal cull. Xn indicates the number of animal treated or culled at that time point. Table shows the number of animals developing primary and recurrence tumours, lung metastasis and lymph node metastasis.

4.3.2 Orthotopic surgical excision model

To improve the clinical relevance of the model we attempted to excise orthotopic LY2 tumours five days after inoculation. We chose the parental cell line as it reliably forms overt primary tumours that can be easily palpated unlike the luciferase stable cells which grow into very small tumours. The model was technically challenging as the surgical procedure had to be performed under injection rather than inhalation

anaesthesia. By the time of excision, tumours were found to involve the masseter muscle and complete tumour resection couldn't be achieved without damaging adjacent structures despite the use of surgical microscope. Two of the five mice perished in the perioperative period, likely due to the trauma of surgery and injection anaesthesia. The remaining three mice developed early recurrence and they had to be culled at day 16. By then they all had lung and lymph node metastasis (Fig 4.13).

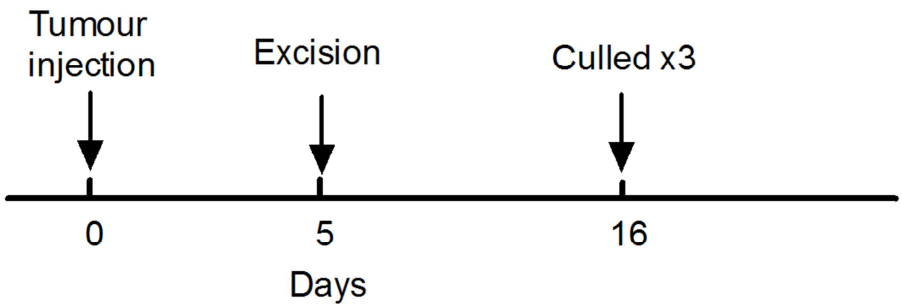

Cell line	Primary tumour	Recurrent tumour	Lung mets	Node mets
LY2	5/5	3/5 (two mice died at time of excision	3/3	3/3

Fig 4.13 Timeline, recurrence and metastasis rates in Orthotopic surgical excision HNSCC murine model using LY2 cells.

$2x10^6$ LY2 and LY2-RLuc cells were injected orthotopically in the right cheek of 5 BABL/c female mice. Tumour were excised at day 5. Animals were monitored for tumour recurrence and weight loss. Lungs and lymph nodes were harvested at the point of animal sacrifice, fixed and stained to evaluate metastasis. The graph shows time line of tumour progress. Table shows the number of animals developing primary and recurrence tumours, lung metastasis and lymph node metastasis.

4.4 Chapter four results summery

- SCC7 and SCC7-RLuc tumours grow rapidly, do not metastasis and the animals remain well with no weight loss or cachexia. It is a poorly representative model of head and neck clinical scenario
- B4B8 orthotopic tumours grow slowly and do not metastasise. It can be used to represent a locally advancing HNSCC tumour
- LY2 tumours grow rapidly and metastasise to lung and lymph nodes
- LY2-RLuc cells do not always form overt primary tumours and they grow slower than the parental cells tumours
- LY2-RLuc tumours retained their capacity to metastasise to lung and lymph nodes.
- Neither of the LY2 models is a true representative of HNSCC. However the can be used to simulate certain aspects of the human disease

Chapter five: Virus-infected cancer cell vaccine in head and neck cancer model

5.1 *In vitro* validation of the suitability of the HNSCC cell lines for oncolytic virus treatment

5.1.1 MTS cell killing assay in B4B8 and LY2 parental and luciferase-expressing cells

Based on our findings in the proof of concept experiments we decided, for the remainder of this study, to use a homologous adenovirus vaccination regimen using our triple deleted adenovirus AdTD-C. As discussed in the introduction the unique triple gene deletions; *E1ACR2*, *E1B19K* and *E3gp19K* of this virus resulted in a safer and cancer selective virus with the ability to induce higher levels of antitumour immunity when compared to the *dl1520* virus.

MTS cell killing assay was used to confirm the susceptibility of the three HNSCC cell lines to oncolytic viral infection and to estimate the MOI required for the vaccination experiments. B4B8, LY2 were sensitive to adenovirus infection with EC50 values of 11 and 6 pfu/cell respectively, while SCC7 was very resistant (Fig 5.1 A-D). All cell lines were sensitive to vaccinia virus infection with EC50 values between 0.2 and 1.6 pfu/cell (Fig 5.1 E-H). Based on these results we decided to use an MOI=20 pfu/cell to infect B4B8 and LY2 cells for vaccination and efficacy experiments. Due to its resistance to adenovirus infection and the shortcomings of its animal model, SCC7 cell line was deemed unsuitable for this study.

In order to confirm that transduction and stable expression of Renilla luciferase does not interfere with the infectability of the B4B8 and LY2 cell lines, MTS assay was repeated and resulted in similar EC50 values compared to the parental cell lines (Fig 5.2).

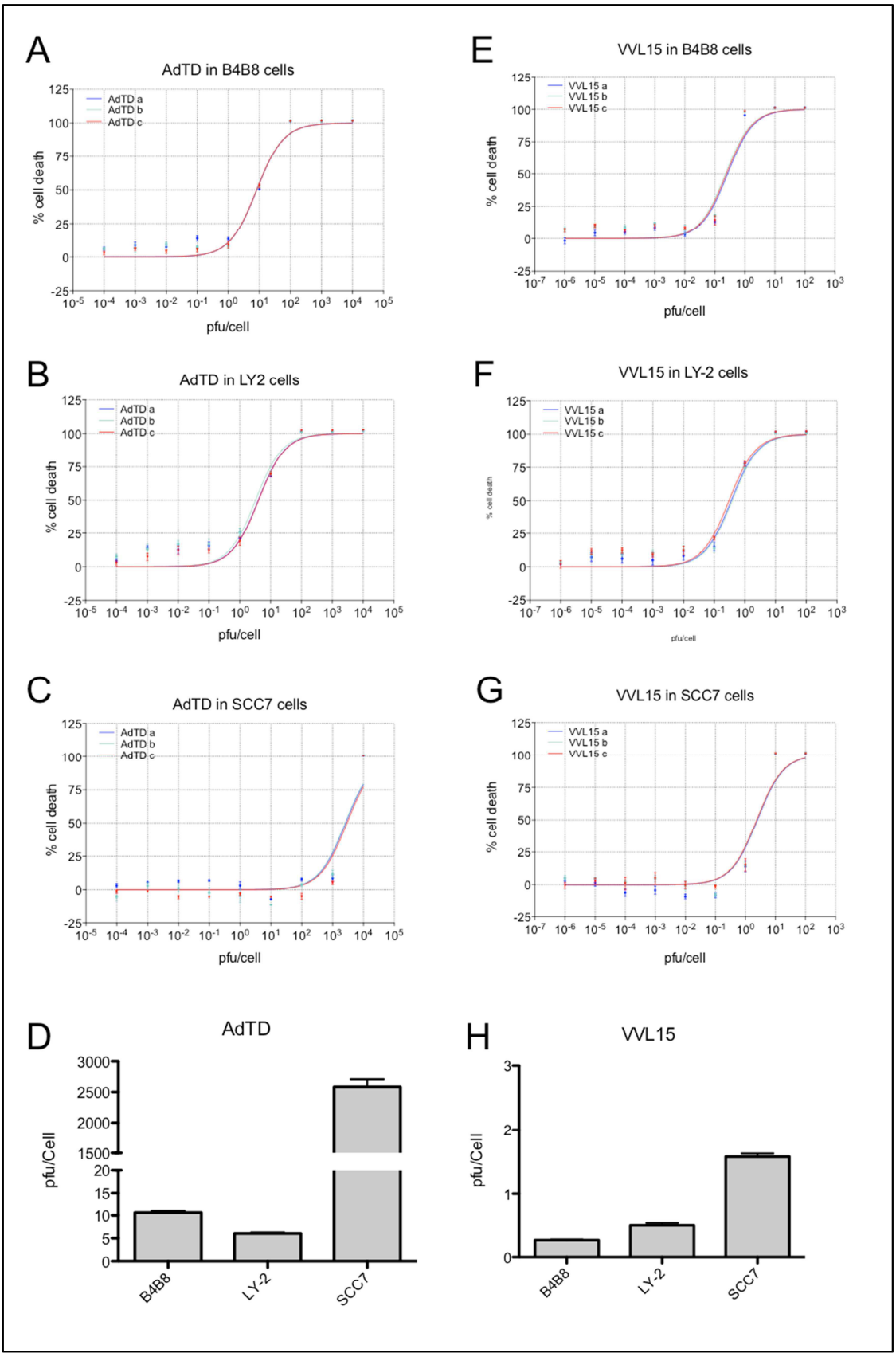
A
AdTD in B4B8 cells
AdTD a
AdTD b
AdTD c
% cell death
pfu/cell
B
AdTD in LY2 cells
C
AdTD in SCC7 cells
D
AdTD
pfu/Cell
B4B8
LY-2
SCC7
E
VVL15 in B4B8 cells
VVL15 a
VVL15 b
VVL15 c
F
VVL15 in LY-2 cells
G
VVL15 in SCC7 cells
H
VVL15

Fig 5.1 MTS cell killing assay in murine HNSCC cell lines.

B4B8, LY2 and SCC7 cells were infected with 1:10 serial dilutions of AdTD-C (top dilution MOI=1x10^4 pfu/cell) or VVL15 (Top dilution MOI=100 pfu/cell). Figures represent dose-response curve for A) AdTD in B4B8, B) AdTD in LY2, C) AdTD in SCC7, D) EC50 values of all cell lines, E) VVL15 in B4B8, F) VVL15 in LY2, G) VVL15 in SCC7 and H) EC50 values of all cell lines. Data shown is a representative of two independent experiments.

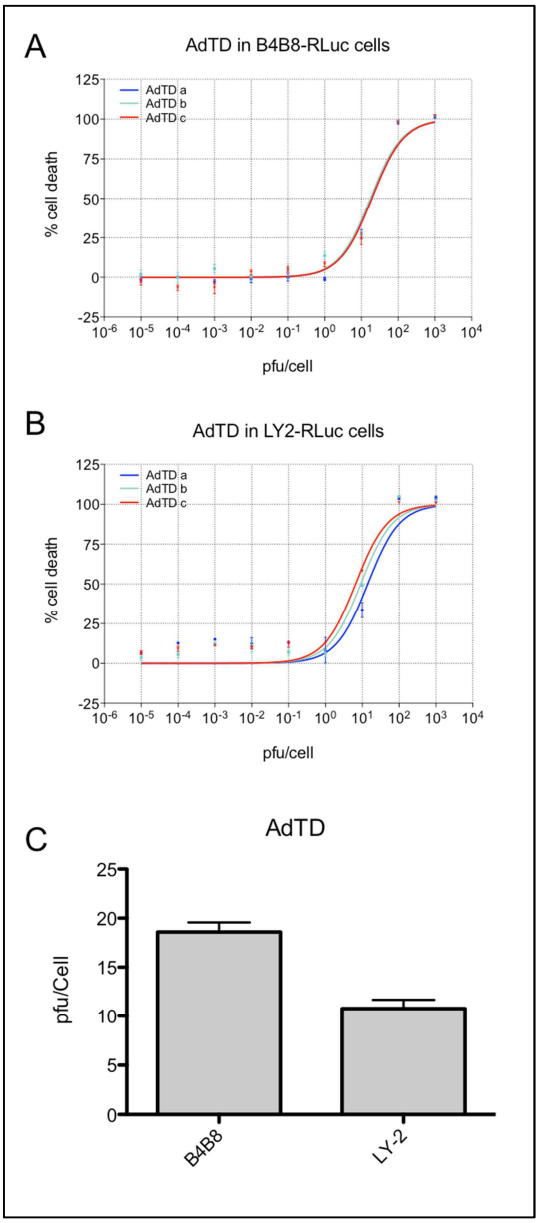

Fig 5.2 MTS cell killing assay in murine HNSCC cell lines stably expressing Renilla luciferase.

B4B8-RLuc and LY2-RLuc cells were infected with 1:10 serial dilutions of AdTD-C (top dilution MOI=1x10^3 pfu/cell). Figures represent dose-response curve for A) AdTD in B4B8 -RLuc, B) AdTD in LY2-RLuc and C) EC50 values of both cell lines.

5.1.2 Adenovirus replication

Replication assay showed that AdTD-C virus did not replicate in any of the HNSCC cell lines tested (Fig 5.3). However, as demonstrated in the pancreatic cancer models, the lack of viral replication did not result in reduction of the antitumour immunity, as measured by IFN-γ release assay, or vaccine efficacy. This will be further tested later in this chapter.

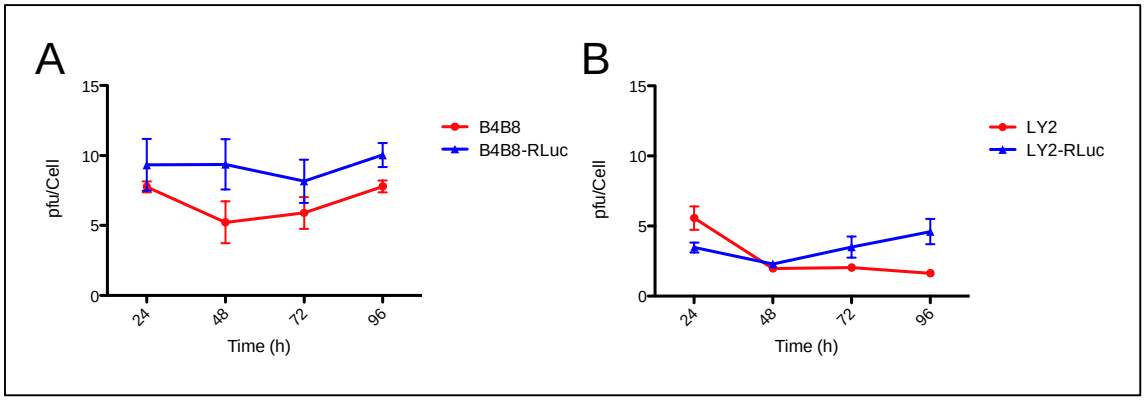

Fig 5.3 Triple-deleted adenovirus does not replicate in murine HNSCC cells.
B4B8, B4B8-RLuc, LY2 and LY2-RLuc cells were plated in 6-well plate at $2x10^5$ cell/well and infected with AdTD-C at MOI=20 pfu/cell. Cell lysate were then harvested at 24, 48, 72 and 96 hours. Viral titers were determined using TCID50 assay. Each virus/cell line/ time point combination was performed in triplicates. Figures represent A) AdTD-C replication in B4B8 cell lines. B) AdTD-C replication in LY2 cell lines. Points represent mean TCID50 value of three corresponding wells. Error bars represent standard error of means (SEM).

5.1.3 Validation of VICCV safety

Before embarking on *in vivo* experiments we validated if the combination of adenovirus infection and mitomycin can kill tumour cells to prevent a tumour developing at the vaccination site. This is particularly relevant in this model as adenovirus is replication-deficient in the LY2 and B4B8 cell lines. Our results showed that the LY2 cells were more sensitive to Adenovirus infection compared to B4B8, which goes to confirm our MTS dose-response results. In the LY2 cells both adenovirus and combination treatment resulted in similar levels of cell killing over 4 days periods. In contrast, adenovirus infection alone was not sufficient to kill all the B4B8 cells (Fig 5.4).

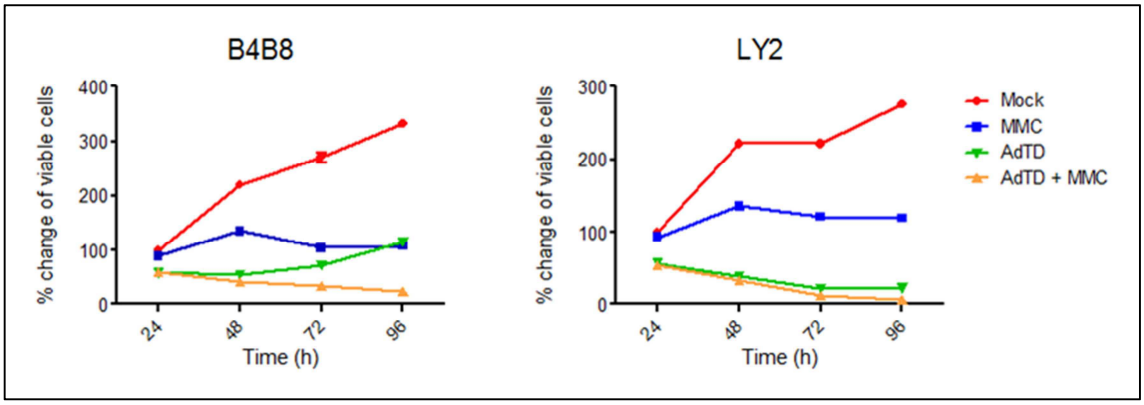

Fig 5.4 Combination of AdTD virus infection and mitomycin can kill HNSCC cells.
$5x10^4$ B4B8 and LY2 cells were plated in triplicate in 24-wells plate. They were then infected with AdTD at MOI=20pfu/cell; treated with MMC or a combination. 100µl of MTS reagent was added to each well at 24, 48, 72 and 96 hours and incubated at 37° for one hour. All plates at different time points were normalised by subtracting background values. The mean optical density of untreated cells at 24 hours was designated the arbitrary unit 100%. Change of optical density correlates to the metabolic activity of viable cells in each well. Points represent the mean of three corresponding wells. Error bars represent standard error of means (SEM).

5.2 Induction of tumour specific immunity following VICCV in HNSCC model

5.2.1 VICCV using parental cell lines infected with AdTD virus

An IFN-γ release assay was performed to test the ability of the VICCV to induce an antitumour immunity in HNSCC animal model. Five groups of animals (n=3) were vaccinated with either PBS, mitomycin (MMC)-treated LY2 (50 µg/ml), MMC-treated B4B8 cells, LY2 cells pre-infected with AdTD virus (MOI=20 pfu/cell) then treated with MMC or B4B8 cells pre-infected with AdTD virus then treated with MMC. Two weeks later the animals received homologues boost injections following the same protocol. Two weeks later mice were culled and IFN-γ release assay was performed.

Splenocytes were stimulated using either the same cell line or cross-stimulated using the other HNSCC cell line to represent an autologous vs. allogeneic vaccination. In addition, to test the specificity of the antitumour immunity splenocytes were stimulated

a control cell line, JC (murine breast cancer). Antitumour immunity was significantly higher in mice vaccinated with B4B8 + AdTD + MMC compared to those vaccinated with MMC-treated cells or naïve mice (Fig. 5.5 A). When cross-stimulated with LY2 cells, this group (B4B8 + AdTD + MMC) expressed the highest level of IFN-γ. However that was not statistically different to the levels expressed when stimulated with the JC control cell line (Fig. 5.5 B-C).

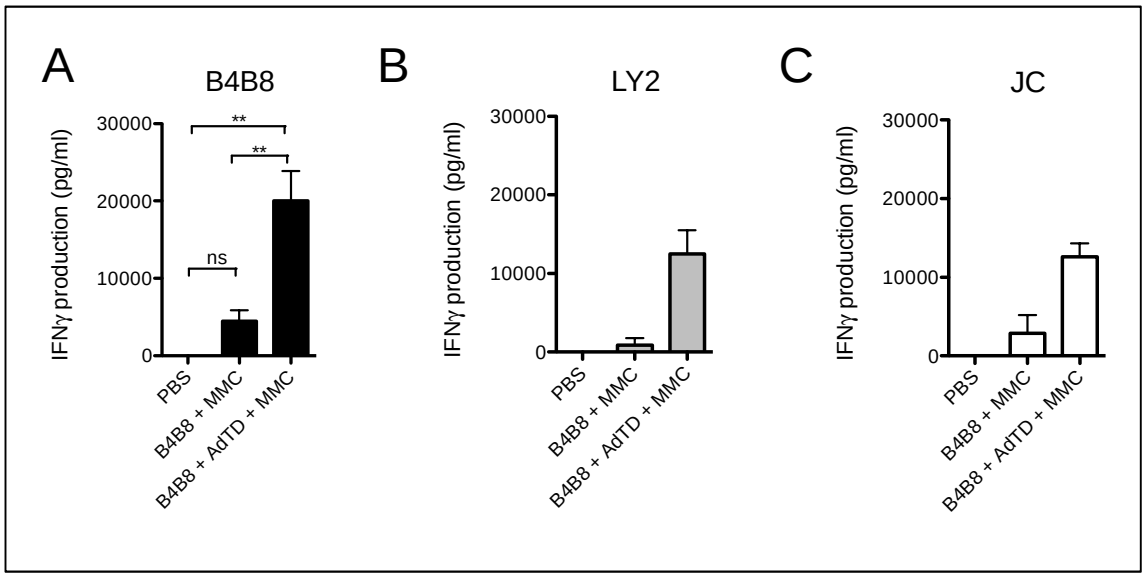

Fig 5.5 VICCV using B4B8 cells induced a tumour-specific immune response.
Three groups of BALB/c mice (n=3) were vaccinated with PBS, MMC-treated B4B8 cells or AdTD pre-infected cells with MMC secondary treatment. Mice were similarly boosted two weeks later. Spleens were harvested and processed two weeks after boost. Isolated splenocytes were incubated for 72 hours with proliferation-arrested A) B4B8 cells, B) LY2 cells or C) JC control cells. IFNγ production, as an indicator of CD8 activation, in the supernatant was measured by ELISA. IFNγ levels were normalized by subtracting background release from non-stimulated splenocytes. One-way ANOVA with Tukey post-hoc test was used to compare groups. Columns represent the means ± SEM; asterisks denote the significance levels as comparing: ns non-significant; * $p \leq 0.05$; ** $p \leq 0.01$; *** $p \leq 0.001$.

On the other hand, mice vaccinated with LY2 + AdTD + MMC resulted in a general trend of a higher IFN-γ expression compared to the other two vaccination groups, however that did not reach statistical significance (Fig 5.6). Splenocytes expressed higher levels of IFN-γ when stimulated with the “autologous” B4B8 cells, compared to

LY2 and JC cells. However that did not reach statistical difference. This observation suggests that B4B8 cells are probably more immunogenic compared to LY2.

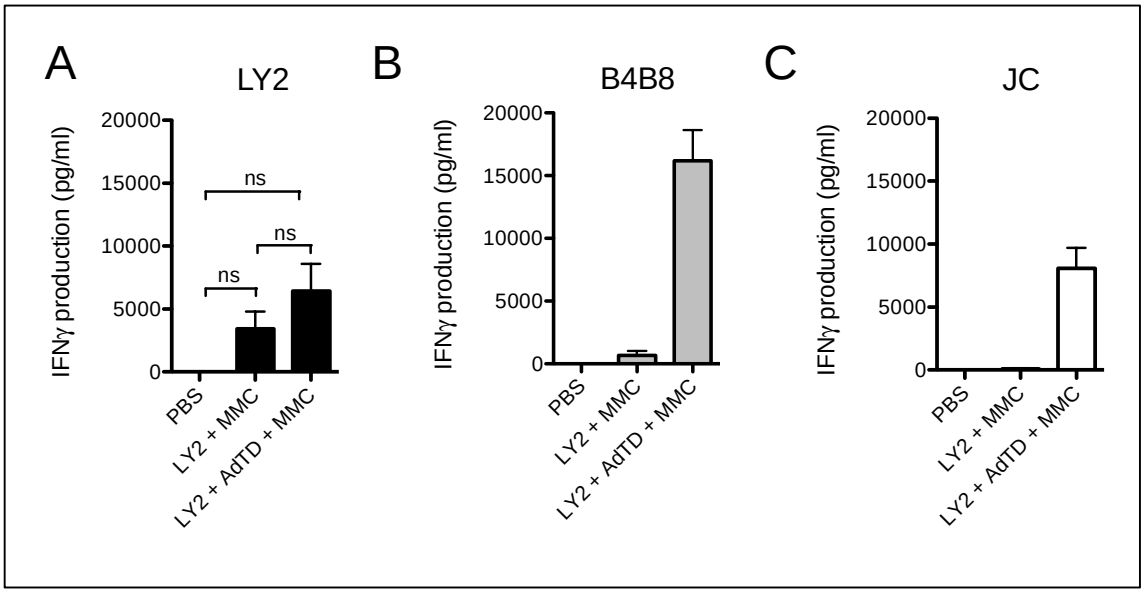

Fig 5.6 VICCV using LY2 cells did not result in a statistically significant tumour-specific immune response.

Three groups of BALB/c mice (n=3) were vaccinated with PBS, MMC-treated LY2 cells or AdTD pre-infected cells with MMC secondary treatment. Mice were similarly boosted two weeks later. Spleens were harvested and processed two weeks after boost. Isolated splenocytes were incubated for 72 hours with proliferation-arrested A) LY2 cells, B) B4B8 cells or C) JC control cells. IFNγ production, as an indicator of CD8 activation, in the supernatant was measured by ELISA. IFNγ levels were normalized by subtracting background release from non-stimulated splenocytes. One-way ANOVA with Tukey post-hoc test was used to compare groups. Columns represent the means ± SEM; asterisks denote the significance levels as comparing: ns non-significant; * $p \leq 0.05$; ** $p \leq 0.01$; *** $p \leq 0.001$.

5.2.2 VICCV using LY2-RLuc cells infected with AdTD virus

As mentioned previously, the LY2-RLuc cell line appears to be suitable model to simulate recurrence of HNSCC following surgical excision. To evaluate the suitability of this cell line for VICCV regimen we repeated the IFN-γ assay using LY2-RLuc cell line. We hoped that this experiment would help us understand if increased immunogenicity

(likely against Luciferase) is behind the slower growth rate of the LY2-RLuc tumours compared to the parental cells.

Mice were vaccinated with LY2-Rluc cells treated with mitomycin or the same cells pre-infected with AdTD virus then treated with mitomycin. Splenocytes harvested from vaccinated animals were then stimulated *in vitro* with either LY2-RLuc or parental cells. Immune responses as measured by means of secreted IFN-γ showed no significant difference between the two cell lines (Fig 5.7 A and B).

In addition we stimulated these splenocytes with either B4B8 or B4B8-RLuc cells. The immune response appears to be much stronger (**, One way ANOVA with Tuekey post hoc test) compared to that generated against LY2 cells (Fig 5.7 C and D). These results appear to be very similar to that obtained when mice were vaccinated with LY2 parental cells as shown in the previous section.

Since immune response does not appear to be the cause for reduced growth rate of LY2-RLuc tumours we investigated if the transfixion of luciferase has led to growth attenuation of these cells. Cell proliferation rate appears to be slower in luciferase-expressing cells and more so in LY2 compared to B4B8 (Fig 5.8).

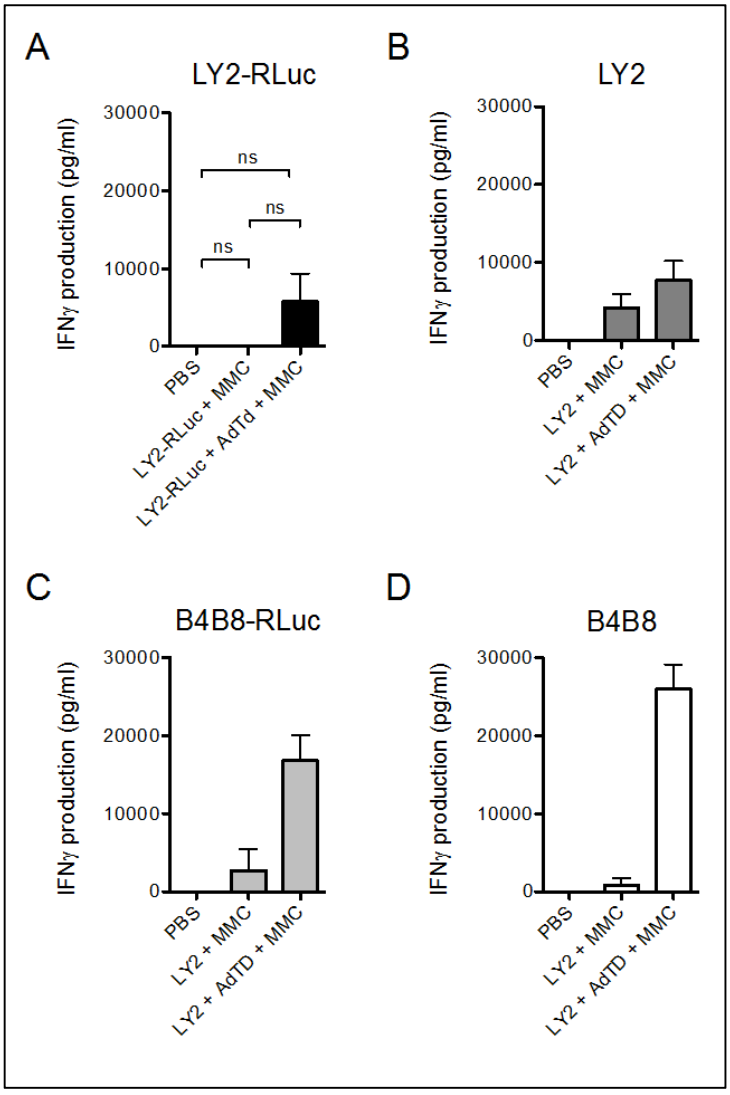

Fig 5.7 VICCV using LY2-RLuc cells did not result in a statistically significant tumour-specific immune response.

Three groups of BALB/c mice (n=3) were vaccinated with PBS, MMC-treated LY2-RLuc cells or AdTD pre-infected cells with MMC secondary treatment. Mice were similarly boosted two weeks later. Spleens were harvested and processed two weeks after boost. Isolated splenocytes were incubated for 72 hours with proliferation-arrested A) LY2-RLuc cells, B) LY2 cells, C) B4B8-RLuc cells or D) B4B8 cells. IFNγ production, as an indicator of CD8 activation, in the supernatant was measured by ELISA. IFNγ levels were normalized by subtracting background release from non-stimulated splenocytes. One-way ANOVA with Tukey post-hoc test was used to compare groups. Columns represent the means ± SEM; asterisks denote the significance levels as comparing: ns non-significant; * $p \leq 0.05$; ** $p \leq 0.01$; *** $p \leq 0.001$.

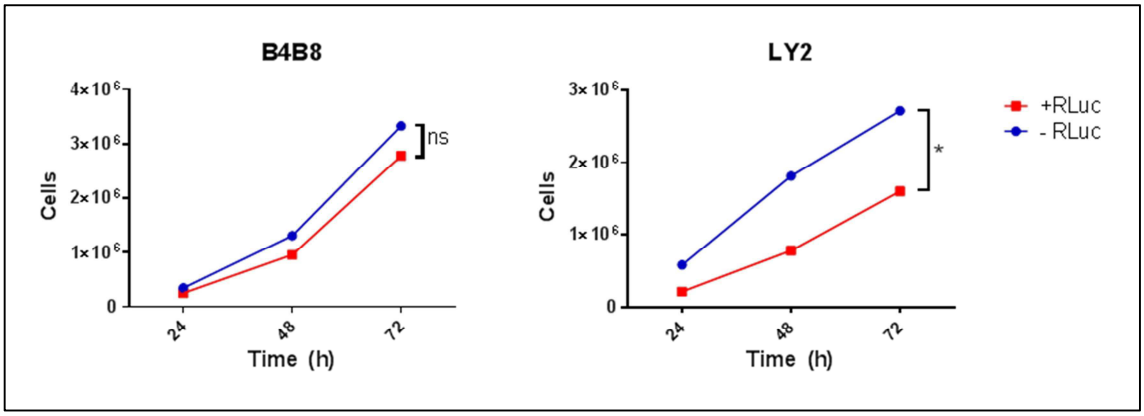

Fig 5.8 Stable transduction of Renilla luciferase gene attenuates the proliferation of LY2 cells.

$2x10^5$ cells of B4B8, B4B8-RLuc, LY2 and LY2-RLuc were plated in triplicate in 6-wells plate. Number of viable cells was counted at 24, 48 and 72 hours. Two-way ANOVA with Bonferroni post-hoc test was used to compare groups. Points represent the means ± SEM; asterisks denote the significance levels as comparing: ns non-significant; * $p \leq 0.05$; ** $p \leq 0.01$; *** $p \leq 0.001$.

5.3 Efficacy of VICCV in HNSCC model

In order to test the therapeutic potential of the VICCV we used an orthotopic tumour model using B4B8 parental cell line. This model simulates a clinical scenario of an advanced unrespectable head and neck cancer. We injected $3x10^6$ cells into the right cheek of 30 female BALB/c mice. Mice were grouped in cages of five animals. Cages were randomised to treatment group using random numbers generator on Microsoft Excel software. Tumour size and weight were recorded twice a week. Mice were sacrificed according to Home Office guidelines if showing signs of tumour ulceration, bleeding, dyspnoea, distress or severe cachexia, if tumour size reached 1.44 cm^2 or if they lost 20% of total body weight. Vaccination with AdTD pre-infected B4B8 cells with a secondary treatment of mitomycin C resulted in an initial regression and slower tumour growth (Fig. 5.9 A). On the long term the vaccinated group had a longer median survival of 79 days compared to 64 and 69.5 of the PBS and MMC groups respectively. Although this difference did not reach statistical significance there was a trend of longer

survival in the AdTD vaccination group with three animals surviving past 110 days (Fig. 5.9 B).

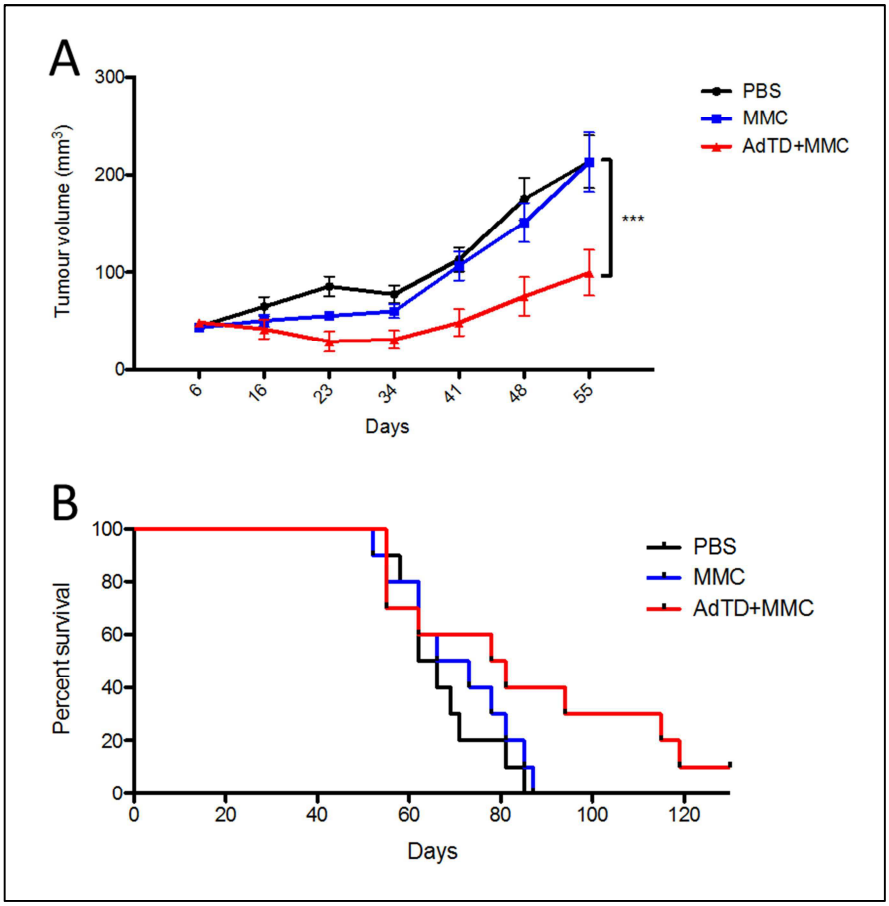

Fig 5.9 Efficacy of VICCV in B4B8 orthotopic tumour model.

Three groups of BALB/c mice (n=10) were inoculated in the right check with $3x10^6$ B4B8 tumour cells. Seven days later animals were randomized to three groups and vaccinated with PBS, MMC-treated B4B8 cells or AdTD pre-infected cells plus MMC secondary treatment. Mice were similarly boosted two weeks later. A) The graph shows tumour growth rates of the three treatment groups until the first animal in each group was culled. Two-way ANOVA with Bonferroni post-hoc test was used to compare groups. Points represent the means ± SEM; asterisks denote the significance levels as comparing: ns non-significant; * $p \leq 0.05$; ** $p \leq 0.01$; *** $p \leq 0.001$. B) Kaplan-Meier survival curve showing a trend of longer survival in the AdTD vaccination group although that did not reach statistical significance.

5.4 Functional mechanisms

To help understand the mechanisms behind the antitumour efficacy we looked into different aspects of the immunological response including T cell response, PAMPs expression and antigen presenting cells activation.

5.4.1 Immunophenotyping of T cells following VICCV using parental cell lines

Using fluorescence cytometry, we investigated the changes in the immune profile of T cells is response to vaccination with virus-infected HNSCC cells in comparison to naïve mice and those vaccinated with MMC-treated matching cells. From the same experiment described above, splenocytes were stained for CD3, CD4 and CD8 expression and profiled into cytotoxic T cells (CD3+ CD8+) and helper T cells (CD3+ CD4+) following the gating strategy discussed previously.

In addition, cells were stained for the secondary lymphoid organs homing cell adhesion molecule, CD62L and the cell surface glycoprotein, CD44. The latter is upregulated in activated memory T cells while CD62L expression is lost in both effector and effector memory T cells allowing them to circulate in peripheral tissues. Based on these two markers T_{EM} was defined as $CD44^{Hi}CD62L^{Lo}$ and T_{CM} as $CD44^{Hi}CD62L^{Hi}$.

Vaccination with B4B8 cells pre-infected with AdTD virus plus MMC showed a significantly higher level of CD8+ T_{EM} population, and a proportional drop in T_{CM} population, compared to naïve mice or those vaccinated with MMC-treated cells. Similar trend was observed in mice vaccinated with LY2 cells however it did not reach statistical significance (Fig 5.10 A).

Similar pattern was observed in the CD4+ population albeit less dramatic (Fig. 5.10 B).

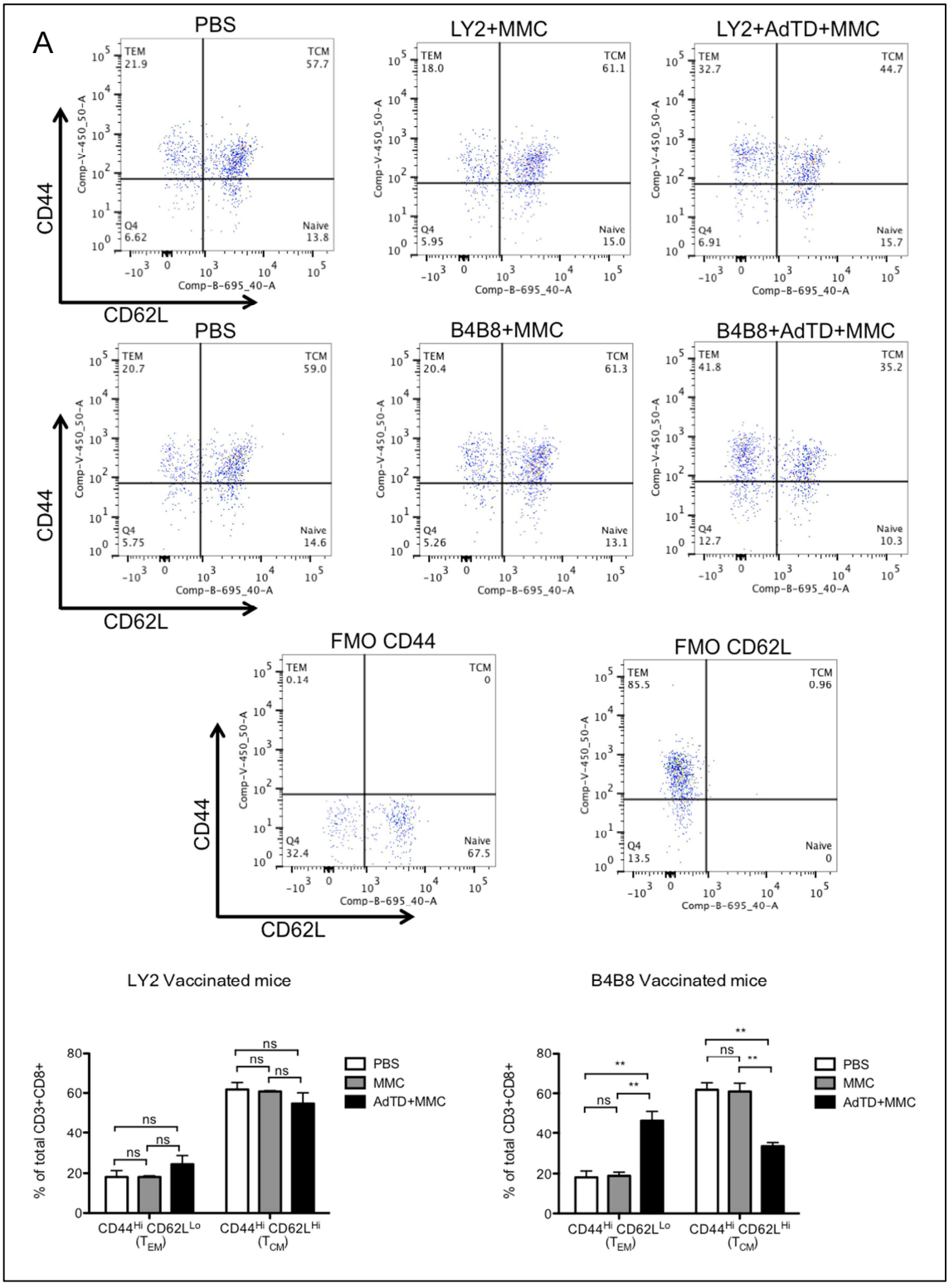
A
PBS
LY2+MMC
LY2+AdTD+MMC
B4B8+MMC
B4B8+AdTD+MMC
FMO CD44
FMO CD62L
CD44
CD62L
Comp-V-450_50-A
Comp-B-695_40-A
TEM
TCM
Naive
Q4
LY2 Vaccinated mice
B4B8 Vaccinated mice
% of total CD3+CD8+
PBS
MMC
AdTD+MMC
ns
**
CD44Hi CD62LLo (TEM)
CD44Hi CD62LHi (TCM)

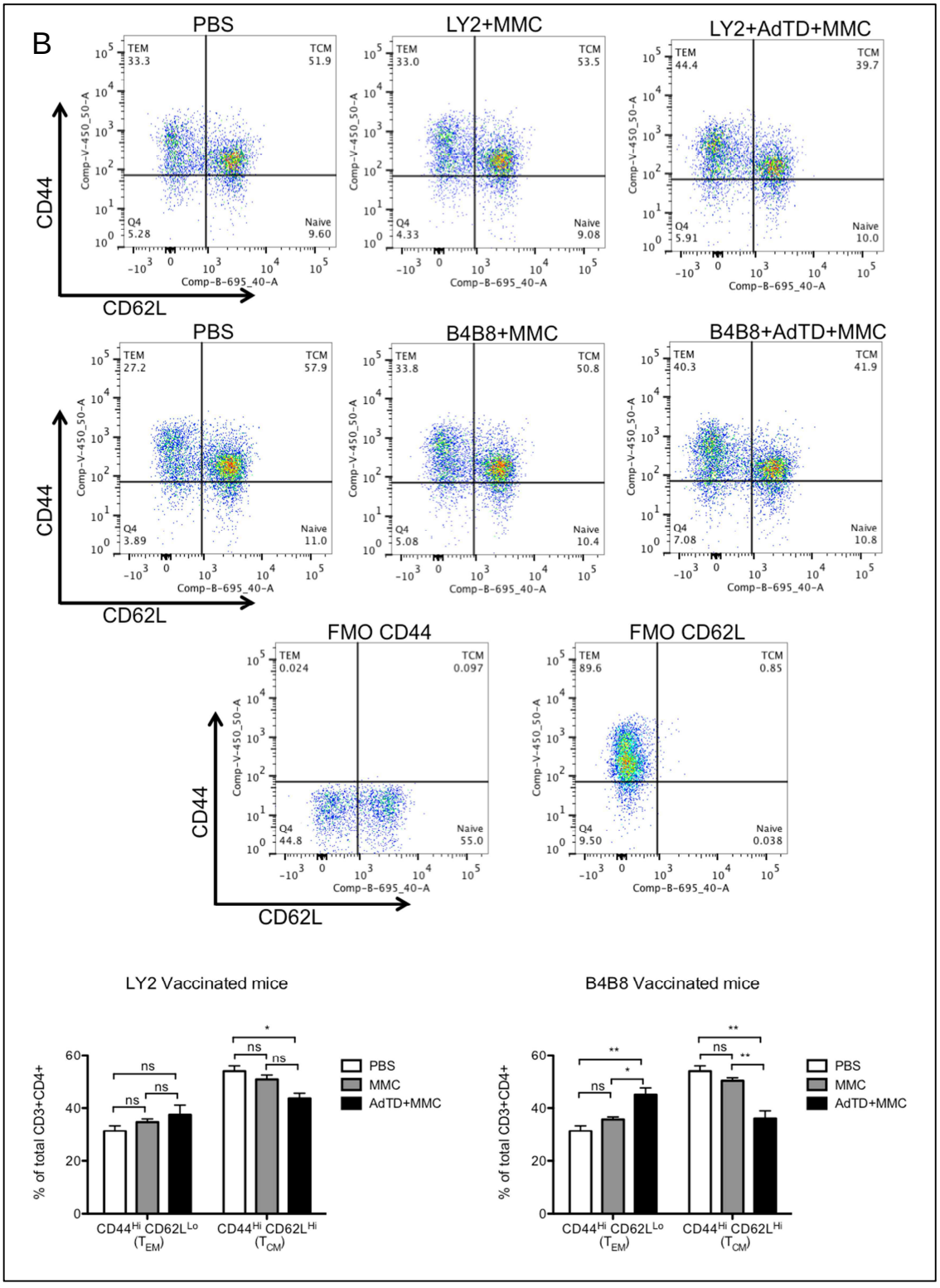
B
PBS
LY2+MMC
LY2+AdTD+MMC
B4B8+MMC
B4B8+AdTD+MMC
FMO CD44
FMO CD62L
CD44
CD62L
TEM
TCM
Naive
Comp-V-450_50-A
Comp-B-695_40-A
LY2 Vaccinated mice
B4B8 Vaccinated mice
% of total CD3+CD4+
PBS
MMC
AdTD+MMC
ns

Fig 5.10 VICCV with HNSCC cells pre-infected with AdTD virus enhances the generation of an effector memory T cell population.

Five groups of BALB/c mice (n=3) were vaccinated with PBS, MMC-treated LY2 cells, MMC-treated B4B8 cells or AdTD pre-infected cells with MMC secondary treatment. Mice were similarly boosted two weeks later. Spleens were harvested and processed two weeks after boost. Splenocytes were stained for CD3, CD4, CD8, CD44, CD62L and profiled into various populations using fluorescence cytometry. A) shows the change of the CD8+ T_{EM} and T_{CM} populations. The top row shows a dot plot three representative mice one of each LY2 treatment group. The second row shows the B4B8 vaccination groups. The third row shows the gating strategy using samples stained for all colours except CD44 (FMO CD44) or CD62L (FMO CD62L). The bar charts depict the effector and central memory populations out of the total CD8+ population in the LY2 and B4B8 vaccination groups. B) shows similar changes in the CD4+ populations. One-way ANOVA with Tukey post-hoc test was used to compare groups. Columns represent the means ± SEM; asterisks denote the significance levels as comparing: ns non-significant; * $p \leq 0.05$; ** $p \leq 0.01$; *** $p \leq 0.001$.

5.4.1.2 Immunophenotyping of T cells following VICCV LY2-RLuc cells

Similarly we investigated the immune response and the change in T cell populations following VICCV using LY2-RLuc cells pre-infected with AdTD virus then treated with MMC. Treatment group mice showed a small increase in effector memory population more prominent in the cytotoxic CD8+ population (Fig 5.11). These changes were almost identical to those seen with parental cells.

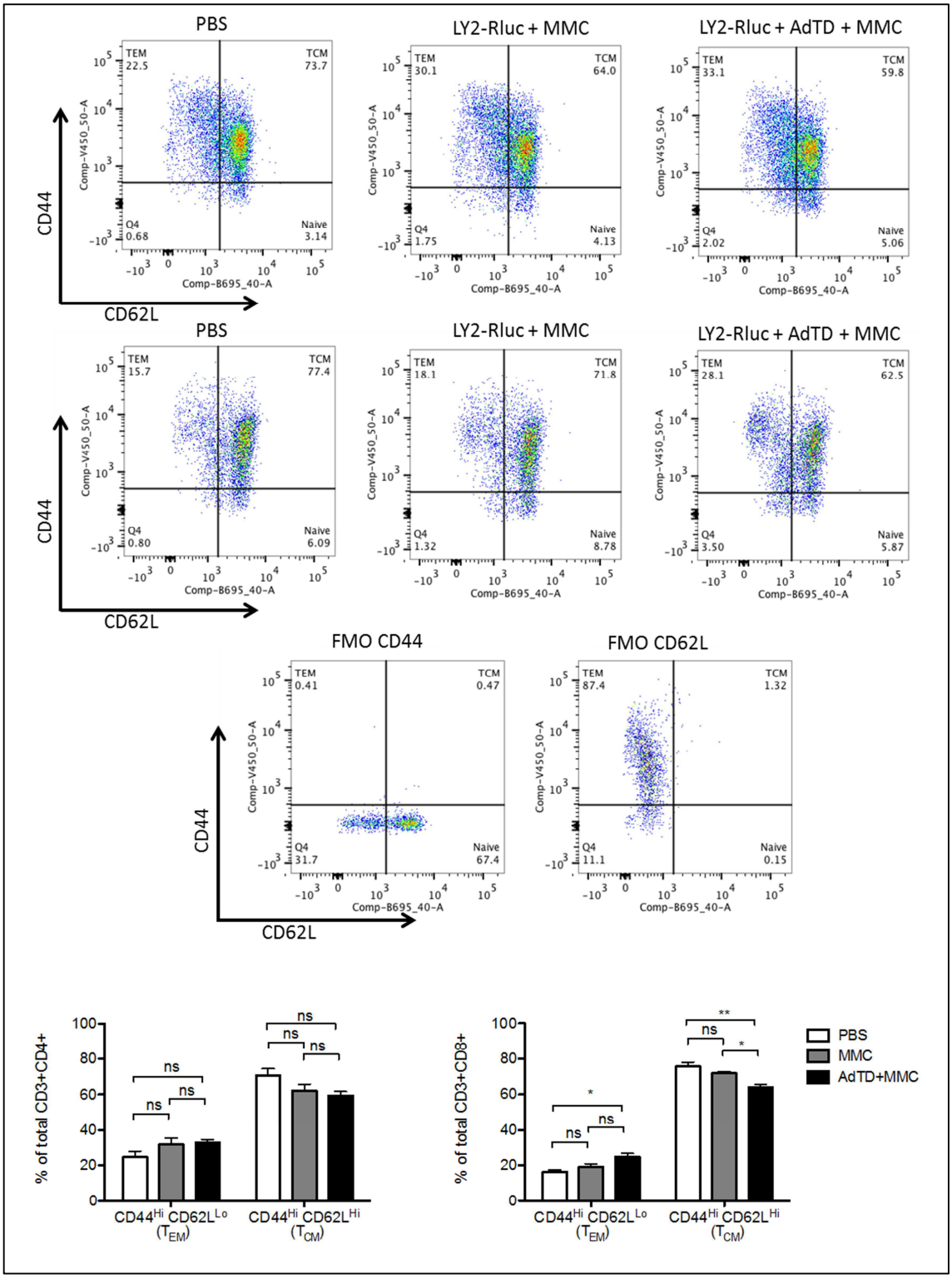
PBS
LY2-Rluc + MMC
LY2-Rluc + AdTD + MMC
TEM 22.5
TCM 73.7
Q4 0.68
Naive 3.14
TEM 30.1
TCM 64.0
Q4 1.75
Naive 4.13
TEM 33.1
TCM 59.8
Q4 2.02
Naive 5.06
PBS
LY2-Rluc + MMC
LY2-Rluc + AdTD + MMC
TEM 15.7
TCM 77.4
Q4 0.80
Naive 6.09
TEM 18.1
TCM 71.8
Q4 1.32
Naive 8.78
TEM 28.1
TCM 62.5
Q4 3.50
Naive 5.87
FMO CD44
FMO CD62L
TEM 0.41
TCM 0.47
Q4 31.7
Naive 67.4
TEM 87.4
TCM 1.32
Q4 11.1
Naive 0.15
CD44
CD62L
Comp-V450_50-A
Comp-B695_40-A
% of total CD3+CD4+
% of total CD3+CD8+
CD44Hi CD62LLo (TEM)
CD44Hi CD62LHi (TCM)
PBS
MMC
AdTD+MMC
ns
*
**

Fig 5.11 VICCV with LY2-RLuc cells pre-infected with AdTD virus induces a modest increase in CD8+ effector memory T cell population.

Three groups of BALB/c mice (n=3) were vaccinated with PBS, MMC-treated LY2 cells or AdTD pre-infected cells with MMC secondary treatment. Mice were similarly boosted two weeks later. Spleens were harvested and processed two weeks after boost. Splenocytes were stained for CD3, CD4, CD8, CD44, CD62L and profiled into various populations using fluorescence cytometry. The top row shows dot plots of CD4+ cells of three representative mice one of each LY2 treatment group. The second row shows CD8+ population. The third row shows the gating strategy using samples stained for all colours except CD44 (FMO CD44) or CD62L (FMO CD62L). The bar charts depict the effector and central memory populations out of the total CD4+ and DC8+ population. One-way ANOVA with Tukey post-hoc test was used to compare groups. Columns represent the means ± SEM; asterisks denote the significance levels as comparing: ns non-significant; * $p \leq 0.05$; ** $p \leq 0.01$; *** $p \leq 0.001$.

5.4.2 PAMPs expression following AdTD infection of HNSCC cells

Despite lack of replication in B4B8 and LY2 cells, early and late viral proteins were still being expressed following triple-deleted adenovirus infection. In keeping with our previous findings in pancreatic cancer model, mitomycin C doesn't appear to affect viral proteins production (Fig 5.12)

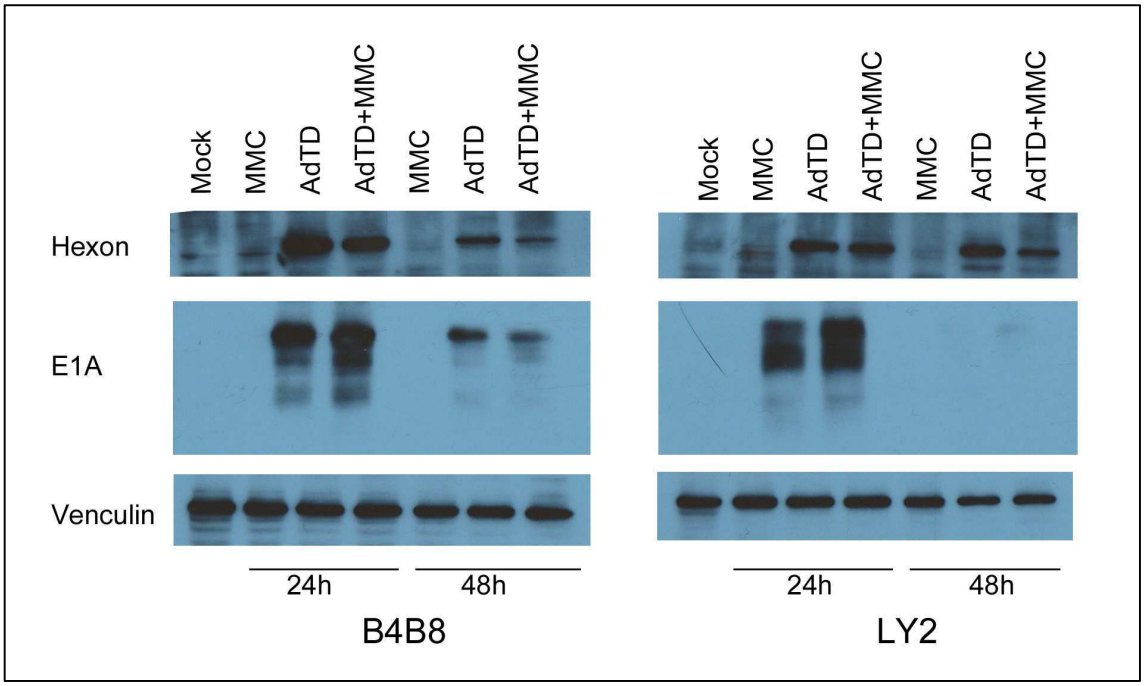

Fig 5.12 Mitomycin C secondary treatment does not affect viral protein production following AdTD infection.

B4B8 and LY2 cells were treated with MMC at a concentration 50µg/ml, infected with AdTD at MOI=20 pfu/cell or a combination treatment. Cell lysate were then harvested at 24 and 48 hours for western blotting using primary antibodies against adenovirus E1A and hexon proteins. Venculin was used as a loading control.

5.4.3 Dendritic cells activation following VICCV

As part of the experiment described in section 5.2.1, local draining lymph nodes (right inguinal) were harvested and mashed to obtain a lymphocyte single cell suspension as described previously. Cells were stained for CD11c, MHCII and CD80. Dendritic cells population (CD11c+ MHCII+) was isolated using fluorescence cytometry. In addition dendritic cells were isolated similarly from the harvested spleens of these mice. The percentage of activated dendritic cells (CD80+) was determined. There was no demonstrable difference between the various vaccination groups (Fig 5.13). While disappointing, the result was not surprising as the total number of DCs out of the total lymphocytes population was very small. This meant that the slightest change to the FACS gating led to large percentage variation. In addition, the samples were obtained

two weeks after boost injection, while DC activation and migration to local lymph nodes to activate T cells takes place within the first few days after antigen exposure.

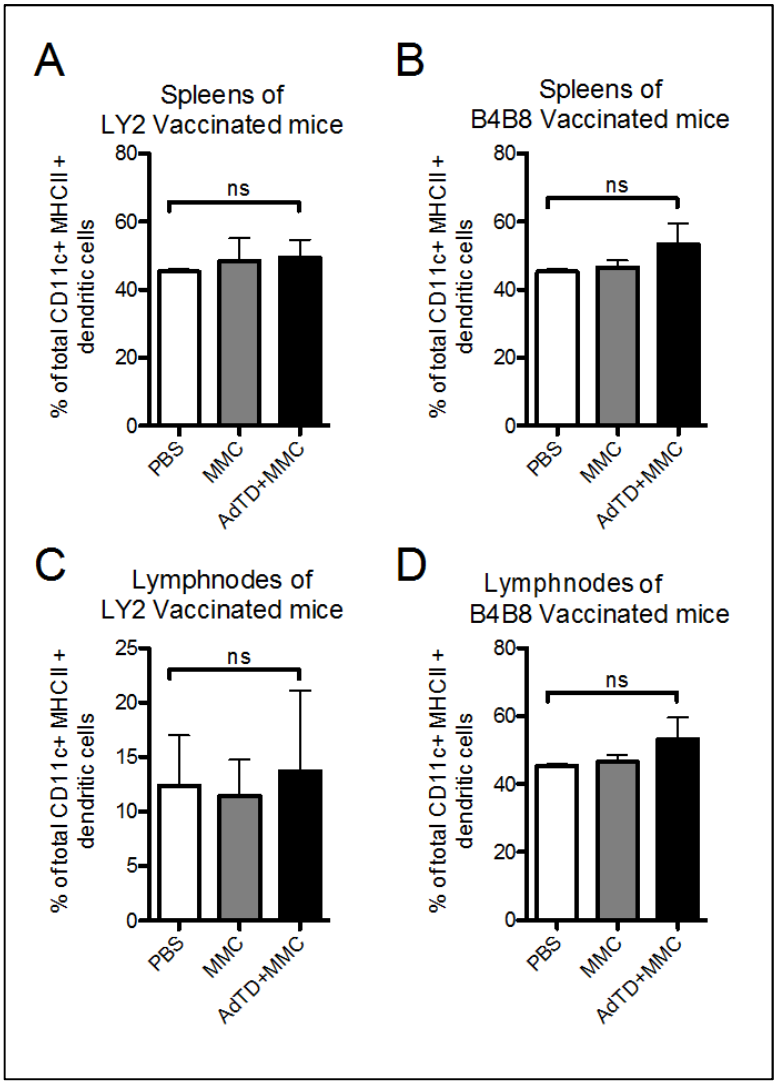

Fig 5.13 Dendritic cell activation following VICCV.

Five groups of BALB/c mice (n=3) were vaccinated with PBS, MMC-treated LY2 cells, MMC-treated B4B8 cells or AdTD pre-infected cells with MMC secondary treatment. Mice were similarly boosted two weeks later. Spleens and inguinal lymph nodes were harvested and processed two weeks after boost. Cells were stained for CD11c, MHCII and CD80. Dendritic cells (CD11c+ MHCII+) were selected using florescence cytometry. The graphs show the percentage of activated DCs (CD80+) of the total DC populations in A, B) spleens and D, C) lymph nodes. One-way ANOVA with Tukey post-hoc test was used to compare groups. Columns represent the means ± SEM; asterisks denote the significance levels as comparing: ns non-significant; * $p \leq 0.05$; ** $p \leq 0.01$; *** $p \leq 0.001$.

5.5 Chapter five results summery

- LY2 and B4B8 cells, and their luciferase-expressing sub-clones, were susceptible to adenovirus infection
- Neither cell supported adenovirus replication
- Adding a secondary treatment of mitomycin did not affect the virus ability to kill these cells. In fact, combination treatment resulted in better cell killing in B4B8 cells.
- Mitomycin treatment did not affect viral protein production as seen previously in pancreatic cell lines.
- Vaccinating mice with B4B8 cells pre-infected with AdTD virus and treated with mitomycin resulted in significantly higher immune response compared to vaccination with cells treated with mitomycin alone. This immune response was cell line-specific.
- Vaccination with LY2 pre-infected cells showed a trend towards a better immune response however that did not reach statistical significance. Similar results were seen in mice vaccinated with LY2-RLuc cells
- In mice vaccinated with LY2 or LY2-RLuc, there was a much higher IFN-γ response against B4B8 cells. This suggests that B4B8 cells are more immunogenic compared to LY2
- Vaccination with B4B8 cells pre-infected with AdTD virus led to an increase in effector memory T cells of both CD4+ and CD8+ phonotypes
- This effect was much smaller in LY2 vaccinated mice
- In an orthotopic tumour model of B4B8 our vaccination regimen led to a decrease in tumour growth rate and a trend towards increased survival of these mice

Chapter six: Construction and validation of CCL25-armed triple-deleted adenovirus

6.1 Construction of AdTD-CCL25

Following cloning of CCL25 gene in the *AdTD* vector (*Section 2.6 and appendix I*), 16 colonies were picked from AdTD-CCL25 transformation and grown in Kanamycin-LB overnight. DNA of each was extracted and PCR performed to confirm insertion and direction of CCL25 gene (Fig 6.1).

Based on the PCR results, DNA extracted from colonies 2 and 4 were sent for sequencing using E3gp19K primers. Correct sequence and direction of colony 2 was confirmed, while colony 4 showed a missing segment of the CCL25 gene. *AdTD-CCL25* vector from colony 2 and *AdTD* were linearised using PacI digestion (*Appendix I*). They were subsequently transfected into HEK293 cells to produce AdTD-CCL25 and AdTD-C viruses. CPE was observed for both viruses. 100 µl of each transfection lysate was used for virus primary expansion. DNA of each virus was extracted from residual lysate and used to validate the triple-gene deletion and the insertion of CCL25 gene using Ad5 standard primers set [388] and CCL25 primers respectively (Fig 6.2, 6.3 and table 6.1). In addition supernatant was collected to confirm CCL25 expression using ELISA.

Once confirmed both viruses were expanded, purified, titrated and stored at -80℃.

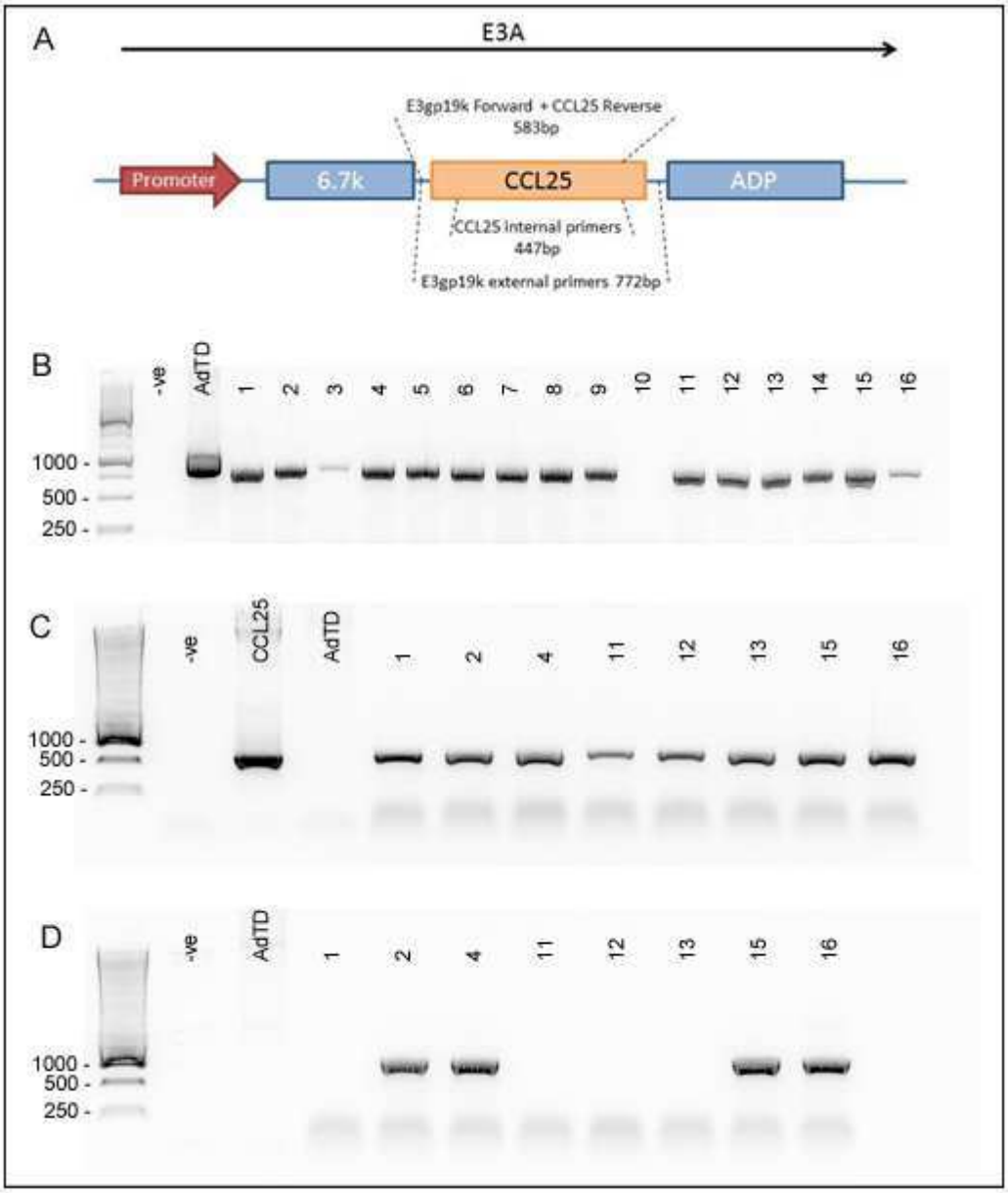

Fig 6.1 PCR confirmation and clone selection of AdTD-CCL25 virus.

Following cloning of murine CCL25 gene into the *AdTD* vector, DNA was transformed into competent E.Coli and grown on kanamycin-agar dish overnight. DNA extracted using Miniprep kit, PCR performed and run on agarose gel. A) a schematic diagram of the CCL25 gene inserted into the gp19k region of the Adenovirus E3 gene. Broken lines demonstrate the three primers sets and the expected size of the PCR fragments. ADP is Adenovirus death gene. B) shows PCR product of all colonies using E3gp19k external primers. Correct colonies showed a smaller amplified fragment compared to AdTD control. C) shows further PCR confirmation using CCL25 internal primers. All tested colonies showed a DNA fragment identical in size to CCL25 control. D) shows PCR product obtained using E3gp19k forward primer and CCL25 reverse primer. Amplified fragment shows correct orientation of inserted CCL25 gene in colonies 2, 4,15 and 16.

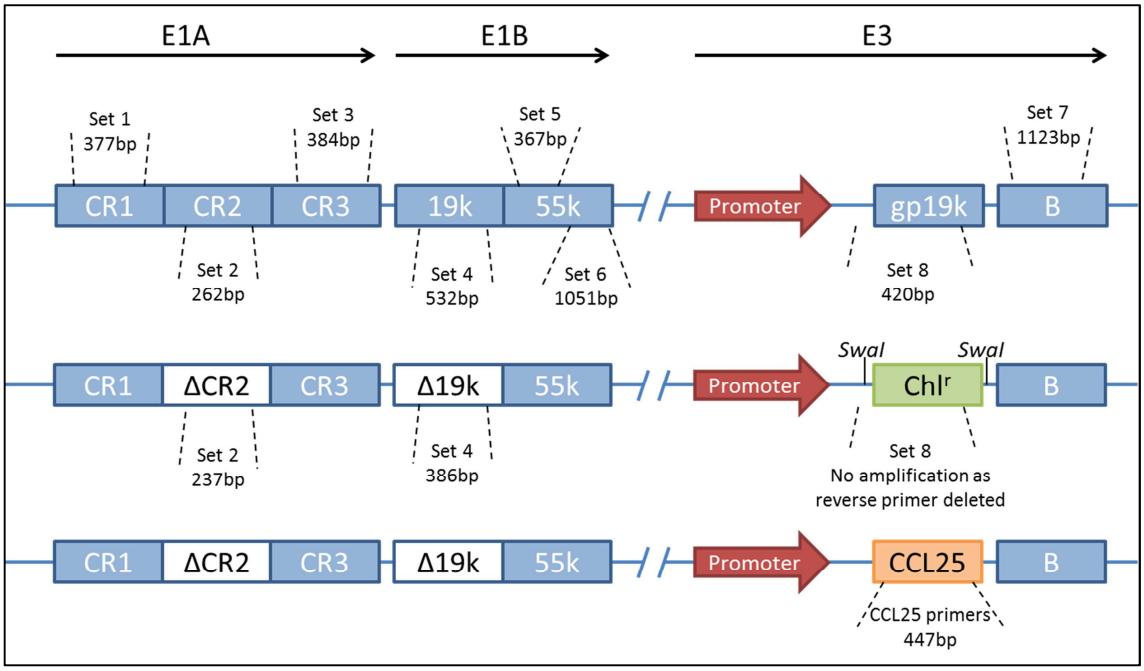

Fig 6.2 Vectors map showing gene deletions and PCR expected fragment size using Ad5 standard 1-8 primer sets and CCL25 primers.

AdTD-C and AdTD-CCL25 vectors used in this study in comparison to wild type adenovirus 5 (WT Ad5). Triple gene deletions at E1A-CR2, E1B-19k and E3GP19K regions are demonstrated. AdTD-C backbone virus contains Chloramphenicol resistant gene (Chl^r) for clone selection flanked by two SwaI restriction enzyme sites. AdTD-CCL25 virus was cloned by insertion of CCL25 gene at that region to replace the Chl^r gene *(Section 2.6).* Ad5 standard 1-8 primer sets and CCL25 primers with expected PCR fragment size are demonstrated on the relevant regions.

Table 6.1 Expected size of amplified segment using standard Ad5 primer sets

Set	5' binding site	3' binding site	Target gene	Expected size (bp)
1	476	853	E1A start	377
2	767	1029	E1A-CR2	262
3	1069	1453	E1A end	384
4	1554	2086	E1B-19k	532
5	2073	2440	E1B-55k	367
6	2383	3434	E1B-55k	1051
7	29915	31038	E3B	1123
8	28715	29135	E3-gp19K	420

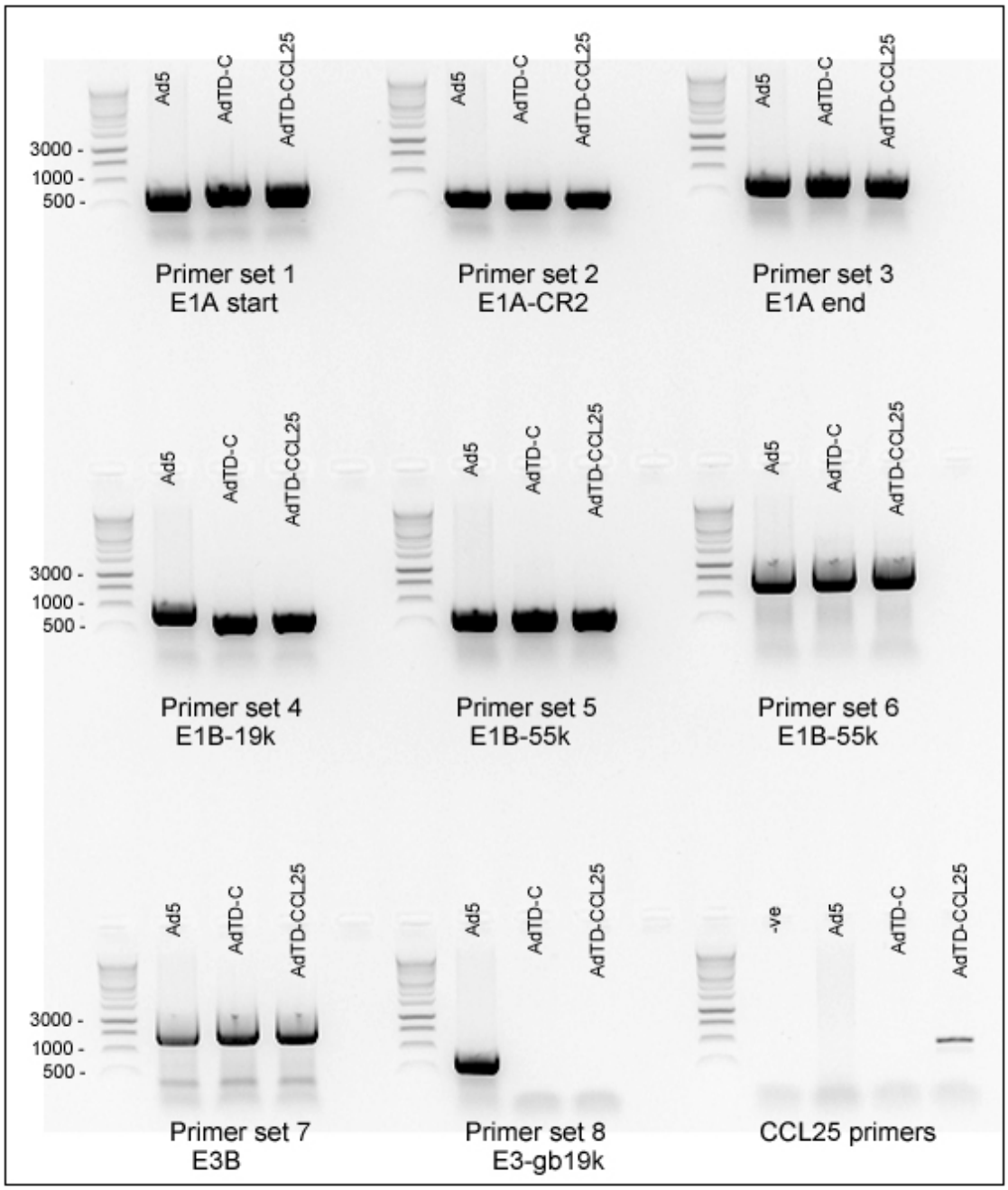

Fig 6.3 Validation of AdTD-CCL25 virus using Ad5 standard 1-8 primer pairs and CCL25 primers.

DNA was extracted from purified AdTD-C and AdTD-CCL25 virus using DNA extraction kit and used for PCR reactions. Reduction of fragment size can be seen in primer set 2 and 4 corresponding to deletions in the E1A-CR2 and E1B-19k regions respectively. Primer set 8 showed complete lack of DNA amplification as the reverse primer of the set is within the deleted region. Finally PCR reaction using CCL25 primers confirmed the presence of CCL25 gene in the expanded and purified virus.

6.2 Validation of replication, CCL25 expression and cell killing of AdTD-CCL25 in a panel of pancreatic cancer cell lines

6.2.1 Replication and CCL25 expression at MOI=50 pfu/cell

CCL25 expression was confirmed in murine pancreatic cancer cell lines; DT6606, TB11381 and pkpa130200 (Fig 6.4 A). Interestingly, CCL25 was expressed from all cell lines however its levels dropped dramatically after 24 hours. Although this observation could be explained by the short half-life of CCL25 in culture at 37℃, one would expect a continuous CCL25 expression from viral-infected cells to replenish the denatured protein until all cells are dead. In addition, viral replication assay of the same experiment showed no replication of AdTD-CCL25 virus in all three cell lines contrary to the control virus (Fig 6.5 B).

Various different hypotheses could explain these results; they will be discussed in details in the discussion chapter (Chapter 8). In this experiment we used our adenovirus standard dose of MOI=50pfu/cell. To get a more accurate replication data and to help explain the previous findings we proceeded to perform an MTS cell killing assay. This will quantify the potency of each virus and allow us to repeat replication assay based on the EC50 value.

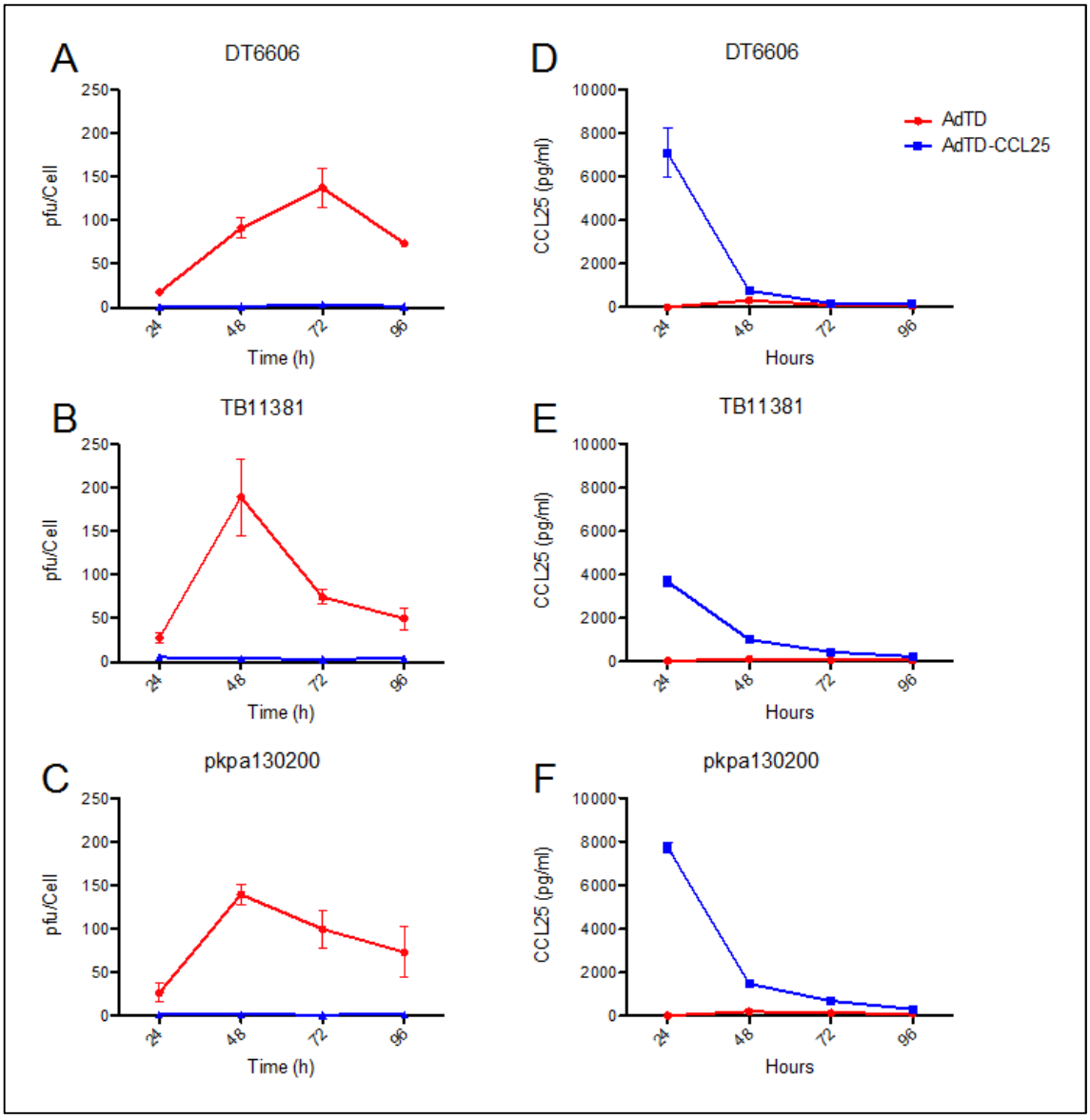

Fig 6.4 AdTD viral replication and CCL25 expression in murine pancreatic cancer cells.

DT6606, TB11381 and pkpa130200 cells were plated in 6-well plate at $2x10^5$ cell/well and infected with AdTD-C and AdTD-CCL25 virus at MOI=50 pfu/cell. A-C) represents change of viral titer over a 4 days time course. Cell lysate were then harvested at 24, 48, 72 and 96 hours. Viral titers were determined using TCID50 assay. Each virus/cell line/ time point combination was performed in triplicates. D-E) shows change of CCL25 expression as measured by ELISA in the supernatant over the time course. Points represent mean CCL25 concentration or TCID50 value of three corresponding wells. Error bars represent standard error of means (SEM).

6.2.2 MTS cell killing assay in murine and human pancreatic cell lines

MTS cell killing assay in DT6606, TB11381 and in human pancreatic cancer cell lines SUIT2 showed AdTD-CCL25 to be ten to twenty folds more potent at cell killing (Fig 6.5).

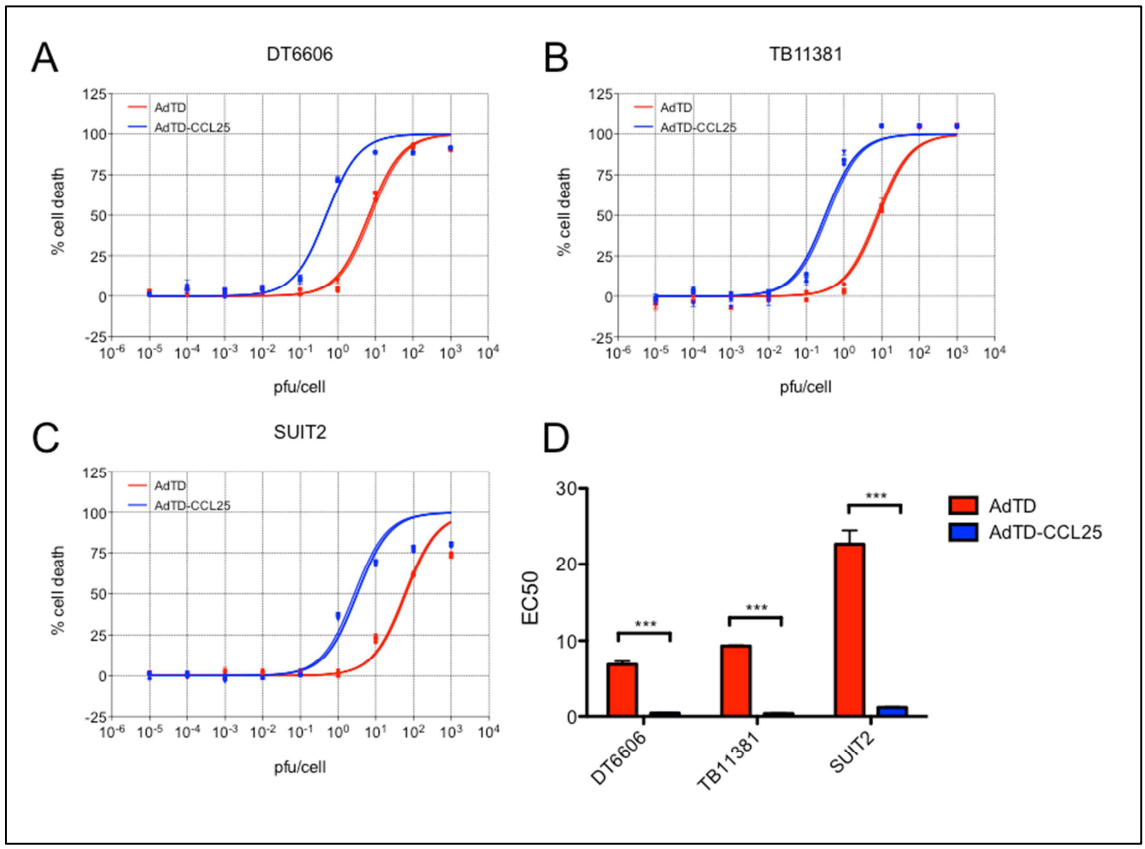

Fig 6.5 AdTD-CCL25 virus is more potent than AdTD-C virus in murine and human pancreatic cancer cell lines.

DT6606, TB11381 and SUIT2 cells were infected with 1:10 serial dilutions of AdTD-C or AdTD-CCL25 (top dilution MOI=1x10^3 pfu/cell) Figures represent dose-response curve for both viruses in A) DT6606, B) TB11381 and C) SUIT2. D) Represents EC50 values of all cell lines. Un-paired *t*-test was used to compare the two viruses. Columns represent EC50 value means ± SEM; asterisks denote the significance levels as comparing: ns non-significant; * p ≤ 0.05; ** p ≤ 0.01; *** p ≤ 0.001.

6.2.3 Viral replication and CCL25 expression at MOI=10 pfu/cell

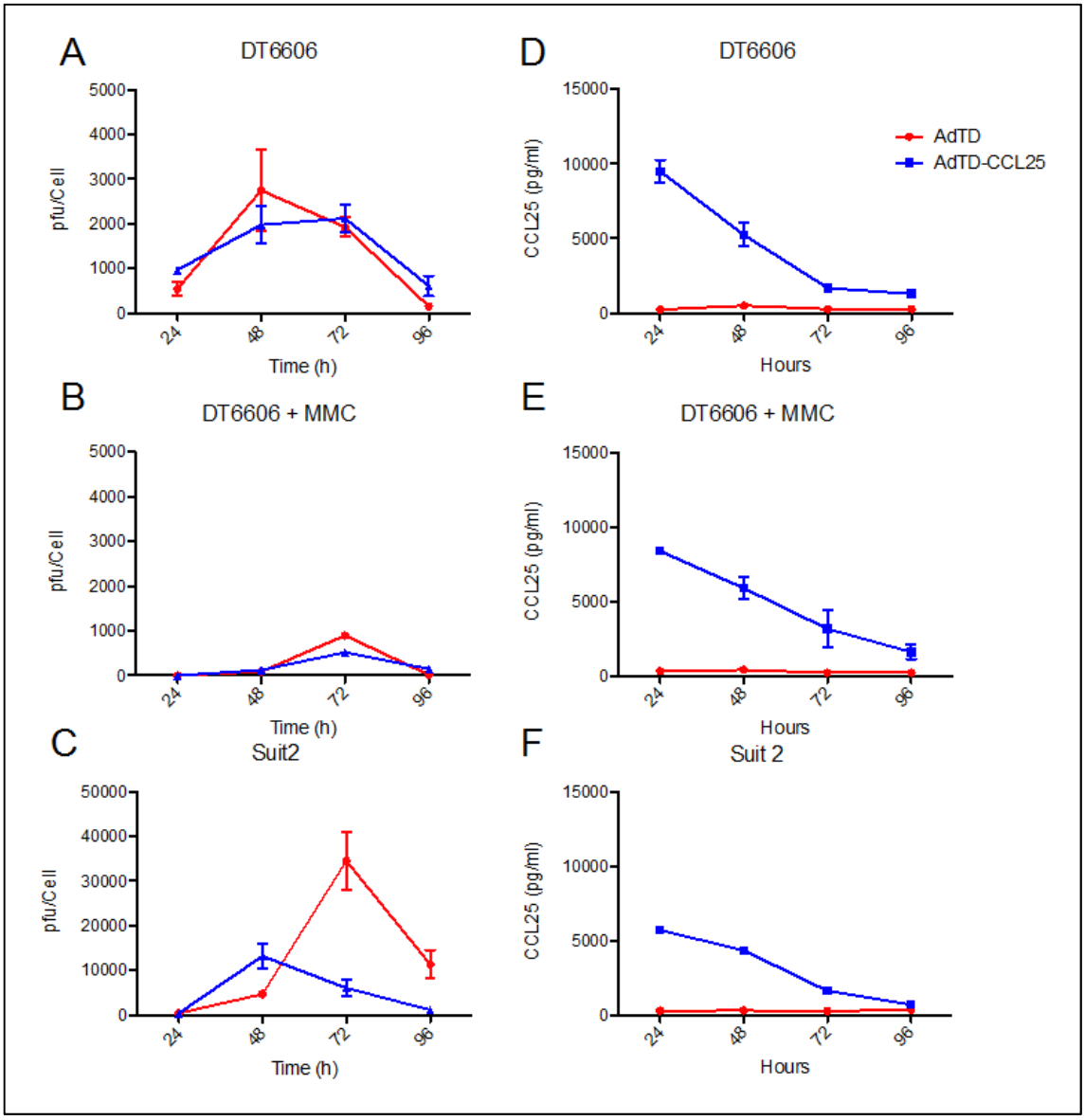

Fig 6.6 AdTD viral replication and CCL25 expression in murine and human pancreatic cancer cells.

DT6606 and SUIT2 cells were plated in 6-well plate at $2x10^5$ cell/well and infected with AdTD-C and AdTD-CCL25 virus at MOI=10 pfu/cell. In addition one group of DT6606 cells were treated with mitomycin C for 2 hours after viral infection before all samples were washed twice in PBS. A-C) represents change of viral titer over a 4 days time course. Cell lysate were then harvested at 24, 48, 72 and 96 hours. Viral titers were determined using TCID50 assay. Each virus/cell line/ time point combination was performed in triplicates. D-E) shows change of CCL25 expression as measured by ELISA in the supernatant over the time course Points represent mean CCL25 concentration or TCID50 value of three corresponding wells. Error bars represent standard error of means (SEM).

Repeat viral replication and CCL25 expression using a lower MOI of 10 pfu/cell showed a more persistent CCL25 expression and confirmed both viruses to be replication competent in DT6606 and SUIT2 cell lines. Additionally, treating DT6606 cells with mitomycin after viral infection did not affect CCL25 expression but reduced viral replication in keeping with previous results (Fig 6.6). This will be particularly relevant to *in vivo* experiments as our vaccination protocol requires a secondary treatment with mitomycin prior to injection.

6.3 Comparing AdTD-C vs AdTD-CCL25 cell killing potency

Daily microscopic examination of the various experiments described in the previous section highlighted an interesting observation that AdTD-CCL25 virus kills cultured cells at a much faster rate compared to the AdTD-C control virus. Since CCL25 gene expression is driven by an early adenovirus promoter we hypothesised that CCL25 will start to be expressed in the first few hours after viral infection. This was confirmed in the DT6606 cell line (Fig 6.7). A synergistic effect of CCL25 and adenovirus infection could explain the early cell killing witnessed and be behind the increase potency of the AdTD-CCL25 virus.

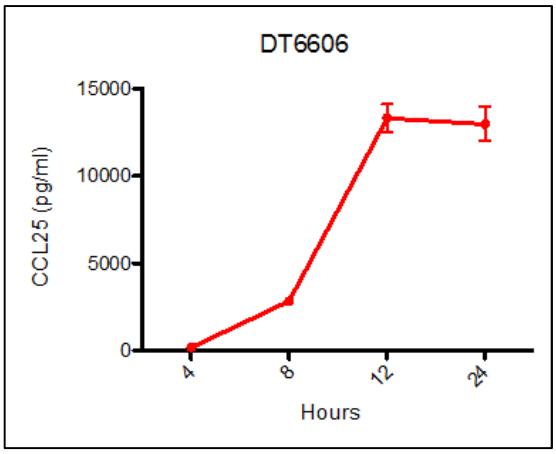

Fig 6.7 CCL25 expression levels peak at 12 hours after AdTD-CCL25 infection.
DT6606 cells were plated in 6-well plate at $2x10^5$ cells/well and infected with AdTD-CCL25 virus at MOI=10 pfu/cell. The graph shows change of CCL25 as measured by ELISA in the supernatant over a 24 period. Points represent mean CCL25 concentration of three separate wells. Error bars represent standard error of means (SEM).

To further examine this hypothesis, the difference of cell killing ability over a time course and its correlation with CCL25 levels was tested in a panel of murine cell lines. Combining these results showed cells behaved in three distinctive manners.

The first group including CMT93, DT6606, TB11381 and 4T1, cell lines were all sensitive to adenovirus infection with the AdTD-CCL25 virus consistently more potent at cell killing compared to control virus. CCL25 levels peaked early on then dropped sharply towards the late time points (Fig 6.8 and 6.9). SCC7 and CT26 cells were more resistant to adenovirus infection with no demonstrable difference between the two viruses. It appears that these two cell lines support early virus protein synthesis evident by the gradual increase of CCL25, under the control of early virus promoter, over the time course (Fig 6.10). LLC cells were not sensitive to either virus and did not express CCL25 (Fig 6.11) suggesting that the resistant to adenovirus infection is probably at the cell entry level. In addition, CCL25 was not directly toxic in two of the most sensitive cell lines; TB11381 and CMT93 (Fig 6.12)

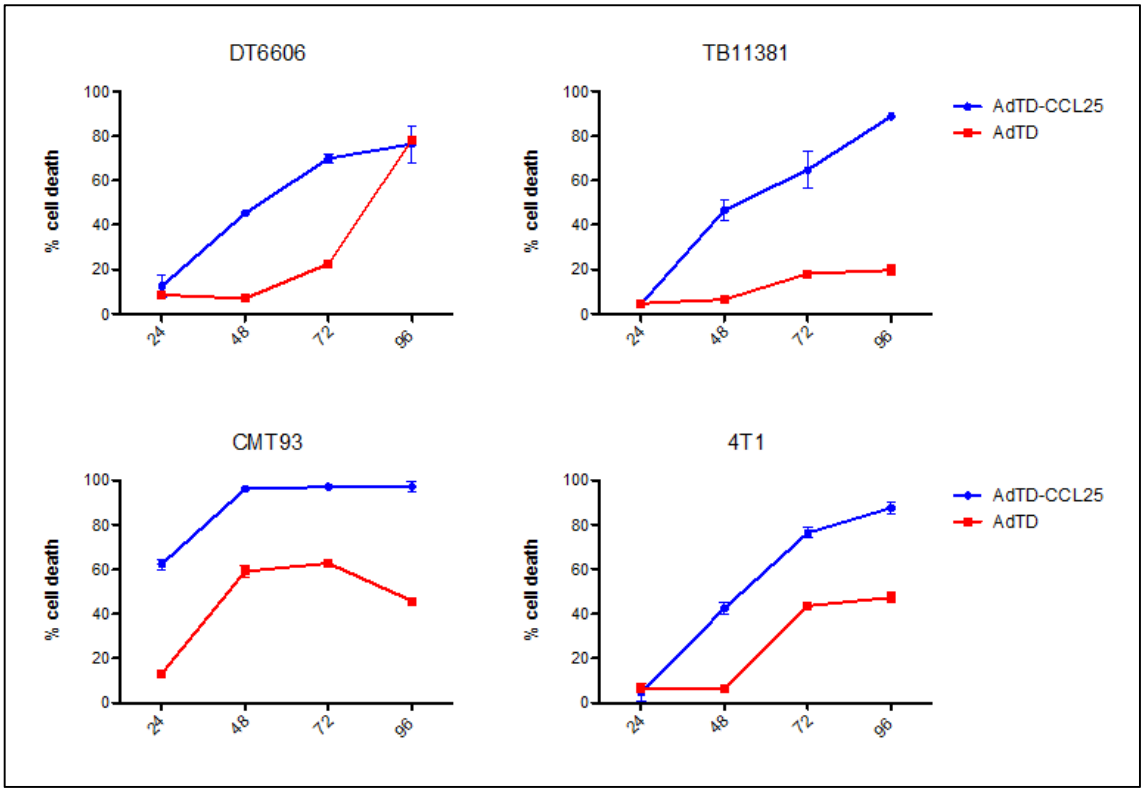

Fig 6.8 AdTD-CCL25 is more potent than AdTD-C in a panel of murine cell lines.
DT6606, TB11381, CMT93 and 4T1 cells were plated in 6-well plates at $2x10^5$ cell/well and infected with AdTD-C and AdTD-CCL25 virus at MOI=10 pfu/cell. The percentage of cell killing was then determined using an MTS assay. Points represent the mean percentage of dead cells in three independent wells. Error bars represent standard error of means (SEM).

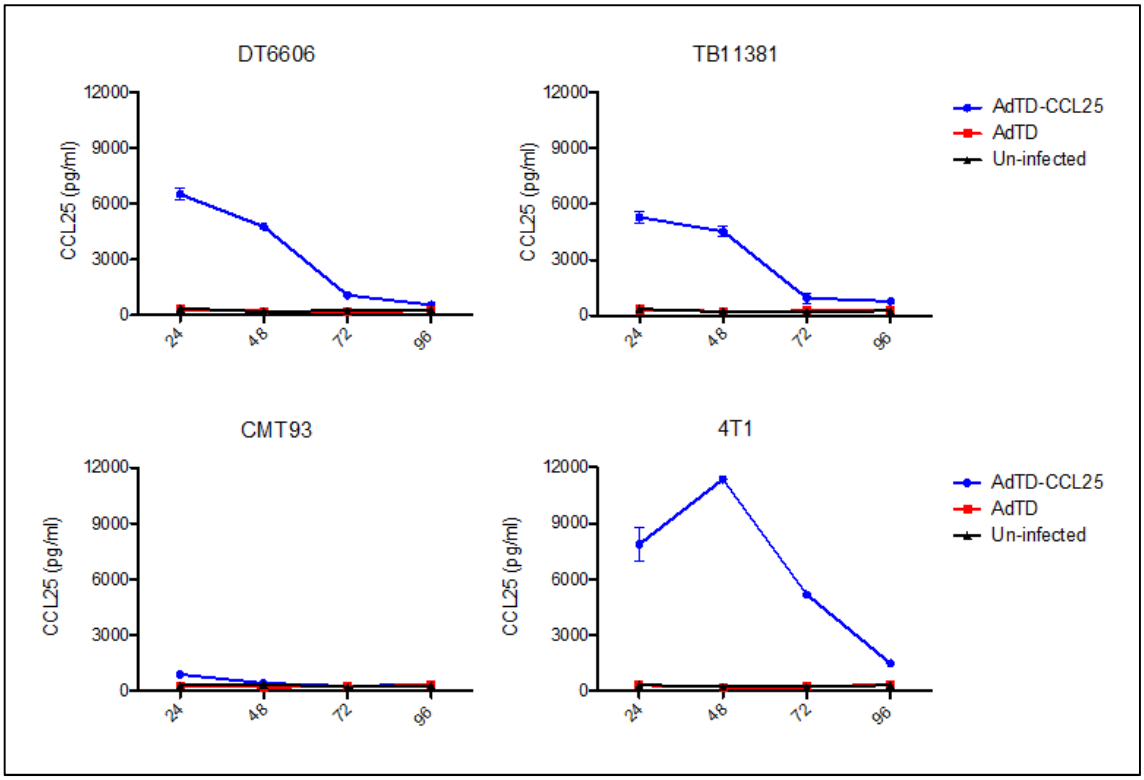

Fig 6.9 CCL25 expression in a panel of murine cell lines.

DT6606, TB11381, CMT93 and 4T1 cells were plated in 6-well plates at $2x10^5$ cell/well and infected with AdTD-C and AdTD-CCL25 virus at MOI=10 pfu/cell. The graphs show change of CCL25 as measured by ELISA in the supernatant over a four days time course. Points represent mean CCL25 concentration of three independent wells. Error bars represent standard error of means (SEM).

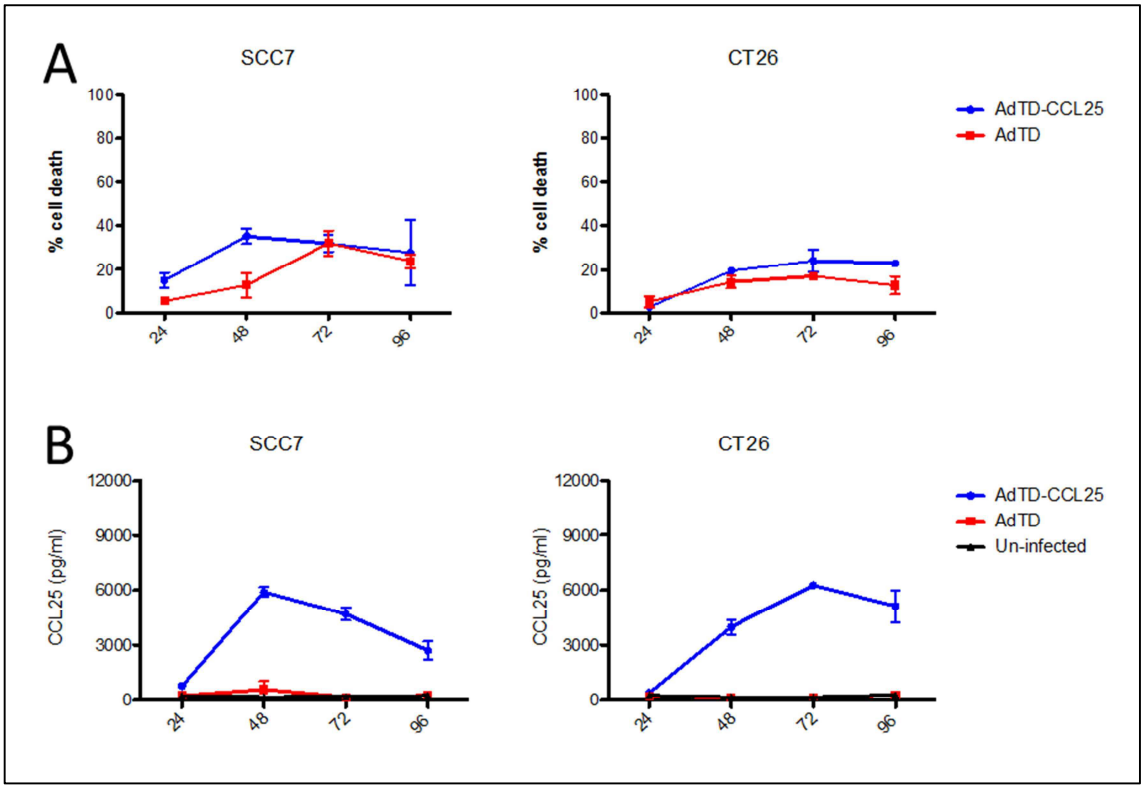

Fig 6.10 AdTD-CCL25 shows similar potency compared to AdTD-C in a CT26 and SCC7 murine cell lines.

Cells were plated in 6-well plates at $2x10^5$ cell/well and infected with AdTD-C and AdTD-CCL25 virus at MOI=10 pfu/cell. The percentage of cell killing was then determined using an MTS assay. A) shows the percentage of dead cells over a 4 days time course. Points represent the mean percentage of dead cells in three independent wells. B) show change of CCL25 as measured by ELISA in the supernatant over the same time period. Points represent mean CCL25 concentration of three independent wells. Error bars represent standard error of means (SEM).

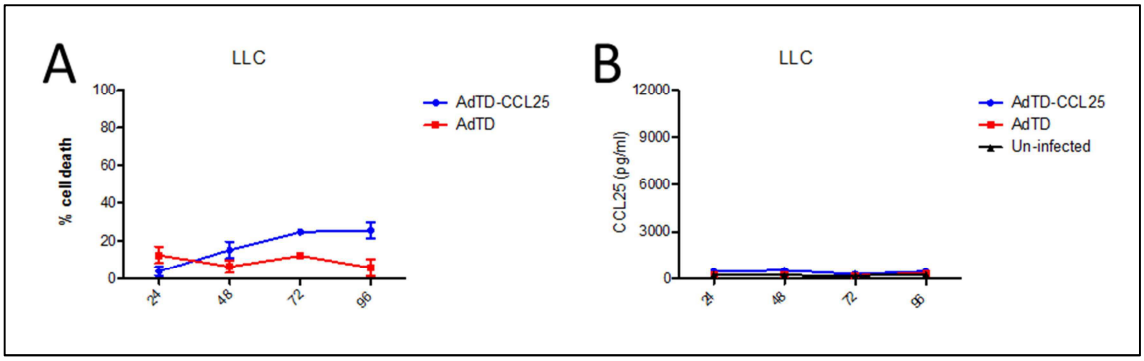

Fig 6.11 LLC cells are resistant to adenovirus infection and do not express CCL25 after AdTD-CCL25 virus infection.

LLC cells were plated in 6-well plates at $2x10^5$ cell/well and infected with AdTD-C and AdTD-CCL25 virus at MOI=10 pfu/cell. The percentage of cell killing was then determined using an MTS assay. A) shows the percentage of dead cells over a 4 days time course. Points represent the mean percentage of dead cells in three independent wells. B) shows change of CCL25 as measured by ELISA in the supernatant over the same time period. Points represent mean CCL25 concentration of three independent wells. Error bars represent standard error of means (SEM).

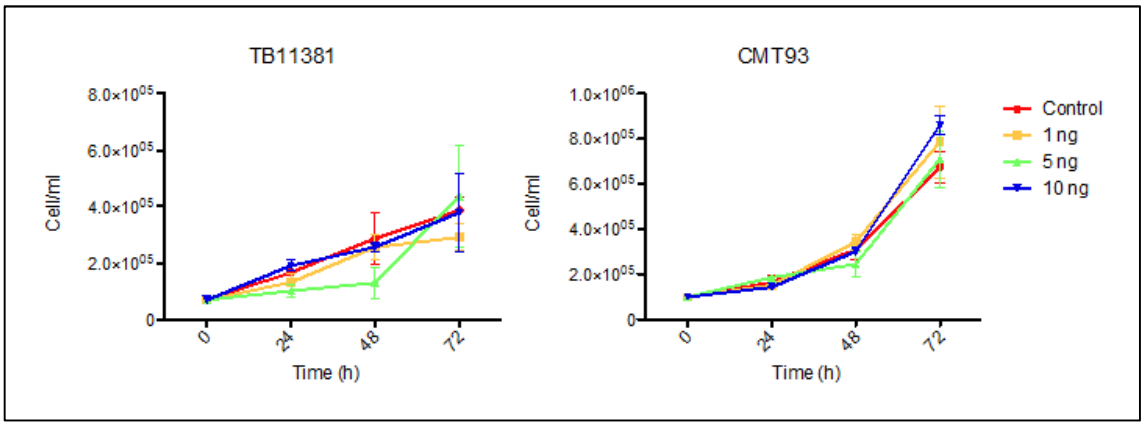

Fig 6.12 CCL25 has no direct toxicity on TB11381 and CMT93 cells.

Cells were plated in 6-well plates at $1x10^5$ cell/ml. CCL25 was added to the media to a final concentration of 1, 5 and 10 ng/ml. Untreated cells were used as a control. 24 hours later cells were trypsinised and the number of viable cells was determined using trypan blue exclusion test. The same was repeated at 48 and 72 hours. Points represent the mean number of viable cells in three independent wells. Error bars represent standard error of means (SEM).

Miss A Ibrahim, an MsC student working in our lab under my supervision, further examined the differences between AdTD-C and AdTD-CCL25 at every stage of the viral life cycle. Her results showed an earlier viral DNA replication and protein expression in cells infected with AdTD-CCL25. Her results are included in appendix III.

Due to the fact that the main direction of my work is cancer vaccination, I did not continue this line of investigation. It would have been interesting to look at the difference between these cell lines and their response to adenovirus infection at a molecular level especially that both adenovirus and CCL25/CCR9 interacts with the PI3K/AKT and the Notch signalling pathways [398-402]. This work will be continued by other colleagues in our lab as further insight into these relations might provide a platform to enhance the oncolytic efficacy of adenovirus.

6.4 Chapter six results summery

- CCL25 gene was successfully cloned into the E3 region of a triple-deleted adenovirus
- The cloned virus AdTD-CCL25 was replication competent
- CCL25 expression was confirmed in a panel of murine cell lines infected with the recombinant virus
- AdTD-CCL25 appears to be more potent at killing cancer cells compared to the parental virus due to an unknown mechanism

Chapter seven: VICCV using CCL25-armed adenovirus in pancreatic cancer model

Antitumour immune response induction following distant vaccination, as is the case in our regimen, may not be sufficient to induce a therapeutic effect. T cells trafficking to the tumour site is an integral part of the immune response. As discussed previously, we hypothesised that vaccination with pancreatic tumour cells pre-infected with AdTD-CCL25 might induce expression of α4β7 integrin on T cells leading to pancreas homing. This is mediated via the interaction between α4β7 and cell adhesion molecule MAdCAM-1.

7.1 Induction of α4β7 T cell phenotype following vaccination with DT6606 cells pre-infected with AdTD-CCL25

7.1.1 Subcutaneous vaccination

Our first aim was to test the hypothesis that T cell priming in the presence of the gut homing chemokine, CCL25, will result in the induction of gut homing phenotype characterised by the expression of α4β7 integrin. Mice were vaccinated subcutaneously with DT6606 cells pre-infected with AdTD-CCL25. Control groups of PBS, MMC-treated cells and AdTD-C pre-infected cells were also tested. One week after boost mice were culled and lymphocytes were isolated from spleen, local draining lymph node (inguinal) and distant lymph node (axillary). Percentage of CD8+ cells (Fig 7.1) and CD4+ cells (Fig 7.2) expressing α4β7 integrin and CCR9 were determined using florescence cytometry. This preliminary experiment showed an increase level of T cells expressing α4β7 integrin (more prominent in CD4+) in the AdTD-CCL25 group but no increase in CCR9. This would suggest that this increase is the result of CCL25

expression from pre-infected tumour cells rather than an upregulation of its receptor CCR9.

7.1.2 Intraperitoneal vaccination

In parallel to the above-mentioned experiment we vaccinated mice via intraperitoneal injections. This is based on the hypothesis that vaccination within a certain anatomical location would induce a homing phenotype to that organ. However, this was not the case for either CD8 (Fig 7.3) or CD4 (Fig 7.4) cells. Expression of α4β7 integrin was fairly similar between all vaccination groups with no added advantage of CCL25.

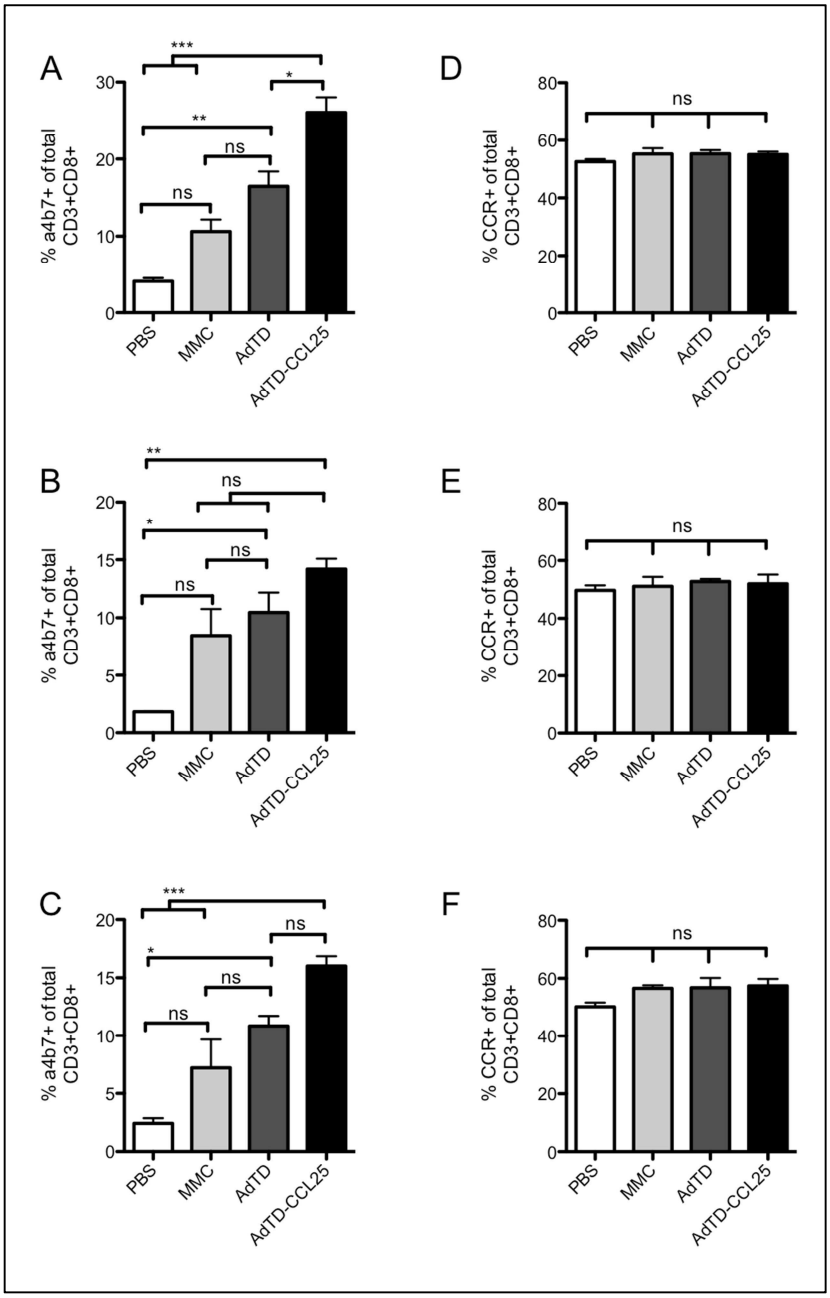

Fig 7.1 Induction α4β7 integrin on CD8+ T cells following subcutaneous vaccination with tumour cell pre-infected with AdTD-CCL25.

Four groups of C57BL/6 mice (n=3) were subcutaneously vaccinated with homologous prime/boost regimen using PBS or DT6606 cells treated with MMC, AdTD-C or AdTD-CCL25 virus. Spleens were harvested and processed one week after boost. Isolated splenocytes were stained for CD3, CD4, CD8, α4β7 and CCR9. Percentage of CD3+CD8+ cells expressing α4β7 in A) spleen, B) inguinal and C) axillary lymph nodes. D, E and F) represent CCR9 expression in the same organs respectively. One-way ANOVA with Tukey post-hoc test was used to compare groups. Columns represent the means ± SEM; asterisks denote the significance levels as comparing: ns non-significant; * $p \leq 0.05$; ** $p \leq 0.01$; *** $p \leq 0.001$.

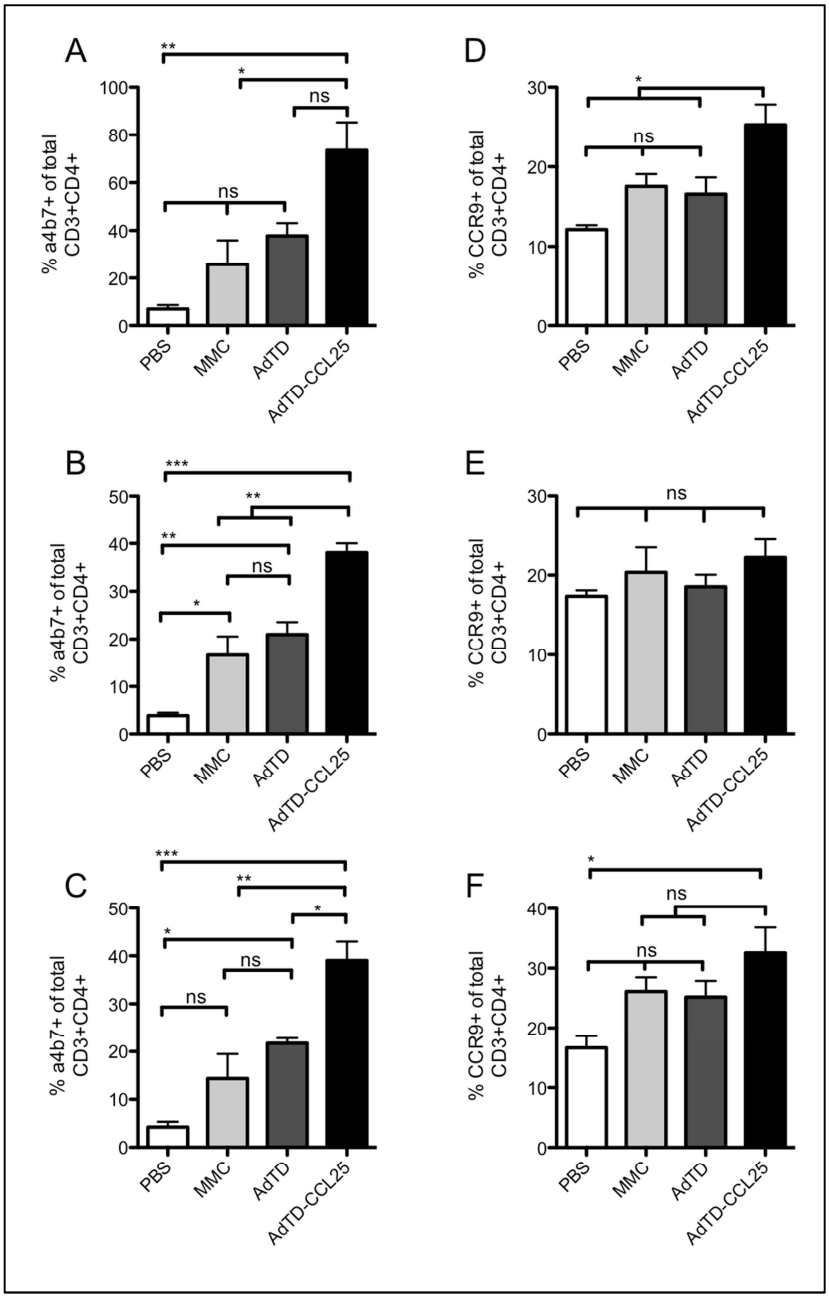

Fig 7.2 Induction α4β7 integrin on CD4+ T cells following subcutaneous vaccination with tumour cell pre-infected with AdTD-CCL25.

Four groups of C57BL/6 mice (n=3) were subcutaneously vaccinated with homologous prime/boost regimen using PBS or DT6606 cells treated with MMC, AdTD-C or AdTD-CCL25 virus. Spleens were harvested and processed one week after boost. Isolated splenocytes were stained for CD3, CD4, CD8, α4β7 and CCR9. Percentage of CD3+CD4+ cells expressing α4β7 in A) spleen, B) inguinal and C) axillary lymph nodes. D, E and F) represent CCR9 expression in the same organs respectively. One-way ANOVA with Tukey post-hoc test was used to compare groups. Columns represent the means ± SEM; asterisks denote the significance levels as comparing: ns non-significant; * $p \leq 0.05$; ** $p \leq 0.01$; *** $p \leq 0.001$.

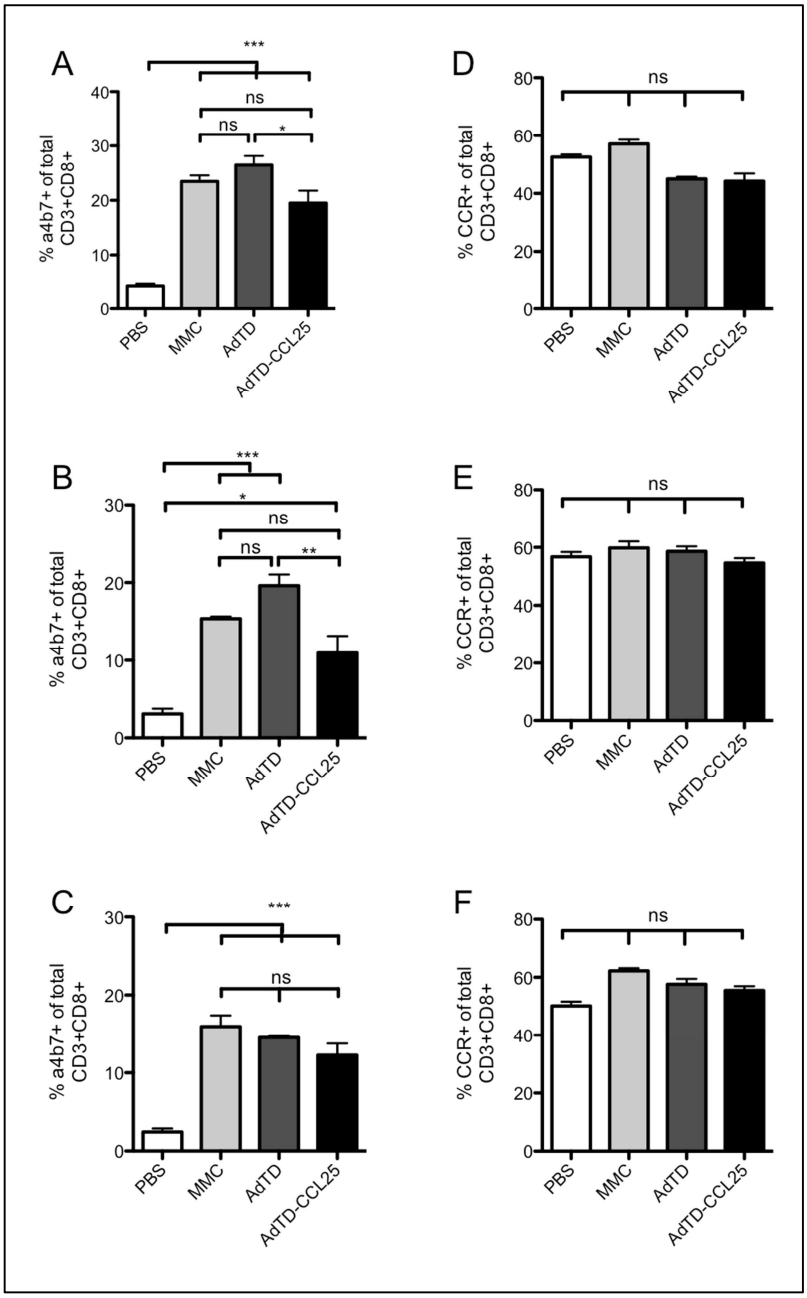

Fig 7.3 Induction α4β7 integrin on CD8+ T cells following intraperitoneal vaccination with tumour cell pre-infected with AdTD-CCL25.

Four groups of C57BL/6 mice (n=3) were subcutaneously vaccinated with homologous prime/boost regimen using PBS or DT6606 cells treated with MMC, AdTD-C or AdTD-CCL25 virus. Spleens were harvested and processed one week after boost. Isolated splenocytes were stained for CD3, CD4, CD8, α4β7 and CCR9. Percentage of CD3+CD8+ cells expressing α4β7 in A) spleen, B) mesenteric and C) axillary lymph nodes. D, E and F) represent CCR9 expression in the same organs respectively. One-way ANOVA with Tukey post-hoc test was used to compare groups. Columns represent the means ± SEM; asterisks denote the significance levels as comparing: ns non-significant; * $p \leq 0.05$; ** $p \leq 0.01$; *** $p \leq 0.001$.

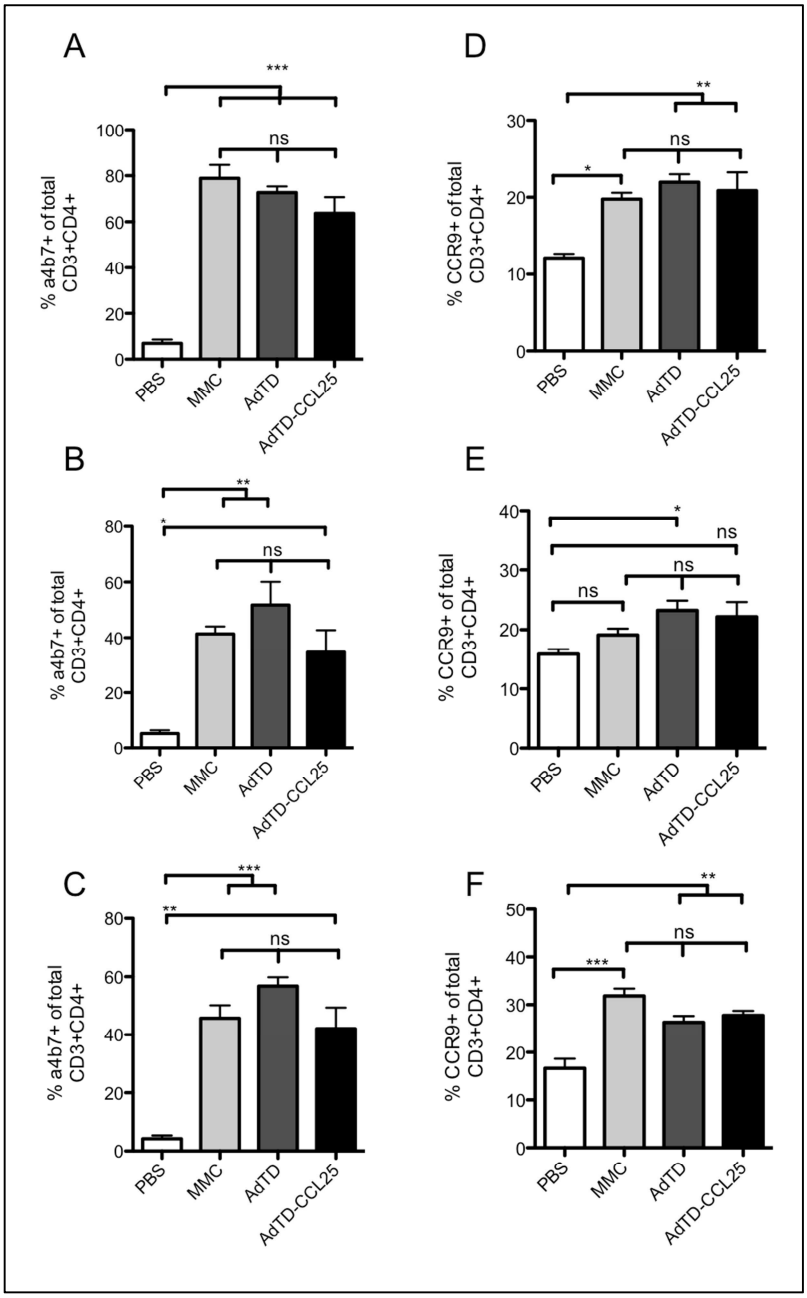

Fig 7.4 Induction α4β7 integrin on CD4+ T cells following intraperitoneal vaccination with tumour cell pre-infected with AdTD-CCL25.

Four groups of C57BL/6 mice (n=3) were subcutaneously vaccinated with homologous prime/boost regimen using PBS or DT6606 cells treated with MMC, AdTD-C or AdTD-CCL25 virus. Spleens were harvested and processed one week after boost. Isolated splenocytes were stained for CD3, CD4, CD8, α4β7 and CCR9. Percentage of CD3+CD4+ cells expressing α4β7 in A) spleen, B) mesenteric and C) axillary lymph nodes. D, E and F) represent CCR9 expression in the same organs respectively. One-way ANOVA with Tukey post-hoc test was used to compare groups. Columns represent the means ± SEM; asterisks denote the significance levels as comparing: ns non-significant; * $p \leq 0.05$; ** $p \leq 0.01$; *** $p \leq 0.001$.

7.2 Efficacy of AdTD-CCL25 VICCV in transgenic pancreatic cancer model

Based on our observation above and on the increased potency of the AdTD-CCL25 virus (MTS assay results in chapter 6), we decided to use an MOI=5 pfu/cell and a subcutaneous vaccination route. Since treatment with mitomycin C does not seem to affect CCL25 production (Fig 6.7) and to enhance the safety of vaccination regimen we decided to add MMC as a secondary treatment in keeping with our previous work. KPC transgenic mice (K-ras$^{LSL.G12D/+}$; p53$^{R172H/+}$; PdxCre) were vaccinated subcutaneously at 10 weeks old with DT6606 cell pre-infected with either AdTD-CCL25 or AdTD-C control virus and then treated with MMC. These mice recapitulate the natural sequence of genetic and histological changes seen in human pancreatic cancer. By 10 weeks of age they would have developed early pancreatic ductal adenocarcinoma (PDAC) tumours. Due to the aggressive disease progression in this mouse model we decided to boost after two weeks rather than four.

Our efficacy experiment showed a trend towards increased survival in both viral vaccination groups compared to PBS (Fig. 7.5). Although this survival increase did not reach statistical difference, it represents a positive result in our opinion. In this experiment we vaccinated the mice with $2x10^6$ pre-infected cells in keeping with our previous work. There is convincing evidence from clinical trials that antitumour immune response is dose-dependent in whole cell vaccines [403]. We speculate that vaccination with higher dose will enhance our vaccine efficacy. This will be necessary to overcome the aggressive tumour process in KPC mice.

On the other hand, there was no difference between the two viral vaccine groups. This will be examined in detail in the following sections.

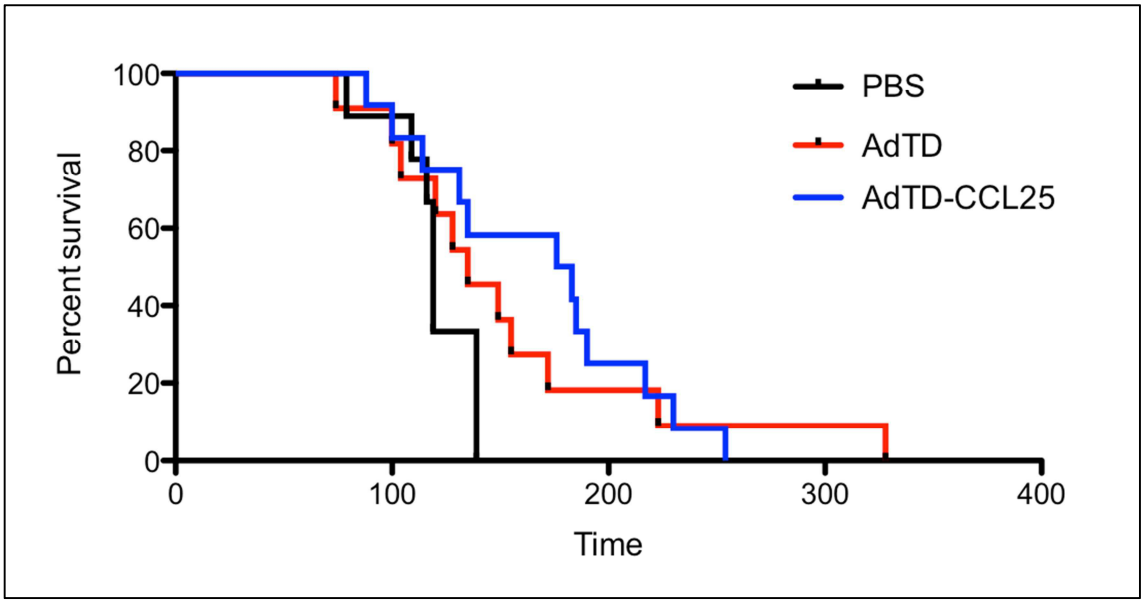

Fig 7.5 VICCV using AdTD-CCL25 virus did not increase survival in KPC mice.
KPC mice were randomised at weaning into one of three treatment groups: PBS (n=10), VICCV using AdTD-C (n=12) virus or AdTD-CCL25 (n=13). Each mouse in the VICCV groups received a subcutaneous injection of $2x10^6$ DT6606 cells pre-infected with corresponding virus at MOI=5 pfu/cell then treated with MMC for 2 hours at ten weeks old then boosted two weeks later. Mice were monitored twice a week and culled according to home office guidelines. Kaplan-Meier survival curve showing no overall difference between the groups ($p>0.05$). The author designed the experiment, wrote the protocol and analysed the data. This experiment was performed by staff at the Sino-British Research Centre for Molecular Oncology, Zhengzhou University, Zhengzhou, China.

7.3 Gut homing and antitumour immunity induction by VICCV regimen using DT6606 and AdTD-CCL25 virus

In the efficacy experiment, cells were treated with MMC prior to injection. In addition we used a lower MOI and a shorter prime-boost interval. These were different from the conditions used in the preliminary experiment described above (section 7.1).

Concurrently with the efficacy study we tried to validate that these changes did not affect the induction of α4β7 integrin on T cells.

Mice were vaccinated with DT6606 cells pre-infected with AdTD-CCL25 or AdTD-C control virus and treated with MMC. The experiment had two arms with the only difference is the prime/boost interval.

7.3.1 Induction of antitumour immunity

In keeping with our previous experience, vaccinated mice showed stronger anti-tumour immune response, evident by higher levels of IFN-γ secreted from *ex vivo* splenocytes stimulated by tumour cells, compared to PBS-vaccinated mice. There was no difference in IFN-γ levels between the two viruses or the different prime/boost intervals (Fig 7.6).

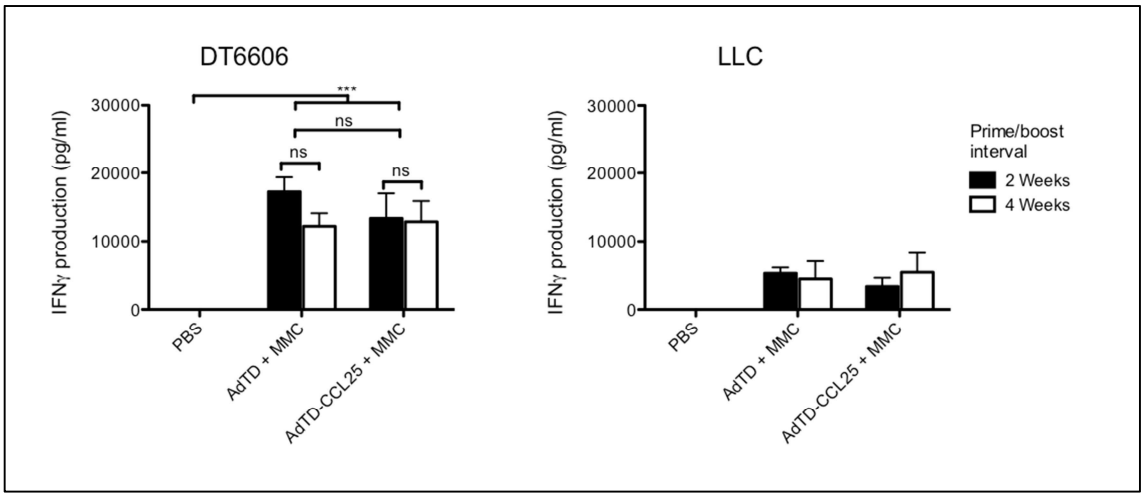

Fig 7.6 Induction of antitumour immunity following VICCV using AdTD-CCL25 virus. Six groups of C57BL/6 mice (n=3) were subcutaneously vaccinated with homologous prime/boost regimen using PBS or DT6606 cells treated with AdTD-C or AdTD-CCL25 virus followed by a secondary treatment with mitomycin C. Mice were boosted either two or four weeks later. Spleens were harvested and processed one week after boost. Isolated splenocytes were incubated for 72 hours with proliferation-arrested DT6606 cells or LLC cells. IFNγ production, as an indicator of CD8 activation, in the supernatant was measured by ELISA. IFNγ levels were normalized by subtracting background release from non-stimulated splenocytes. Two-way ANOVA with Bonferroni post-hoc test was used to compare groups. Columns represent the means ± SEM; asterisks denote the significance levels as comparing: ns non-significant; * $p \leq 0.05$; ** $p \leq 0.01$; *** $p \leq 0.001$.

7.3.2 Induction of T cells gut-homing phenotype

In the same experiment described above, splenocytes were stained for CD3, CD4 and CD8. Percentage of T cells expressing α4β7 integrin was determined using fluorescence cytometry. Contrary to our preliminary experiment we didn't detect any difference between the AdTd-CCL25 group and the control virus or even the PBS treated mice (Fig 7.7).

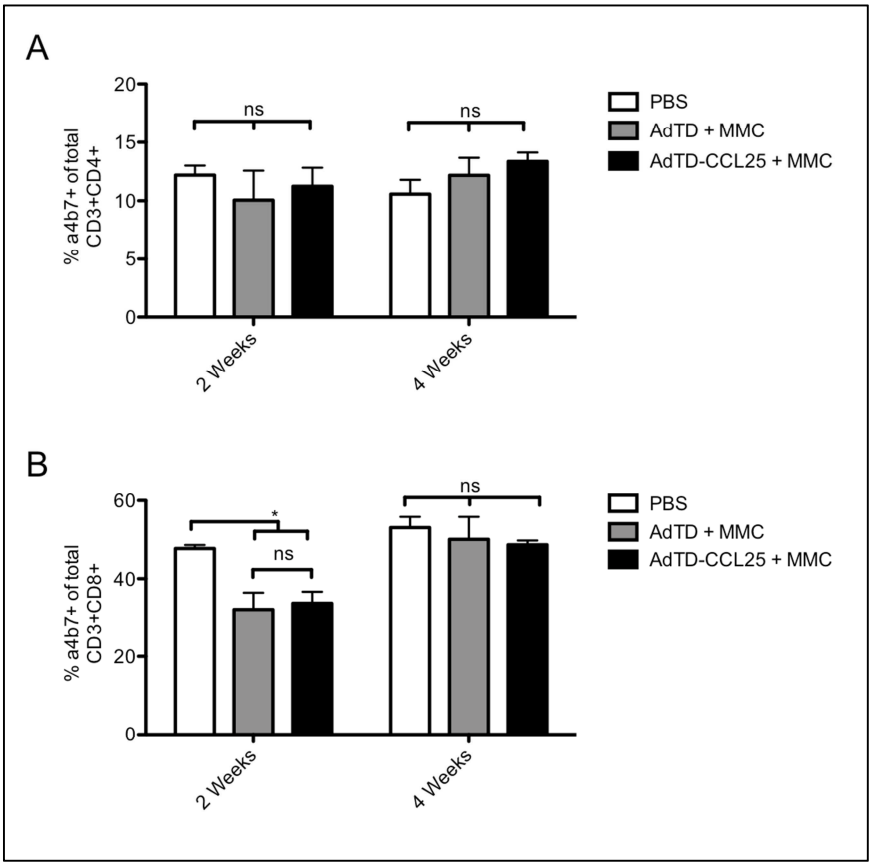

Fig 7.7 Induction α4β7 integrin on CD8+ and CD4+ T cells following subcutaneous vaccination with tumour cell pre-infected with AdTD-CCL25.
In the same experiment described above (fig 7.6) isolated splenocytes were stained for CD3, CD4, CD8, α4β7 and CCR9. Fig A) shows the percentage of CD3+CD8+ cells expressing α4β7. Fig B) shows expression on CD3+CD4+. The two groups in each graph represent different prime/boost intervals. Two-way ANOVA with Bonferroni post-hoc test was used to compare groups. Columns represent the means ± SEM; asterisks denote the significance levels as comparing: ns non-significant; * $p \leq 0.05$; ** $p \leq 0.01$; *** $p \leq 0.001$.

Of note, the percentage of CD8+ cells expressing α4β7 integrin in this experiment was significantly higher compared to all other experiments including the PBS group. This is

likely to be caused by technical issues at flowcytometry stage as the Laser voltages were set too narrowly which meant differentiating various populations was difficult despite the kind assistance of our FACS Lab manager. The experiment was included for the sake of completion. However the results interpretation needs to be treated with caution.

7.4 VICCV using AdTD-CCL25 virus in TB11381 cell line.

Following the border line results of the efficacy studies and the failure to induce α4β7 in the matching functional study we decided to test our hypothesis using TB11381 murine pancreatic cell line.

In two separate experiments, C57BL/6 mice were vaccinated using TB11381 cells pre-infected with AdTD-CCL25 and treated with mitomycin C. In the first experiment an MOI=5 was used (Fig 7.8) and an MOI=25 in the second (Fig 7.9). Neither dose induced a higher expression of α4β7 integrin compared to control treatments.

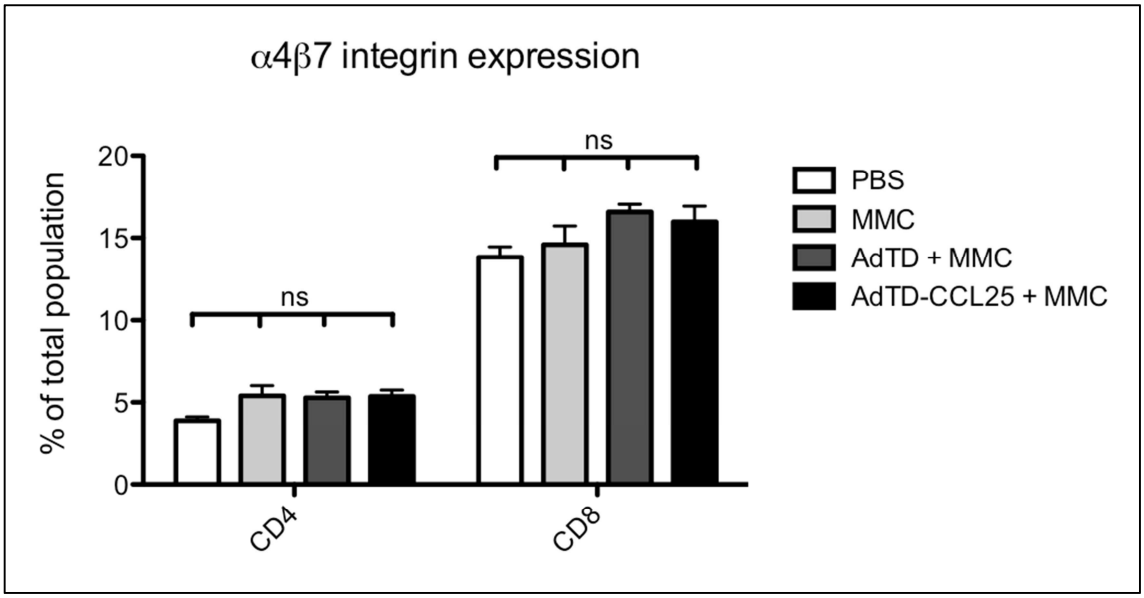

Fig 7.8 Induction α4β7 integrin on CD8+ and CD4+ T cells following subcutaneous vaccination with TB11381 tumour cell pre-infected with AdTD-CCL25.

Four groups of C57BL/6 mice (n=3) were subcutaneously vaccinated with homologous prime/boost regimen using PBS or DT6606 cells treated with mitomycin C, AdTD-C or AdTD-CCL25 virus at an MOI=25 pfu/cell followed by a secondary treatment with mitomycin C. Mice were boosted four weeks later. Spleens were harvested and processed one week after boost. Isolated splenocytes were stained for CD3, CD4, CD8 and α4β7. The graph shows the percentage of CD3+CD8+ or CD3+CD4+ cells expressing α4β7. One-way ANOVA with Tukey post-hoc test was used to compare groups. Columns represent the means ± SEM; asterisks denote the significance levels as comparing: ns non-significant; * $p \leq 0.05$; ** $p \leq 0.01$; *** $p \leq 0.001$.

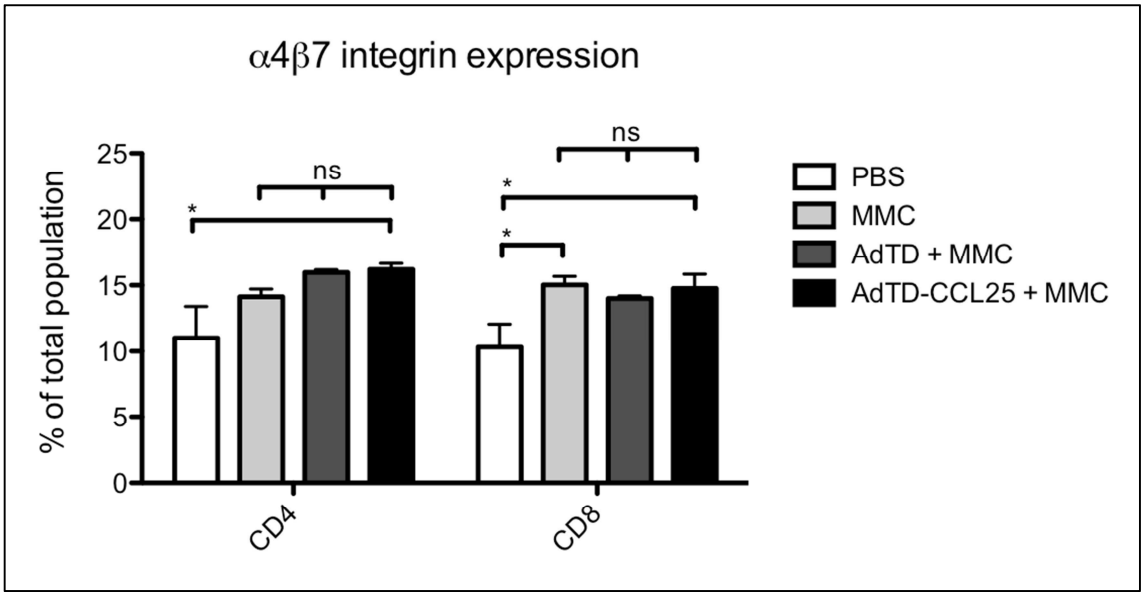

Fig 7.9 Induction α4β7 integrin on CD8+ and CD4+ T cells following subcutaneous vaccination with TB11381 tumour cell pre-infected with AdTD-CCL25.

Four groups of C57BL/6 mice (n=3) were subcutaneously vaccinated with homologous prime/boost regimen using PBS or DT6606 cells treated with mitomycin C, AdTD-C or AdTD-CCL25 virus at an MOI=5 pfu/cell followed by a secondary treatment with mitomycin C. Mice were boosted four weeks later. Spleens were harvested and processed one week after boost. Isolated splenocytes were stained for CD3, CD4, CD8 and α4β7. The graph shows the percentage of CD3+CD8+ or CD3+CD4+ cells expressing α4β7. One-way ANOVA with Tukey post-hoc test was used to compare groups. Columns represent the means ± SEM; asterisks denote the significance levels as comparing: ns non-significant; * $p \leq 0.05$; ** $p \leq 0.01$; *** $p \leq 0.001$.

Due to the lack of efficacy and the negative results in three separate experiments we decided not to pursue this line of investigation any further. The disparity between these experiments and our preliminary one will be discussed in further detail in the discussion chapter.

7.5 Dissection of the immune response following VICCV using TB11381 cells

7.5.1 Induction of antitumour immunity

Repeating the α4β7 induction experiment using TB11381 cells provided us with an opportunity to validate the VICCV regimen in a third model in addition to the DT6606 and the HNSCC cell lines tested in previous chapters.

Vaccination of mice with TB11381 cells pre-infected with either virus resulted in an increased IFN-γ production from splenocytes when incubated with their cognate tumour cells. This was a tumour-specific response as stimulation with LLC cells resulted in significantly lower levels (AdTD p=0.0099, AdTD-CCL25 p= 0.0413) (Fig 7.10)

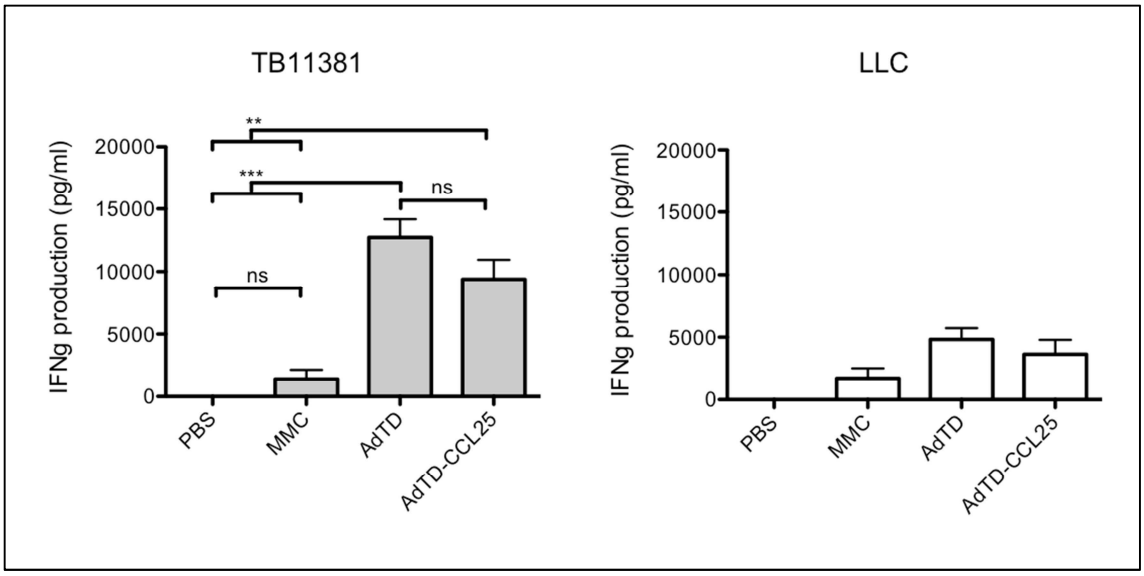

Fig 7.10 VICCV using TB11381 cells induced a tumour-specific immune response.
Four groups of C57BL/6 mice (n=3) were vaccinated with PBS, MMC-treated TB11381 cells or cells pre-infected with AdTD-C or AdTD-CCL25 virus plus MMC secondary treatment. Mice were similarly boosted four weeks later. Spleens were harvested and processed one week after boost. Isolated splenocytes were incubated for 72 hours with proliferation-arrested TB11381 cells or LLC control cells. IFNγ production, as an indicator of CD8 activation, in the supernatant was measured by ELISA. IFNγ levels were normalized by subtracting background release from non-stimulated splenocytes. One-way ANOVA with Tukey post-hoc test was used to compare groups. Columns represent the means ± SEM; asterisks denote the significance levels as comparing: ns non-significant; * $p \leq 0.05$; ** $p \leq 0.01$; *** $p \leq 0.001$.

7.5.2 Immunophenotyping of T cell response following VICCV using TB11381 cells

Similar to our findings in HNSCC model, vaccination with pre-infected TB11381 cells resulted in an increase in effector memory T cells ($CD44^{Hi}CD62L^{Lo}$) in both CD4+ (Fig 7.11) and CD8+ Cells (Fig 7.12).

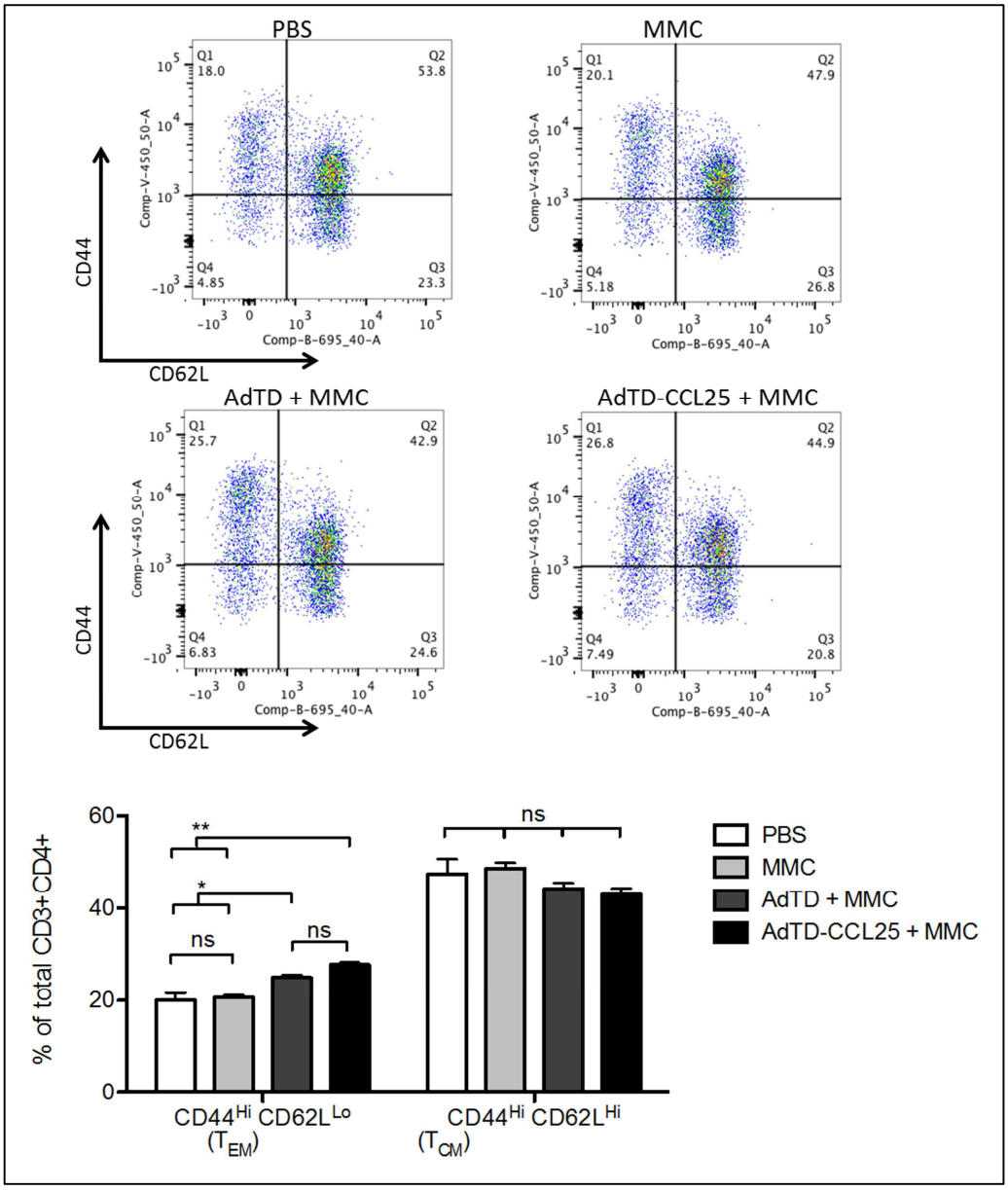

Fig 7.11 VICCV with TB11381 cells pre-infected with AdTD virus enhances the generation of an effector memory CD4+ population.

Four groups of mice (n=3) were vaccinated with PBS, MMC-treated TB11381 cells or cells pre-infected with AdTD or AdTD-CCL25 plus MMC secondary treatment. Mice were similarly boosted four weeks later. Spleens were harvested and processed one week after boost. Splenocytes were stained for CD3, CD4, CD8, CD44, CD62L and profiled into various populations using fluorescence cytometry. The dot plots show a representative mouse one of each treatment group. The bar charts depict the effector and central memory populations out of the total DC4+ population. One-way ANOVA with Tukey post-hoc test was used to compare groups. Columns represent the means ± SEM; asterisks denote the significance levels as comparing: ns non-significant; * $p \leq 0.05$; ** $p \leq 0.01$; *** $p \leq 0.001$.

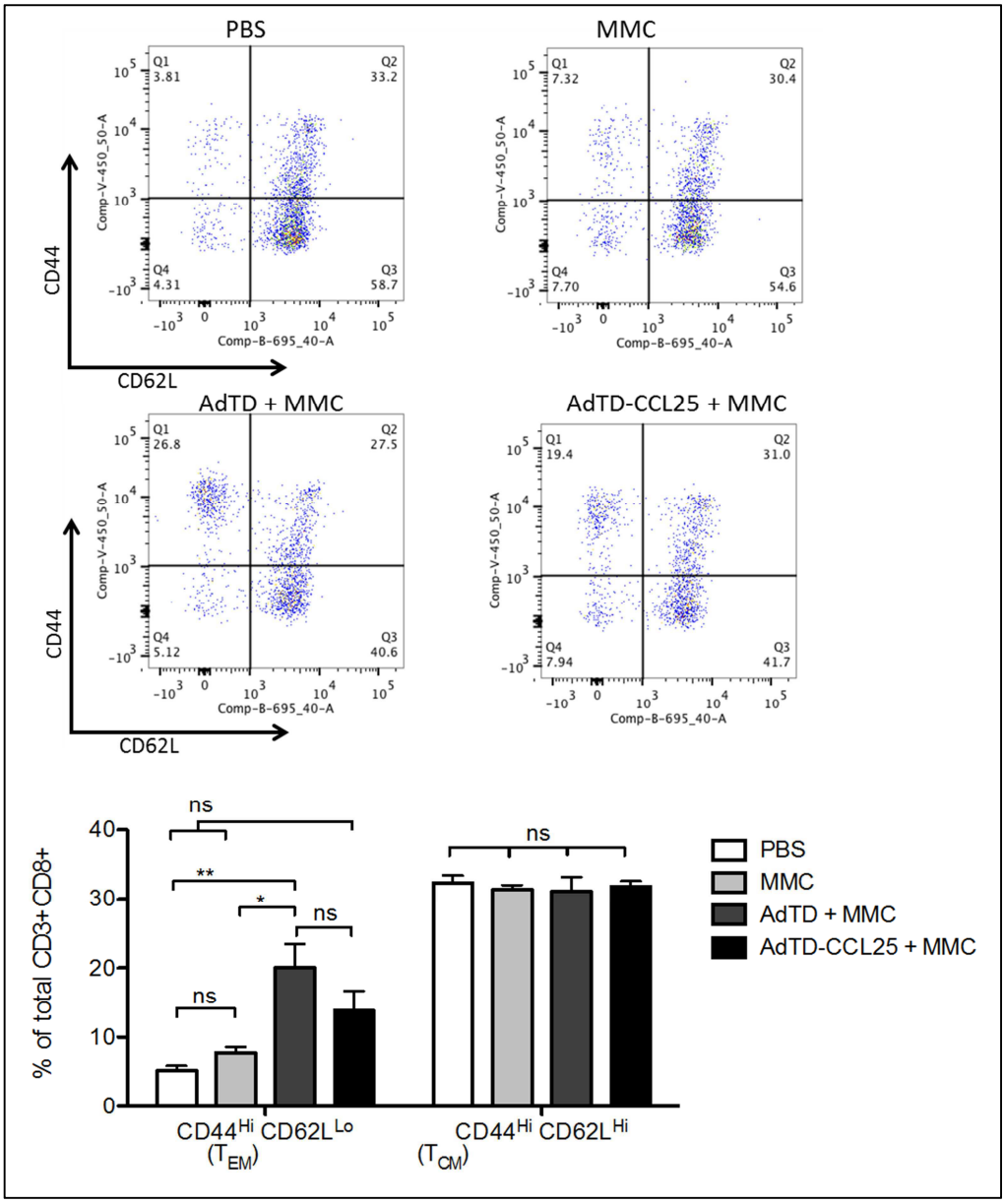

Fig 7.12 VICCV with TB11381 cells pre-infected with AdTD virus enhances the generation of an effector memory CD8+ population.

Four groups of mice (n=3) were vaccinated with PBS, MMC-treated TB11381 cells or cells pre-infected with AdTD or AdTD-CCL25 plus MMC secondary treatment. Mice were similarly boosted four weeks later. Spleens were harvested and processed one week after boost. Splenocytes were stained for CD3, CD4, CD8, CD44, CD62L and profiled into various populations using fluorescence cytometry. The dot plots show a representative mouse one of each treatment group. The bar charts depict the effector and central memory populations out of the total DC8+ population. One-way ANOVA with Tukey post-hoc test was used to compare groups. Columns represent the means ± SEM; asterisks denote the significance levels as comparing: ns non-significant; * $p \leq 0.05$; ** $p \leq 0.01$; *** $p \leq 0.001$.

7.6 Chapter seven results summery

- Subcutaneous vaccination with pancreatic cancer cells pre-infected with AdTD-CCL25 virus resulted in an increase in T cells expressing α4β7 integrin.
- No such increase was seen when mice were vaccinated intraperitoneally.
- Repeat experiments after adding secondary treatment of mitomycin was not successful. There was no difference between vaccination groups in three independent experiments.
- Vaccinating KPC mice with DT6606 cells pre-treated with AdTD or AdTD-CCL25 led to an increase in survival. However there was no significant statistical difference between the two viral groups.
- In keeping with our previous experience, vaccination with DT6606 or TB11381 pancreatic cancer cells pre-treated with either adenovirus resulted in a tumour specific immune response.
- Similarly, there was an increase in effector memory T cells in both viral groups compared to control.

Chapter eight: Discussion

8.1 Proof of concept

8.1.1 Efficacy of virus-infected cancer cell vaccine

There is abundant evidence in the literature that the immune system plays a major role in the anti-tumour effect of OVs [6-9]. Our group has shown recently that intratumoural (IT) injection of AdV followed by VV in a Syrian hamster subcutaneous pancreatic tumour model led to complete regression of the tumours. More importantly, we have demonstrated that this treatment induced a T cell-mediated tumour specific immunity capable of protecting treated animals against tumour re-challenge [80].

The current study utilises these findings to develop a prime/boost virus-infected cancer cell vaccine (VICCV). Cancer cells treated with either AdV or VV for 4 hours and 2 hours respectively were injected subcutaneously in the animal. This short period of exposure to the virus allows enough time for attachment and internalisation. After cell injection, the virus continues its life cycle and replication *in vivo* leading to cell lysis and immunogenic cell death. The released DAMPs and PAMPs activate DCs which co-present TAA to T cells resulting in an anti-tumour immunity.

In our proof of concept experiment, VICCV resulted in an anti-tumour immunity capable of protecting the animals from tumour re-challenge up to three times the vaccination dose ($2x10^6$ and $6x10^6$ cells for vaccination and re-challenge respectively). Higher tumour re-challenge doses seem to overwhelm the immune system and the VICCV lost its protective ability. This result was in keeping with evidence from clinical trials. It is well documented that tumour vaccination and immunotherapy does not work well in patients with high tumour burden [404, 405].

Other groups have shown effective anti-tumour immunity using a similar approach with other OVs. Vaccination with NDV-infected cells resulted in protective anti-tumour immunity in pre-clinical experiments [259, 406, 407] and clinical trials [262, 327, 408, 409]. Similarly, vaccination with tumour cells infected with vesicular stomatitis virus led to protective anti-tumour immunity [410].

8.1.2 Homologous vs. heterologous prime/boost VICCV

Prime-boost vaccination is a long established strategy to generate long-lasting immunity [411, 412]. In the context of viral vectors vaccination, heterologous prime-boost where two different viral vectors are used may be required to circumvent the anti-viral immunity against the prime virus [413].

Our group has tested the VICCV regimen in Syrian hamster subcutaneous tumour model. The vaccination led to protective immunity preventing tumour progression on tumour re-challenge. In the Syrian hamster model all viral groups were significantly better than vaccination with MMC-treated cells. Prime vaccination with Ad5-infected cells followed by boost with VVL15-infected cells resulted in the highest level of protection against tumour re-challenge compared to other prime/boost combinations [Wang et al, unpublished data] (Fig 8.1). The results of the efficacy study in the Syrian hamster model seems to reflect our group's previous experience [80] that heterologous treatment with AdV-infected cells prime and VV-infected cells boost offers the best protection against tumour progression.

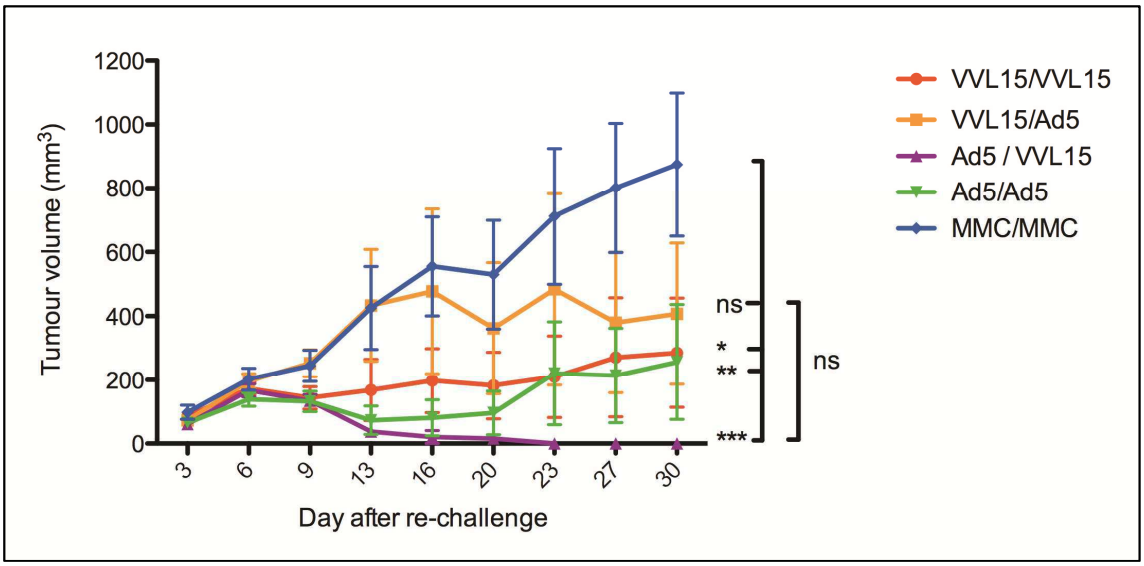

Fig 8.1 Vaccination with virus-infected tumour cells can induce a protective antitumour immunity.

Five groups of Syrian Hamsters (n= 9 or 10) were vaccinated (Prime) with HPD-1NR cells pre-treated with Mitomycin (MMC), Adeno Virus (Ad) or Vaccinia Virus (VV). Four weeks later vaccination was repeated (boost). The animals were challenged two weeks after boost with HPD-1NR cells ($1x10^7$ cells) via subcutaneous injection and tumours' sizes were monitored over 30 days period. Two-way ANOVA test with Bonferroni post-test analysis was used to compare various groups.

The picture seems slightly different in the mouse model.

As a measure of tumour-specific immunity we used IFN-γ release assay. This assay is based on the release of IFN-γ when CD8 cells are activated by their cognate epitope-MHC complex. In each experiment, mice were vaccinated with tumour cells pre-treated with an oncolytic virus or with MMC as a control. In some experiments, more control groups were introduced using Rx or MTX-treated cells to compare the anti-tumour immunity induced by the secondary treatment alone vs. virus plus treatment. All experiments included a PBS-treated group to exclude non-specific immunity caused by animal related factors such as general or injection site infection, general anaesthesia and so forth. Two weeks after boost mice were euthanized and spleens were harvested. We incubated isolated splenocytes with proliferation-arrested target tumour

cells, control tumour cells or media only. The latter group was used as a measure of non-specific IFN-γ released from other cells, mainly natural killer cells. The background IFN-γ was then deducted from the total released in each target and control tumour samples and the difference was represented on column chart. This measure should correlate to the level of specific tumour/antigen immunity.

IFN-γ assay results in the mouse model showed that priming the animals with AdV-infected cells offered a significant increase in anti-tumour immunity when compared to VV-infected cells or control groups. There was a general trend of a higher immune response in homologues (AdV/AdV) compared to heterologous vaccination (AdV/VV) although that did not reach statistical significance. These results were accurately reflected in the prime/boost efficacy study in subcutaneous model.

8.1.3 Safety and translatability of the VICCV

Injecting viable tumour cells, albeit virus-infected, as a vaccine raises few safety and ethical concerns that will impact the potential translatability of our VICCV. First, can we guarantee all injected tumour cells will be virus-infected? Even if they were all infected, does that guarantee all cells will be killed by the OV? Second, can we reliably monitor the injected tumour cells for early detection of cell survival? What form of monitoring is required? Finally, in case some injected cells survived the viral infection and developed a tumour in injection site, what would be the rescue plan?

To overcome these challenges the safety of the VICCV needs to be enhanced. One approach would be to use higher MOI for viral infection. However, that will increase the toxicity of the treatment due to a higher viral dose. Alternatively, we can monitor cells, via a labelling system incorporated in the OV, to guarantee all injected cells are infected. The third approach, that we adapted, would be to add a secondary treatment

to arrest the proliferation of vaccine cells prior to injection in the form of irradiation or a chemotherapeutic agent.

After validating the required doses of Rx, MMC and MTX to arrest the proliferation of vaccination tumour cell lines, the effect of these treatments on viral replication was tested. Irradiation led to moderate reduction of viral replication while MMC and MTX treatment led to the complete arrest of AdV replication and a significant reduction of VV's.

Contrary to our expectations, this reduction of viral replication did not lead to reduction in anti-tumour immunity. These findings were later confirmed in murine HNSCC cells where adenovirus is replication-defective. This seems to reflect other groups experience were vaccination with non-replicating OVs did not impact anti-tumour immunity [410]. We speculated that despite the lack of viral replication, the virus in combination with secondary treatment was still killing vaccination cells resulting in the release of the required DAMPs and PAMPs to generate an effective anti-tumour immunity. This was confirmed in the HNSCC model. Adenovirus in these cell lines was replication defective however it was still capable of killing the cells. Adding mitomycin did not reduce cell killing. To the contrary, it resulted in better cell killing in the B4B8 cell line (Fig 5.4).

While, in-depth investigation of immunogenic cell death mechanisms is beyond the scope of this study and is the subject of a PhD project of another team member [El-Khouri *et al*, unpublished data], I investigated the effect of secondary treatments on PAMPs release in the form of viral proteins and viral DNA. Radiation and MMC seem to have little impact on viral proteins production and viral DNA replication while MTX resulted in some reduction in both.

From these results it appears that a strong anti-tumour immunity requires a viral infection with sufficient dose to kill tumour cells and release associated DAMPs and PAMPs. Virus replication does not seem to be a deciding factor in the overall success of the cancer vaccine.

8.2 HNSCC animal model

8.2.1 Pros and cons of the HNSCC tumour models

SCC7 and SCC7-RLuc cell lines were very consistent at developing primary tumours either subcutaneously or orthotopically. The luciferase stable transduction doesn't seem to affect the viability of these cells or how they behave *in vivo*. SCC7 tumours grew rapidly to reach the maximum size limit within two to three weeks. However, despite the large tumour size these animals remained well throughout with steady weight increase and no sign of cachexia or muscle wasting. Metastatic disease was limited in this model. We only observed a single lung metastasis in one out of 20 animals tested. This seems to contradict the finding of the original paper describing the orthotopic model were they found lung and lymph node metastasis in 15 out 20 animals tested [414]. However other authors using this model could not replicate these results when using the tumour model [415]. Various authors have used the SCC7 cells as a metastatic model by injecting these cells in the mouse tail vain [415-417]. However in our opinion this is a poor representation of the tumour spread seen in head and neck cancer patients. It simply represents tumour embolus in distant organs bypassing the continuous natural process of tumour cells invasion and migration. Another potential shortcoming of this tumour model is the tissue origin of these cells. Despite its wide use as a HNSCC cell line, the SCC7 cells originated from a spontaneously occurring SCC of the abdominal wall of the C3H mice rather than their upper aerodigestive tract [418].

B4B8 is a murine SCC cell line derived from BALB/c oral keratinocytes treated with the chemical carcinogen 4NQO before being transplanted and re-isolated in SCID mice [381]. Tumours derived from this cell line show histological features of well-differentiated squamous cell carcinoma [381, 394]. In our experiments we found tumours originating from this cell line to be slow growing with no lung or lymph node metastasis, similar to previously published studies [394, 419]. This growth and metastasis pattern does not accurately resemble human disease progression however; we believe this to be a useful model to represent an unrespectable locally advancing disease. In particular, this could be a useful model to test vaccination and other immunotherapy treatments where the longer survival of the animal allows a sufficient timeframe for repeated vaccination boosts and development of a strong immune response. The stable transduction of the B4B8 cells doesn't seem to affect the ability of these cells to form tumours *in vivo*.

LY2 cells were isolated from lymph node metastasis after inoculation with PAM212 squamous cell carcinoma cells [382]. The latter is a spontaneously transformed cell line derived from neonatal keratinocytes of male BALB/c mice [383]. The LY2 cells exhibits a more aggressive growth and metastatic phenotype compared to the parental line [382]. In our experience subcutaneous and orthotopic tumours derived from this cell line grow rapidly to reach maximum size limit between two and three weeks. The tumour had a high affinity to lungs and lymph nodes with almost all animals showing metastasis to both organs. The only exception was the orthotopic tumour model where we did not observe any lung metastasis. In this experiment we injected $5x10^6$ cells into the right cheeks of the animals. All the animals in this experiment were culled at day 16, while the time required for overt lung metastasis to form is around three weeks [394]. We believe that the tumour dose used was probably too high resulting in the

rapid demise of these animals. Over all, the orthotopic LY2 model (possibly using a lower number of injected cells) is the most accurate representative of the human head and neck cancer out of the three cell lines.

Contrary to the other two cell lines, transfecting LY2 cells with Renilla luciferase did change the phenotype of these cells. The LY2-RLuc has a reduced ability to form primary tumours and resulted in a slower growth rate. In the orthotopic tumour model we reported tumour formation rate between 10 to 20%. In contrast, all animals in the subcutaneous model ($5x10^6$ injection dose) formed tumours, albeit slow growing. This low tumour formation rate in the orthotopic model is likely to be due to our inability to differentiate small slow-growing tumours from the underlying masseter muscle by manual palpation. IVIS luminescence imaging system would have helped to show small tumours embedded into the muscle. Unfortunately the imaging system, along with most of the Biological Services Unit (animal house) and the animal imaging suit, were unavailable for large parts of this study due to refurbishment. The rate of lung and lymph node metastasis is slightly reduced compared to parental cells which make the luciferase tumour model even closer to the human disease. Another added benefit of this model is the prolonged survival of these animals in comparison to parental cells making it more suitable model for vaccination and immunotherapy approaches.

8.2.2 Surgical excision model

Treatment of most head and cancers would involve surgical resection of the tumour and the main cause for mortality is locoregional recurrence. To simulate this clinical scenario we used our cells in a surgical excision model. Despite the lack of metastasis of the SCC7 model we decided to test it as there is evidence that surgical excision can promote metastasis and stimulate the growth of any minimal residual disease [420]. In our experiment most animals developed local recurrence between 7 to 10 days after

excision that grew in a similar pattern to the primary tumour leading to the animals needing to be culled almost three weeks later. This surgical model had the same shortcomings described previously. There was no lung or lymph node metastasis and the animals remained well until the point of sacrifice.

Similarly the LY2 and LY2-RLuc cells behaved in a predictable manner in the subcutaneous surgical excision model. The growth rates and metastasis were in keeping with our previous results. Of note all mice in these groups developed skin ulceration at injection site leading to early excision in four out of ten mice. This early excision didn't lead to reduction in metastasis however it might prove problematic for experiments requiring intratumoural injections. I attempted an orthotopic surgical excision model using LY2 parental cells however this was a significantly challenging model as described previously limiting its applicability.

Subcutaneous tumour models in general do not reflect site-specific tumour growth and metastasis behaviour related to different blood supply, immune cell composition, local stromal components and site-specific organ invasion. The latter is particularly relevant to HNSCC where dysphagia and dyspnoea caused by tumours involving the upper aerodigestive tract are some of the key features of the human head and neck cancers. However flank tumours are not without their advantages. They are easy to access and measure, surgical excision is fairly simple, they drain to inguinal nodes which are easy to assess clinically and simple to harvest and finally, the lack of impingement on the upper aerodigestive tract allows longer survival and humane care of the animals. Regardless of which model is used one needs to keep in mind that a model is just that, a model. Models' shortcomings, differences in biology and host response between human and mouse need to be taken into account when extrapolating experimental data into human disease [421, 422].

8.3 VICCV in head and neck cancers

8.3.1 Model validation

Since this was our lab first experience with the B4B8 and the LY2 cells we aimed to validate these cells suitability for oncolytic viral therapy. MTS cell killing assay showed both cell lines to be amenable to adenovirus infection with an EC50 value of around 10 pfu/cell for both cell lines. Based on this we decided to use a dose of 20 pfu/cell for all our *in vivo* and *in vitro* experiment in keeping with our previous work (working dose approximately double the EC50 value). To the contrary SCC7 cells were very resistant to adenovirus infection with an EC50 value over 2,500 pfu/cell which meant these cells will not be suitable for my VICCV treatment. All three cell lines were amenable to vaccinia virus infection. Luciferase stable cell lines were similarly sensitive to adenovirus infection with slightly higher EC50 values. The two experiments (parental vs. stable) were performed independently. A variety of factors could affect the outcome of this assay including media, cells, incubation period between cell plating and infection, and viral exposure to room temperature making the comparison of two independent experiments difficult. The moderate increase of EC50 value is probably within the margin of variability of the MTS assay.

As is the case with the majority of murine cells, the LY2 and B4B8 cells and their luciferase stable cell lines did not support human adenovirus replication. Based on our proof of concept data we speculated that this lack of replication would not affect antitumour immunity. Our INFγ assay results discussed in the next section seems to support this hypothesis.

8.3.2 VICCV-induced antitumour immunity

In two independent experiments we measured IFN-γ released from splenocytes of vaccinated mice as an indicator of antitumour immunity. In the first of these experiments mice were vaccinated with B4B8 or LY2 parental cells. As expected, splenocytes of mice vaccinated with B4B8 cells pre-infected with AdTD and treated with mitomycin released the highest level of IFN-γ when stimulated *in vitro* with B4B8 cells indicating the highest level of antitumour immunity compared to naïve mice or mice vaccinated with MMC treated cells. In addition, the highest IFN-γ was against B4B8 cells compared to LY2 or the JC control cell line indicating a cell-specific immune response.

The results were not as predictable in the LY2 vaccinated mice. Firstly there was no significant difference in immune response between mice vaccinated with virus-infected cells and the other treatment group or even naïve mice. Secondly there was no difference if splenocytes were stimulated with LY2 cells or JC cells. Interestingly, immune response was significantly higher when splenocytes were stimulated with B4B4. This difference between the two cell lines suggests that B4B8 cells are more immunogenic than LY2 cells. We speculate that some tumour antigens sre expressed in a much higher level in B4B8. High throughput sequencing might provide some answers if it can identify the presence of neoantigens in both cell lines.

In the second experiment we vaccinated mice with LY2-RLuc cells. The results appear to be very similar to these of the parental cell lines. B4B8 cells were significantly more immunogenic compared to LY2. Luciferase transduction does not seem to increase the immunogenicity of these cells however it attenuates their growth and duplication rates.

8.3.3 T cell activation and effector memory induction as a response to VICCV

The introduction of an antitumour immune memory is key to the success of any tumour vaccine. Effector memory cells and CD8+ in particular play a crucial rule in the immune response to cancer. These cells have lost their lymphoid tissue homing capacity and primarily populate peripheral tissues. They play a sentinel role and are capable of immediate activation and expansion when faced with their cognate antigen to generate a strong antitumour response. In experimental tumour models the induction of CD8+ T_{EM} phenotype lasted up to five months after tumour resection and was capable to protect animals against tumour re-challenge either intradermally or intravenously [423]. In a clinical setting the induction of T_{EM} phenotype correlated with better survival and antitumour response [424, 425].

In our head and neck cancer model we tested if vaccination with adenovirus pre-infected cells can lead to activation of T cells and development of a memory phenotype. Our results demonstrated that vaccination with pre-infected B4B8 cells results in an increase in the T_{EM} population of both CD4+ and CD8+ cells, and a proportional drop of the T_{CM} population. This increase was less prominent and did not reach statistical significance for either LY2 or LY2-RLuc vaccinated mice.

It is to be acknowledged that the increase in effector memory is not purely related to antitumour immunity as part of the increase of this population is derived from T cell targeting adenovirus than tumour cells. The distinction between the two groups could be technically difficult to assess. One way would be to use viral antigen pentamer to detect antiviral T cells. Other members of our lab [El-Khouri *et al*, unpublished data] attempted this experiment using vaccinia virus antigen B8R without success as the total percentage of these cells out of the total population was less than 1% making data interpretation unreliable. Nevertheless, we believe this T_{EM} increase to be mainly in the

antitumour population as, firstly, the total starting viral dose is very small and large proportion of it will be invariably lost in the infection and multiple wash steps. Only a small proportion of the total virus volume will be carried into the animal. In addition these cell lines do not support adenovirus replication keeping the total viral particles count relatively small. Secondly, the disparity between the two cell lines suggests that this increase in T_{EM} population is probably derived from the tumour specific subset rather than an antiviral population as both cell lines where infected at same MOI and the same number of cells were used for vaccination.

8.3.4 Efficacy of the VICCV in head and neck cancer model

To test if this anti-B4B8 immune response can translate into efficacy we tested our VICCV as a therapeutic vaccine in a locally advancing disease model. Mice were inoculated orthotopically in the right cheek and the tumours were allowed to grow for a week before the prime vaccination using adenovirus pre-infected B4B8 cells at a distant site (right flank). Animals were boosted twice at two weeks intervals. Up to day 55 when the first animal was culled in each treatment group there was a significant slowing of the tumour growth. This led to a trend increase in the overall survival of these animals however that did not reach statistical difference. Although on the surface these results were not as impressive as our previous efficacy results in DT6606 subcutaneous inoculation model (*Chapter 3*) were complete tumour rejection was achieved; this orthotopic model is a lot more realistic and closer to a real clinical scenario. The orthotopic site of the tumour and its impingement on the upper aerodigestive tract (not dissimilar to HNSCC patients) meant other factors such as feeding and breathing affected the overall survival of these animals. In a true clinical scenario such factors could be overcome, even in unresectable tumours, via assisted breathing and feeding i.e. insertion of tracheostomy tube or tumour debulking and enteral feeding methods.

The lack of significant tumour regression in our vaccination model should not be interpreted as a failure of the vaccine. Evidence from clinical trials using the poxvirus-based PROSTVAC vaccine (also known as PSA-TRICOM) showed that the reduction of tumour growth rate is more important for the overall survival than rapid tumour regression seen with chemotherapy [426]. The findings of these trials supports the notion that cancer vaccines are most effective when used in patient with low tumour burden. Combining vaccination with other traditional treatments that can significantly reduce tumour volume such as surgery or chemotherapy (as the case in the PROSTVAC trials) will theoretically lead to a much improved overall survival. The paradigm of increase survival in vaccination patients despite the lack of tumour regression is further explored below (Fig 8.2). Although this theoretical model is based on prostate cancer trials we believe it to be particularly applicable to head and neck cancer patients were the biggest killer is locoregional recurrence secondary to minimal residual disease post surgical excision. Cancer vaccination in this group could significantly slow down the growth rate of the recurrent disease leading to increased patients' survival.

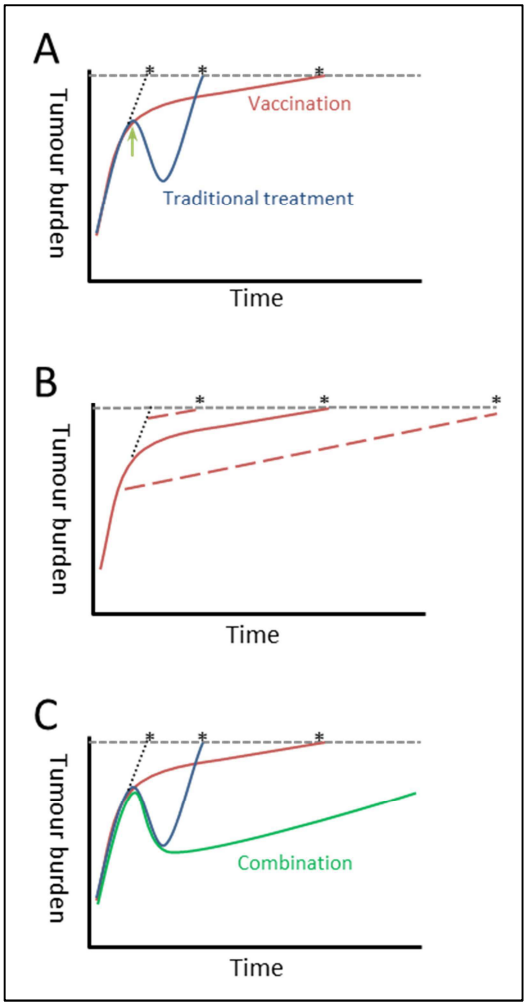

Fig 8.2 Vaccination vs traditional cancer therapies.

A) Traditional cancer treatment including surgery and chemoradiotherapy lead to rapid tumour regression followed by rapid increase while vaccination therapy leads to slowing of tumour growth rate leading to increased survival. Arrow represent treatment point, * denotes terminal point and broken line shows growth curve if left untreated. Graph B) shows the effect of tumour burden at the initiation of vaccination on the overall survival of the patient. Overall survival can be enhanced by initiating vaccination at an earlier time point. Graph C) shows the effect of combining vaccination with traditional cancer treatment resulting in a significant increase of overall survival. This model is based on PROSTVAC clinical trials data. Figure adapted from [421].

8.4 VICCV using AdTD-CCL25 virus

8.4.1 Why is AdTD-CCL25 more potent at killing cancer cells? Or is it?

The increased efficacy of AdTD-CCL25 virus was first noted during daily observation of infected cells in viral validation experiments (replication and CCL25 expression). It became apparent that the CCL25-armed virus killed the cells at much earlier time point compared to control virus. These results were confirmed in our first virus validation experiment (Fig 6.5) using an MOI=50 pfu/cell. This is our standard dose for adenovirus infection in DT6606 and TB11381 cell lines. In this experiment we found that CCL25 levels dropped rapidly after 24 hours, and the AdTD-armed virus didn't replicate in these cells.

Various different reasons could explain these results. Firstly, viral titration is incorrect which means the AdTD-CCL25 was being delivered in a much higher dose. Secondly, AdTD-CCL25 is replication-defective. Thirdly, AdTD-CCL25 is more potent at killing cancer cells compared to control virus possibly due to a synergistic effect between adenovirus and CCL25.

Initially each of the two viruses was titrated independently at the point of mass production. The TCID50 assay, by its very nature, could be affected by viability of JH293 cells used in titration or variation of assay conditions such as media, incubation temperature, etc. Titration of both viruses was repeated by the author and independently by my colleagues Mr M Yuan and Miss A Ibrahim (results not shown) showing consistent values.

Once satisfied with the titration, I proceeded to calculate the EC50 value for each virus in the cell lines of interest. The MTS assay showed the AdTD-CCL25 virus to be around 20 times more potent compared to control virus. This meant that our starting dose of MOI=50 pfu/cell was too high. Repeat replication experiment using an MOI=10 pfu/cell (Fig 6.7) exclude the second hypothesis and showed that the AdTD-CCL25 virus was replication competent in the cell lines of interest. As expected, the virus replicated better in human cell line SUIT2 compared to murine ones.

Our final hypothesis was that the AdTD-CCL25 virus was more potent at killing cancer cells. That could be either due to a better, earlier replication of AdTD-CCL25 virus leading to rapid killing of all cells within the first 24 hours; or it could be related to CCL25 toxicity killing these cells within the first 24 hours preventing viral replication. The latter was fairly simple to exclude as recombinant CCL25 protein was not directly

toxic to cells (Fig 6.11). This left us with the possibility that the AdTD-CCL25 virus is in fact more potent at cell killing. This was confirmed in a number of murine cell lines (Fig 6.8). Simultaneously we looked into CCL25 expression in these cell lines. We could not demonstrate a correlation between the level of CCL25 and viral potency suggesting no synergistic effect between the two. This was later confirmed by my MSc student Ms A Ibrahim as she found that adding recombinant CCL25 to backbone AdTD virus did not increase its cell killing ability. She went on to demonstrate that AdTD-CCL25 virus has a faster life cycle including earlier DNA replication and viral protein synthesis due to an as-yet unexplained mechanism.

However, and of a potentially critical importance, when we titrated the viruses using a picogreen assay we had paradoxical results. This assay measures the number of viral particles (vp) based on the amount of viral DNA in the purified viral stock. It does not distinguish between viable and dead virus particles. To the contrary, the TCID50 assay is a functional assay measuring viable infectious viral units. The vp/pfu ratio for our in-house produced adenoviruses is around 10:1 – 20:1. This was correct for the AdTD-C virus however the ratio was around 700:1 for the CCL25-armed virus. This could simply represent a poor quality batch of the AdTD-CCL25 virus and suggest the possibility of direct toxicity of the cells. It is however difficult to explain how this direct toxicity affects a variety of cell lines but does not affect the JH293 cells (when both viruses added in equal volumes to the JH293 cells during the TCID50 assay, the control virus was almost ten fold better at killing cells). Furthermore, when Ms Ibrahim tested the difference between the two viruses in terms of life cycle she used both methods of titration and came to similar conclusion.

In conclusion, we are still to explain the difference in cell killing potency between the two viruses and the paradox of picogreen vs TCID50 titration. More work need to be

done in this area possibly looking at a molecular level and the interaction between the virus and CCL25 pathway.

8.4.2 Induction of T cells gut-homing phenotype secondary to AdTD-CCL25 VICCV

In our pilot experiment when we vaccinated mice with pancreatic cancer cell lines pre-infected with AdTD-CCL25 virus via subcutaneous route we achieved significant increase in T cells expression α4β7 integrin in spleens, local and distant lymph nodes. The increase was more prominent in CD4+ cells. Contrary to our expectations, and our collaborators experience, we did not detect this increase when vaccinating the mice intraperitoneally. We speculated that this difference was related to the anatomical nature of the vaccination site. Subcutaneous vaccination will keep all the injected cells in close proximity allowing viral spread between the cells resulting in CCL25 to be expressed to a high level in a sustained fashion. To the contrary, intraperitoneal injection will lead to tumour cells being dispersed around the abdominal cavity possibly limiting viral spread between the cells.

Based on the success of the pilot experiment we moved to add a secondary treatment of mitomycin to bring it in line with our pre-infected cell vaccination. Unfortunately we could not replicate the pilot experiment success despite repeating the experiment in different pancreatic cancer cell lines using different viral dose. I scrutinised my methods closely and re-analysed my flowcytometry results using different gating strategies with the help of experienced members of the team but the results were consistent (with the exception of CD8+ cells in the DT6606 vaccination experiment as explained previously, *Section 7.3.2*). The main difference between the experiments was the addition of mitomycin. Although I have validated that CCL25 expression is maintained with MMC treatment, we know from our proof of concept data that it significantly reduces viral replication. Similar to intraperitoneal vaccination, the lack of

viral replication and cell to cell spread might limit the level and sustainability of the CCL25. This remains largely speculative explanation. It would have been interesting to measure CCL25 levels at the site of vaccination although it might be technically challenging and will require a large number of animals. A more realistic approach would have been to fuse CCL25 with a reporter gene such as green florescent protein where expression levels could be monitored with IVIS imaging in real time with having to sacrifice animals at each time point. In light of time limit of this study and most importantly the limited efficacy results in KPC mice we decided not to pursue this line of investigation any further.

8.4.3 Antitumour immunity in the AdTD-CCL25 vaccination model

Although the model failed to deliver a statistically significant therapeutic effect in the KPC mice or an increase expression of α4β7 integrin it did provide us with vital information on antitumour immune response in a second tumour model.

IFN-γ assay in both DT6606 and TB11381 were in line with my previous results in the HNSCC model and the proof of concept experiments. Infecting the cells with adenovirus prior to injecting them resulted in a strong cell-specific immune response. Arming the virus with CCL25 gene does not change this response. Similarly the pattern of T cell activation and the increase in effector memory population following vaccination with TB11381 cells was very similar to that generated after vaccination with B4B8 cells.

8.4.4 Prime/boost interval

Deciding the prime/boost schedule for our VICCV regimen was a subject of much debate at the early stages of this project. Most published literature suggests an interval between two to three months [427, 428]. However it was difficult to extrapolate this data to our vaccine as most of these studies are based on infectious diseases data

from human trials rather than cancer vaccine. In addition most of vaccination trials use antibody response rather than cellular response as a determining factor. Finally the difference in biology, immune response and tumour growth rates between human and mouse complicates matter further. At the end we decided to take a pragmatic approach and chose a four weeks interval. However, rapid tumour growth in KPC transgenic mice dictated a shorter interval. We compared anti tumour immune response after vaccination with pre-infected DT6606 cells with different vaccination interval (Fig7.6). There was no significance different between two and four weeks. We decided to use two weeks in our efficacy results for both KPC mice and the B4B8 orthotopic model.

Irrespective of what the “optimal” interval is, it remains only relevant to this experiment. We do not believe such interval will translate well to human trials due to the differences mentioned above. Vaccination schedule should be decided based on actual patients’ data and it might need to be incorporated in phase I/II trial.

8.5 Potential for improvement and clinical applicability

8.5.1 Enhancing antitumour immunity using combination therapies

Combining oncolytic virotherapy, including our pre-infected cell vaccine, with other cancer treatments is an area of great promise. Traditionally, chemotherapy was not believed to be compatible with cancer vaccination due to myeloid suppression and the resultant immunodeficiency. However, evidence from basic research and clinical trials seems to support the use of combination therapy [429]. One such example in pancreatic cancer is Gemcitabine. It can suppress Myloid-derived suppressor cells (MDSC) in the tumour microenvironment resulting in a stronger anti-tumour immune response [430]. On the other hand, gemcitabine is a nucleoside analogue that inhibits DNA synthesis including that of double stranded DNA viruses [431]. Using these

agents in a sequential rather than combination manner might be the key to effective therapy [432].

Similarly, combining our VICCV with immune checkpoints inhibitors is an area that requires more investigation and optimisation. PD-1 and CTLA-4 inhibitors might enhance the OV-induced antitumour immunity by creating a favorable immune profile in the tumour microenvironment [433, 434]. We tested our DT6606 and the HNSCC cell lines for expression PDL-1 (Fig 8.3) with the LY2 cells showing the highest expression levels making them a potential model for combination therapy.

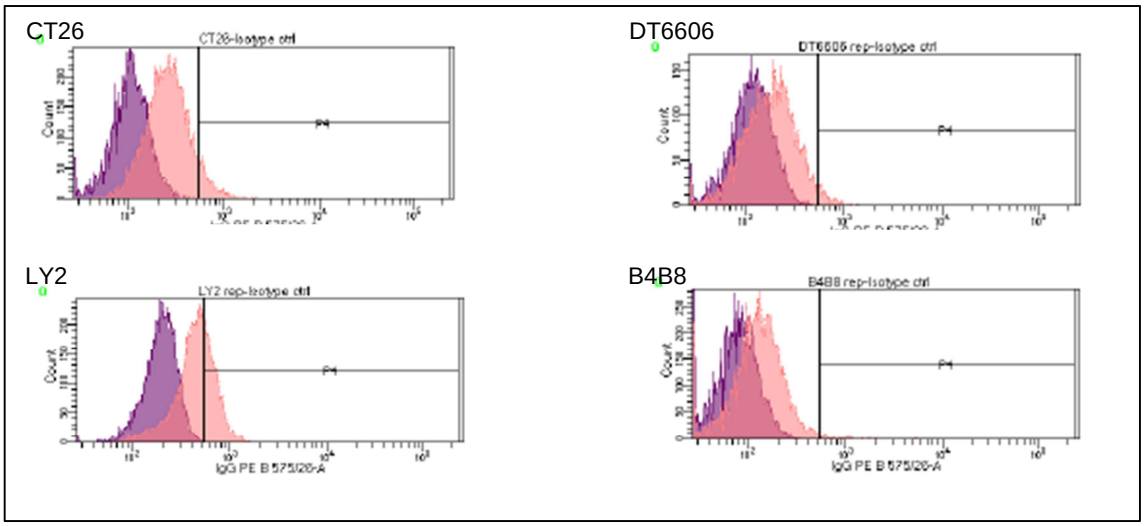

Fig 8.3 PDL-1 expression in a panel of murine cell lines.
1x10^6 DT6606, LY2 and B4B8 cells were stained for PDL-1 using anti-mouse PDL-1 antibodies PE 1:200 or Isotype Control Mouse IgG1 PE (eBioscience, San Diego, CA, USA) . CT26 cells were used as a positive control as we have confirmed their expression of PDL-1 previously using Western Blot. Expression levels were measured using florescence cytometry.

8.5.2 Enhancing immune response using cytokines-armed viruses

One of the main advantages of viruses as vaccine vectors is their ability to accommodate transgenes, including cytokines, and express them to a high level. Using

cytokines-armed adenovirus in my VICCV regimen can enhance the resultant antitumour immune response. Rational selection of different cytokines for prime and boost based on function can enhance the various stages of the developing immune response. We speculate that using a cytokine that can enhance antigen presentation, such as GM-CSF and Fms-like tyrosine kinase 3 ligand (Flt3L), for prime and a cytokine that can stimulate a T-cell response, such as IL-12 or IL-21, for boost will elicit the strongest antitumour immune response.

Our group has a well-established track record working with cytokines armed oncolytic viruses. IL-12 armed triple-deleted adenovirus [P Wang et al, unpublished data] or Lister strain vaccinia virus [J Ahmed *et al*, unpublished data] has shown better efficacy and stronger antitumour immunity compared to backbone virus in pancreatic and lung tumour models. Similarly our group has found that intratumoural injection of vaccinia virus armed with IL-10 dampened antiviral immune response resulting in prolonged viral persistence in pancreatic tumours. This led to stronger anti-tumour immunity and improved survival in both subcutaneous and transgenic pancreatic cancer mouse models [28]. Although these experiments were all direct antitumour injection it seems that the resultant immune response is an, if not the most, important factor behind the efficacy. In all these experiments the addition of the cytokine did not significantly change the potency of the virus *in vitro* but enhanced it *in vivo* highlighting the role of the immune system.

8.5.3 CXCR3-mediated T cell homing

Although our CCL25-induced gut homing experiment was largely unsuccessful we still believe there is enough merit in the approach to warrant further investigation. Evidence from preclinical experimental work shows that CXCR3-mediated T cell homing plays an important role in antitumour immunity [435]. In addition it plays a role trafficking CD8+

cells to virus infected cells [436]. We have shown in one pilot experiment that our VICCV using adenovirus-infected DT6606 cells can lead to an increase CD4+ and CD8+ T cells expressing CXCR3 (Fig 8.4).

We are currently constructing a triple deleted adenovirus expressing the CXCR3-ligand CXCL10. We would like to combine this virus with our vaccination. We are hypothesising that intratumoural injection of the CXCL10-armed virus will enhance T cell trafficking to the tumour site. Alternatively, other approaches that enhance the production of CXCL10 via the activation of the Toll-like receptors could be used in combination with our vaccination regimen. One such approach is to combine vaccination with polyinosinic-polycytidylic acid stabilised by lysine and carboxymethylcellulose (poly-ICLC) [437]. If successful, these combinations could represent a promising new strategy to target tumour cells.

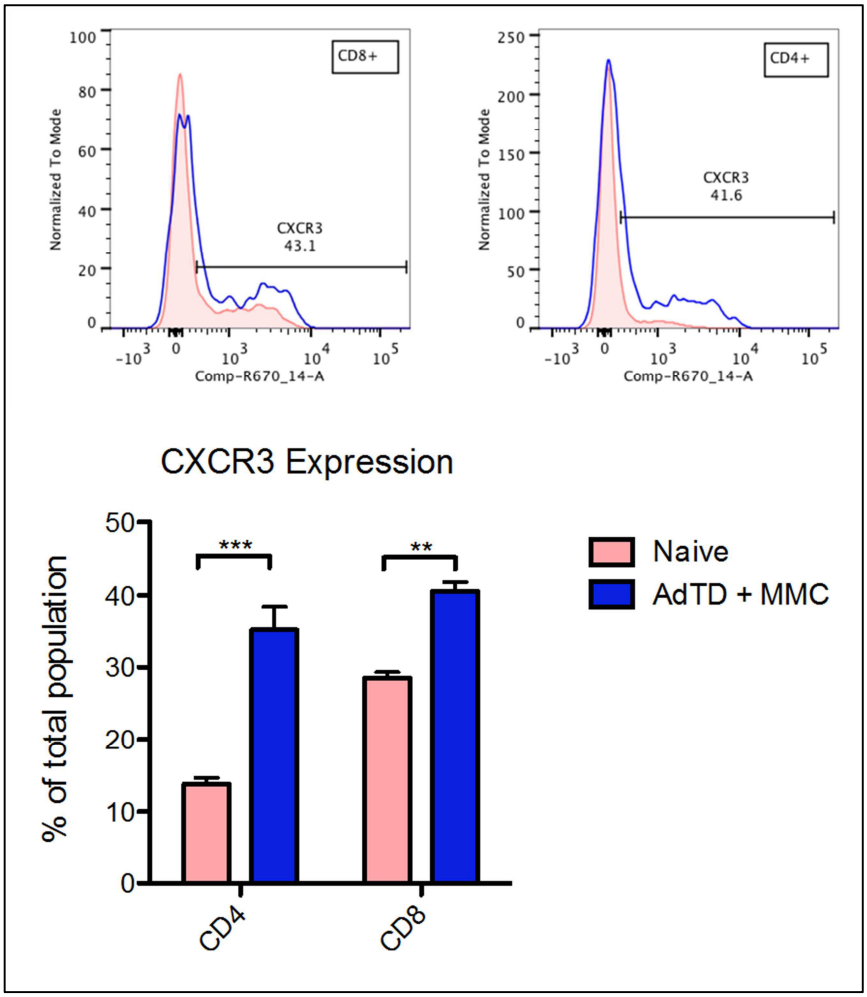

Fig 8.4 VICCV increased the proportion of T cells expressing CXCR3.
Two groups of mice (n=3) were vaccinated with either PBS or DT6606 cells pre-infected with AdTD plus MMC secondary treatment. Mice were similarly boosted four weeks later. Spleens were harvested and processed one week after boost. Splenocytes were stained for CD3, CD4, CD8, CXCR3 and profiled into various populations using fluorescence cytometry. The line graphs show a representative mouse of each treatment group. The bar charts depict the CXCR3+ cells out of the total CD4+ and CD8+ populations in naïve and vaccinated mice. One-way ANOVA with Tukey post-hoc test was used to compare groups. Columns represent the means ± SEM; asterisks denote the significance levels as comparing: ns non-significant; * $p \leq 0.05$; ** $p \leq 0.01$; *** $p \leq 0.001$.

8.6 Conclusion and future work

Virus infected cancer cell vaccine is a promising strategy in the fight against cancer. It utilises oncolytic viruses' ability to kill tumour cells in a combination of immunogenic and non-immunogenic cell death modes providing the immune system with the "danger

signal” required to induce an antitumour immune response. This danger signal is likely to be a combination of danger- and pathogen-associated molecular patterns.

We have shown that our vaccination regimen can induce a tumour-specific immune response capable of protecting the animals against tumour re-challenge. In addition, our VICCV can enhance the pool of the effector memory T cells in a variety of tumour models. We have demonstrated our vaccination efficacy in subcutaneous tumour models where vaccinated mice were able to reject tumour cells on re-challenge. The efficacy was less impressive in orthotopic HNSCC model and in the transgenic pancreatic tumour model. In general, immunotherapeutic treatments are less effective when used as monotherapy in advanced tumours. Most current clinical trials use a combination of immunotherapy and traditional cancer treatments. Although such combination was not tested in the thesis, we believe this will be true for our vaccination.

This project has brought this vaccination regimen one step closer to a clinical trial by enhancing the safety of the proposed treatment via the addition of a secondary treatment in the form of radiation or chemotherapeutic agents to arrest the replication of the injected tumour cells. Further work is required to establish the safest and most effective secondary treatment. We can see a great potential in combining the virus pre-infection with a chemotherapeutic agent that can further enhance the immune response.

In the immediate future, we will be testing our VICCV in other head and neck cancer models such as LY2-RLuc and HCPC-1 in Syrian Hamsters. The latter provides the opportunity to excise orthotopic tumours in combination with vaccination. The next step

would be to test other treatment combination such as chemoradiotherapy and immune checkpoints inhibitors.

On the long term, we believe this vaccination has the potential to go into clinical trials. I envisage this to be an effective treatment after surgical excision in head and neck cancer with advanced nodal disease and extracapsular tumour spread. These patients would be at a great risk of locoregional recurrence due to minimal residual disease. An effective vaccination targeting these micro metastasis would hopefully slowdown this process.

Another potential clinical application would be to combine our VICCV with neoadjuvant intratumoural oncolytic viral injection. In this treatment the injected oncolytic virus will result in direct tumour lysis and induce an antitumour immune response, effectively an *in situ* vaccination. Following surgical excision and chemoradiotherapy the patient will receive repeated boost injections of VICCV using a different virus to pre-infect the cells.

I do believe there is merit, and a clinical need, for this vaccination regimen. I hope I will be in a position to bring it to the clinic in the not too distant future.

Appendix I: AdTD-CCL25 cloning enzymatic reactions

AdTD vector digestion with SwaI

Plasmid DNA	6 µl (852.6 ng/µl)	
SwaI	5 µl	
BSA	1 µl	
NEB Buffer 3	10 µl	
H_2O	78 µl	→ 25°for 4 hours

AdTD vector dephosphorylation

Digestion reaction	100 µl	
rSAP	5 µl	→ 37°for 1 hours

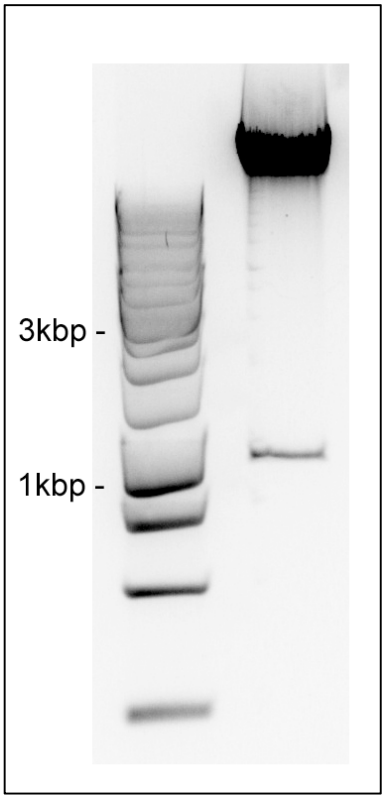

Fig i.1 Confirmation of SwaI digestion of *AdTD* vector.
AdTD vector was digested with SwaI restriction enzyme as described above then dephsphorylated with recombinant Shrimp Alkaline Phosphatase (rSAP). 5µl of the enzymatic reaction were diluted in 15µl of water and run on agarose gel. Image shows digested fragment size as expected (1093bp)

pCMV6-Entry-mCCL25-MycDDK digestion with EcoRI

Plasmid DNA	8 µl (621 ng/µl)	
EcoRI	3 µl	
EcoRI Buffer	5 µl	
H_2O	34 µl	→ 37°for 2 hours

EcoRI digestion site blunting

EcoRI reaction	50 µl	
dNTP	5 µl	
DTT	3 µl	
Blunting enzyme mix	2 µl	→ RT for 15 minutes, DNA extracted using GFX extraction kit and eluted in 40µl H_2O

pCMV6-Entry-mCCL25-MycDDK second digestion with SmaI

Extraced DNA	40 µl	
SmaI	3 µl	
NEB CS Buffer	5 µl	
BSA	0.5 µl	
H_2O	1.5 µl	→ 25°for 2 hours, Run on gel, Insert DNA band cut out and extracted using GFX extraction kit

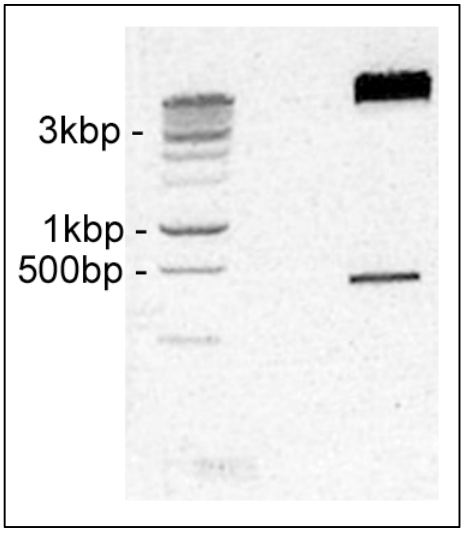

Fig i.2 Confirmation of double digestion of *pCMV6-Entry-mCCL25-MycDDK* vector.
pCMV6-Entry-mCCL25-MycDDK vector was sequentially digested with EcoRI and SmaI restriction enzymes as described above. 5µl of the enzymatic reaction were diluted in 15µl of water and run on agarose gel. Image shows digested fragment size as expected (497bp).

AdTD-CCL25 Ligation

	AdTD-CCL25	**Vector Control**	
AdTD vector DNA	1 µl (202 ng/µl)	1 µl (202 ng/µl)	
CCL25 insert DNA	6 µl (19 ng/µl)	-	
T4 DNA Ligase	1 µl	1 µl	
Ligase Buffer	1 µL	1 µL	
H_2O	1 µl	7 µl	→ 16°overnight

AdTD-CCL25 Colony 2 and *AdTD* plasmid digestion with PacI

	AdTD-CCL25	**AdTD**	
Plasmid DNA	40 µl (214.2 ng/µl)	23 µl (434.8 ng/µl)	
PacI	6 µl	6 µl	
NEB CS Buffer	10 µl	10 µl	
H_2O	34 µl	61 µl	→ 37°for 2 hours

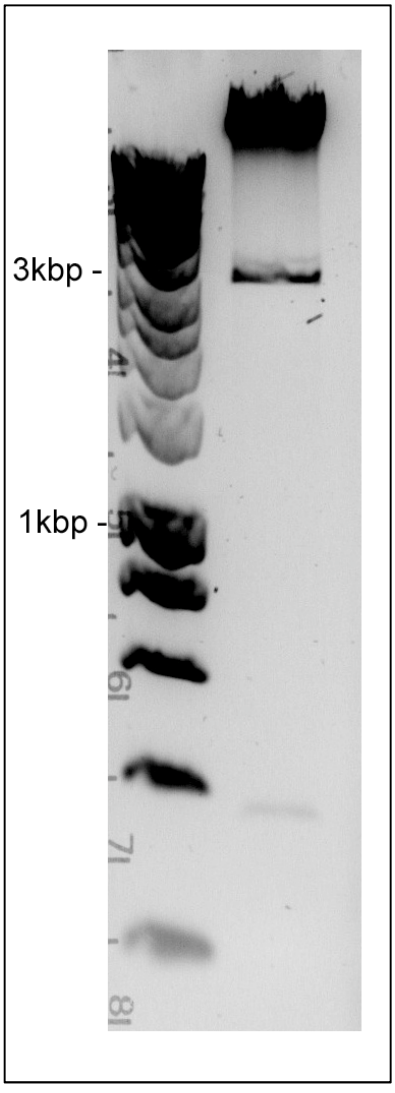

Fig i.3 Confirmation of PacI digestion of *AdTD-CCL25 colony 2* vector.

DNA from AdTD-CCL25 ligation reaction was transformed into E.Coli and grown on kanamycin-agar dish. Correct ligation was confirmed with PCR and sequencing from colony 2 (section 6.1). DNA extracted from colony 2 of *AdTD-CCL25* was digested with PacI restriction enzyme as described above. 5µl of the enzymatic reaction were diluted in 15µl of water and run on agarose gel. Image shows digested fragment size as expected (2864bp).

Appendix II: Buffers and Western blot gels

Buffer	Composition	Storage
FACS Buffer	Sterile PBS + 1% BSA	4 ℃
ACK lysis buffer	0.15 M NH_4Cl + 10 mM $KHCO_3$ + 0.1 mM Na_2EDTA in H_2O (pH to 7.2-7.4)	RT
NP40 Protein lysis buffer	50 mM Tris (pH7.4) + 150 mM NaCl + 10 mM CaCl2 + 1% NP40 + 1 protease inhibitor tablet (*Roche Applied Science, #11873580001)* in H_2O (for 50 ml)	-20 ℃
5X loading buffer	50 mM Tris, 4% SDS, 10% glycerol, 5% Mercaptoethanol, 0.01% Bromophenol Blue	-20 ℃
WB running buffer	10 % of 10 X Tris-Glycine-SDS Buffer (*National Diagnostic*s) + 90% H_2O	RT
WB transfer buffer	10% of 10 X Tris-Glycine Buffer (*National Diagnostic*s) + 10% methanol + 80% H_2O	RT
WB Blocking buffer	10% of 10 X Tris-buffered saline (TBS, *National diagnostics*) + 0.1% Tween-20 (*Sigma Aldrich*) + 5% skimmed powder milk (*Sigma Aldrich)* in H_2O	RT
WB washing buffer (TBST)	10% of 10 X Tris-buffered saline (TBS, *National diagnostics*) + 0.1% Tween-20 (*Sigma Aldrich*) in H_2O	RT

	8% gel	10% gel	12% gel	Stacking gel
ProtoGel (30%)	5.4 ml	6.6 ml	8 ml	1.3 ml
4x ProtoGel Resolving buffer	5 ml	5 ml	5 ml	-
4x ProtoGel Stacking buffer	-	-	-	2.5 ml
H_2O	9.4 ml	8.2 ml	6.8 ml	6.1 ml
TEMED	20 µl	20 µl	20 µl	10 µl
10% ammonium persulfate (APS)	200 µl	200 µl	200 µl	50 µl

Appendix III: Further investigation into the effect of CCL25 onto adenovirus life cycle

Disclaimer: this section was written by Miss A. Ibrahim and formed part of her MSc thesis. The concept of this study and all experiments were designed by C. Al Yaghchi. Experimental work was carried out by A. Ibrahim under my supervision.

III.I Viral titration

*The stock viruses were quantified by titration in both a $TCID_{50}$ assay and a picogreen assay, yielding concentrations in plaque-forming units (PFU)/ml and viral particles (vp)/ml, respectively (**Table 5**). The PFU/ml values were used for infection in cell cytotoxicity assays while both values were used in infection for viral DNA and protein quantification.*

Table 5. Virus concentrations determined by viral titration assays

Virus vector	PFU/ml*	Viral particles/ml**
Ad-TD	$9.74x10^9$	$1.81x10^{11}$
Ad-TD-CCL25	$1.32x10^9$	$9.24x10^{11}$

** as determined by $TCID_{50}$ assay*

*** as determined by picogreen assay*

For comparative reasons and to ensure that we are not over-infecting the cell by using the PFU/ml concentrations, both MOIs of 100 vp/cell and 10 PFU/cell infections were used to quantify viral protein and DNA.

III.II Cell cytotoxicity

*A cell kill dose-response assay was done to determine an appropriate multiplicity of infection (MOI) for the proceeding experiments. A PFU/cell of 10^0 and 10^1 allowed 50% cell kill with Ad-TD-CCL25 and Ad-TD, respectively in both TB11381 and 4T1 cells (**Figure 8**). As a result, we decided to continue with an MOI of 10 PFU/cell for the infections going forward. The EC_{50} values were determined from the variable slope. The mean EC_{50} values for Ad-TD in TB11381 and 4T1 cells are 32.55 and 15.78 PFU/cell, respectively and 5.04 and 0.63 PFU/cell for Ad-TD-CCL25. Ad-TD-CCL25 is more potent than Ad-TD in both TB11381 (p=0.0001) and 4T1 (p=0.0005) cell lines (**Figure 9**).*

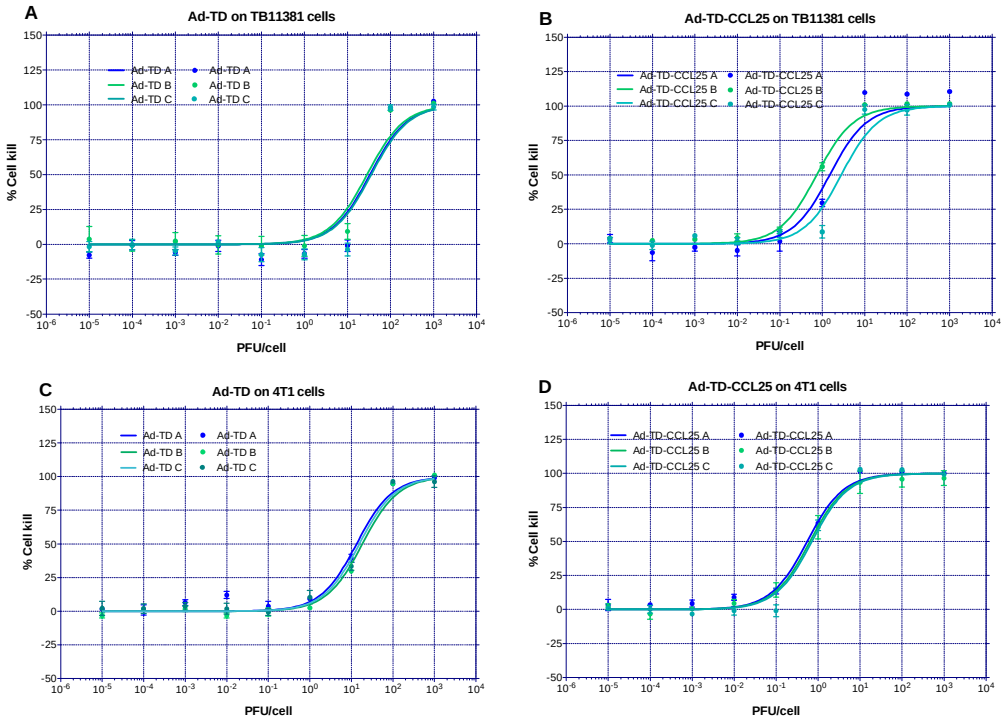

Figure 8. Ad-TD and Ad-TD-CCL25 viral dose-response curves in TB11381 and 4T1 cell lines. (A) *and* ***(B)*** *dose-response curves for Ad-TD- and Ad-TD-CCL25-infected TB11381 cells, respectively.* ***(C)*** *and* ***(D)*** *dose-response curves for Ad-TD- and Ad-TD-CCL25-infected 4T1 cells, respectively. The cells were infected with serial dilutions (1:10) of either virus in six replicates per three separate plates. The curves were constrained to fit between 0 and 100% cell kill using GraphPad Prism 5.0 software.*

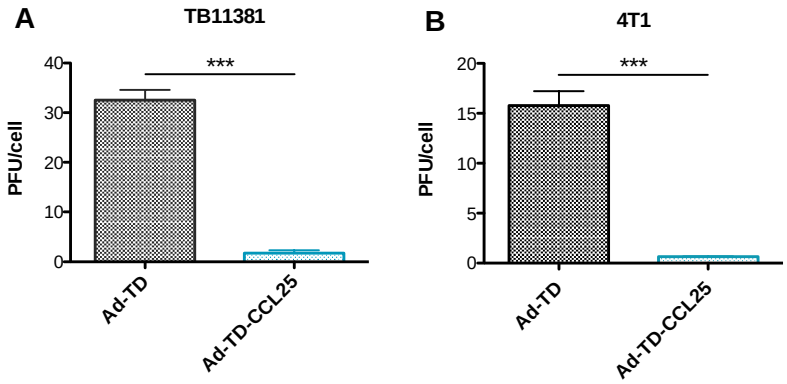

Figure 9. Ad-TD-CCL25 is significantly more potent than Ad-TD. *Graphical representation of the 50% effective concentrations (EC_{50}) in* ***(A)*** *TB11381 and* ***(B)*** *4T1 cells determined by the non-linear regression of the dose-response curves. The*

statistical analysis was conducted using an unpaired student t-test. ***(A)*** ****, p=0.0001;* ***(B)*** ****, p=0.0005.*

*Cell cytotoxicity was then assessed at a MOI of 10 PFU/cell at four time points (24, 48, 72, 96 hr) in order to determine differences between the two viral vectors over time. The cell cytotoxicity of Ad-TD + recombinant CCL25 (20 ng/ml) was also assessed to determine any direct effect CCL25 exerts on the cells. Ad-TD + recombinant CCL25 behaved similarly to Ad-TD, and did not demonstrate increased toxicity or increased potency (****Figure 10****). Ad-TD-CCL25 was significantly more cytotoxic than Ad-TD (p<0.05) and Ad-TD + rCCL25 (p<0.01).*

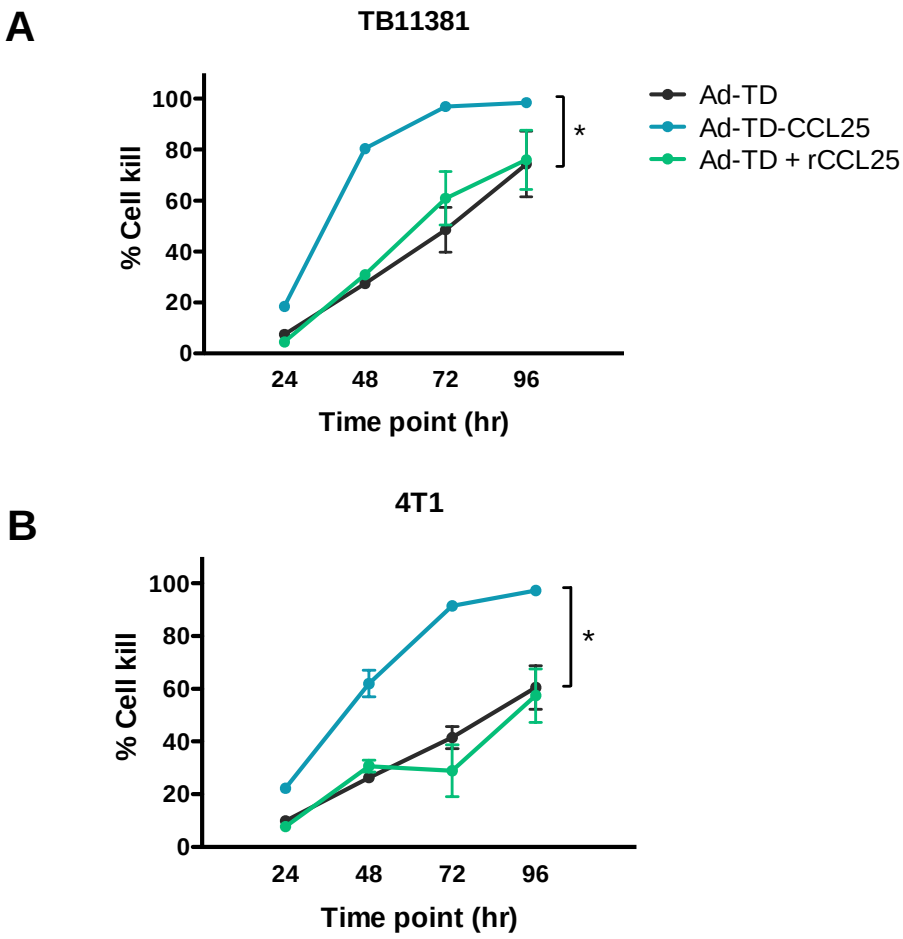

Figure 10. Ad-TD-CCL25 is more cytotoxic than Ad-TD over time. (A) *TB11381 and* ***(B)*** *4T1 cells were infected with either Ad-TD, Ad-TD-CCL25 or Ad-TD + recombinant CCL25 (20 ng/ml). MOI = 10 PFU/cell. Each biological time point was assayed in triplicates. The percentage cell kill was significantly higher with Ad-TD-CCL25-infected cells compared to Ad-TD and Ad-TD + CCL25. The statistical analysis was conducted using a one-way ANOVA. *, p<0.05.*

*In this same experiment, cell cytotoxicity was assessed before and after a four hour wash post-infection, a time point when CCL25 is not being produced by Ad-TD-CCL25. This investigated whether CCL25 produced by Ad-TD-CCL25 after the four hours increases the internalization of the viral particles that remained in the medium in the unwashed samples. Ad-TD-CCL25 was not shown to undergo increased internalization in both cell lines; no significant differences were seen in cell kill when comparinig if the viruses were washed or not washed away (**Figure 11**).*

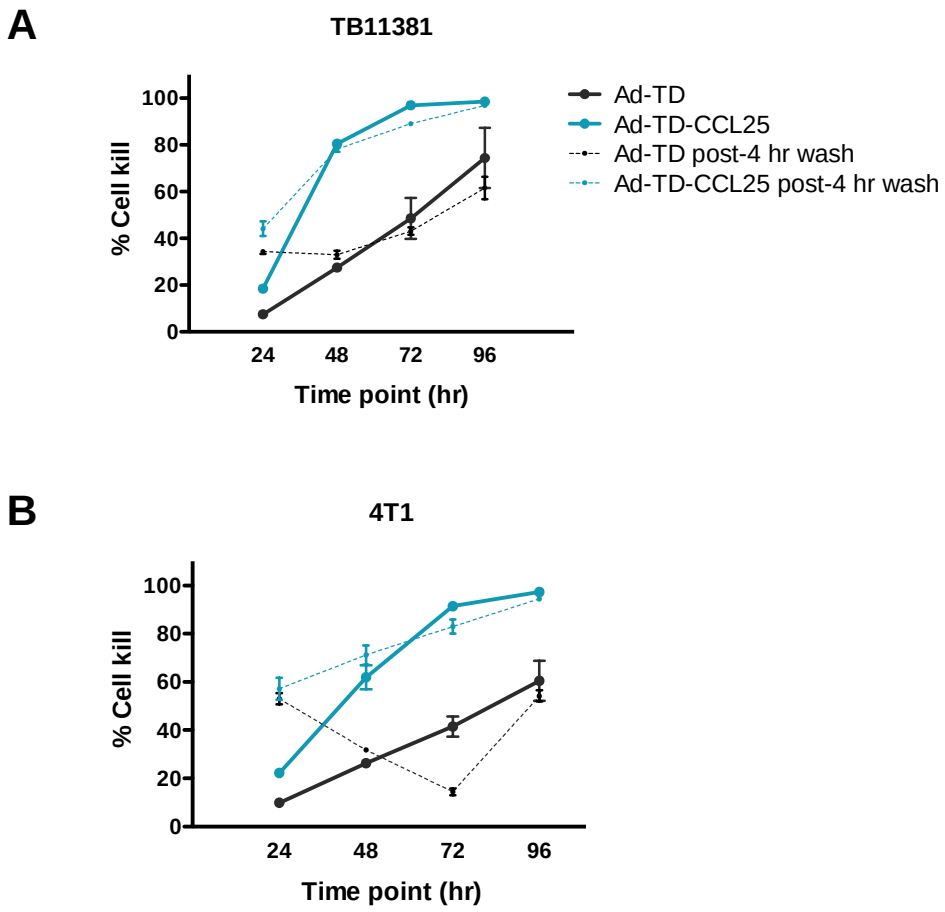

Figure 11. Ad-TD-CCL25 does not exhibit increased internalization. (A) *TB11381 and* ***(B)*** *4T1 cells were infected with either Ad-TD or Ad-TD-CCL25 with or without a wash four hours post-infection. MOI = 10 PFU/cell. Each biological time point was assayed in triplicates. There were no statistically significant differences observed in cell cytotoxicity after washing away the virus in both viral vectors. The statistical analysis was conducted using a students t-test.*

III.III Viral protein expression

*The TB11381 cell line was chosen for further investigation of viral protein and DNA quantification. In order to determine if replication occurs quicker in Ad-TD-CCL25-infected cells, we performed Western Blotting for one early and one late-transcribed protein, E1A and hexon, respectively. Ad-TD-CCL25-infected samples expressed E1A (55 kDa) as early as 12 hours p.i. and at a higher level than Ad-TD (**Figure 12A**). Densitometric analysis revealed a 23 fold difference and a 15 fold difference in E1A expression at 12 and 24 hours, respectively. A similar observation was seen with hexon; Ad-TD-CCL25-infected TB11381 cells expressed hexon (108 kDa) as early as 24 hours (80 fold difference), while Ad-TD still did not express hexon at 48 hours (29.62 fold difference). As expected, the earlier time points and mock-infected samples do not express E1A or hexon. **Figure 12B** is a Western Blot also probed for E1A and hexon, however the TB11381 cells were infected with 100 vp/cell in order to study any differences in the two infection methods. In these samples, E1A was also expressed as early as 12 hours, and densitometric analysis shows very similar expression at 24 hours between Ad-TD and Ad-TD-CCL25 (1.107). At 48 hours, Ad-TD-CCL25 expresses E1A almost two folds higher than Ad-TD. The trend is not as consisent with hexon expression levels, which will be discussed below.*

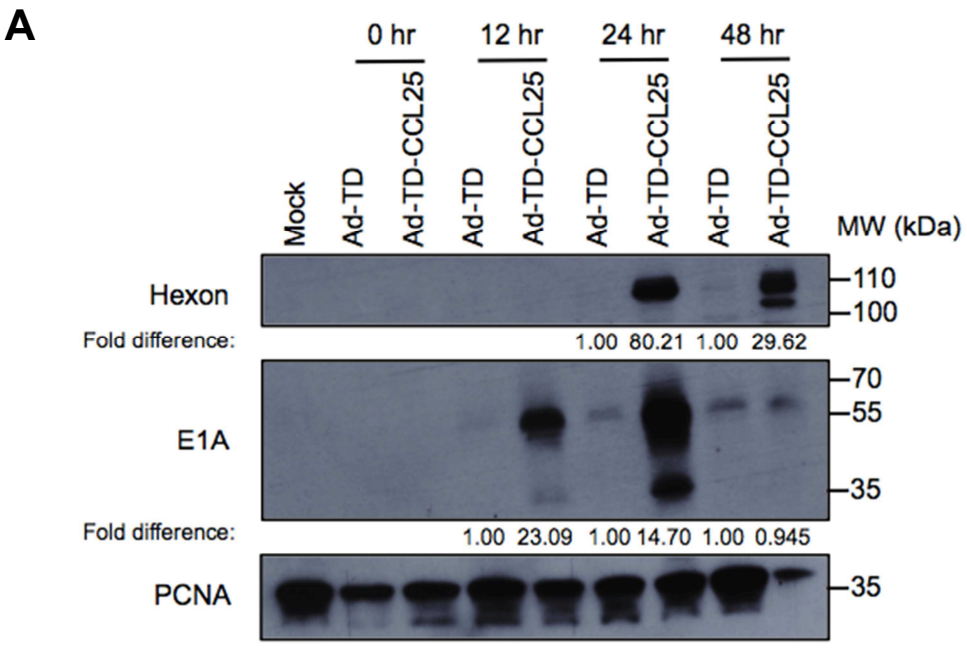

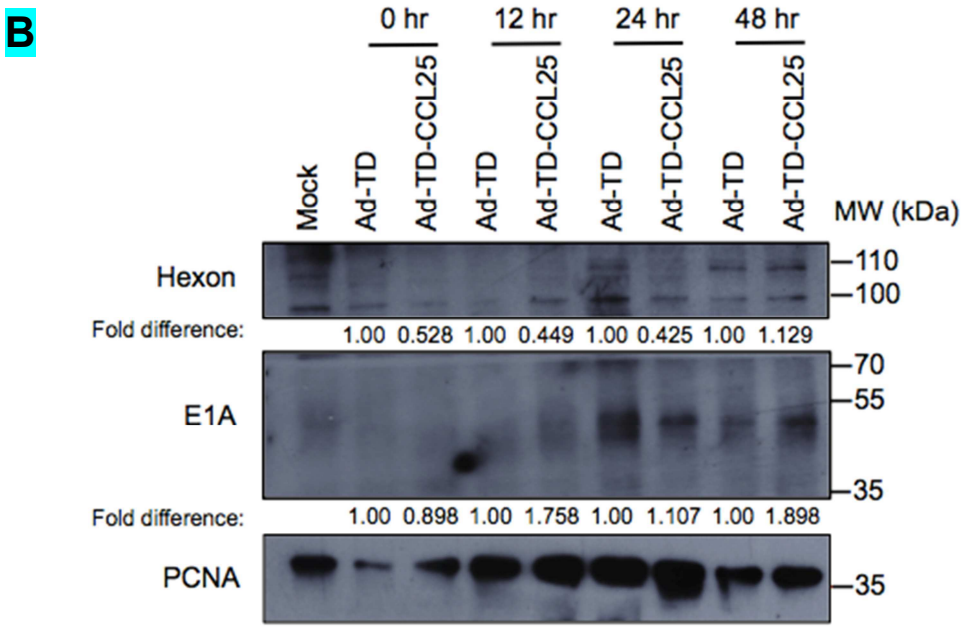

Figure 12. Ad-TD-CCL25-infected cells express viral proteins earlier. *TB11381 cells were infected with Ad-TD or Ad-TD-CCL25* ***(A)*** *MOI = 10 PFU/cell and* ***(B)*** *100 vp/cell, and cell lysates were collected for protein harvest at 0, 12, 24 and 48 hours post-infection. Western blotting was used to assess protein levels of early protein, E1A and late coating protein, hexon. Relative densities were calculated using Image Studio™ Lite Software 5.0.21. The blots are representatives of two repeated experiments. PCNA was used as a loading control.*

II.IV Viral DNA replication

*Lastly, we investigated viral DNA replication using qPCR. The intracellular DNA copy numbers were determined as measured by E2A levels. Ad-TD-CCL25-infected TB11381 cells had higher E2A copy numbers compared to Ad-TD at 24 hours in both PFU/cell (**Figure 13A** p=0.0005) and vp/cell infected cells (**Figure 13B** p=0.0103). In the PFU/cell-infected cells **(Figure 13A)**, Ad-TD-CCL25-infected cells also had higher E2A copy numbers at 48 hours (p=0.0223). The data is represented as a fold change in order to distinguish any differences between the two methods of infection. Overall, the two methods resulted in similar results.*

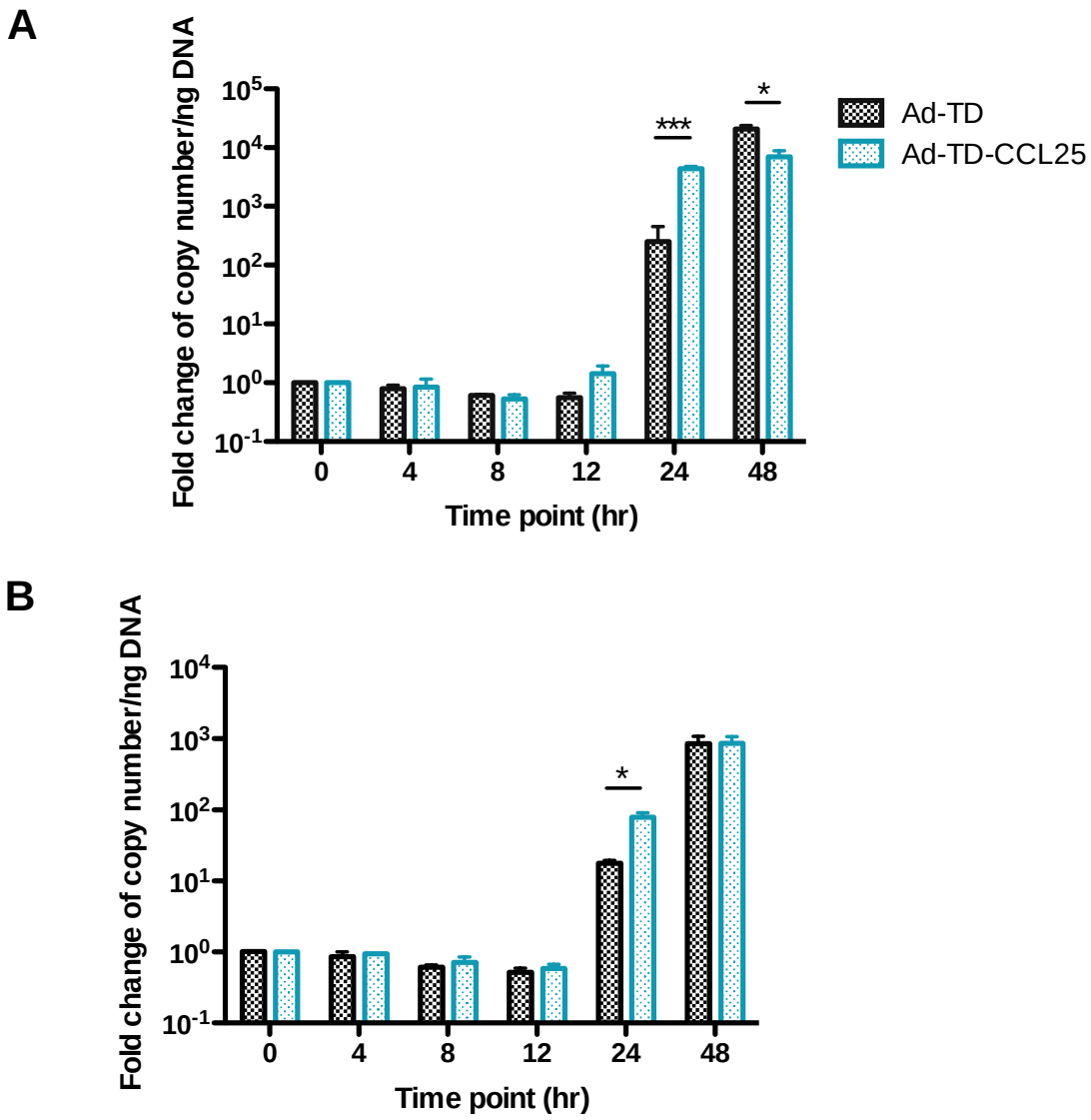

Figure 13. Ad-TD-CCL25 replicates more rapidly than Ad-TD. *TB11381 cells were infected with Ad-TD or Ad-TD-CCL25* ***(A)*** *MOI = 10 PFU/cell* ***(B)*** *MOI = 100 vp/cell, and DNA was purified from the samples. Quantitative PCR (qPCR) was used to determine the intracellular viral DNA copy number as measured by E2A levels (by comparison to an Ad5 standard curve) at 4, 8, 12, 24 and 48 hours post-infection (t=0). Each sample was assayed in triplicate and each time point assay was performed in biological triplicates. The results are presented as the fold change compared to t=0, which was arbitrarily set to 1. E2A was not amplified in the mock-infected sample (not shown). The statistical analysis was conducted using an unpaired two-tailed student t-test at each time point.* ***(A)*** **, p=0.0223; ***, p=0.0005* ***(B)*** **, p=0.0108.*

IV. DISCUSSION

IV.I Characterization of Ad-TD-CCL25 virus vector

Virion replication and CCL25 production

*The first step in validating the new viral vector Ad-TD-CCL25 as an oncolytic virus was to characterize its ability to infect, replicate in as well as lyse cancer cell lines. Preliminary work performed by Chad Al-Yaghchi demonstrated that Ad-TD-CCL25, like its backbone virus, Ad-TD, is replication-competent and unlike Ad-TD, produces CCL25 upon replication (**Figure 6**). This demonstrates that the cloning of CCL25 into the viral genome does not affect the replication competency of Ad-TD-CCL25, and moreover, that the CCL25 transgene is transcribed and its soluble product is released during virion assembly. Theoretically, CCL25 produced by the OV should attract immune cells such as T-cells to the site of infection i.e. the tumour site, and as a result, enhance antitumour effects in vivo[41]. Studies investigating the chemotaxis of chemokine-expressing oncolytic viruses demonstrate migration of immune cells towards the OV-infected cells in vitro and in vivo[41,42]. Oncolytic vaccinia virus expressing CCL5 induced lymphocyte chemotaxis, increased persistence of the virus within the tumour and enhanced therapeutic benefits when combined with a DC vaccine[41]. An adenovirus expressing CCL5 also correlated with an increase in proinflammatory cytokines, DC infiltration and antigen-specific $CD8^+$ T-cell responses[42]. Therefore, Ad-TD-CCL25 should possess similar chemotaxis properties. The ability of the OV to not only directly lyse cells more efficiently (which is only accounted for a small part of OV-mediated antitumour effects) but also attract the immune system will allow Ad-TD-CCL25 to be an effective therapy.*

Viral titration

Titration of the two viruses was determined by two separate assays, which yielded different units of measure. The $TCID_{50}$ assay determines the ability of the virus to form a plaque per unit of volume (PFU/ml), therefore is a functional measurement of the virions. The picogreen assay, however, determines the viral particle count per unit of volume, a quantitative measurement. The viral particle count for Ad-TD-CCL25 was 700x more concentrated than in PFU/ml, which may be owed to the quality of the viral particles i.e. the presence of high levels of immature virions. A possible explanation for the discrepancy is that the increased potency of Ad-TD-CCL25 allows for more cell

death of the JH293 cells during titration, thus the viral particles that are harvested and purified may not be fully packaged virions.

Viral cytotoxicity

*A cell cytotoxicity assay at various dilutions of the viruses was done to determine the half maximal effective concentrations (EC_{50}) and thus an appropriate MOI for all further infections performed in this study. Ad-TD killed 50% of the cells at a MOI of 10^1 while Ad-TD-CCL25 killed 50% of the cells at a MOI of 10^0 PFU/cell. This means that Ad-TD-CCL25 is more potent, and if we use MOI of 10 PFU/cell, technically the Ad-TD virus added at infection is 10 fold higher than it should be to be equally infectious as Ad-TD-CCL25. Therefore, any differences noted in the further investigations such as protein expression and gene copy numbers are dramatic. My results confirm preliminary data (**Figure 7**), demonstrating increased potency exhibited by Ad-TD-CCL25 compared to Ad-TD. Cell kill was then determined at a MOI of 10 PFU/cell, where Ad-TD-CCL25 was significantly more cytotoxic over four days. Ad-TD + recombinant CCL25 behaved similarly to Ad-TD alone, concluding that the transcription of CCL25 by Ad-TD-CCL25 in someway is involved in its increased potency. Moreover, this also demonstrates that CCL25 is not cytotoxic (this was also confirmed in a specific assay by our laboratory- data not shown).*

IV.II Investigating viral internalization

In order to determine if the reason for increased potency occurred at viral internalization, the virus was washed away after four hours post-infection. This allowed for only the viral particles that have attached and internalized within that time to replicate within the cells. Since CCL25 is not expressed by Ad-TD-CCL25 within the first four hours, if there was increased cell kill without a virus wash, it would suggest that CCL25 somehow increased the amount of virus that is being internalized. Therefore, since no significant differences in the results were seen, we can conclude that the internalization of the virus was independent of the CCL25 in the growth medium. Our laboratory has previously shown that vascular endothelial growth factor (VEGF)-A produced by tumour cells promoted vaccinia virus (VV) entry into host cells through activation of the Akt pathway and was associated with increased potency of the virus[43]. Similarly, Cheshenko et al demonstrated that silencing of Akt prevented calcium release, which blocked viral entry and inhibited plaque formation by 90%

compared to the control[44]. It was thus hypothesized that CCL25 through binding to CCR9 on host cells and signaling through PI3K/Akt may promote viral entry. Ad is internalized very efficiently; approximately 85% of the added viral particles are internalized within 10 minutes of attachment[23]. It would thus be necessary to wash away the virus earlier (e.g. 10 minutes to 2 hours) in order to ensure that the maximal amount of virus has not entered within that time. This experiment can be improved investigating viral attachment, internalization and trafficking within the cell, using qPCR[45]. To assess binding, the cells should be left in the cold for one hour post-infection and then washed with cold buffer to remove unbound virus particles. This is because at 37℃, viral attachment and entry is promoted. The cells can then be collected for total DNA preparation and qPCR analysis. For assessing internalization, the washed cells are placed at 37℃ for various intervals and the attached, but uninternalized viral particles can be removed with 2 mg/ml of substilin reagent and the cells can be collected for DNA preparation. Next, the nuclear fractions can be separated using a kit (NE-PER nuclear and cytoplasmic kit, Pierce, Thermo Scientific) in order to assess trafficking into the nuclear pore. If there are differences in the viral genome copy numbers, it would suggest differences at either one of these points in the viral lifecycle, which should then be investigated further (discussed below). It is possible that through binding of CCL25 on CCR9 on the tumour cells, attachment, internalization or trafficking of Ad-TD-CCL25 may enhanced, leading to increased replication and/or potency. Wang et al showed that carcinoembryonic antigen-related adhesion molecule 6 (CEACAM6) blocked adenovirus trafficking to the nucleus through the Src pathway, which interfered with the cytoskeleton of cancer cells, resulting in attenuated infectability by adenovirus[45].

IV.III Viral protein expression

*The greater potency of Ad-TD-CCL25 was thought to possibly be due to quicker transcription and translation of viral proteins that are necessary for replication or virion assembly. The Ad chromosome carries five early (E) transcription units, two delayed and one major late unit. Protein was harvested from Ad-TD and Ad-TD-CCL25-infected cells and probed for an early protein E1A, as well as for hexon, a late viral coating protein in a Western blot (**Figure 12**). E1A expression was detected earlier (at 12 hours) in Ad-TD-CCL25-infected TB11381 cells compared to Ad-TD-infected cells. E1A is the first transcription unit to be expressed in the host nucleus. E1A activates transcription by binding to cellular transcription factors and promotes host cell entry into the S phase of the cell cycle[23]. Therefore, earlier E1A transcription may suggest faster*

*replication of Ad-TD-CCL25, which may account for its increased potency. Hexon was also detected earlier with Ad-TD-CCL25 (at 24 hours) (**Figure 12A**), which further proves this hypothesis, as the coating protein is needed to complete virion packaging in the cytosol and release from the host cell[23]. In **Figure 12B**, we observed that E1A is slightly higher expressed in Ad-TD-CCL25-infected cells, however hexon seems to be expressed at higher levels in Ad-TD-infected cells. This can be explained by the higher amount of Ad-TD mature infectious particles that are entering the cells. When using vp/cell concentrations, there are 10 infectious Ad-TD viral particles per cell added to the medium compared to one infectious Ad-TD-CCL25 viral particle. This should thus result in more virus entering the cells and thus higher (or equal) viral protein expression in the Ad-TD infected cells compared to the Ad-TD-CCL25-infected cells.*

IV.IV Viral DNA replication

*E2A, also known as DBP (DNA-binding protein) is primarily responsible for initiating DNA replication[23]. Therefore, the E2A gene was chosen to investigate differences in DNA replication between the two viral vectors. The qPCR results (**Figure 13**) show significant differences in E2A amplification in Ad-TD-CCL25-infected TB11381 cells at 24 hours, and although not statistically significant, a similar trend at 48 hours (**Figure 13B**). These results suggest that DNA replication is occurring more rapidly in Ad-TD-CCL25, and is consistent with the Western Blots described above. In **Figure 13B,** a slight increase (not statistically significant) is seen at 12 hours between the two virus copy numbers, which may also suggest quicker replication in Ad-TD-CCL25. E1A expression was detected as early as 12 hours, thereby complimenting these findings.*

*On the contrary, in **Figure 13A**, Ad-TD-infected cells had a higher fold change in copy number compared to Ad-TD-CCL25, which is most likely due to more cell death with Ad-TD-CCL25, which was observed under the microscope before harvest. The quality of Ad-TD-CCL25 viral particles merits more investigation. That said, as described above, at a MOI of 10 PFU/cell, Ad-TD is technically 10 fold more concentrated than Ad-TD-CCL25, therefore this may just signify increased cell kill with Ad-TD-CCL25, thereby making it a more effective oncolytic virus.*

Appendix IV: Review article

Review

For reprint orders, please contact: reprints@futuremedicine.com

Immunotherapy

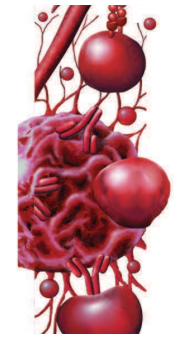

Vaccinia virus, a promising new therapeutic agent for pancreatic cancer

The poor prognosis of pancreatic cancer patients signifies a need for radically new therapeutic strategies. Tumor-targeted oncolytic viruses have emerged as attractive therapeutic candidates for cancer treatment due to their inherent ability to specifically target and lyse tumor cells as well as induce antitumor effects by multiple action mechanisms. Vaccinia virus has several inherent features that make it particularly suitable for use as an oncolytic agent. In this review, we will discuss the potential of vaccinia virus in the management of pancreatic cancer in light of our increased understanding of cellular and immunological mechanisms involved in the disease process as well as our extending knowledge in the biology of vaccinia virus.

Keywords: immunotherapy • oncolytic virus • pancreatic cancer • vaccinia virus

Chadwan Al Yaghchi[1], Zhongxian Zhang[2], Ghassan Alusi[1], Nicholas R Lemoine[1,2] & Yaohe Wang*[,1,2]

[1]Centre for Molecular Oncology, Barts Cancer Institute, Queen Mary University of London, UK

[2]National Centre for International Research in Cell & Gene Therapy, Sino-British Research Centre for Molecular Oncology, Zhengzhou University, China

*Author for correspondence:
Tel.: +44 207 882 3596
Yaohe.wang@qmul.ac.uk

Pancreatic cancer remains one of the most difficult cancers to diagnose and treat. It is the fifth most common cause of cancer death in the UK with 1 and 5 years survival of 20.8 and 3.3%, respectively. These figures have hardly improved since the early 1970s [1]. Complete surgical resection remains the only curative treatment. Unfortunately, less than 20% of pancreatic tumors are amenable to surgical excision at the time of diagnosis. However, even with complete surgical resection prognoses remains poor with 5 years survival around 20% [2,3]. Gemcitabine is the main chemotherapeutic agent approved for advanced pancreatic cancer. Despite being shown to improve life expectancy compared with 5-flurouracil, effect remains modest with median survival around 6 months [4]. Combining gemcitabin therapy with erlotinib led to minimal increase in life expectancy from 5.9 to 6.2 months [5]. Therefore, new treatment strategies are clearly imperative.

Vaccinia virus (VV) has played a prominent role in one of the greatest achievements in medical history: the eradication of smallpox (caused by Variola virus). Since then, VV has been developed as a vector for vaccines against infectious diseases such HIV, influenza, malaria and tuberculosis as well as in immunotherapies [6] and oncolytic therapies for cancer [7,8]. With regards to the latter, the earliest studies, which mainly used replication attenuated VV recombinants for fear of toxicity, were relatively disappointing in the clinic. Replication competent VVs retain their ability to lyse tumor cells and spread through tumor tissue. Recent advances in DNA recombinant technology enabling the rational manipulation of the viral backbone, coupled with the ever increasing knowledge gains in the fields of molecular virology and cancer cell biology have aided the development of safe and efficacious tumor-targeted oncolytic VVs. These are currently at the forefront of the most promising novel anticancer agents.

In this review, we will explore the potential of tumor-targeted oncolytic VV in the management of pancreatic cancer in light of our increased understanding of cellular and immunological mechanisms involved in the disease process as well as our extending knowledge in the biology of VV.

Future Medicine part of fsg

Tumor-targeted oncolytic viruses as a new class of cancer therapeutics

Targeted therapy of cancer using oncolytic viruses (OV) has generated much interest over the past decades in the light of the limited efficacy and the significant side effects of standard cancer therapeutics for advanced disease [9]. OVs have become an increasingly popular anticancer therapy platform due to their ability to selectively infect and lyse tumor cells (Figure 1). Cancer selectivity of OVs could be a result of natural tropism [10,11] or via genetic modification [9]. OVs can target multiple cellular pathways [12–14] minimizing the risk of tumor resistance and induce different modes of cell death [15–18]. In addition, OVs can break down the immunosuppressive tumor microenvironment and induce a long-lasting tumor-specific immunity [19,20] (Figure 2). OVs can specifically deliver therapeutic proteins into tumors at increasing levels following viral replication within the malignant cells. Furthermore, OVs can function in synergy with conventional cancer treatments of chemoradiotherapy [21–24]. Finally, OVs as a treatment platform are amenable to adjustment and development following our ever-increasing understanding of cancer cells, the virus and host immune responses to both tumor and virus.

H101, an adenovirus with *E1B 55K* gene deletion (Oncorine; Shanghai Sunway Biotech, Shanghai, China) was licensed in China in 2005 as the world's first OV for treatment of head and neck cancer when combined with chemotherapy [25]. The similar virus, *dl1520* (also known as, ONYX-015) has been administered by intratumoral injection under CT guidance into locally advanced primary tumors of pancreatic cancer patients in Phase I/II trials. The treatments were well tolerated, but no objective responses were seen in any of the patients with virus alone, and only 10% (2/21) patients showed objective response when gemcitabine was used in combination [26–28]. Another virus that entered clinical trials is HF10, a Herpes Simplex virus armed with granulocyte-macrophage colony-stimulating factor (GM-CSF). Phase I trial of intratumoral injection into nonresectable pancreatic tumors proved to be safe with some encouraging clinical results [29]. These early results warrant further investigation to seek more powerful agents for this cancer.

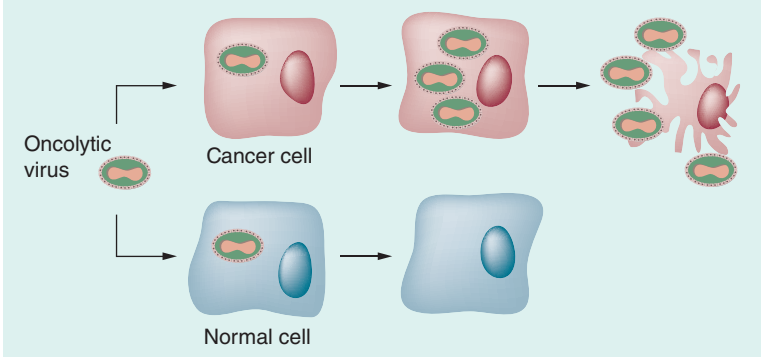

Figure 1. Tumor selectivity of oncolytic viruses. Tumor-targeted oncolytic viruses can exploit defective cellular pathways in cancer cells (top). oncolytic viruses can infect and replicate in cancer cells leading to cell lysis and release of viral particles. These in turn infect neighbor tumor cells and so forth. In normal cells (bottom) cellular defense mechanisms prevents viral replications.

Favorable features of vaccinia virus for cancer treatment

VV is a member the poxvirus family. It is a double-stranded DNA virus ~192 kbp in size. It can be stably accommodate up to 25 kbp of cloned exogenous DNA [30]. Structurally, it consists of a core region composed of viral DNA and a various viral enzymes including RNA polymerase and polyA polymerase encased in a lipoprotein core membrane. The outer layer of the virus consists of double lipid membrane envelope [31,32]. VV has two major forms of infectious virions; the intracellular mature virions, as described above, which is released upon cell lysis and the extracellular enveloped virion released from the cells via cell membrane fusion. The latter has an additional lipid bilayer membrane wrapped around the intracellular mature virion particle.

VV has many inherent characteristics that make it an ideal choice for oncolytic virotherapy. VV has a short life cycle of 8 h that takes place in its entirety in the cytoplasm eliminating the risk of genome integration. Replication usually starts 2 h after infection, at which time the host cell nucleic acid synthesis shuts down as all cellular resources are directed toward viral replication [33,34]. Cell lyses takes place between 12 and 48 h releasing packaged viral particles. Furthermore, the virus does not depend on host mechanisms for mRNA transcription making it less susceptible to biological changes of the host cell [33,35].

Unlike other OVs, VV does not have a specific surface receptor for cell entry allowing it to infect a wide range of cells unhindered by the lack of expression of said receptor. They depend on a number of membrane fusion pathways for cell entry [36,37].

The existence of various antigenically distinct forms of the mature virus allows it to evade host immune system. extracellular enveloped virion form of the virus is encapsulated in a host-derived envelope, with incorporated viral proteins, that contains several host complement control proteins [38–40]. In addition, VV infected cells secret Vaccinia complement control protein which binds an inactivate C4b and C3B inhibiting the classic and alternative complement activation pathways [41–43]. VV therefore can be disseminated relatively unharmed in the blood stream to reach distant tumors allowing

systemic delivery of the virus [44], which is more suitable for the treatment of the advanced pancreatic cancer.

The hypoxic nature of pancreatic cancer contributes to its aggressive and treatment-resistant phenotype. In contrast to adenovirus [45], we have found that hypoxic conditions did not affect replication, viral proteins production, cytotoxicity and transgene expression of the Lister strain of VV [46]. These results suggest that VV could be suitable for management of pancreatic cancers and potentially other hypoxic tumors.

Finally, VV has a good safety track record following its use as a vaccine for over a century. Minor and less severe side effects include fever, rash and inadvertent inoculation. Moderate-to-severe side effects include eeczema vaccinatum, generalized vaccinia, progressive vaccinia and postvaccinial encephalitis [47]. Sides effects are rare with an incident of less than 1:10,000 and severe side effects in particular are extremely rare [48]. Genetically modified recombinant VV could be potentially safer due to their tumor selectivity. Recent clinical trial of JX-594 virus in hepatocellular carcinoma showed the treatment to be well tolerated with mainly flu-like symptoms in all patients and a single severe side effect [8].

How Vaccinia virus selectively kills cancer cells by multiple action mechanisms

VV has a natural tropism to cancer cells [49,50]. The virus can utilize activated molecular pathways in tumor cells to aid its replication [51–53]. In fact, many of the hallmarks of cancer [54] make tumor cells susceptible to viral replication including immune escape, sustained cell proliferation and resisting cell death. In the case of VV, the EGFR family [55], potentially plays an important role in tumor selectivity. The viral SPGF, an EGF-like growth factor carried by VV, can activate host cellular pathways leading to increased viral replication [56]. In addition, Ras–GTP-activating protein S3H domain-binding protein, overexpressed in most human cancers [57], plays a role in VV replication by complementing the activity of the VITF-2 [58].

Various approaches can be utilized to enhance tumor selectivity of OVs. The virus depends for its replication in normal cells on a set of genes that prepare the cell resources for viral replication and block apoptotic pathways. Deleting these genes will limit the virus ability to replicate in normal cells. However, these pathways are often disrupted in cancer cells allowing the mutant virus to replicate despite the defective genes. One such example is the disruption of the vaccinia thymidine kinase gene (*TK* gene) affecting the virus ability to synthesize deoxyribonucleotides [59,60]. Normal cells have a much smaller reserve of deoxyribonucleotides, compared with tumor cells, limiting the ability of VV to replicate. Another example is the deletion of the *B18R* gene encoding the secreted IFN-binding protein that blocks IFNα signaling [61]. In normal cells, this gene deletion attenuates viral replication due to IFN antiviral effect while cancer cells remain permissive to VV replication as IFN signaling is often disrupted [62,63]. In addition, altering the expression of crucial vaccinia viral gene by microRNA also enables tumor-specific viral replication, which is a potentially novel and versatile platform for engineering VVs for cancer virotherapy [64].

GLV-1h68 is a replication-competent VV targeted at tumor cells by mutation of *J2R* (encoding thymidine kinase) and *A56R* (encoding hemagglutinin) loci. This virus was shown to be effective against human pancreatic cancer cell line *in vitro* and in nude mice xenografts. Importantly this efficacy was enhanced

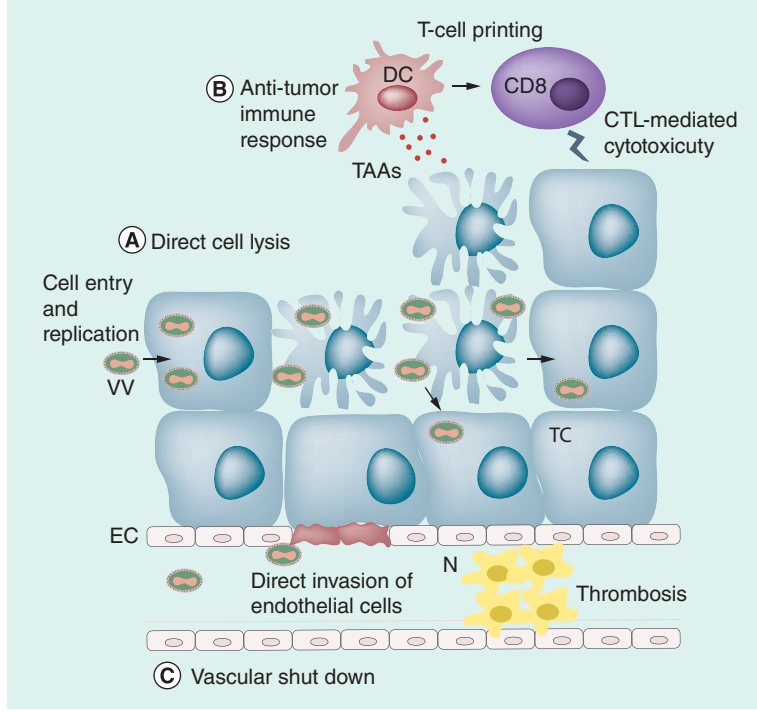

Figure 2. Multiple modes of actions of tumor-targeted oncolytic viruses.
Oncolytic viruses (OV) can kill cancer cells via a variety of mechanisms. First, they directly infect, replicate and lyse tumor cells sparing normal cells. Released virions can infect neighbor tumor cells and so forth. Second, OVs can induce immunogenic cell death associated with the release of pathogen-associated molecular patterns and damage-associated molecular patterns. In addition viral infection results in the release of cytokine and chemokines deviating the immune response toward a cytotoxic profile. Dendritic cells can pick tumor-associated antigens released from lysed tumor cells and prime $CD8^+$ T cells to induce a tumor-specific immune response. Third, OV infection can result in vascular shutdown caused by direct viral invasion of endothelial cells and thrombosis caused by cytokine-mediated neutrophils accumulation.
CD8: Cytotoxic T cell; DC: Dendritic cell; EC: Endothelial cell; N: Neutrophil; TAA: Tumor-associated antigen; TC: Tumor cell; VV: Vaccinia virus.

when virus therapy was combined with gemcitabine and cisplatin [65]. GLV-1h151, a virus with similar gene deletions but different marker proteins transgenes [66], was found to be effective *in vivo* and *in vitro* against human pancreatic cancer cell lines. Combining the virus with radiotherapy resulted in a synergistic antitumor effect [67].

In addition to direct cell lysis, VV can utilize vascular shut down to kill noninfected tumor cells [44,68–69]. This is believed to be caused by accumulation of neutrophils in blood vessels, mediated by cytokines and chemokines, leading to intravascular thrombosis [69]. In addition, VV can infect and destroy tumor-associated endothelial cells further contributing to vascular collapse [62]. Although this process has not been specifically shown in pancreatic tumors, we believe it to play an important role in the multimechanistic antitumor effect of VV, as pancreatic cancers are often well-vascularised and high microvascular density correlates with poor outcome after surgical excision [70]. To further capitalize on this process we have rationally armed Lister strain VV with endostatin–angiostaten fusion gene, a well-documented angiogenesis inhibitor [71]. The resultant VVhAE virus proved to be tumor selective *in vitro* and *in vivo*. It resulted in suppression of angiogenesis and prolonged survival of mice bearing human pancreatic cancer xenografts [50].

Vaccinia virus as immunomodulatory agent

The ability of OVs to alter the immune composition of the, ordinarily, immune-suppressive tumor microenvironment led to a new line of thinking of their mechanism of action. Large body of evidence suggests that antitumor immunity, where the virus is acting as an oncotropic immunomodulator, is the key determinant of a successful onclytic virotherapy [72–74].

VV kills cancer cells via a combination of necrosis and immunogenic apoptosis resulting in the release of damage associated molecular patterns [75–78] and pathogen associated molecular patterns [79–81] as well as the release of viral antigens into the tumor. This process leads to a strong inflammatory response that can overcome the immune suppression within the tumor microenvironment. In addition, tumor cell lysis releases tumor-associated antigens (TAA) into this inflammatory environment. Dendritic cells recruited by the virus can in turn pick up these exposed TAAs and cross-prime $CD8^+$ T cells resulting in a potent antitumor adaptive immune response. It has been demonstrated that an oncolytic VV (JX549) could induce tumor-specific immunity in human cancer patients [82] and preclinical study [20]. Therefore, oncolytic virotherapy may be considered as a method of vaccination *in situ*, enabling the adaptive immune response to clear residual disease as well remote metastatic cancer cells and provide long-term surveillance against relapse.

In the context of vaccination, heterologous prime-boost immunization regimen using recombinant adenovirus prime and VV boost has been shown to enhance $CD8^+$ T-cell immunogenicity with protective efficacy against malaria in a mouse model [83,84]. So, it seems logical that combining two different OVs for cancer treatment may induce a stronger tumor-specific immunity. We have, for the first time, combined the use of oncolytic adenovirus and VV, in a prime-boost strategy, for treatment of established tumors in the hope to harness the host immune response to the infected tumor cells. We found that sequential treatment via intratumoral injection with oncolytic adenovirus followed by oncolytic VV resulted in complete eradication of subcutaneous pancreatic cancer grafts in Syrian hamsters. More importantly, the surviving animals developed a long-lasting tumor-specific immune response that protected them against tumor rechallenge. This process was shown to be T-cell dependent [20].

Arming VV with various cytokines and chemokines can further enhance its antitumor activity. IL-10, a cytokine produced by Th2 T cells, is a potent inhibitor of antiviral immune response [85]. We have found that arming VV with IL-10 dampened antiviral immune response resulting in prolonged viral persistence in pancreatic tumors. This led to stronger antitumor immunity and improved survival in both subcutaneous and transgenic pancreatic cancer mouse models [86].

Vaccinia virus as vaccine vector

The first use of a recombinant virus armed with an antigen from a different organism as a vaccine vector was reported over 30 years ago. VV armed with hepatitis B surface antigen gene was able to induce a protective immunity against hepatitis in chimpanzees [87,88]. Since then there has been a great progress in recombinant VV vaccines in the veterinary field [89,90]. Unfortunately this success did not extend to human infectious diseases vaccines, mainly due to the lengthy and more stringent process for human licensing, with only a handful of recombinant VV vectors in current clinical trials [91–94].

One of the significant challenges for cancer vaccination lies in developing strategies to improve the delivery of antigens to antigen-presenting cells *in vivo*, allowing effective antigen processing and presentation and activation of a potent immune response against a unique background of immune tolerance toward 'self' TAAs. Viral vectors have become attractive antigen delivery systems as they mimic a natural viral infection, resulting in induction of cytokines and co-stimulatory molecules

that provide a powerful adjuvant effect and elicit potent cellular immunity [74,95].

Survivin is a member of the inhibitor of apoptosis family expressed in a variety of cancers. It plays a crucial role in tumor survival and drug resistance [96]. It is expressed during embryonic development but absent from differentiated cells [97]. Survivin is overexpressed in 70–80% of pancreatic cancers and is associated with resistance to chemoradiotherapy [98,99]. Vaccination with Vaccinia Ankara virus, a nonreplicating attenuated VV strain, armed with survivin induced survivin-specific CD8+ immune response resulting in a modest antitumor effect. When combined gemcitabine antitumor immunity and efficacy improved significantly. This is likely to be related to gemcitabine suppression of myeloid-derived suppressor cells [100].

The only VV-based cancer vaccine to enter clinical trials is PANVAC-V, a VV expressing carcinoembryonic antigen and mucin-1, both highly expressed in pancreatic cancers. The two antigens were packaged with three costimulatory molecules: B7.1 (cluster of differentiation 80), ICAM-1 (intracellular adhesion molecule one) and LFA-3 (leukocyte function-associated antigen-3) known collectively as TRICOM. To further enhance the immune response, the vaccination was delivered as a heterologous prime/boost regimen using a nonreplicating fowlpox vector expressing the same antigens and costimulatory molecules (PANVAC-F) [101]. GM-CSF was administered at the injection site as an adjuvant to enhance local antigen processing and presentation. In a Phase I clinical trial, the vaccine was found to be safe and well tolerable. It generated an antigen-specific immune response toward carcinoembryonic antigen and mucin-1 which correlated with increased survival [102]. However, Phase III trial (NCT00088660) targeting patients with metastatic pancreatic cancer who failed gemcitabine treatment failed to meet its therapeutic targets and was terminated [103]. The vaccine is currently under investigation for direct intratumoral injection under endoscopic ultrasound guidance with encouraging results of Phase I trial [104].

Future perspective

There has been a great interest in VV in recent years. Its safety, cancer tropism, amenability to genetic modification and ability to target solid tumors via a variety of mechanism of actions have made it a near-perfect onclytic virus to target pancreatic cancers. Nevertheless, as with any new therapeutic agents VV therapy need to overcome many hurdles and challenges before it enters routine clinical practice.

The first challenge is the selection of the right VV strain. The nonvaccine strain Western Reserve (WR) VV is widely used in the lab. JX-963, a GM-CSF armed mutant of WR VV with deletion of both the Thymidine Kinase and the Viral Growth Factor gene, has been reported as the most potent tumor-targeted oncolytic VV [52]. Other strains, such as the European vaccine Lister strain, are largely untested. We recently evaluated the antitumor potency and biodistribution of different VV strains using *in vitro* and *in vivo* models of cancer, including pancreatic cancer models. The Lister strain virus with Thymidine Kinase gene deletion (VVΔTK) demonstrated superior antitumor potency and cancer-selective replication *in vitro* and *in vivo*, compared with WRDD, especially in human cancer cell lines and immune-competent hosts. Further investigation of functional mechanisms revealed that Lister VVΔTK presented favorable viral biodistribution within the tumors, with lower levels of proinflammatory cytokines compared with WRDD, suggesting that Lister strain may induce a diminished host inflammatory response [105]. Our comprehensive study indicates that the Lister strain VV with TK deletion is a particularly promising VV strain for the development of the next generation of tumor-targeted oncolytic therapeutics. We anticipate that more and more people will use the Lister stain of VV as a backbone to develop new OVs for cancer treatment in the future.

Further genetic modifications of VV might enhance its oncolytic ability. Disruption of the *N1L* gene reduces virulence and inhibits VV replication in the brain reducing the risk postvaccinial encephalitis, a rare but significant complication of VV vaccination [106,107]. Our unpublished work on *N1L*-deleted VV suggests that *N1L*-deleted VV resulted in a superior antitumor efficacy compared with N1L-intact VV [Ahmed J *et al.*, Unpublished Data]. In addition, arming the new generation of VV with immune-modulatory genes or other therapeutic genes that enhance the antitumor immunity is a future for cancer treatment using tumor-targeted OVs.

Achieving the right immune response is of a paramount importance. Increasingly safer viruses permits the use of higher doses to maximize therapeutic effect [8], however higher viral load might deviate the immune response toward antiviral immunity resulting in rapid viral clearance and reduced antitumor immunity. Manipulating the immune system with cytokine-armed viruses is not without its risks including serious autoimmune side effects [108].

Systemic delivery of VV is particularly relevant in pancreatic cancer as most pancreatic tumors present with distant metastasis at the time of diagnosis. One such virus (JX594) has recently been shown to effectively target tumors after intravenous infusion, making it an ideal OV for treatment of inaccessible tumors such

as pancreatic cancer [7]. To date, the systemic delivery of OVs has been shown to be safe but not efficacious mainly due to the rapid clearance of these agents by the immune system [109]. When designing new strategy to enhance the systemic delivery of VV lessons can be learnt from other OVs. Serotype exchange [110,111], engineering new serotypes [112] and the use of chemical shielding [113] have been successfully used with other OVs. In fact the latter strategy have been used to modify the nonreplicating Vaccinia Ankara vaccine vector to circumvent pre-existing anti-VV immunity [114]. Other approaches include pharmacologically modifying the immune response to reduce the neutralization of the systemically delivered OVs [115–117].

Combining oncolytic virotherapy with traditional cancer treatments is an area of great promise. Gemcitabine can suppress myloid-derived suppressor cells in the tumor microenvironment resulting in a stronger antitumor immune response [118]. On the other hand, gemcitabine is a nucleoside analogue that inhibits DNA synthesis including that of double-stranded DNA viruses [119]. Using these agents in a sequential rather than combination manner might be the key to effective therapy [120]. Similarly, combining OVs with immune checkpoints inhibitors is an area that requires more investigation and optimization. PD-1 and CTLA-4 inhibitors might enhance the OV-induced antitumor immunity by creating a favorable immune profile in the tumor microenvironment [121,122].

Despite the challenges, the field of oncolytic virotherapy is generating a great interest of both researchers and pharmaceutical companies alike. The recent US FDA approval of talimogene laherparapvec (T-VEC, an engineered herpes simplex virus-1 expressing GM-CSF), for the treatment of melanoma has given the field a much needed boost. As safety and efficacy data start to accumulate the process of licensing new OVs will get easier. We anticipate other cytokine- and chemokine-armed viruses to enter clinical practice within the next few years. In addition, combining OVs with immune checkpoint therapies, monoclonal antibodies and CAR-T therapies will be an area of major research interest in the near future. Combining immune checkpoint antibodies with other immune-stimulating agents such as conventional drugs, targeted agents and most of all OVs, may increase the tumor types and individual patient profiles in which a durable clinical benefit can be achieved. OVs are finally being recognized for their ability to stimulate antitumor immunity, and with anti-CTLA-4 and anti-PD-1 agents on the market, OVs may finally have met their perfect match. It has never been a more promising era for cancer immunotherapy and personalized medicine.

We believe at the current rate of development it will not be long before OVs are part of routine clinical practice.

Financial & competing interests disclosure

This project was funded by the Medical Research Council of the UK (MR/MD15696/1), Ministry of Sciences and Technology, China (2013DFG32080) and the UK Charity Pancreatic Cancer Research Fund as well Pancreatic Cancer Research UK. The authors have no other relevant affiliations or financial involvement with any organization or entity with a financial interest in or financial conflict with the subject matter or materials discussed in the manuscript apart from those disclosed.

No writing assistance was utilized in the production of this manuscript.

Executive summary

- Pancreatic cancer is one of the most aggressive human cancers, without effective therapies.
- Tumor-targeted oncolytic viruses is a new class of cancer therapeutic agents.
- Oncolytic Vaccinia virus (VV) has distinctive features that make it ideal for treatment of pancreatic cancer.
- The antitumor efficacy of oncolytic VV can be further improved by modification of viral genes and arming the virus with therapeutic genes.
- Combination of oncolytic VV with other cancer therapies could be the future for treatment of pancreatic cancer.

References

1 Cancer Research UK. Pancreatic cancer key stats. Cancer Research UK (2014).

2 Allison DC, Piantadosi S, Hruban RH *et al.* DNA content and other factors associated with ten-year survival after resection of pancreatic carcinoma. *J. Surg. Oncol.* 67(3), 151–159 (1998).

3 Garcea G, Dennison AR, Pattenden CJ *et al.* Survival following curative resection for pancreatic ductal adenocarcinoma. A systematic review of the literature. *JOP* 9(2), 99–132 (2008).

4 Burris HA 3rd, Moore MJ, Andersen J *et al.* Improvements in survival and clinical benefit with gemcitabine as first-line therapy for patients with advanced pancreas cancer: a randomized trial. *J. Clin. Oncol.* 15(6), 2403–2413 (1997).

5 Moore MJ, Goldstein D, Hamm J *et al.* Erlotinib plus gemcitabine compared with gemcitabine alone in patients with advanced pancreatic cancer: a Phase iii trial of the national cancer institute of canada clinical trials group. *J. Clin. Oncol.* 25(15), 1960–1966 (2007).

6 Moss B. Reflections on the early development of poxvirus vectors. *Vaccine* 31(39), 4220–4222 (2013).

7 Breitbach CJ, Burke J, Jonker D *et al.* Intravenous delivery of a multi-mechanistic cancer-targeted oncolytic poxvirus in humans. *Nature* 477(7362), 99–102 (2011).

8 Heo J, Reid T, Ruo L *et al.* Randomized dose-finding clinical trial of oncolytic immunotherapeutic vaccinia jx-594 in liver cancer. *Nat. Med.* 19(3), 329–336 (2013).

9 Wong HH, Lemoine NR, Wang Y. Oncolytic viruses for cancer therapy: overcoming the obstacles. *Viruses* 2(1), 78–106 (2010).

10 Fiola C, Peeters B, Fournier P *et al.* Tumor selective replication of newcastle disease virus: association with defects of tumor cells in antiviral defence. *Int. J. Cancer* 119(2), 328–338 (2006).

11 Krishnamurthy S, Takimoto T, Scroggs RA, Portner A. Differentially regulated interferon response determines the outcome of newcastle disease virus infection in normal and tumor cell lines. *J. Virol.* 80(11), 5145–5155 (2006).

12 Liu XY, Qiu SB, Zou WG *et al.* Effective gene-virotherapy for complete eradication of tumor mediated by the combination of htrail (tnfsf10) and plasminogen k5. *Mol. Ther.* 11(4), 531–541 (2005).

13 Zhang Y, Gu J, Zhao L *et al.* Complete elimination of colorectal tumor xenograft by combined manganese superoxide dismutase with tumor necrosis factor-related apoptosis-inducing ligand gene virotherapy. *Cancer Res.* 66(8), 4291–4298 (2006).

14 Freytag SO, Rogulski KR, Paielli DL *et al.*A novel three-pronged approach to kill cancer cells selectively: concomitant viral, double suicide gene, and radiotherapy. *Hum. Gene Ther.* 9(9), 1323–1333 (1998).

15 Diaconu I, Cerullo V, Hirvinen ML *et al.* Immune response is an important aspect of the antitumor effect produced by a CD40L-encoding oncolytic adenovirus. *Cancer Res.* 72(9), 2327–2338 (2012).

16 Miyamoto S, Inoue H, Nakamura T *et al.* Coxsackievirus b3 is an oncolytic virus with immunostimulatory properties that is active against lung adenocarcinoma. *Cancer Res.* 72(10), 2609–2621 (2012).

17 Donnelly OG, Errington-Mais F, Steele L *et al.* Measles virus causes immunogenic cell death in human melanoma. *Gene Ther.* 20(1), 7–15 (2013).

18 Liikanen I, Ahtiainen L, Hirvinen ML *et al.* Oncolytic adenovirus with temozolomide induces autophagy and antitumor immune responses in cancer patients. *Mol. Ther.* 21(6), 1212–1223 (2013).

19 Kaufman HL, Kim DW, Deraffele G *et al.* Local and distant immunity induced by intralesional vaccination with an oncolytic herpes virus encoding gm-csf in patients with stage iiic and iv melanoma. *Ann. Surg. Oncol.* 17(3), 718–730 (2010).

20 Tysome JR, Li X, Wang S *et al.* A novel therapeutic regimen to eradicate established solid tumors with an effective induction of tumor-specific immunity. *Clin. Cancer Res.* 18(24), 6679–6689 (2012).

21 Nishizaki M, Meyn RE, Levy LB *et al.* Synergistic inhibition of human lung cancer cell growth by adenovirus-mediated wild-type p53 gene transfer in combination with docetaxel and radiation therapeutics in vitro and in vivo. *Clin. Cancer Res.* 7(9), 2887–2897 (2001).

22 Dai MH, Zamarin D, Gao SP *et al.* Synergistic action of oncolytic herpes simplex virus and radiotherapy in pancreatic cancer cell lines. *Br. J. Surg.* 97(9), 1385–1394 (2010).

23 Miranda E, Maya Pineda H, Oberg D *et al.* Adenovirus-mediated sensitization to the cytotoxic drugs docetaxel and mitoxantrone is dependent on regulatory domains in the e1acr1 gene-region. *PLoS ONE* 7(10), e46617 (2012).

24 Cherubini G, Kallin C, Mozetic A *et al.* The oncolytic adenovirus addeltadelta enhances selective cancer cell killing in combination with DNA-damaging drugs in pancreatic cancer models. *Gene Ther.* 18(12), 1157–1165 (2011).

25 Garber K. China approves world's first oncolytic virus therapy for cancer treatment. *J. Natl Cancer Inst.* 98(5), 298–300 (2006).

26 Hecht JR, Bedford R, Abbruzzese JL *et al.* A Phase i/ii trial of intratumoral endoscopic ultrasound injection of onyx-015 with intravenous gemcitabine in unresectable pancreatic carcinoma. *Clin. Cancer Res.* 9(2), 555–561 (2003).

27 Kirn D. Replication-selective oncolytic adenoviruses: virotherapy aimed at genetic targets in cancer. *Oncogene* 19(56), 6660–6669 (2000).

28 Mulvihill S, Warren R, Venook A *et al.* Safety and feasibility of injection with an e1b-55 kda gene-deleted, replication-selective adenovirus (onyx-015) into primary carcinomas of the pancreas: a Phase i trial. *Gene Ther.* 8(4), 308–315 (2001).

29 Nakao A, Kasuya H, Sahin TT *et al.* A Phase I dose-escalation clinical trial of intraoperative direct intratumoral injection of HF10 oncolytic virus in non-resectable patients with advanced pancreatic cancer. *Cancer Gene Ther.* 18(3), 167–175 (2011).

30 Smith GL, Moss B. Infectious poxvirus vectors have capacity for at least 25 000 base pairs of foreign DNA. *Gene* 25(1), 21–28 (1983).

31 Griffiths G, Roos N, Schleich S, Locker JK. Structure and assembly of intracellular mature vaccinia virus: thin-section analyses. *J. Virol.* 75(22), 11056–11070 (2001).

32 Griffiths G, Wepf R, Wendt T *et al.* Structure and assembly of intracellular mature vaccinia virus: isolated-particle analysis. *J. Virol.* 75(22), 11034–11055 (2001).

33 Broyles SS. Vaccinia virus transcription. *J. Gen. Virol.* 84(Pt 9), 2293–2303 (2003).

34 Mallardo M, Leithe E, Schleich S *et al.* Relationship between vaccinia virus intracellular cores, early mrnas, and DNA replication sites. *J. Virol.* 76(10), 5167–5183 (2002).

35 Joklik WK. Vaccinia virus deoxyribonucleic acid: a genome replicating in the cytoplasm. *Res. Publ. Assoc. Res. Nerv. Ment. Dis.* 44, 87–101 (1968).

36 Mercer J, Knebel S, Schmidt FI *et al.* Vaccinia virus strains use distinct forms of macropinocytosis for host-cell entry. *Proc. Natl Acad. Sci. USA* 107(20), 9346–9351 (2010).

37 Moss B. Poxvirus entry and membrane fusion. *Virology* 344(1), 48–54 (2006).

38 Putz MM, Midgley CM, Law M, Smith GL. Quantification of antibody responses against multiple antigens of the two

infectious forms of vaccinia virus provides a benchmark for smallpox vaccination. *Nat. Med.* 12(11), 1310–1315 (2006).

39 Vanderplasschen A, Mathew E, Hollinshead M *et al.* Extracellular enveloped vaccinia virus is resistant to complement because of incorporation of host complement control proteins into its envelope. *Proc. Natl Acad. Sci. USA* 95(13), 7544–7549 (1998).

40 Vanderplasschen A, Hollinshead M, Smith GL. Antibodies against vaccinia virus do not neutralize extracellular enveloped virus but prevent virus release from infected cells and comet formation. *J. Gen. Virol.* 78(Pt 8), 2041–2048 (1997).

41 Girgis NM, Dehaven BC, Fan X *et al.* Cell surface expression of the vaccinia virus complement control protein is mediated by interaction with the viral a56 protein and protects infected cells from complement attack. *J. Virol.* 82(9), 4205–4214 (2008).

42 Kotwal GJ, Isaacs SN, Mckenzie R *et al.* Inhibition of the complement cascade by the major secretory protein of vaccinia virus. *Science* 250(4982), 827–830 (1990).

43 Sahu A, Isaacs SN, Soulika AM, Lambris JD. Interaction of vaccinia virus complement control protein with human complement proteins: factor i-mediated degradation of C3B to IC3B1 inactivates the alternative complement pathway. *J. Immunol.* 160(11), 5596–5604 (1998).

44 Kirn DH, Wang Y, Liang W, Contag CH, Thorne SH. Enhancing poxvirus oncolytic effects through increased spread and immune evasion. *Cancer Res.* 68(7), 2071–2075 (2008).

45 Pipiya T, Sauthoff H, Huang YQ *et al.* Hypoxia reduces adenoviral replication in cancer cells by downregulation of viral protein expression. *Gene Ther.* 12(11), 911–917 (2005).

46 Hiley CT, Yuan M, Lemoine NR, Wang Y. Lister strain vaccinia virus, a potential therapeutic vector targeting hypoxic tumours. *Gene Ther.* 17(2), 281–287 (2010).

47 Center for Disease Control and Prevention. Vaccinia (smallpox) vaccine: recommendations of the Advisory Committee On Immunization Practices (ACIP). *MMWR* 2001 (RR-10), 50, 7-11 (2001).

48 Haim M, Gdalevich M, Mimouni D *et al.* Adverse reactions to smallpox vaccine: the israel defense force experience, 1991 to 1996. A comparison with previous surveys. *Mil. Med.* 165(4), 287–289 (2000).

49 Zeh HJ, Bartlett DL. Development of a replication-selective, oncolytic poxvirus for the treatment of human cancers. *Cancer Gene Ther.* 9(12), 1001–1012 (2002).

50 Tysome JR, Briat A, Alusi G *et al.* Lister strain of vaccinia virus armed with endostatin-angiostatin fusion gene as a novel therapeutic agent for human pancreatic cancer. *Gene Ther.* 16(10), 1223–1233 (2009).

51 Parato KA, Breitbach CJ, Le Boeuf F *et al.* The oncolytic poxvirus jx-594 selectively replicates in and destroys cancer cells driven by genetic pathways commonly activated in cancers. *Mol. Ther.* 20(4), 749–758 (2012).

52 Thorne SH, Hwang TH, O'Gorman WE *et al.* Rational strain selection and engineering creates a broad-spectrum, systemically effective oncolytic poxvirus, jx-963. *J. Clin. Invest.* 117(11), 3350–3358 (2007).

53 Yu YA, Shabahang S, Timiryasova TM *et al.* Visualization of tumors and metastases in live animals with bacteria and vaccinia virus encoding light-emitting proteins. *Nat. Biotechnol.* 22(3), 313–320 (2004).

54 Hanahan D, Weinberg RA. Hallmarks of cancer: the next generation. *Cell* 144(5), 646–674 (2011).

55 Yarden Y. The egfr family and its ligands in human cancer. Signalling mechanisms and therapeutic opportunities. *Eur. J. Cancer* 37(Suppl. 4), S3–S8 (2001).

56 Yang H, Kim SK, Kim M *et al.* Antiviral chemotherapy facilitates control of poxvirus infections through inhibition of cellular signal transduction. *J. Clin. Invest.* 115(2), 379–387 (2005).

57 Guitard E, Parker F, Millon R *et al.* G3bp is overexpressed in human tumors and promotes S Phase entry. *Cancer Lett.* 162(2), 213–221 (2001).

58 Katsafanas GC, Moss B. Vaccinia virus intermediate stage transcription is complemented by ras-gtpase-activating protein Sh3 domain-binding protein (g3bp) and cytoplasmic activation/proliferation-associated protein (p137) individually or as a heterodimer. *J. Biol. Chem.* 279(50), 52210–52217 (2004).

59 Mccart JA, Ward JM, Lee J *et al.* Systemic cancer therapy with a tumor-selective vaccinia virus mutant lacking thymidine kinase and vaccinia growth factor genes. *Cancer Res.* 61(24), 8751–8757 (2001).

60 Puhlmann M, Brown CK, Gnant M *et al.* Vaccinia as a vector for tumor-directed gene therapy: biodistribution of a thymidine kinase-deleted mutant. *Cancer Gene Ther.* 7(1), 66–73 (2000).

61 Colamonici OR, Domanski P, Sweitzer SM *et al.* Vaccinia virus *B18r* gene encodes a type I interferon-binding protein that blocks interferon alpha transmembrane signaling. *J. Biol. Chem.* 270(27), 15974–15978 (1995).

62 Kirn DH, Wang Y, Le Boeuf F *et al.* Targeting of interferon-beta to produce a specific, multi-mechanistic oncolytic vaccinia virus. *PLoS Med.* 4(12), e353 (2007).

63 Luker KE, Hutchens M, Schultz T *et al.* Bioluminescence imaging of vaccinia virus: effects of interferon on viral replication and spread. *Virology* 341(2), 284–300 (2005).

64 Hikichi M, Kidokoro M, Haraguchi T *et al.* MicroRNA regulation of glycoprotein B5r in oncolytic vaccinia virus reduces viral pathogenicity without impairing its antitumor efficacy. *Mol. Ther.* 19(6), 1107–1115 (2011).

65 Yu YA, Galanis C, Woo Y *et al.* Regression of human pancreatic tumor xenografts in mice after a single systemic injection of recombinant vaccinia virus GLV-1h68. *Mol. Cancer Ther.* 8(1), 141–151 (2009).

66 Haddad D, Chen N, Zhang Q *et al.* A novel genetically modified oncolytic vaccinia virus in experimental models is effective against a wide range of human cancers. *Ann. Surg. Oncol.* 19(Suppl. 3), S665–S674 (2012).

67 Dai MH, Liu SL, Chen NG *et al.* Oncolytic vaccinia virus in combination with radiation shows synergistic antitumor efficacy in pancreatic cancer. *Cancer Lett.* 344(2), 282–290 (2014).

68 Liu TC, Hwang T, Park BH *et al.* The targeted oncolytic poxvirus jx-594 demonstrates antitumoral, antivascular, and anti-HBV activities in patients with hepatocellular carcinoma. *Mol. Ther.* 16(9), 1637–1642 (2008).

69 Breitbach CJ, Paterson JM, Lemay CG *et al.* Targeted inflammation during oncolytic virus therapy severely compromises tumor blood flow. *Mol. Ther.* 15(9), 1686–1693 (2007).

70 Ikeda N, Adachi M, Taki T *et al.* Prognostic significance of angiogenesis in human pancreatic cancer. *Br. J. Cancer* 79(9–10), 1553–1563 (1999).

71 Scappaticci FA, Contreras A, Smith R *et al.* Statin-AE: a novel angiostatin-endostatin fusion protein with enhanced antiangiogenic and antitumor activity. *Angiogenesis* 4(4), 263–268 (2001).

72 Bell J, Mcfadden G. Viruses for tumor therapy. *Cell Host Microbe* 15(3), 260–265 (2014).

73 Tong AW, Senzer N, Cerullo V *et al.* Oncolytic viruses for induction of anti-tumor immunity. *Curr. Pharm. Biotechnol.* 13(9), 1750–1760 (2012).

74 Bartlett DL, Liu Z, Sathaiah M *et al.* Oncolytic viruses as therapeutic cancer vaccines. *Mol. Cancer* 12(1), 103 (2013).

75 Huang B, Sikorski R, Kirn DH, Thorne SH. Synergistic anti-tumor effects between oncolytic vaccinia virus and paclitaxel are mediated by the IFN response and Hmgb1. *Gene Ther.* 18(2), 164–172 (2011).

76 Guo ZS, Naik A, O'malley ME *et al.* The enhanced tumor selectivity of an oncolytic vaccinia lacking the host range and antiapoptosis genes *spi-1* and *spi-2*. *Cancer Res.* 65(21), 9991–9998 (2005).

77 John LB, Howland LJ, Flynn JK *et al.* Oncolytic virus and anti-4–1BB combination therapy elicits strong antitumor immunity against established cancer. *Cancer Res.* 72(7), 1651–1660 (2012).

78 Whilding LM, Archibald KM, Kulbe H *et al.* Vaccinia virus induces programmed necrosis in ovarian cancer cells. *Mol. Ther.* 21(11), 2074–2086 (2013).

79 Zhu J, Martinez J, Huang X, Yang Y. Innate immunity against vaccinia virus is mediated by TLR2 and requires TLR-independent production of IFN-beta. *Blood* 109(2), 619–625 (2007).

80 Barbalat R, Lau L, Locksley RM, Barton GM. Toll-like receptor 2 on inflammatory monocytes induces type I interferon in response to viral but not bacterial ligands. *Nat. Immunol.* 10(11), 1200–1207 (2009).

81 Delaloye J, Roger T, Steiner-Tardivel QG *et al.* Innate immune sensing of modified vaccinia virus ankara (MVA) is mediated by TLR2-TLR6, MDA-5 and the NALP3 inflammasome. *PLoS Pathog.* 5(6), e1000480 (2009).

82 Kim MK, Breitbach CJ, Moon A *et al.* Oncolytic and immunotherapeutic vaccinia induces antibody-mediated complement-dependent cancer cell lysis in humans. *Sci. Transl. Med.* 5(185), 185ra163 (2013).

83 Draper SJ, Moore AC, Goodman AL *et al.* Effective induction of high-titer antibodies by viral vector vaccines. *Nat. Med.* 14(8), 819–821 (2008).

84 Bruña-Romero O, González-Aseguinolaza G, Hafalla JC *et al.* Complete, long-lasting protection against malaria of mice primed and boosted with two distinct viral vectors expressing the same plasmodial antigen. *Proc. Natl Acad. Sci. USA* 98(20), 11491–11496 (2001).

85 Couper KN, Blount DG, Riley EM. Il-10: the master regulator of immunity to infection. *J. Immunol.* 180(9), 5771–5777 (2008).

86 Chard LS, Maniati E, Wang P *et al.* A vaccinia virus armed with interleukin-10 is a promising therapeutic agent for treatment of murine pancreatic cancer. *Clin. Cancer Res.* 21(2), 405–416 (2015).

87 Smith GL, Mackett M, Moss B. Infectious vaccinia virus recombinants that express hepatitis B virus surface antigen. *Nature* 302(5908), 490–495 (1983).

88 Moss B, Smith GL, Gerin JL, Purcell RH. Live recombinant vaccinia virus protects chimpanzees against hepatitis B. *Nature* 311(5981), 67–69 (1984).

89 Meeusen EN, Walker J, Peters A *et al.* Current status of veterinary vaccines. *Clin. Microbiol. Rev.* 20(3), 489–510 (2007).

90 Poulet H, Minke J, Pardo MC *et al.* Development and registration of recombinant veterinary vaccines. The example of the canarypox vector platform. *Vaccine* 25(30), 5606–5612 (2007).

91 Rerks-Ngarm S, Pitisuttithum P, Nitayaphan S *et al.* Vaccination with Alvac and Aidsvax to prevent HIV-1 infection in Thailand. *N. Engl. J. Med.* 361(23), 2209–2220 (2009).

92 Sheehy SH, Duncan CJ, Elias SC *et al.* Phase ia clinical evaluation of the safety and immunogenicity of the plasmodium falciparum blood-stage antigen ama1 in chad63 and mva vaccine vectors. *PLoS ONE* 7(2), e31208 (2012).

93 Sheehy SH, Duncan CJ, Elias SC *et al.* Phase ia clinical evaluation of the plasmodium falciparum blood-stage antigen MSP1 in CHAD63 and MVA vaccine vectors. *Mol. Ther.* 19(12), 2269–2276 (2011).

94 Scriba TJ, Tameris M, Mansoor N *et al.* Modified vaccinia ankara-expressing ag85a, a novel tuberculosis vaccine, is safe in adolescents and children, and induces polyfunctional $CD4^+$ T cells. *Eur. J. Immunol.* 40(1), 279–290 (2010).

95 Draper SJ, Heeney JL. Viruses as vaccine vectors for infectious diseases and cancer. *Nat. Rev. Microbiol.* 8(1), 62–73 (2010).

96 Singh N, Krishnakumar S, Kanwar RK *et al.* Clinical aspects for survivin: a crucial molecule for targeting drug-resistant cancers. *Drug Discov. Today* 20(5),578–587 (2014).

97 Adida C, Crotty PL, Mcgrath J *et al.* Developmentally regulated expression of the novel cancer anti-apoptosis gene survivin in human and mouse differentiation. *Am. J. Pathol.* 152(1), 43–49 (1998).

98 Sarela AI, Verbeke CS, Ramsdale J*et al.* Expression of survivin, a novel inhibitor of apoptosis and cell cycle regulatory protein, in pancreatic adenocarcinoma. *Br. J. Cancer* 86(6), 886–892 (2002).

99 Kami K, Doi R, Koizumi M *et al.* Downregulation of survivin by sirna diminishes radioresistance of pancreatic cancer cells. *Surgery* 138(2), 299–305 (2005).

100 Ishizaki H, Manuel ER, Song GY *et al.* Modified vaccinia ankara expressing survivin combined with gemcitabine generates specific antitumor effects in a murine pancreatic carcinoma model. *Cancer Immunol. Immunother.* 60(1), 99–109 (2011).

101 Petrulio CA, Kaufman HL. Development of the panvac-vf vaccine for pancreatic cancer. *Expert Rev. Vaccines* 5(1), 9–19 (2006).

102 Kaufman HL, Kim-Schulze S, Manson K *et al.* Poxvirus-based vaccine therapy for patients with advanced pancreatic cancer. *J. Transl. Med.* 5, 60 (2007).

103 Therion reports results of Phase 3 panvac-vf trial and announces plans for company sale. PR Newswire 28 June. www.prnewswire.com

104 Riedmann EM. Human vaccines & immunotherapeutics: news. *Hum. Vaccin. Immunother.* 10(7), 1773–1777 (2014).

105 Hughes J, Wang P, Alusi G *et al.* Lister strain vaccinia virus with thymidine kinase gene deletion is a tractable platform for development of a new generation of oncolytic virus. *Gene Ther.*22(6), 476-84 (2015).

106 Billings B, Smith SA, Zhang Z *et al*. Lack of *n1l* gene expression results in a significant decrease of vaccinia virus replication in mouse brain. *Ann. NY Acad. Sci.* 1030, 297–302 (2004).

107 Bartlett N, Symons JA, Tscharke DC, Smith GL. The vaccinia virus N1l protein is an intracellular homodimer that promotes virulence. *J. Gen. Virol.* 83(Pt 8), 1965–1976 (2002).

108 Poutou J, Bunuales M, Gonzalez-Aparicio M *et al.* Safety and antitumor effect of oncolytic and helper-dependent adenoviruses expressing interleukin-12 variants in a hamster pancreatic cancer model. *Gene Ther.* 22(9), 696-706 (2015).

109 Ferguson MS, Lemoine NR, Wang Y. Systemic delivery of oncolytic viruses: hopes and hurdles. *Adv. Virol.* 2012, 805629 (2012).

110 Roberts DM, Nanda A, Havenga MJ *et al.* Hexon-chimaeric adenovirus serotype 5 vectors circumvent pre-existing anti-vector immunity. *Nature* 441(7090), 239–243 (2006).

111 Kuhlmann KF, Van Geer MA, Bakker CT *et al.* Fiber-chimeric adenoviruses expressing fibers from serotype 16 and 50 improve gene transfer to human pancreatic adenocarcinoma. *Cancer Gene Ther.* 16(7), 585–597 (2009).

112 Miest TS, Yaiw KC, Frenzke M *et al.* Envelope-chimeric entry-targeted measles virus escapes neutralization and achieves oncolysis. *Mol. Ther.* 19(10), 1813–1820 (2011).

113 Kim PH, Kim J, Kim TI *et al.* Bioreducible polymer-conjugated oncolytic adenovirus for hepatoma-specific therapy via systemic administration. *Biomaterials* 32(35), 9328–9342 (2011).

114 Naito T, Kaneko Y, Kozbor D. Oral vaccination with modified vaccinia virus ankara attached covalently to TMPEG-modified cationic liposomes overcomes pre-existing poxvirus immunity from recombinant vaccinia immunization. *J. Gen. Virol.* 88(Pt 1), 61–70 (2007).

115 Ikeda K, Ichikawa T, Wakimoto H *et al.* Oncolytic virus therapy of multiple tumors in the brain requires suppression of innate and elicited antiviral responses. *Nat. Med.* 5(8), 881–887 (1999).

116 Ikeda K, Wakimoto H, Ichikawa T *et al.* Complement depletion facilitates the infection of multiple brain tumors by an intravascular, replication-conditional herpes simplex virus mutant. *J. Virol.* 74(10), 4765–4775 (2000).

117 Kambara H, Saeki Y, Chiocca EA. Cyclophosphamide allows for *in vivo* dose reduction of a potent oncolytic virus. *Cancer Res.* 65(24), 11255–11258 (2005).

118 Le HK, Graham L, Cha E *et al.* Gemcitabine directly inhibits myeloid derived suppressor cells in balb/c mice bearing 4T1 mammary carcinoma and augments expansion of T cells from tumor-bearing mice. *Int. Immunopharmacol.* 9(7–8), 900–909 (2009).

119 Watanabe I, Kasuya H, Nomura N *et al.* Effects of tumor selective replication-competent herpes viruses in combination with gemcitabine on pancreatic cancer. *Cancer Chemother. Pharmacol.* 61(5), 875–882 (2008).

120 Wennier ST, Liu J, Li S *et al.*Myxoma virus sensitizes cancer cells to gemcitabine and is an effective oncolytic virotherapeutic in models of disseminated pancreatic cancer. *Mol. Ther.* 20(4), 759–768 (2012).

121 Engeland CE, Grossardt C, Veinalde R *et al.* CTLA-4 and PD-L1 checkpoint blockade enhances oncolytic measles virus therapy. *Mol. Ther.* 22(11), 1949–1959 (2014).

122 Dias JD, Hemminki O, Diaconu I *et al.* Targeted cancer immunotherapy with oncolytic adenovirus coding for a fully human monoclonal antibody specific for CTLA-4. *Gene Ther.* 19(10), 988–998 (2012).

References

1. Yaghchi, C.A., et al., *Vaccinia virus, a promising new therapeutic agent for pancreatic cancer.* Immunotherapy, 2015. **7**(12): p. 1249-58.
2. CRUK. *All cancers combined Key Stats*. [Document] 2015 04/02/2015 09:58; Available from: http://www.cancerresearchuk.org/cancer-info/cancerstats/keyfacts/Allcancerscombined/.
3. Kelly, E. and S.J. Russell, *History of oncolytic viruses: genesis to genetic engineering.* Mol Ther, 2007. **15**(4): p. 651-9.
4. Sinkovics, J., J. Horvath, and M. Szabo-Szabari, *Human cancer vaccines.* Leukemia, 1994. **8 Suppl 1**: p. S194-7.
5. Martuza, R.L., et al., *Experimental therapy of human glioma by means of a genetically engineered virus mutant.* Science, 1991. **252**(5007): p. 854-6.
6. Bell, J. and G. McFadden, *Viruses for tumor therapy.* Cell Host Microbe, 2014. **15**(3): p. 260-5.
7. Cawood, R., et al., *Recombinant viral vaccines for cancer.* Trends Mol Med, 2012. **18**(9): p. 564-74.
8. Bartlett, D.L., et al., *Oncolytic viruses as therapeutic cancer vaccines.* Mol Cancer, 2013. **12**(1): p. 103.
9. Tong, A.W., et al., *Oncolytic viruses for induction of anti-tumor immunity.* Curr Pharm Biotechnol, 2012. **13**(9): p. 1750-60.
10. Liu, X.Y., et al., *Effective gene-virotherapy for complete eradication of tumor mediated by the combination of hTRAIL (TNFSF10) and plasminogen k5.* Mol Ther, 2005. **11**(4): p. 531-41.
11. Zhang, Y., et al., *Complete elimination of colorectal tumor xenograft by combined manganese superoxide dismutase with tumor necrosis factor-related apoptosis-inducing ligand gene virotherapy.* Cancer Res, 2006. **66**(8): p. 4291-8.
12. Freytag, S.O., et al., *A novel three-pronged approach to kill cancer cells selectively: concomitant viral, double suicide gene, and radiotherapy.* Hum Gene Ther, 1998. **9**(9): p. 1323-33.
13. Diaconu, I., et al., *Immune response is an important aspect of the antitumor effect produced by a CD40L-encoding oncolytic adenovirus.* Cancer Res, 2012. **72**(9): p. 2327-38.
14. Miyamoto, S., et al., *Coxsackievirus B3 is an oncolytic virus with immunostimulatory properties that is active against lung adenocarcinoma.* Cancer Res, 2012. **72**(10): p. 2609-21.
15. Donnelly, O.G., et al., *Measles virus causes immunogenic cell death in human melanoma.* Gene Ther, 2013. **20**(1): p. 7-15.
16. Liikanen, I., et al., *Oncolytic adenovirus with temozolomide induces autophagy and antitumor immune responses in cancer patients.* Mol Ther, 2013. **21**(6): p. 1212-23.
17. Nishizaki, M., et al., *Synergistic inhibition of human lung cancer cell growth by adenovirus-mediated wild-type p53 gene transfer in combination with docetaxel and radiation therapeutics in vitro and in vivo.* Clin Cancer Res, 2001. **7**(9): p. 2887-97.

18. Dai, M.H., et al., *Synergistic action of oncolytic herpes simplex virus and radiotherapy in pancreatic cancer cell lines.* Br J Surg, 2010. **97**(9): p. 1385-94.
19. Miranda, E., et al., *Adenovirus-mediated sensitization to the cytotoxic drugs docetaxel and mitoxantrone is dependent on regulatory domains in the E1ACR1 gene-region.* PLoS One, 2012. **7**(10): p. e46617.
20. Cherubini, G., et al., *The oncolytic adenovirus AdDeltaDelta enhances selective cancer cell killing in combination with DNA-damaging drugs in pancreatic cancer models.* Gene Ther, 2011. **18**(12): p. 1157-65.
21. Hanahan, D. and R.A. Weinberg, *Hallmarks of cancer: the next generation.* Cell, 2011. **144**(5): p. 646-74.
22. Chiocca, E.A. and S.D. Rabkin, *Oncolytic viruses and their application to cancer immunotherapy.* Cancer Immunol Res, 2014. **2**(4): p. 295-300.
23. Russell, S.J., K.W. Peng, and J.C. Bell, *Oncolytic virotherapy.* Nat Biotechnol, 2012. **30**(7): p. 658-70.
24. Cattaneo, R., et al., *Reprogrammed viruses as cancer therapeutics: targeted, armed and shielded.* Nat Rev Microbiol, 2008. **6**(7): p. 529-40.
25. Liu, T.C., et al., *The targeted oncolytic poxvirus JX-594 demonstrates antitumoral, antivascular, and anti-HBV activities in patients with hepatocellular carcinoma.* Mol Ther, 2008. **16**(9): p. 1637-42.
26. Park, B.H., et al., *Use of a targeted oncolytic poxvirus, JX-594, in patients with refractory primary or metastatic liver cancer: a phase I trial.* Lancet Oncol, 2008. **9**(6): p. 533-42.
27. Kim, W., et al., *A novel combination treatment of armed oncolytic adenovirus expressing IL-12 and GM-CSF with radiotherapy in murine hepatocarcinoma.* J Radiat Res, 2011. **52**(5): p. 646-54.
28. Chard, L.S., et al., *A vaccinia virus armed with interleukin-10 is a promising therapeutic agent for treatment of murine pancreatic cancer.* Clin Cancer Res, 2015. **21**(2): p. 405-16.
29. Moss, B., *Reflections on the early development of poxvirus vectors.* Vaccine, 2013. **31**(39): p. 4220-2.
30. Breitbach, C.J., et al., *Intravenous delivery of a multi-mechanistic cancer-targeted oncolytic poxvirus in humans.* Nature, 2011. **477**(7362): p. 99-102.
31. Heo, J., et al., *Randomized dose-finding clinical trial of oncolytic immunotherapeutic vaccinia JX-594 in liver cancer.* Nat Med, 2013. **19**(3): p. 329-36.
32. *Vaccinia virus, complete genome - Nucleotide - NCBI*. 2015; Available from: http://www.ncbi.nlm.nih.gov/pubmed/.
33. Baroudy, B.M., S. Venkatesan, and B. Moss, *Incompletely base-paired flip-flop terminal loops link the two DNA strands of the vaccinia virus genome into one uninterrupted polynucleotide chain.* Cell, 1982. **28**(2): p. 315-24.
34. Smith, G.L. and B. Moss, *Infectious poxvirus vectors have capacity for at least 25 000 base pairs of foreign DNA.* Gene, 1983. **25**(1): p. 21-8.
35. Griffiths, G., et al., *Structure and assembly of intracellular mature vaccinia virus: thin-section analyses.* J Virol, 2001. **75**(22): p. 11056-70.
36. Griffiths, G., et al., *Structure and assembly of intracellular mature vaccinia virus: isolated-particle analysis.* J Virol, 2001. **75**(22): p. 11034-55.

37. Mercer, J., et al., *Vaccinia virus strains use distinct forms of macropinocytosis for host-cell entry.* Proc Natl Acad Sci U S A, 2010. **107**(20): p. 9346-51.
38. Moss, B., *Poxvirus entry and membrane fusion.* Virology, 2006. **344**(1): p. 48-54.
39. Moss, B., *Regulation of vaccinia virus transcription.* Annu Rev Biochem, 1990. **59**: p. 661-88.
40. Joklik, W.K., *Vaccinia virus deoxyribonucleic acid: a genome replicating in the cytoplasm.* Res Publ Assoc Res Nerv Ment Dis, 1968. **44**: p. 87-101.
41. Broyles, S.S., *Vaccinia virus transcription.* J Gen Virol, 2003. **84**(Pt 9): p. 2293-303.
42. Mallardo, M., et al., *Relationship between vaccinia virus intracellular cores, early mRNAs, and DNA replication sites.* J Virol, 2002. **76**(10): p. 5167-83.
43. Putz, M.M., et al., *Quantification of antibody responses against multiple antigens of the two infectious forms of Vaccinia virus provides a benchmark for smallpox vaccination.* Nat Med, 2006. **12**(11): p. 1310-5.
44. Vanderplasschen, A., et al., *Extracellular enveloped vaccinia virus is resistant to complement because of incorporation of host complement control proteins into its envelope.* Proc Natl Acad Sci U S A, 1998. **95**(13): p. 7544-9.
45. Vanderplasschen, A., M. Hollinshead, and G.L. Smith, *Antibodies against vaccinia virus do not neutralize extracellular enveloped virus but prevent virus release from infected cells and comet formation.* J Gen Virol, 1997. **78 (Pt 8)**: p. 2041-8.
46. Girgis, N.M., et al., *Cell surface expression of the vaccinia virus complement control protein is mediated by interaction with the viral A56 protein and protects infected cells from complement attack.* J Virol, 2008. **82**(9): p. 4205-14.
47. Kotwal, G.J., et al., *Inhibition of the complement cascade by the major secretory protein of vaccinia virus.* Science, 1990. **250**(4982): p. 827-30.
48. Sahu, A., et al., *Interaction of vaccinia virus complement control protein with human complement proteins: factor I-mediated degradation of C3b to iC3b1 inactivates the alternative complement pathway.* J Immunol, 1998. **160**(11): p. 5596-604.
49. Kirn, D.H., et al., *Enhancing poxvirus oncolytic effects through increased spread and immune evasion.* Cancer Res, 2008. **68**(7): p. 2071-5.
50. Park, S.H., et al., *Phase 1b Trial of Biweekly Intravenous Pexa-Vec (JX-594), an Oncolytic and Immunotherapeutic Vaccinia Virus in Colorectal Cancer.* Mol Ther, 2015. **23**(9): p. 1532-40.
51. Pipiya, T., et al., *Hypoxia reduces adenoviral replication in cancer cells by downregulation of viral protein expression.* Gene Ther, 2005. **12**(11): p. 911-7.
52. Hiley, C.T., et al., *Lister strain vaccinia virus, a potential therapeutic vector targeting hypoxic tumours.* Gene Ther, 2010. **17**(2): p. 281-7.
53. Hiley, C.T., et al., *Vascular endothelial growth factor A promotes vaccinia virus entry into host cells via activation of the Akt pathway.* J Virol, 2013. **87**(5): p. 2781-90.
54. Arulanandam, R., et al., *VEGF-Mediated Induction of PRD1-BF1/Blimp1 Expression Sensitizes Tumor Vasculature to Oncolytic Virus Infection.* Cancer Cell, 2015. **28**(2): p. 210-24.

55. *Vaccinia (smallpox) vaccine: recommendations of the Advisory Committee on Immunization Practices (ACIP)*, in *MMWR 2001*, J.W. Ward, Editor. 2001, Centers for Disease Control and Prevention.
56. Haim, M., et al., *Adverse reactions to smallpox vaccine: the Israel Defense Force experience, 1991 to 1996. A comparison with previous surveys.* Mil Med, 2000. **165**(4): p. 287-9.
57. Zeh, H.J. and D.L. Bartlett, *Development of a replication-selective, oncolytic poxvirus for the treatment of human cancers.* Cancer Gene Ther, 2002. **9**(12): p. 1001-12.
58. Tysome, J.R., et al., *Lister strain of vaccinia virus armed with endostatin-angiostatin fusion gene as a novel therapeutic agent for human pancreatic cancer.* Gene Ther, 2009. **16**(10): p. 1223-33.
59. Parato, K.A., et al., *The oncolytic poxvirus JX-594 selectively replicates in and destroys cancer cells driven by genetic pathways commonly activated in cancers.* Mol Ther, 2012. **20**(4): p. 749-58.
60. Thorne, S.H., et al., *Rational strain selection and engineering creates a broad-spectrum, systemically effective oncolytic poxvirus, JX-963.* J Clin Invest, 2007. **117**(11): p. 3350-8.
61. Yu, Y.A., et al., *Visualization of tumors and metastases in live animals with bacteria and vaccinia virus encoding light-emitting proteins.* Nat Biotechnol, 2004. **22**(3): p. 313-20.
62. Yarden, Y., *The EGFR family and its ligands in human cancer. signalling mechanisms and therapeutic opportunities.* Eur J Cancer, 2001. **37 Suppl 4**: p. S3-8.
63. Yang, H., et al., *Antiviral chemotherapy facilitates control of poxvirus infections through inhibition of cellular signal transduction.* J Clin Invest, 2005. **115**(2): p. 379-87.
64. Guitard, E., et al., *G3BP is overexpressed in human tumors and promotes S phase entry.* Cancer Lett, 2001. **162**(2): p. 213-21.
65. Katsafanas, G.C. and B. Moss, *Vaccinia virus intermediate stage transcription is complemented by Ras-GTPase-activating protein SH3 domain-binding protein (G3BP) and cytoplasmic activation/proliferation-associated protein (p137) individually or as a heterodimer.* J Biol Chem, 2004. **279**(50): p. 52210-7.
66. McCart, J.A., et al., *Systemic cancer therapy with a tumor-selective vaccinia virus mutant lacking thymidine kinase and vaccinia growth factor genes.* Cancer Res, 2001. **61**(24): p. 8751-7.
67. Puhlmann, M., et al., *Vaccinia as a vector for tumor-directed gene therapy: biodistribution of a thymidine kinase-deleted mutant.* Cancer Gene Ther, 2000. **7**(1): p. 66-73.
68. Colamonici, O.R., et al., *Vaccinia virus B18R gene encodes a type I interferon-binding protein that blocks interferon alpha transmembrane signaling.* J Biol Chem, 1995. **270**(27): p. 15974-8.
69. Kirn, D.H., et al., *Targeting of interferon-beta to produce a specific, multi-mechanistic oncolytic vaccinia virus.* PLoS Med, 2007. **4**(12): p. e353.
70. Luker, K.E., et al., *Bioluminescence imaging of vaccinia virus: effects of interferon on viral replication and spread.* Virology, 2005. **341**(2): p. 284-300.

71. Hikichi, M., et al., *MicroRNA regulation of glycoprotein B5R in oncolytic vaccinia virus reduces viral pathogenicity without impairing its antitumor efficacy.* Mol Ther, 2011. **19**(6): p. 1107-15.
72. Huang, B., et al., *Synergistic anti-tumor effects between oncolytic vaccinia virus and paclitaxel are mediated by the IFN response and HMGB1.* Gene Ther, 2011. **18**(2): p. 164-72.
73. Guo, Z.S., et al., *The enhanced tumor selectivity of an oncolytic vaccinia lacking the host range and antiapoptosis genes SPI-1 and SPI-2.* Cancer Res, 2005. **65**(21): p. 9991-8.
74. John, L.B., et al., *Oncolytic virus and anti-4-1BB combination therapy elicits strong antitumor immunity against established cancer.* Cancer Res, 2012. **72**(7): p. 1651-60.
75. Whilding, L.M., et al., *Vaccinia virus induces programmed necrosis in ovarian cancer cells.* Mol Ther, 2013. **21**(11): p. 2074-86.
76. Zhu, J., et al., *Innate immunity against vaccinia virus is mediated by TLR2 and requires TLR-independent production of IFN-beta.* Blood, 2007. **109**(2): p. 619-25.
77. Barbalat, R., et al., *Toll-like receptor 2 on inflammatory monocytes induces type I interferon in response to viral but not bacterial ligands.* Nat Immunol, 2009. **10**(11): p. 1200-7.
78. Delaloye, J., et al., *Innate immune sensing of modified vaccinia virus Ankara (MVA) is mediated by TLR2-TLR6, MDA-5 and the NALP3 inflammasome.* PLoS Pathog, 2009. **5**(6): p. e1000480.
79. Kim, M.K., et al., *Oncolytic and immunotherapeutic vaccinia induces antibody-mediated complement-dependent cancer cell lysis in humans.* Sci Transl Med, 2013. **5**(185): p. 185ra63.
80. Tysome, J.R., et al., *A novel therapeutic regimen to eradicate established solid tumors with an effective induction of tumor-specific immunity.* Clinical Cancer Research, 2012. **18**(24): p. 6679-6689.
81. Breitbach, C.J., et al., *Targeted inflammation during oncolytic virus therapy severely compromises tumor blood flow.* Mol Ther, 2007. **15**(9): p. 1686-93.
82. Hughes, J., et al., *Lister strain vaccinia virus with thymidine kinase gene deletion is a tractable platform for development of a new generation of oncolytic virus.* Gene Ther, 2015.
83. ROWE, W.P., et al., *Isolation of a cytopathogenic agent from human adenoids undergoing spontaneous degeneration in tissue culture.* Proc Soc Exp Biol Med, 1953. **84**(3): p. 570-3.
84. Halldén, G. and G. Portella, *Oncolytic virotherapy with modified adenoviruses and novel therapeutic targets.* Expert Opin Ther Targets, 2012. **16**(10): p. 945-58.
85. Russell, W.C., *Adenoviruses: update on structure and function.* J Gen Virol, 2009. **90**(Pt 1): p. 1-20.
86. Rux, J.J. and R.M. Burnett, *Adenovirus structure.* Hum Gene Ther, 2004. **15**(12): p. 1167-76.
87. San Martín, C., *Latest insights on adenovirus structure and assembly.* Viruses, 2012. **4**(5): p. 847-77.
88. *Human adenovirus 5, complete genome - Nucleotide - NCBI*. 2015; Available from: http://www.ncbi.nlm.nih.gov/pubmed/.

89. Davison, A.J., M. Benko, and B. Harrach, *Genetic content and evolution of adenoviruses.* J Gen Virol, 2003. **84**(Pt 11): p. 2895-908.
90. Tollefson, A.E., et al., *The adenovirus death protein (E3-11.6K) is required at very late stages of infection for efficient cell lysis and release of adenovirus from infected cells.* J Virol, 1996. **70**(4): p. 2296-306.
91. Bergelson, J.M., et al., *Isolation of a common receptor for Coxsackie B viruses and adenoviruses 2 and 5.* Science, 1997. **275**(5304): p. 1320-3.
92. Marttila, M., et al., *CD46 is a cellular receptor for all species B adenoviruses except types 3 and 7.* J Virol, 2005. **79**(22): p. 14429-36.
93. Dechecchi, M.C., et al., *Heparan sulfate glycosaminoglycans are involved in adenovirus type 5 and 2-host cell interactions.* Virology, 2000. **268**(2): p. 382-90.
94. Short, J.J., et al., *Adenovirus serotype 3 utilizes CD80 (B7.1) and CD86 (B7.2) as cellular attachment receptors.* Virology, 2004. **322**(2): p. 349-59.
95. Li, E., et al., *Integrin alpha(v)beta1 is an adenovirus coreceptor.* J Virol, 2001. **75**(11): p. 5405-9.
96. Wickham, T.J., et al., *Integrins alpha v beta 3 and alpha v beta 5 promote adenovirus internalization but not virus attachment.* Cell, 1993. **73**(2): p. 309-19.
97. Li, E., et al., *Adenovirus endocytosis via alpha(v) integrins requires phosphoinositide-3-OH kinase.* J Virol, 1998. **72**(3): p. 2055-61.
98. Meier, O. and U.F. Greber, *Adenovirus endocytosis.* J Gene Med, 2004. **6 Suppl 1**: p. S152-63.
99. Deal, C., A. Pekosz, and G. Ketner, *Prospects for oral replicating adenovirus-vectored vaccines.* Vaccine, 2013. **31**(32): p. 3236-43.
100. Leen, A.M. and C.M. Rooney, *Adenovirus as an emerging pathogen in immunocompromised patients.* Br J Haematol, 2005. **128**(2): p. 135-44.
101. Alvarez, R.D. and D.T. Curiel, *A phase I study of recombinant adenovirus vector-mediated intraperitoneal delivery of herpes simplex virus thymidine kinase (HSV-TK) gene and intravenous ganciclovir for previously treated ovarian and extraovarian cancer patients.* Hum Gene Ther, 1997. **8**(5): p. 597-613.
102. Nemunaitis, J., et al., *Phase II trial of intratumoral administration of ONYX-015, a replication-selective adenovirus, in patients with refractory head and neck cancer.* J Clin Oncol, 2001. **19**(2): p. 289-98.
103. HUEBNER, R.J., et al., *Studies on the use of viruses in the treatment of carcinoma of the cervix.* Cancer, 1956. **9**(6): p. 1211-8.
104. SOUTHAM, C.M., M.R. HILLEMAN, and J.H. WERNER, *Pathogenicity and oncolytic capacity of RI virus strain RI-67 in man.* J Lab Clin Med, 1956. **47**(4): p. 573-82.
105. GEORGIADES, J., et al., *Research on the oncolytic effect of APC viruses in cancer of the cervix uteri; preliminary report.* Biul Inst Med Morsk Gdansk, 1959. **10**: p. 49-57.
106. Engler, H., et al., *Acute hepatotoxicity of oncolytic adenoviruses in mouse models is associated with expression of wild-type E1a and induction of TNF-alpha.* Virology, 2004. **328**(1): p. 52-61.

107. Raper, S.E., et al., *Fatal systemic inflammatory response syndrome in a ornithine transcarbamylase deficient patient following adenoviral gene transfer.* Mol Genet Metab, 2003. **80**(1-2): p. 148-58.
108. Zhang, W.W., et al., *Generation and identification of recombinant adenovirus by liposome-mediated transfection and PCR analysis.* Biotechniques, 1993. **15**(5): p. 868-72.
109. Peng, Z., *Current status of gendicine in China: recombinant human Ad-p53 agent for treatment of cancers.* Hum Gene Ther, 2005. **16**(9): p. 1016-27.
110. Nemunaitis, J., *Head and neck cancer: response to p53-based therapeutics.* Head Neck, 2011. **33**(1): p. 131-4.
111. Senzer, N. and J. Nemunaitis, *A review of contusugene ladenovec (Advexin) p53 therapy.* Curr Opin Mol Ther, 2009. **11**(1): p. 54-61.
112. Tian, G., et al., *Multiple hepatic arterial injections of recombinant adenovirus p53 and 5-fluorouracil after transcatheter arterial chemoembolization for unresectable hepatocellular carcinoma: a pilot phase II trial.* Anticancer Drugs, 2009. **20**(5): p. 389-95.
113. Wold, W.S. and K. Toth, *Adenovirus vectors for gene therapy, vaccination and cancer gene therapy.* Curr Gene Ther, 2013. **13**(6): p. 421-33.
114. Saukkonen, K. and A. Hemminki, *Tissue-specific promoters for cancer gene therapy.* Expert Opin Biol Ther, 2004. **4**(5): p. 683-96.
115. Shirakawa, T., et al., *Long-term outcome of phase I/II clinical trial of Ad-OC-TK/VAL gene therapy for hormone-refractory metastatic prostate cancer.* Hum Gene Ther, 2007. **18**(12): p. 1225-32.
116. Small, E.J., et al., *A phase I trial of intravenous CG7870, a replication-selective, prostate-specific antigen-targeted oncolytic adenovirus, for the treatment of hormone-refractory, metastatic prostate cancer.* Mol Ther, 2006. **14**(1): p. 107-17.
117. Bischoff, J.R., et al., *An adenovirus mutant that replicates selectively in p53-deficient human tumor cells.* Science, 1996. **274**(5286): p. 373-6.
118. Heise, C., et al., *ONYX-015, an E1B gene-attenuated adenovirus, causes tumor-specific cytolysis and antitumoral efficacy that can be augmented by standard chemotherapeutic agents.* Nat Med, 1997. **3**(6): p. 639-45.
119. Barker, D.D. and A.J. Berk, *Adenovirus proteins from both E1B reading frames are required for transformation of rodent cells by viral infection and DNA transfection.* Virology, 1987. **156**(1): p. 107-21.
120. Lane, D.P., *Cancer. p53, guardian of the genome.* Nature, 1992. **358**(6381): p. 15-6.
121. Goodrum, F.D. and D.A. Ornelles, *p53 status does not determine outcome of E1B 55-kilodalton mutant adenovirus lytic infection.* J Virol, 1998. **72**(12): p. 9479-90.
122. O'Shea, C.C., et al., *Heat shock phenocopies E1B-55K late functions and selectively sensitizes refractory tumor cells to ONYX-015 oncolytic viral therapy.* Cancer Cell, 2005. **8**(1): p. 61-74.
123. O'Shea, C.C., et al., *Late viral RNA export, rather than p53 inactivation, determines ONYX-015 tumor selectivity.* Cancer Cell, 2004. **6**(6): p. 611-23.
124. Chiocca, E.A., et al., *A phase I open-label, dose-escalation, multi-institutional trial of injection with an E1B-Attenuated adenovirus, ONYX-015, into the*

peritumoral region of recurrent malignant gliomas, in the adjuvant setting. Mol Ther, 2004. **10**(5): p. 958-66.
125. Galanis, E., et al., *Phase I-II trial of ONYX-015 in combination with MAP chemotherapy in patients with advanced sarcomas.* Gene Ther, 2005. **12**(5): p. 437-45.
126. Kirn, D., *Oncolytic virotherapy for cancer with the adenovirus dl1520 (Onyx-015): results of phase I and II trials.* Expert Opin Biol Ther, 2001. **1**(3): p. 525-38.
127. Makower, D., et al., *Phase II clinical trial of intralesional administration of the oncolytic adenovirus ONYX-015 in patients with hepatobiliary tumors with correlative p53 studies.* Clin Cancer Res, 2003. **9**(2): p. 693-702.
128. Nemunaitis, J., et al., *Intravenous infusion of a replication-selective adenovirus (ONYX-015) in cancer patients: safety, feasibility and biological activity.* Gene Ther, 2001. **8**(10): p. 746-59.
129. Nemunaitis, J., et al., *A phase I trial of intravenous infusion of ONYX-015 and enbrel in solid tumor patients.* Cancer Gene Ther, 2007. **14**(11): p. 885-93.
130. Opyrchal, M., I. Aderca, and E. Galanis, *Phase I clinical trial of locoregional administration of the oncolytic adenovirus ONYX-015 in combination with mitomycin-C, doxorubicin, and cisplatin chemotherapy in patients with advanced sarcomas.* Methods Mol Biol, 2009. **542**: p. 705-17.
131. Reid, T.R., et al., *Effects of Onyx-015 among metastatic colorectal cancer patients that have failed prior treatment with 5-FU/leucovorin.* Cancer Gene Ther, 2005. **12**(8): p. 673-81.
132. Vasey, P.A., et al., *Phase I trial of intraperitoneal injection of the E1B-55-kd-gene-deleted adenovirus ONYX-015 (dl1520) given on days 1 through 5 every 3 weeks in patients with recurrent/refractory epithelial ovarian cancer.* J Clin Oncol, 2002. **20**(6): p. 1562-9.
133. Thomas, M.A., et al., *E4orf1 limits the oncolytic potential of the E1B-55K deletion mutant adenovirus.* J Virol, 2009. **83**(6): p. 2406-16.
134. Wang, Y., et al., *E3 gene manipulations affect oncolytic adenovirus activity in immunocompetent tumor models.* Nat Biotechnol, 2003. **21**(11): p. 1328-35.
135. Spurrell, E., et al., *STAT1 interaction with E3-14.7K in monocytes affects the efficacy of oncolytic adenovirus.* J Virol, 2014. **88**(4): p. 2291-300.
136. Garber, K., *China approves world's first oncolytic virus therapy for cancer treatment.* J Natl Cancer Inst, 2006. **98**(5): p. 298-300.
137. Heise, C., et al., *An adenovirus E1A mutant that demonstrates potent and selective systemic anti-tumoral efficacy.* Nat Med, 2000. **6**(10): p. 1134-9.
138. Han, J., et al., *The E1B 19K protein blocks apoptosis by interacting with and inhibiting the p53-inducible and death-promoting Bax protein.* Genes Dev, 1996. **10**(4): p. 461-77.
139. Perez, D. and E. White, *E1B 19K inhibits Fas-mediated apoptosis through FADD-dependent sequestration of FLICE.* J Cell Biol, 1998. **141**(5): p. 1255-66.
140. Liu, T.C., et al., *An E1B-19 kDa gene deletion mutant adenovirus demonstrates tumor necrosis factor-enhanced cancer selectivity and enhanced oncolytic potency.* Mol Ther, 2004. **9**(6): p. 786-803.

141. Leitner, S., et al., *Oncolytic adenoviral mutants with E1B19K gene deletions enhance gemcitabine-induced apoptosis in pancreatic carcinoma cells and anti-tumor efficacy in vivo.* Clin Cancer Res, 2009. **15**(5): p. 1730-40.
142. Bennett, E.M., et al., *Cutting edge: adenovirus E19 has two mechanisms for affecting class I MHC expression.* J Immunol, 1999. **162**(9): p. 5049-52.
143. McSharry, B.P., et al., *Adenovirus E3/19K promotes evasion of NK cell recognition by intracellular sequestration of the NKG2D ligands major histocompatibility complex class I chain-related proteins A and B.* J Virol, 2008. **82**(9): p. 4585-94.
144. Hawkins, L.K., et al., *Gene delivery from the E3 region of replicating human adenovirus: evaluation of the 6.7 K/gp19 K region.* Gene Ther, 2001. **8**(15): p. 1123-31.
145. Dunn, G.P., L.J. Old, and R.D. Schreiber, *The immunobiology of cancer immunosurveillance and immunoediting.* Immunity, 2004. **21**(2): p. 137-48.
146. Dunn, G.P., L.J. Old, and R.D. Schreiber, *The three Es of cancer immunoediting.* Annu Rev Immunol, 2004. **22**: p. 329-60.
147. Garrido, F., et al., *Implications for immunosurveillance of altered HLA class I phenotypes in human tumours.* Immunol Today, 1997. **18**(2): p. 89-95.
148. Garrido, F. and I. Algarra, *MHC antigens and tumor escape from immune surveillance.* Adv Cancer Res, 2001. **83**: p. 117-58.
149. Hicklin, D.J., F.M. Marincola, and S. Ferrone, *HLA class I antigen downregulation in human cancers: T-cell immunotherapy revives an old story.* Mol Med Today, 1999. **5**(4): p. 178-86.
150. Johnsen, A.K., et al., *Deficiency of transporter for antigen presentation (TAP) in tumor cells allows evasion of immune surveillance and increases tumorigenesis.* J Immunol, 1999. **163**(8): p. 4224-31.
151. Staveley-O'Carroll, K., et al., *Induction of antigen-specific T cell anergy: An early event in the course of tumor progression.* Proc Natl Acad Sci U S A, 1998. **95**(3): p. 1178-83.
152. Jacobs, J.F., et al., *Regulatory T cells in melanoma: the final hurdle towards effective immunotherapy?* Lancet Oncol, 2012. **13**(1): p. e32-42.
153. Yokokawa, J., et al., *Enhanced functionality of CD4+CD25(high)FoxP3+ regulatory T cells in the peripheral blood of patients with prostate cancer.* Clin Cancer Res, 2008. **14**(4): p. 1032-40.
154. Lee, I., et al., *Recruitment of Foxp3+ T regulatory cells mediating allograft tolerance depends on the CCR4 chemokine receptor.* J Exp Med, 2005. **201**(7): p. 1037-44.
155. Curiel, T.J., et al., *Specific recruitment of regulatory T cells in ovarian carcinoma fosters immune privilege and predicts reduced survival.* Nat Med, 2004. **10**(9): p. 942-9.
156. Zou, W., *Regulatory T cells, tumour immunity and immunotherapy.* Nat Rev Immunol, 2006. **6**(4): p. 295-307.
157. Mantovani, A. and A. Sica, *Macrophages, innate immunity and cancer: balance, tolerance, and diversity.* Curr Opin Immunol, 2010. **22**(2): p. 231-7.
158. Murdoch, C., et al., *The role of myeloid cells in the promotion of tumour angiogenesis.* Nat Rev Cancer, 2008. **8**(8): p. 618-31.

159. Munn, D.H., et al., *Potential regulatory function of human dendritic cells expressing indoleamine 2,3-dioxygenase.* Science, 2002. **297**(5588): p. 1867-70.
160. Are, C., et al., *The role of transforming growth factor-beta in suppression of hepatic metastasis from colon cancer.* HPB (Oxford), 2010. **12**(7): p. 498-506.
161. de la Cruz-Merino, L., et al., *Role of transforming growth factor beta in cancer microenvironment.* Clin Transl Oncol, 2009. **11**(11): p. 715-20.
162. Maeda, H. and A. Shiraishi, *TGF-beta contributes to the shift toward Th2-type responses through direct and IL-10-mediated pathways in tumor-bearing mice.* J Immunol, 1996. **156**(1): p. 73-8.
163. Gabrilovich, D., *Mechanisms and functional significance of tumour-induced dendritic-cell defects.* Nat Rev Immunol, 2004. **4**(12): p. 941-52.
164. Gabrilovich, D.I., et al., *Production of vascular endothelial growth factor by human tumors inhibits the functional maturation of dendritic cells.* Nat Med, 1996. **2**(10): p. 1096-103.
165. Parry, R.V., et al., *CTLA-4 and PD-1 receptors inhibit T-cell activation by distinct mechanisms.* Mol Cell Biol, 2005. **25**(21): p. 9543-53.
166. Linsley, P.S., et al., *Human B7-1 (CD80) and B7-2 (CD86) bind with similar avidities but distinct kinetics to CD28 and CTLA-4 receptors.* Immunity, 1994. **1**(9): p. 793-801.
167. Wing, K., et al., *CTLA-4 control over Foxp3+ regulatory T cell function.* Science, 2008. **322**(5899): p. 271-5.
168. Peggs, K.S., et al., *Blockade of CTLA-4 on both effector and regulatory T cell compartments contributes to the antitumor activity of anti-CTLA-4 antibodies.* J Exp Med, 2009. **206**(8): p. 1717-25.
169. Ishida, Y., et al., *Induced expression of PD-1, a novel member of the immunoglobulin gene superfamily, upon programmed cell death.* EMBO J, 1992. **11**(11): p. 3887-95.
170. Freeman, G.J., et al., *Engagement of the PD-1 immunoinhibitory receptor by a novel B7 family member leads to negative regulation of lymphocyte activation.* J Exp Med, 2000. **192**(7): p. 1027-34.
171. Keir, M.E., et al., *Tissue expression of PD-L1 mediates peripheral T cell tolerance.* J Exp Med, 2006. **203**(4): p. 883-95.
172. Blank, C., et al., *PD-L1/B7H-1 inhibits the effector phase of tumor rejection by T cell receptor (TCR) transgenic CD8+ T cells.* Cancer Res, 2004. **64**(3): p. 1140-5.
173. Dong, H., et al., *Tumor-associated B7-H1 promotes T-cell apoptosis: a potential mechanism of immune evasion.* Nat Med, 2002. **8**(8): p. 793-800.
174. Taube, J.M., et al., *Colocalization of inflammatory response with B7-h1 expression in human melanocytic lesions supports an adaptive resistance mechanism of immune escape.* Sci Transl Med, 2012. **4**(127): p. 127ra37.
175. Bogen, B., *Peripheral T cell tolerance as a tumor escape mechanism: deletion of CD4+ T cells specific for a monoclonal immunoglobulin idiotype secreted by a plasmacytoma.* Eur J Immunol, 1996. **26**(11): p. 2671-9.
176. Lauritzsen, G.F., et al., *Clonal deletion of thymocytes as a tumor escape mechanism.* Int J Cancer, 1998. **78**(2): p. 216-22.

177. Vanderbilt University. School of, M. and F.M. Burnet, *The clonal selection theory of acquired immunity*. 1959, Cambridge: CUP.
178. BILLINGHAM, R.E., L. BRENT, and P.B. MEDAWAR, *Acquired tolerance of skin homografts.* Ann N Y Acad Sci, 1955. **59**(3): p. 409-16.
179. BILLINGHAM, R.E., L. BRENT, and P.B. MEDAWAR, *The antigenic stimulus in transplantation immunity.* Nature, 1956. **178**(4532): p. 514-9.
180. Bretscher, P. and M. Cohn, *A theory of self-nonself discrimination.* Science, 1970. **169**(3950): p. 1042-9.
181. Lafferty, K.J. and A.J. Cunningham, *A new analysis of allogeneic interactions.* Aust J Exp Biol Med Sci, 1975. **53**(1): p. 27-42.
182. Janeway, C.A., et al., *Cross-linking and conformational change in T-cell receptors: role in activation and in repertoire selection.* Cold Spring Harb Symp Quant Biol, 1989. **54 Pt 2**: p. 657-66.
183. Matzinger, P., *The danger model: a renewed sense of self.* Science, 2002. **296**(5566): p. 301-5.
184. Jounai, N., et al., *Recognition of damage-associated molecular patterns related to nucleic acids during inflammation and vaccination.* Front Cell Infect Microbiol, 2012. **2**: p. 168.
185. Guo, Z.S., Z. Liu, and D.L. Bartlett, *Oncolytic Immunotherapy: Dying the Right Way is a Key to Eliciting Potent Antitumor Immunity.* Front Oncol, 2014. **4**: p. 74.
186. Workenhe, S.T. and K.L. Mossman, *Oncolytic virotherapy and immunogenic cancer cell death: sharpening the sword for improved cancer treatment strategies.* Mol Ther, 2014. **22**(2): p. 251-6.
187. Tang, D., et al., *PAMPs and DAMPs: signal 0s that spur autophagy and immunity.* Immunol Rev, 2012. **249**(1): p. 158-75.
188. Zhu, J., X. Huang, and Y. Yang, *Innate immune response to adenoviral vectors is mediated by both Toll-like receptor-dependent and -independent pathways.* J Virol, 2007. **81**(7): p. 3170-80.
189. Nociari, M., et al., *Sensing infection by adenovirus: Toll-like receptor-independent viral DNA recognition signals activation of the interferon regulatory factor 3 master regulator.* J Virol, 2007. **81**(8): p. 4145-57.
190. Iacobelli-Martinez, M. and G.R. Nemerow, *Preferential activation of Toll-like receptor nine by CD46-utilizing adenoviruses.* J Virol, 2007. **81**(3): p. 1305-12.
191. Endo, Y., et al., *Virus-mediated oncolysis induces danger signal and stimulates cytotoxic T-lymphocyte activity via proteasome activator upregulation.* Oncogene, 2008. **27**(17): p. 2375-81.
192. Myskiw, C., et al., *RNA species generated in vaccinia virus infected cells activate cell type-specific MDA5 or RIG-I dependent interferon gene transcription and PKR dependent apoptosis.* Virology, 2011. **413**(2): p. 183-93.
193. Obeid, M., et al., *Calreticulin exposure dictates the immunogenicity of cancer cell death.* Nat Med, 2007. **13**(1): p. 54-61.
194. Obeid, M., et al., *Leveraging the immune system during chemotherapy: moving calreticulin to the cell surface converts apoptotic death from "silent" to immunogenic.* Cancer Res, 2007. **67**(17): p. 7941-4.

195. Inoue, H. and K. Tani, *Multimodal immunogenic cancer cell death as a consequence of anticancer cytotoxic treatments.* Cell Death Differ, 2014. **21**(1): p. 39-49.
196. Kroemer, G., et al., *Classification of cell death: recommendations of the Nomenclature Committee on Cell Death 2009.* Cell Death Differ, 2009. **16**(1): p. 3-11.
197. Boozari, B., et al., *Antitumoural immunity by virus-mediated immunogenic apoptosis inhibits metastatic growth of hepatocellular carcinoma.* Gut, 2010. **59**(10): p. 1416-26.
198. Kaufman, H.L., et al., *Local and distant immunity induced by intralesional vaccination with an oncolytic herpes virus encoding GM-CSF in patients with stage IIIc and IV melanoma.* Ann Surg Oncol, 2010. **17**(3): p. 718-30.
199. Dreux, M. and F.V. Chisari, *Viruses and the autophagy machinery.* Cell Cycle, 2010. **9**(7): p. 1295-1307.
200. Levine, B. and V. Deretic, *Unveiling the roles of autophagy in innate and adaptive immunity.* Nat Rev Immunol, 2007. **7**(10): p. 767-77.
201. Baird, S.K., et al., *Oncolytic adenoviral mutants induce a novel mode of programmed cell death in ovarian cancer.* Oncogene, 2008. **27**(22): p. 3081-90.
202. Ito, H., et al., *Autophagic cell death of malignant glioma cells induced by a conditionally replicating adenovirus.* J Natl Cancer Inst, 2006. **98**(9): p. 625-36.
203. Colunga, A.G., J.M. Laing, and L. Aurelian, *The HSV-2 mutant DeltaPK induces melanoma oncolysis through nonredundant death programs and associated with autophagy and pyroptosis proteins.* Gene Ther, 2010. **17**(3): p. 315-27.
204. Meng, C., et al., *Newcastle disease virus triggers autophagy in U251 glioma cells to enhance virus replication.* Arch Virol, 2012. **157**(6): p. 1011-8.
205. Dengjel, J., et al., *Autophagy promotes MHC class II presentation of peptides from intracellular source proteins.* Proc Natl Acad Sci U S A, 2005. **102**(22): p. 7922-7.
206. Li, Y., et al., *Efficient cross-presentation depends on autophagy in tumor cells.* Cancer Res, 2008. **68**(17): p. 6889-95.
207. Uhl, M., et al., *Autophagy within the antigen donor cell facilitates efficient antigen cross-priming of virus-specific CD8+ T cells.* Cell Death Differ, 2009. **16**(7): p. 991-1005.
208. Wei, J., et al., *Influenza A infection enhances cross-priming of CD8+ T cells to cell-associated antigens in a TLR7- and type I IFN-dependent fashion.* J Immunol, 2010. **185**(10): p. 6013-22.
209. Gauvrit, A., et al., *Measles virus induces oncolysis of mesothelioma cells and allows dendritic cells to cross-prime tumor-specific CD8 response.* Cancer Res, 2008. **68**(12): p. 4882-92.
210. Plotkin, S.A., *Vaccines: past, present and future.* Nat Med, 2005. **11**(4 Suppl): p. S5-11.
211. Ault, K.A. and F.I.S. Group, *Effect of prophylactic human papillomavirus L1 virus-like-particle vaccine on risk of cervical intraepithelial neoplasia grade 2, grade 3, and adenocarcinoma in situ: a combined analysis of four randomised clinical trials.* Lancet, 2007. **369**(9576): p. 1861-8.

212. Paavonen, J., et al., *Efficacy of a prophylactic adjuvanted bivalent L1 virus-like-particle vaccine against infection with human papillomavirus types 16 and 18 in young women: an interim analysis of a phase III double-blind, randomised controlled trial.* Lancet, 2007. **369**(9580): p. 2161-70.
213. Chang, M.H., et al., *Universal hepatitis B vaccination in Taiwan and the incidence of hepatocellular carcinoma in children. Taiwan Childhood Hepatoma Study Group.* N Engl J Med, 1997. **336**(26): p. 1855-9.
214. Chang, M.H., et al., *Prevention of hepatocellular carcinoma by universal vaccination against hepatitis B virus: the effect and problems.* Clin Cancer Res, 2005. **11**(21): p. 7953-7.
215. Pejawar-Gaddy, S. and O.J. Finn, *Cancer vaccines: accomplishments and challenges.* Crit Rev Oncol Hematol, 2008. **67**(2): p. 93-102.
216. Kawakami, Y., et al., *Cloning of the gene coding for a shared human melanoma antigen recognized by autologous T cells infiltrating into tumor.* Proc Natl Acad Sci U S A, 1994. **91**(9): p. 3515-9.
217. Kawakami, Y., et al., *Identification of a human melanoma antigen recognized by tumor-infiltrating lymphocytes associated with in vivo tumor rejection.* Proc Natl Acad Sci U S A, 1994. **91**(14): p. 6458-62.
218. van der Bruggen, P., et al., *A gene encoding an antigen recognized by cytolytic T lymphocytes on a human melanoma.* Science, 1991. **254**(5038): p. 1643-7.
219. Southall, P.J., et al., *Immunohistological distribution of 5T4 antigen in normal and malignant tissues.* Br J Cancer, 1990. **61**(1): p. 89-95.
220. Starzynska, T., et al., *Prognostic significance of 5T4 oncofetal antigen expression in colorectal carcinoma.* Br J Cancer, 1994. **69**(5): p. 899-902.
221. Van den Eynde, B., et al., *The gene coding for a major tumor rejection antigen of tumor P815 is identical to the normal gene of syngeneic DBA/2 mice.* J Exp Med, 1991. **173**(6): p. 1373-84.
222. Wolfel, T., et al., *A p16INK4a-insensitive CDK4 mutant targeted by cytolytic T lymphocytes in a human melanoma.* Science, 1995. **269**(5228): p. 1281-4.
223. Coulie, P.G., et al., *A mutated intron sequence codes for an antigenic peptide recognized by cytolytic T lymphocytes on a human melanoma.* Proc Natl Acad Sci U S A, 1995. **92**(17): p. 7976-80.
224. Weng, T.Y., et al., *DNA vaccine elicits an efficient antitumor response by targeting the mutant Kras in a transgenic mouse lung cancer model.* Gene Ther, 2014. **21**(10): p. 888-96.
225. Finn, O.J., et al., *MUC-1 epithelial tumor mucin-based immunity and cancer vaccines.* Immunol Rev, 1995. **145**: p. 61-89.
226. Argani, P., et al., *Mesothelin is overexpressed in the vast majority of ductal adenocarcinomas of the pancreas: identification of a new pancreatic cancer marker by serial analysis of gene expression (SAGE).* Clin Cancer Res, 2001. **7**(12): p. 3862-8.
227. Li, M., et al., *Mesothelin is a malignant factor and therapeutic vaccine target for pancreatic cancer.* Mol Cancer Ther, 2008. **7**(2): p. 286-96.
228. Cohen, E.P., et al., *Enhancing cellular cancer vaccines.* Immunotherapy, 2009. **1**(3): p. 495-504.
229. Rosenberg, S.A., et al., *Immunologic and therapeutic evaluation of a synthetic peptide vaccine for the treatment of patients with metastatic melanoma.* Nat Med, 1998. **4**(3): p. 321-7.

230. Slingluff, C.L., *The present and future of peptide vaccines for cancer: single or multiple, long or short, alone or in combination?* Cancer J, 2011. **17**(5): p. 343-50.
231. Slingluff, C.L., et al., *Immunologic and clinical outcomes of a randomized phase II trial of two multipeptide vaccines for melanoma in the adjuvant setting.* Clin Cancer Res, 2007. **13**(21): p. 6386-95.
232. Chianese-Bullock, K.A., et al., *A multipeptide vaccine is safe and elicits T-cell responses in participants with advanced stage ovarian cancer.* J Immunother, 2008. **31**(4): p. 420-30.
233. Yu, M. and O.J. Finn, *DNA vaccines for cancer too.* Cancer Immunol Immunother, 2006. **55**(2): p. 119-30.
234. De Marco, F., et al., *DNA vaccines against HPV-16 E7-expressing tumour cells.* Anticancer Res, 2003. **23**(2B): p. 1449-54.
235. Klencke, B., et al., *Encapsulated plasmid DNA treatment for human papillomavirus 16-associated anal dysplasia: a Phase I study of ZYC101.* Clin Cancer Res, 2002. **8**(5): p. 1028-37.
236. Rosenberg, S.A., *Progress in human tumour immunology and immunotherapy.* Nature, 2001. **411**(6835): p. 380-4.
237. Timmerman, J.M., et al., *Idiotype-pulsed dendritic cell vaccination for B-cell lymphoma: clinical and immune responses in 35 patients.* Blood, 2002. **99**(5): p. 1517-26.
238. Titzer, S., et al., *Vaccination of multiple myeloma patients with idiotype-pulsed dendritic cells: immunological and clinical aspects.* Br J Haematol, 2000. **108**(4): p. 805-16.
239. Palucka, K. and J. Banchereau, *Cancer immunotherapy via dendritic cells.* Nat Rev Cancer, 2012. **12**(4): p. 265-77.
240. Palucka, A.K., et al., *Dendritic cells loaded with killed allogeneic melanoma cells can induce objective clinical responses and MART-1 specific CD8+ T-cell immunity.* J Immunother, 2006. **29**(5): p. 545-57.
241. Soares, M.M., V. Mehta, and O.J. Finn, *Three different vaccines based on the 140-amino acid MUC1 peptide with seven tandemly repeated tumor-specific epitopes elicit distinct immune effector mechanisms in wild-type versus MUC1-transgenic mice with different potential for tumor rejection.* J Immunol, 2001. **166**(11): p. 6555-63.
242. Lokhov, P.G. and E.E. Balashova, *Cellular cancer vaccines: an update on the development of vaccines generated from cell surface antigens.* J Cancer, 2010. **1**: p. 230-41.
243. Le, D.T., et al., *Safety and Survival With GVAX Pancreas Prime and Listeria Monocytogenes-Expressing Mesothelin (CRS-207) Boost Vaccines for Metastatic Pancreatic Cancer.* J Clin Oncol, 2015.
244. Yang, S., T.L. Darrow, and H.F. Seigler, *Generation of primary tumor-specific cytotoxic T lymphocytes from autologous and human lymphocyte antigen class I-matched allogeneic peripheral blood lymphocytes by B7 gene-modified melanoma cells.* Cancer Res, 1997. **57**(8): p. 1561-8.
245. Yang, S., et al., *Tumor cells cotransduced with B7.1 and gamma-IFN induce effective rejection of established parental tumor.* Gene Ther, 1999. **6**(2): p. 253-62.

246. Coley, W.B., *FURTHER OBSERVATIONS ON THE CONSERVATIVE TREATMENT OF SARCOMA OF THE LONG BONES.* Ann Surg, 1919. **70**(6): p. 633-60.
247. Tsung, K. and J.A. Norton, *Lessons from Coley's Toxin.* Surg Oncol, 2006. **15**(1): p. 25-8.
248. Morton, D.L., et al., *Prolongation of survival in metastatic melanoma after active specific immunotherapy with a new polyvalent melanoma vaccine.* Ann Surg, 1992. **216**(4): p. 463-82.
249. Morton, D.L., et al., *Prolonged survival of patients receiving active immunotherapy with Canvaxin therapeutic polyvalent vaccine after complete resection of melanoma metastatic to regional lymph nodes.* Ann Surg, 2002. **236**(4): p. 438-48; discussion 448-9.
250. Hoover, H.C., Jr., et al., *Adjuvant active specific immunotherapy for human colorectal cancer: 6.5-year median follow-up of a phase III prospectively randomized trial.* J Clin Oncol, 1993. **11**(3): p. 390-9.
251. Jocham, D., et al., *Adjuvant autologous renal tumour cell vaccine and risk of tumour progression in patients with renal-cell carcinoma after radical nephrectomy: phase III, randomised controlled trial.* Lancet, 2004. **363**(9409): p. 594-9.
252. Vermorken, J.B., et al., *Active specific immunotherapy for stage II and stage III human colon cancer: a randomised trial.* Lancet, 1999. **353**(9150): p. 345-50.
253. Harris, J.E., et al., *Adjuvant active specific immunotherapy for stage II and III colon cancer with an autologous tumor cell vaccine: Eastern Cooperative Oncology Group Study E5283.* J Clin Oncol, 2000. **18**(1): p. 148-57.
254. Krieg, A.M., *The CpG motif: implications for clinical immunology.* BioDrugs, 1998. **10**(5): p. 341-6.
255. Weiner, G.J., et al., *Immunostimulatory oligodeoxynucleotides containing the CpG motif are effective as immune adjuvants in tumor antigen immunization.* Proc Natl Acad Sci U S A, 1997. **94**(20): p. 10833-7.
256. Van Den Eertwegh, A.J.L., R. J. ; Scheper, R. J.; Giaccone, G.; Meijer, C. J.; Bontkes, H. J.; Gruijl, T.D; Hooijberg, E., *Autologous tumor cell vaccination with PF-3512676 (CPG 7909) and GM-CSF followed by subcutaneous PF-3512676 and IFN-alpha for patients with metastatic renal cell carcinoma.* J Clin Oncol, 2006. **24**(18s): p. 2530.
257. Sondak, V.K. and J.A. Sosman, *Results of clinical trials with an allogenic melanoma tumor cell lysate vaccine: Melacine.* Semin Cancer Biol, 2003. **13**(6): p. 409-15.
258. Sosman, J.A. and V.K. Sondak, *Melacine: an allogeneic melanoma tumor cell lysate vaccine.* Expert Rev Vaccines, 2003. **2**(3): p. 353-68.
259. Heicappell, R., et al., *Prevention of metastatic spread by postoperative immunotherapy with virally modified autologous tumor cells. I. Parameters for optimal therapeutic effects.* Int J Cancer, 1986. **37**(4): p. 569-77.
260. Schirrmacher, V., *Clinical trials of antitumor vaccination with an autologous tumor cell vaccine modified by virus infection: improvement of patient survival based on improved antitumor immune memory.* Cancer Immunol Immunother, 2005. **54**(6): p. 587-98.
261. Voit, C., et al., *Intradermal injection of Newcastle disease virus-modified autologous melanoma cell lysate and interleukin-2 for adjuvant treatment of*

melanoma patients with resectable stage III disease. J Dtsch Dermatol Ges, 2003. **1**(2): p. 120-5.
262. Schulze, T., et al., *Efficiency of adjuvant active specific immunization with Newcastle disease virus modified tumor cells in colorectal cancer patients following resection of liver metastases: results of a prospective randomized trial.* Cancer Immunol Immunother, 2009. **58**(1): p. 61-9.
263. Liang, W., et al., *Application of autologous tumor cell vaccine and NDV vaccine in treatment of tumors of digestive tract.* World J Gastroenterol, 2003. **9**(3): p. 495-8.
264. Torre, L.A., et al., *Global cancer statistics, 2012.* CA Cancer J Clin, 2015. **65**(2): p. 87-108.
265. Chaturvedi, A.K., et al., *Worldwide trends in incidence rates for oral cavity and oropharyngeal cancers.* J Clin Oncol, 2013. **31**(36): p. 4550-9.
266. CRUK *Oral cancer statistics*. 2015.
267. CRUK *Laryngeal cancer statistics*. 2015.
268. Marur, S. and A.A. Forastiere, *Head and neck cancer: changing epidemiology, diagnosis, and treatment.* Mayo Clin Proc, 2008. **83**(4): p. 489-501.
269. Thorne, P., D. Etherington, and M.A. Birchall, *Head and neck cancer in the South West of England: influence of socio-economic status on incidence and second primary tumours.* Eur J Surg Oncol, 1997. **23**(6): p. 503-8.
270. Haddad, R.I. and D.M. Shin, *Recent advances in head and neck cancer.* N Engl J Med, 2008. **359**(11): p. 1143-54.
271. Pignon, J.P., et al., *Chemotherapy added to locoregional treatment for head and neck squamous-cell carcinoma: three meta-analyses of updated individual data. MACH-NC Collaborative Group. Meta-Analysis of Chemotherapy on Head and Neck Cancer.* Lancet, 2000. **355**(9208): p. 949-55.
272. Quinn, M., et al., *Cancer Trends in England and Wales 1950- 1999. Studies on Medical and Population Subjects no.66.* 2001, The Stationary Office: London.
273. Rathod, S., et al., *A systematic review of quality of life in head and neck cancer treated with surgery with or without adjuvant treatment.* Oral Oncol, 2015.
274. Jensen, S.B., et al., *A systematic review of salivary gland hypofunction and xerostomia induced by cancer therapies: management strategies and economic impact.* Support Care Cancer, 2010. **18**(8): p. 1061-79.
275. Rathod, S., et al., *Quality-of-life (QOL) outcomes in patients with head and neck squamous cell carcinoma (HNSCC) treated with intensity-modulated radiation therapy (IMRT) compared to three-dimensional conformal radiotherapy (3D-CRT): evidence from a prospective randomized study.* Oral Oncol, 2013. **49**(6): p. 634-42.
276. Fung, C. and J.R. Grandis, *Emerging drugs to treat squamous cell carcinomas of the head and neck.* Expert Opin Emerg Drugs, 2010. **15**(3): p. 355-73.
277. Kuss, I., et al., *Decreased absolute counts of T lymphocyte subsets and their relation to disease in squamous cell carcinoma of the head and neck.* Clin Cancer Res, 2004. **10**(11): p. 3755-62.
278. Hoffmann, T.K., et al., *Spontaneous apoptosis of circulating T lymphocytes in patients with head and neck cancer and its clinical importance.* Clin Cancer Res, 2002. **8**(8): p. 2553-62.

279. Baruah, P., et al., *Decreased levels of alternative co-stimulatory receptors OX40 and 4-1BB characterise T cells from head and neck cancer patients.* Immunobiology, 2012. **217**(7): p. 669-75.
280. Dasgupta, S., et al., *Inhibition of NK cell activity through TGF-beta 1 by down-regulation of NKG2D in a murine model of head and neck cancer.* J Immunol, 2005. **175**(8): p. 5541-50.
281. Bauernhofer, T., et al., *Preferential apoptosis of CD56dim natural killer cell subset in patients with cancer.* Eur J Immunol, 2003. **33**(1): p. 119-24.
282. Dong, G., et al., *Hepatocyte growth factor/scatter factor-induced activation of MEK and PI3K signal pathways contributes to expression of proangiogenic cytokines interleukin-8 and vascular endothelial growth factor in head and neck squamous cell carcinoma.* Cancer Res, 2001. **61**(15): p. 5911-8.
283. Chen, Z., et al., *Expression of proinflammatory and proangiogenic cytokines in patients with head and neck cancer.* Clin Cancer Res, 1999. **5**(6): p. 1369-79.
284. Riedel, F., et al., *Serum levels of interleukin-6 in patients with primary head and neck squamous cell carcinoma.* Anticancer Res, 2005. **25**(4): p. 2761-5.
285. Gokhale, A.S., et al., *Serum concentrations of interleukin-8, vascular endothelial growth factor, and epidermal growth factor receptor in patients with squamous cell cancer of the head and neck.* Oral Oncol, 2005. **41**(1): p. 70-6.
286. López-Albaitero, A., et al., *Role of antigen-processing machinery in the in vitro resistance of squamous cell carcinoma of the head and neck cells to recognition by CTL.* J Immunol, 2006. **176**(6): p. 3402-9.
287. Ferris, R.L., T.L. Whiteside, and S. Ferrone, *Immune escape associated with functional defects in antigen-processing machinery in head and neck cancer.* Clin Cancer Res, 2006. **12**(13): p. 3890-5.
288. Engels, E.A., et al., *Spectrum of cancer risk among US solid organ transplant recipients.* JAMA, 2011. **306**(17): p. 1891-901.
289. Deeb, R., et al., *Head and neck cancer in transplant recipients.* Laryngoscope, 2012. **122**(7): p. 1566-9.
290. Ward, M.J., et al., *Tumour-infiltrating lymphocytes predict for outcome in HPV-positive oropharyngeal cancer.* Br J Cancer, 2014. **110**(2): p. 489-500.
291. Nordfors, C., et al., *CD8+ and CD4+ tumour infiltrating lymphocytes in relation to human papillomavirus status and clinical outcome in tonsillar and base of tongue squamous cell carcinoma.* Eur J Cancer, 2013. **49**(11): p. 2522-30.
292. Cho, Y.A., et al., *Relationship between the expressions of PD-L1 and tumor-infiltrating lymphocytes in oral squamous cell carcinoma.* Oral Oncol, 2011. **47**(12): p. 1148-53.
293. Pretscher, D., et al., *Distribution of immune cells in head and neck cancer: CD8+ T-cells and CD20+ B-cells in metastatic lymph nodes are associated with favourable outcome in patients with oro- and hypopharyngeal carcinoma.* BMC Cancer, 2009. **9**: p. 292.
294. Strome, S.E., et al., *B7-H1 blockade augments adoptive T-cell immunotherapy for squamous cell carcinoma.* Cancer Res, 2003. **63**(19): p. 6501-5.
295. Hatam, L.J., et al., *Immune suppression in premalignant respiratory papillomas: enriched functional CD4+Foxp3+ regulatory T cells and PD-1/PD-L1/L2 expression.* Clin Cancer Res, 2012. **18**(7): p. 1925-35.

296. Malaspina, T.S., et al., *Enhanced programmed death 1 (PD-1) and PD-1 ligand (PD-L1) expression in patients with actinic cheilitis and oral squamous cell carcinoma.* Cancer Immunol Immunother, 2011. **60**(7): p. 965-74.
297. Lyford-Pike, S., et al., *Evidence for a role of the PD-1:PD-L1 pathway in immune resistance of HPV-associated head and neck squamous cell carcinoma.* Cancer Res, 2013. **73**(6): p. 1733-41.
298. Malm, I.J., et al., *Expression profile and in vitro blockade of programmed death-1 in human papillomavirus-negative head and neck squamous cell carcinoma.* Head Neck, 2015. **37**(8): p. 1088-95.
299. Ukpo, O.C., W.L. Thorstad, and J.S. Lewis, *B7-H1 expression model for immune evasion in human papillomavirus-related oropharyngeal squamous cell carcinoma.* Head Neck Pathol, 2013. **7**(2): p. 113-21.
300. Götte, K., et al., *Tumor-associated antigens as possible targets for immune therapy in head and neck cancer: comparative mRNA expression analysis of RAGE and GAGE genes.* Acta Otolaryngol, 2002. **122**(5): p. 546-52.
301. Young, M.R., et al., *Oral premalignant lesions induce immune reactivity to both premalignant oral lesions and head and neck squamous cell carcinoma.* Cancer Immunol Immunother, 2007. **56**(7): p. 1077-86.
302. Rabassa, M.E., et al., *MUC1 expression and anti-MUC1 serum immune response in head and neck squamous cell carcinoma (HNSCC): a multivariate analysis.* BMC Cancer, 2006. **6**: p. 253.
303. Chow, V., et al., *Prognostic significance of serum p53 protein and p53 antibody in patients with surgical treatment for head and neck squamous cell carcinoma.* Head Neck, 2001. **23**(4): p. 286-91.
304. Beckhove, P., et al., *Rapid T cell-based identification of human tumor tissue antigens by automated two-dimensional protein fractionation.* J Clin Invest, 2010. **120**(6): p. 2230-42.
305. Dadian, G., et al., *Immune changes in peripheral blood resulting from locally directed interleukin-2 therapy in squamous cell carcinoma of the head and neck.* Eur J Cancer B Oral Oncol, 1993. **29B**(1): p. 29-34.
306. Whiteside, T.L., et al., *Evidence for local and systemic activation of immune cells by peritumoral injections of interleukin 2 in patients with advanced squamous cell carcinoma of the head and neck.* Cancer Res, 1993. **53**(23): p. 5654-62.
307. De Stefani, A., et al., *Improved survival with perilymphatic interleukin 2 in patients with resectable squamous cell carcinoma of the oral cavity and oropharynx.* Cancer, 2002. **95**(1): p. 90-7.
308. Verastegui, E., et al., *A natural cytokine mixture (IRX-2) and interference with immune suppression induce immune mobilization and regression of head and neck cancer.* Int J Immunopharmacol, 1997. **19**(11-12): p. 619-27.
309. Berinstein, N.L., et al., *Increased lymphocyte infiltration in patients with head and neck cancer treated with the IRX-2 immunotherapy regimen.* Cancer Immunol Immunother, 2012. **61**(6): p. 771-82.
310. Wolf, G.T., et al., *Novel neoadjuvant immunotherapy regimen safety and survival in head and neck squamous cell cancer.* Head Neck, 2011. **33**(12): p. 1666-74.

311. Rubin Grandis, J., et al., *Levels of TGF-alpha and EGFR protein in head and neck squamous cell carcinoma and patient survival.* J Natl Cancer Inst, 1998. **90**(11): p. 824-32.
312. Ang, K.K., et al., *Impact of epidermal growth factor receptor expression on survival and pattern of relapse in patients with advanced head and neck carcinoma.* Cancer Res, 2002. **62**(24): p. 7350-6.
313. Li, S., et al., *Structural basis for inhibition of the epidermal growth factor receptor by cetuximab.* Cancer Cell, 2005. **7**(4): p. 301-11.
314. Srivastava, R.M., et al., *Cetuximab-activated natural killer and dendritic cells collaborate to trigger tumor antigen-specific T-cell immunity in head and neck cancer patients.* Clin Cancer Res, 2013. **19**(7): p. 1858-72.
315. Vermorken, J.B., et al., *Platinum-based chemotherapy plus cetuximab in head and neck cancer.* N Engl J Med, 2008. **359**(11): p. 1116-27.
316. Bonner, J.A., et al., *Radiotherapy plus cetuximab for locoregionally advanced head and neck cancer: 5-year survival data from a phase 3 randomised trial, and relation between cetuximab-induced rash and survival.* Lancet Oncol, 2010. **11**(1): p. 21-8.
317. van Schalkwyk, M.C., et al., *Design of a phase I clinical trial to evaluate intratumoral delivery of ErbB-targeted chimeric antigen receptor T-cells in locally advanced or recurrent head and neck cancer.* Hum Gene Ther Clin Dev, 2013. **24**(3): p. 134-42.
318. Teknos, T.N., et al., *Elevated serum vascular endothelial growth factor and decreased survival in advanced laryngeal carcinoma.* Head Neck, 2002. **24**(11): p. 1004-11.
319. Argiris, A., et al., *Cetuximab and bevacizumab: preclinical data and phase II trial in recurrent or metastatic squamous cell carcinoma of the head and neck.* Ann Oncol, 2013. **24**(1): p. 220-5.
320. Strauss, L., et al., *The frequency and suppressor function of CD4+CD25highFoxp3+ T cells in the circulation of patients with squamous cell carcinoma of the head and neck.* Clin Cancer Res, 2007. **13**(21): p. 6301-11.
321. Badoual, C., et al., *PD-1-expressing tumor-infiltrating T cells are a favorable prognostic biomarker in HPV-associated head and neck cancer.* Cancer Res, 2013. **73**(1): p. 128-38.
322. Van den Eynde, B., et al., *A new family of genes coding for an antigen recognized by autologous cytolytic T lymphocytes on a human melanoma.* J Exp Med, 1995. **182**(3): p. 689-98.
323. Kienstra, M.A., et al., *Identification of NY-ESO-1, MAGE-1, and MAGE-3 in head and neck squamous cell carcinoma.* Head Neck, 2003. **25**(6): p. 457-63.
324. Lu, J., et al., *TAP-independent presentation of CTL epitopes by Trojan antigens.* J Immunol, 2001. **166**(12): p. 7063-71.
325. Voskens, C.J., et al., *Induction of MAGE-A3 and HPV-16 immunity by Trojan vaccines in patients with head and neck carcinoma.* Head Neck, 2012. **34**(12): p. 1734-46.
326. Goswitz, V.C. and Z.P. Sawicki, *Cancer therapy based on a mechanism of action for controlling the immune system and the resulting patent portfolio.* Recent Pat Endocr Metab Immune Drug Discov, 2013. **7**(1): p. 1-10.

327. Karcher, J., et al., *Antitumor vaccination in patients with head and neck squamous cell carcinomas with autologous virus-modified tumor cells.* Cancer Res, 2004. **64**(21): p. 8057-61.
328. Gleich, L.L., et al., *Therapeutic decision making in stages III and IV head and neck squamous cell carcinoma.* Arch Otolaryngol Head Neck Surg, 2003. **129**(1): p. 26-35.
329. Fukunaga, A., et al., *CD8+ tumor-infiltrating lymphocytes together with CD4+ tumor-infiltrating lymphocytes and dendritic cells improve the prognosis of patients with pancreatic adenocarcinoma.* Pancreas, 2004. **28**(1): p. e26-31.
330. Ene-Obong, A., et al., *Activated pancreatic stellate cells sequester CD8+ T cells to reduce their infiltration of the juxtatumoral compartment of pancreatic ductal adenocarcinoma.* Gastroenterology, 2013. **145**(5): p. 1121-32.
331. Watt, J. and H.M. Kocher, *The desmoplastic stroma of pancreatic cancer is a barrier to immune cell infiltration.* Oncoimmunology, 2013. **2**(12): p. e26788.
332. *Pancreatic Cancer Key Stats*. 2014 23/03/2015]; Available from: http://publications.cancerresearchuk.org/downloads/Product/CS_KF_PANCREAS.pdf.
333. Allison, D.C., et al., *DNA content and other factors associated with ten-year survival after resection of pancreatic carcinoma.* J Surg Oncol, 1998. **67**(3): p. 151-9.
334. Garcea, G., et al., *Survival following curative resection for pancreatic ductal adenocarcinoma. A systematic review of the literature.* JOP, 2008. **9**(2): p. 99-132.
335. Burris, H.A., 3rd, et al., *Improvements in survival and clinical benefit with gemcitabine as first-line therapy for patients with advanced pancreas cancer: a randomized trial.* J Clin Oncol, 1997. **15**(6): p. 2403-13.
336. Moore, M.J., et al., *Erlotinib plus gemcitabine compared with gemcitabine alone in patients with advanced pancreatic cancer: a phase III trial of the National Cancer Institute of Canada Clinical Trials Group.* J Clin Oncol, 2007. **25**(15): p. 1960-6.
337. Gjertsen, M.K., et al., *Intradermal ras peptide vaccination with granulocyte-macrophage colony-stimulating factor as adjuvant: Clinical and immunological responses in patients with pancreatic adenocarcinoma.* Int J Cancer, 2001. **92**(3): p. 441-50.
338. Ramanathan, R.K., et al., *Phase I study of a MUC1 vaccine composed of different doses of MUC1 peptide with SB-AS2 adjuvant in resected and locally advanced pancreatic cancer.* Cancer Immunol Immunother, 2005. **54**(3): p. 254-64.
339. Kimura, Y., et al., *Clinical and immunologic evaluation of dendritic cell-based immunotherapy in combination with gemcitabine and/or S-1 in patients with advanced pancreatic carcinoma.* Pancreas, 2012. **41**(2): p. 195-205.
340. Bauer, C., et al., *Dendritic cell-based vaccination of patients with advanced pancreatic carcinoma: results of a pilot study.* Cancer Immunol Immunother, 2011. **60**(8): p. 1097-107.
341. Dranoff, G., et al., *Vaccination with irradiated tumor cells engineered to secrete murine granulocyte-macrophage colony-stimulating factor stimulates*

potent, specific, and long-lasting anti-tumor immunity. Proc Natl Acad Sci U S A, 1993. **90**(8): p. 3539-43.
342. Thomas, A.M., et al., *Mesothelin-specific CD8(+) T cell responses provide evidence of in vivo cross-priming by antigen-presenting cells in vaccinated pancreatic cancer patients.* J Exp Med, 2004. **200**(3): p. 297-306.
343. Le, D.T., et al., *Safety and survival with GVAX pancreas prime and Listeria Monocytogenes-expressing mesothelin (CRS-207) boost vaccines for metastatic pancreatic cancer.* J Clin Oncol, 2015. **33**(12): p. 1325-33.
344. Butcher, E.C., *Leukocyte-endothelial cell recognition: three (or more) steps to specificity and diversity.* Cell, 1991. **67**(6): p. 1033-6.
345. von Andrian, U.H. and C.R. Mackay, *T-cell function and migration. Two sides of the same coin.* N Engl J Med, 2000. **343**(14): p. 1020-34.
346. Ebert, L.M., P. Schaerli, and B. Moser, *Chemokine-mediated control of T cell traffic in lymphoid and peripheral tissues.* Mol Immunol, 2005. **42**(7): p. 799-809.
347. Zlotnik, A. and O. Yoshie, *Chemokines: a new classification system and their role in immunity.* Immunity, 2000. **12**(2): p. 121-7.
348. Rossi, D. and A. Zlotnik, *The biology of chemokines and their receptors.* Annu Rev Immunol, 2000. **18**: p. 217-42.
349. Warnock, R.A., et al., *Molecular mechanisms of lymphocyte homing to peripheral lymph nodes.* J Exp Med, 1998. **187**(2): p. 205-16.
350. Bargatze, R.F., M.A. Jutila, and E.C. Butcher, *Distinct roles of L-selectin and integrins alpha 4 beta 7 and LFA-1 in lymphocyte homing to Peyer's patch-HEV in situ: the multistep model confirmed and refined.* Immunity, 1995. **3**(1): p. 99-108.
351. Girard, J.P. and T.A. Springer, *High endothelial venules (HEVs): specialized endothelium for lymphocyte migration.* Immunol Today, 1995. **16**(9): p. 449-57.
352. Sallusto, F., et al., *Two subsets of memory T lymphocytes with distinct homing potentials and effector functions.* Nature, 1999. **401**(6754): p. 708-12.
353. Mora, J.R. and U.H. von Andrian, *T-cell homing specificity and plasticity: new concepts and future challenges.* Trends Immunol, 2006. **27**(5): p. 235-43.
354. Wherry, E.J., et al., *Lineage relationship and protective immunity of memory CD8 T cell subsets.* Nat Immunol, 2003. **4**(3): p. 225-34.
355. Marzo, A.L., et al., *Initial T cell frequency dictates memory CD8+ T cell lineage commitment.* Nat Immunol, 2005. **6**(8): p. 793-9.
356. Berlin, C., et al., *Alpha 4 beta 7 integrin mediates lymphocyte binding to the mucosal vascular addressin MAdCAM-1.* Cell, 1993. **74**(1): p. 185-95.
357. Wagner, C.C., D.L. Haller, and M.E. Olbrisch, *Relapse prevention treatment for liver transplant patients.* J Clin Psychol Med Settings, 1996. **3**(4): p. 387-98.
358. Zabel, B.A., et al., *Human G protein-coupled receptor GPR-9-6/CC chemokine receptor 9 is selectively expressed on intestinal homing T lymphocytes, mucosal lymphocytes, and thymocytes and is required for thymus-expressed chemokine-mediated chemotaxis.* J Exp Med, 1999. **190**(9): p. 1241-56.
359. Hosoe, N., et al., *Demonstration of functional role of TECK/CCL25 in T lymphocyte-endothelium interaction in inflamed and uninflamed intestinal mucosa.* Am J Physiol Gastrointest Liver Physiol, 2004. **286**(3): p. G458-66.

360. Nakache, M., et al., *The mucosal vascular addressin is a tissue-specific endothelial cell adhesion molecule for circulating lymphocytes.* Nature, 1989. **337**(6203): p. 179-81.
361. Kantele, A., et al., *Cutaneous lymphocyte antigen expression on human effector B cells depends on the site and on the nature of antigen encounter.* Eur J Immunol, 2003. **33**(12): p. 3275-83.
362. Kantele, A., et al., *Differential homing commitments of antigen-specific T cells after oral or parenteral immunization in humans.* J Immunol, 1999. **162**(9): p. 5173-7.
363. Campbell, D.J. and E.C. Butcher, *Rapid acquisition of tissue-specific homing phenotypes by CD4(+) T cells activated in cutaneous or mucosal lymphoid tissues.* J Exp Med, 2002. **195**(1): p. 135-41.
364. Svensson, M., et al., *CCL25 mediates the localization of recently activated CD8alphabeta(+) lymphocytes to the small-intestinal mucosa.* J Clin Invest, 2002. **110**(8): p. 1113-21.
365. Johansson-Lindbom, B., et al., *Selective generation of gut tropic T cells in gut-associated lymphoid tissue (GALT): requirement for GALT dendritic cells and adjuvant.* J Exp Med, 2003. **198**(6): p. 963-9.
366. Mora, J.R., et al., *Selective imprinting of gut-homing T cells by Peyer's patch dendritic cells.* Nature, 2003. **424**(6944): p. 88-93.
367. Mora, J.R., et al., *Reciprocal and dynamic control of CD8 T cell homing by dendritic cells from skin- and gut-associated lymphoid tissues.* J Exp Med, 2005. **201**(2): p. 303-16.
368. Iwata, M., et al., *Retinoic acid imprints gut-homing specificity on T cells.* Immunity, 2004. **21**(4): p. 527-38.
369. Sigmundsdottir, H., et al., *DCs metabolize sunlight-induced vitamin D3 to 'program' T cell attraction to the epidermal chemokine CCL27.* Nat Immunol, 2007. **8**(3): p. 285-93.
370. Briskin, M., et al., *Human mucosal addressin cell adhesion molecule-1 is preferentially expressed in intestinal tract and associated lymphoid tissue.* Am J Pathol, 1997. **151**(1): p. 97-110.
371. Grant, A.J., et al., *MAdCAM-1 expressed in chronic inflammatory liver disease supports mucosal lymphocyte adhesion to hepatic endothelium (MAdCAM-1 in chronic inflammatory liver disease).* Hepatology, 2001. **33**(5): p. 1065-72.
372. Ala, A., et al., *Mucosal addressin cell adhesion molecule (MAdCAM-1) expression is upregulated in the cirrhotic liver and immunolocalises to the peribiliary plexus and lymphoid aggregates.* Dig Dis Sci, 2013. **58**(9): p. 2528-41.
373. Lind, A., et al., *The immune cell composition in Barrett's metaplastic tissue resembles that in normal duodenal tissue.* PLoS One, 2012. **7**(4): p. e33899.
374. Phillips, J.M., K. Haskins, and A. Cooke, *MAdCAM-1 is needed for diabetes development mediated by the T cell clone, BDC-2.5.* Immunology, 2005. **116**(4): p. 525-31.
375. Hänninen, A., et al., *Vascular addressins are induced on islet vessels during insulitis in nonobese diabetic mice and are involved in lymphoid cell binding to islet endothelium.* J Clin Invest, 1993. **92**(5): p. 2509-15.

376. Nummer, D., et al., *Role of tumor endothelium in CD4+ CD25+ regulatory T cell infiltration of human pancreatic carcinoma.* J Natl Cancer Inst, 2007. **99**(15): p. 1188-99.
377. Sandoval, F., et al., *Mucosal imprinting of vaccine-induced CD8$^+$ T cells is crucial to inhibit the growth of mucosal tumors.* Sci Transl Med, 2013. **5**(172): p. 172ra20.
378. Hingorani, S.R., et al., *Preinvasive and invasive ductal pancreatic cancer and its early detection in the mouse.* Cancer Cell, 2003. **4**(6): p. 437-50.
379. Hingorani, S.R., et al., *Trp53R172H and KrasG12D cooperate to promote chromosomal instability and widely metastatic pancreatic ductal adenocarcinoma in mice.* Cancer Cell, 2005. **7**(5): p. 469-483.
380. Sweeney, C.L., et al., *Methotrexate exacerbates tumor progression in a murine model of chronic myeloid leukemia.* J Pharmacol Exp Ther, 2002. **300**(3): p. 1075-84.
381. Thomas, G.R., et al., *Decreased expression of CD80 is a marker for increased tumorigenicity in a new murine model of oral squamous-cell carcinoma.* Int J Cancer, 1999. **82**(3): p. 377-84.
382. Chen, Z., et al., *Metastatic variants derived following in vivo tumor progression of an in vitro transformed squamous cell carcinoma line acquire a differential growth advantage requiring tumor-host interaction.* Clin Exp Metastasis, 1997. **15**(5): p. 527-37.
383. Yuspa, S.H., et al., *A survey of transformation markers in differentiating epidermal cell lines in culture.* Cancer Res, 1980. **40**(12): p. 4694-703.
384. Rosenfeldt, M.T., et al., *p53 status determines the role of autophagy in pancreatic tumour development.* Nature, 2013. **504**(7479): p. 296-300.
385. Workman, P., et al., *Guidelines for the welfare and use of animals in cancer research.* Br J Cancer, 2010. **102**(11): p. 1555-77.
386. Timiryasova, T.M., et al., *Vaccinia virus-mediated expression of wild-type p53 suppresses glioma cell growth and induces apoptosis.* Int J Oncol, 1999. **14**(5): p. 845-54.
387. Kretschmer, P.J., et al., *Development of a transposon-based approach for identifying novel transgene insertion sites within the replicating adenovirus.* Mol Ther, 2005. **12**(1): p. 118-27.
388. Chroboczek, J., F. Bieber, and B. Jacrot, *The sequence of the genome of adenovirus type 5 and its comparison with the genome of adenovirus type 2.* Virology, 1992. **186**(1): p. 280-5.
389. REED, L.J. and H. MUENCH, *A SIMPLE METHOD OF ESTIMATING FIFTY PER CENT ENDPOINTS.* American Journal of Epidemiology, 1938. **27**(3): p. 493-497.
390. Strober, W., *Trypan blue exclusion test of cell viability.* Curr Protoc Immunol, 2001. **Appendix 3**: p. Appendix 3B.
391. Michaud, M., et al., *Autophagy-dependent anticancer immune responses induced by chemotherapeutic agents in mice.* Science, 2011. **334**(6062): p. 1573-7.
392. Workenhe, S.T., et al., *Combining oncolytic HSV-1 with immunogenic cell death-inducing drug mitoxantrone breaks cancer immune tolerance and improves therapeutic efficacy.* Cancer Immunol Res, 2013. **1**(5): p. 309-19.

393. Gulley, J.L., R.A. Madan, and J. Schlom, *Impact of tumour volume on the potential efficacy of therapeutic vaccines.* Curr Oncol, 2011. **18**(3): p. e150-7.
394. Vigneswaran, N., et al., *Hypoxia-induced autophagic response is associated with aggressive phenotype and elevated incidence of metastasis in orthotopic immunocompetent murine models of head and neck squamous cell carcinomas (HNSCC).* Exp Mol Pathol, 2011. **90**(2): p. 215-25.
395. Shah, J.P., *Patterns of cervical lymph node metastasis from squamous carcinomas of the upper aerodigestive tract.* Am J Surg, 1990. **160**(4): p. 405-9.
396. Candela, F.C., K. Kothari, and J.P. Shah, *Patterns of cervical node metastases from squamous carcinoma of the oropharynx and hypopharynx.* Head Neck, 1990. **12**(3): p. 197-203.
397. Coatesworth, A.P., A. Tsikoudas, and K. MacLennan, *The cause of death in patients with head and neck squamous cell carcinoma.* J Laryngol Otol, 2002. **116**(4): p. 269-71.
398. Hayward, S.D., *Viral interactions with the Notch pathway.* Semin Cancer Biol, 2004. **14**(5): p. 387-96.
399. Chen, H.J., et al., *Chemokine 25-induced signaling suppresses colon cancer invasion and metastasis.* J Clin Invest, 2012. **122**(9): p. 3184-96.
400. Sharma, P.K., et al., *CCR9 mediates PI3K/AKT-dependent antiapoptotic signals in prostate cancer cells and inhibition of CCR9-CCL25 interaction enhances the cytotoxic effects of etoposide.* Int J Cancer, 2010. **127**(9): p. 2020-30.
401. Liu, Q. and D.A. Muruve, *Molecular basis of the inflammatory response to adenovirus vectors.* Gene Ther, 2003. **10**(11): p. 935-40.
402. Liu, Q., et al., *Akt/protein kinase B activation by adenovirus vectors contributes to NFkappaB-dependent CXCL10 expression.* J Virol, 2005. **79**(23): p. 14507-15.
403. Jaffee, E.M., et al., *Novel allogeneic granulocyte-macrophage colony-stimulating factor-secreting tumor vaccine for pancreatic cancer: a phase I trial of safety and immune activation.* J Clin Oncol, 2001. **19**(1): p. 145-56.
404. Johnson, R.S., A.I. Walker, and S.J. Ward, *Cancer vaccines: will we ever learn?* Expert Rev Anticancer Ther, 2009. **9**(1): p. 67-74.
405. Rosenberg, S.A., J.C. Yang, and N.P. Restifo, *Cancer immunotherapy: moving beyond current vaccines.* Nat Med, 2004. **10**(9): p. 909-15.
406. Schirrmacher, V. and R. Heicappell, *Prevention of metastatic spread by postoperative immunotherapy with virally modified autologous tumor cells. II. Establishment of specific systemic anti-tumor immunity.* Clin Exp Metastasis, 1987. **5**(2): p. 147-56.
407. von Hoegen, P., et al., *Prevention of metastatic spread by postoperative immunotherapy with virally modified autologous tumor cells. III. Postoperative activation of tumor-specific CTLP from mice with metastases requires stimulation with the specific antigen plus additional signals.* Invasion Metastasis, 1989. **9**(2): p. 117-33.
408. Herold-Mende, C., et al., *Antitumor immunization of head and neck squamous cell carcinoma patients with a virus-modified autologous tumor cell vaccine.* Adv Otorhinolaryngol, 2005. **62**: p. 173-83.

409. Steiner, H.H., et al., *Antitumor vaccination of patients with glioblastoma multiforme: a pilot study to assess feasibility, safety, and clinical benefit.* J Clin Oncol, 2004. **22**(21): p. 4272-81.
410. Lemay, C.G., et al., *Harnessing oncolytic virus-mediated antitumor immunity in an infected cell vaccine.* Mol Ther, 2012. **20**(9): p. 1791-9.
411. Mincheff, M., et al., *Naked DNA and adenoviral immunizations for immunotherapy of prostate cancer: a phase I/II clinical trial.* Eur Urol, 2000. **38**(2): p. 208-17.
412. Ramshaw, I.A. and A.J. Ramsay, *The prime-boost strategy: exciting prospects for improved vaccination.* Immunol Today, 2000. **21**(4): p. 163-5.
413. Marshall, J.L., et al., *Phase I study in advanced cancer patients of a diversified prime-and-boost vaccination protocol using recombinant vaccinia virus and recombinant nonreplicating avipox virus to elicit anti-carcinoembryonic antigen immune responses.* J Clin Oncol, 2000. **18**(23): p. 3964-73.
414. O'Malley, B.W., et al., *A new immunocompetent murine model for oral cancer.* Arch Otolaryngol Head Neck Surg, 1997. **123**(1): p. 20-4.
415. Khurana, D., et al., *Characterization of a spontaneously arising murine squamous cell carcinoma (SCC VII) as a prerequisite for head and neck cancer immunotherapy.* Head Neck, 2001. **23**(10): p. 899-906.
416. Ning, N., et al., *Cancer stem cell vaccination confers significant antitumor immunity.* Cancer Res, 2012. **72**(7): p. 1853-64.
417. Park, K., et al., *The attenuation of experimental lung metastasis by a bile acid acylated-heparin derivative.* Biomaterials, 2007. **28**(16): p. 2667-76.
418. Hirst, D.G., J.M. Brown, and J.L. Hazlehurst, *Enhancement of CCNU cytotoxicity by misonidazole: possible therapeutic gain.* Br J Cancer, 1982. **46**(1): p. 109-16.
419. Gleich, L.L., et al., *Alloantigen gene therapy for head and neck cancer: evaluation of animal models.* Head Neck, 2003. **25**(4): p. 274-9.
420. Coffey, J.C., et al., *Excisional surgery for cancer cure: therapy at a cost.* Lancet Oncol, 2003. **4**(12): p. 760-8.
421. Mestas, J. and C.C. Hughes, *Of mice and not men: differences between mouse and human immunology.* J Immunol, 2004. **172**(5): p. 2731-8.
422. Herman, G.E., *Mouse models of human disease: lessons learned and promises to come.* ILAR J, 2002. **43**(2): p. 55-6.
423. Zhang, P., et al., *Induction of postsurgical tumor immunity and T-cell memory by a poorly immunogenic tumor.* Cancer Res, 2007. **67**(13): p. 6468-76.
424. Speiser, D.E., et al., *A novel approach to characterize clonality and differentiation of human melanoma-specific T cell responses: spontaneous priming and efficient boosting by vaccination.* J Immunol, 2006. **177**(2): p. 1338-48.
425. Powell, D.J., et al., *Transition of late-stage effector T cells to CD27+ CD28+ tumor-reactive effector memory T cells in humans after adoptive cell transfer therapy.* Blood, 2005. **105**(1): p. 241-50.
426. Schlom, J., *Therapeutic cancer vaccines: current status and moving forward.* J Natl Cancer Inst, 2012. **104**(8): p. 599-613.
427. Castiglione, F., et al., *How the interval between prime and boost injection affects the immune response in a computational model of the immune system.* Comput Math Methods Med, 2012. **2012**: p. 842329.

428. Sallusto, F., et al., *From vaccines to memory and back.* Immunity, 2010. **33**(4): p. 451-63.
429. Ramakrishnan, R. and D.I. Gabrilovich, *Novel mechanism of synergistic effects of conventional chemotherapy and immune therapy of cancer.* Cancer Immunol Immunother, 2013. **62**(3): p. 405-10.
430. Le, H.K., et al., *Gemcitabine directly inhibits myeloid derived suppressor cells in BALB/c mice bearing 4T1 mammary carcinoma and augments expansion of T cells from tumor-bearing mice.* Int Immunopharmacol, 2009. **9**(7-8): p. 900-9.
431. Watanabe, I., et al., *Effects of tumor selective replication-competent herpes viruses in combination with gemcitabine on pancreatic cancer.* Cancer Chemother Pharmacol, 2008. **61**(5): p. 875-82.
432. Wennier, S.T., et al., *Myxoma virus sensitizes cancer cells to gemcitabine and is an effective oncolytic virotherapeutic in models of disseminated pancreatic cancer.* Mol Ther, 2012. **20**(4): p. 759-68.
433. Engeland, C.E., et al., *CTLA-4 and PD-L1 checkpoint blockade enhances oncolytic measles virus therapy.* Mol Ther, 2014. **22**(11): p. 1949-59.
434. Dias, J.D., et al., *Targeted cancer immunotherapy with oncolytic adenovirus coding for a fully human monoclonal antibody specific for CTLA-4.* Gene Ther, 2012. **19**(10): p. 988-98.
435. Hensbergen, P.J., et al., *The CXCR3 targeting chemokine CXCL11 has potent antitumor activity in vivo involving attraction of CD8+ T lymphocytes but not inhibition of angiogenesis.* J Immunother, 2005. **28**(4): p. 343-51.
436. Hickman, H.D., et al., *CXCR3 chemokine receptor enables local CD8(+) T cell migration for the destruction of virus-infected cells.* Immunity, 2015. **42**(3): p. 524-37.
437. Zhu, X., et al., *Poly-ICLC promotes the infiltration of effector T cells into intracranial gliomas via induction of CXCL10 in IFN-alpha and IFN-gamma dependent manners.* Cancer Immunol Immunother, 2010. **59**(9): p. 1401-9.